Smart Materials for Subsea Buoyancy Control

by

Paul Molloy (M.Sc.)

Submitted in partial fulfilment of the requirements for the Degree of
Doctor of Philosophy

University of Glasgow
Glasgow Marine Technology Centre

July 2000

Abstract

Buoyancy control is needed in small autonomous underwater devices to enable greater flexibility in measurements in the ocean. This project has examined a number of ways in which buoyancy changes might be achieved. Firstly, an extensive review of the mechanisms by which various marine organisms control their buoyancy was undertaken. There is a tremendous diversity of natural buoyancy control mechanisms, but most of these mechanisms produce only slow (and small) changes in buoyancy.

Studies were carried out on the behaviour of polymer gel systems that exhibit large volume changes under the influence of solvent composition and/or temperature. The effects of salinity were investigated, from 5 parts per thousand (ppt) to 35ppt, on hydrolysed polyacrylamide gels, over the temperature range of 5°C to 40°C. It was found that the gels decreased in volume in the solutions, this effect being most pronounced in the 35ppt solution. As temperature increased, the volume changes were observed to decrease. The cyclical volumetric strain behaviour of the polyacrylamide gels, by alternate exposure to saline solutions and distilled water, resulted in significant (~200%) volume changes induced over periods of 2 days. In a second study, the density change associated with the volumetric strain of polymeric materials was investigated in poly(N-isopropylacrylamide), NIPA, gels. The temperature-sensitive NIPA gels, immersed in distilled water or seawater solutions at temperatures ranging from 5°C to 50°C, exhibited volume changes of over 800%, and density changes of 30-40%. NIPA gels exhibit a faster response time than polyacrylamide gels, and their density and volume changes have potential application in buoyancy change.

Experiments were also performed on NiTi shape memory alloys (SMA), which change in length and mechanical properties with temperature. A controllable parallel-plate device was constructed, linked by four helical SMA springs, which exerted significant axial forces with the application of temperature. The device is capable of producing substantial volume changes if contained in a suitable enclosure. It is currently on loan to the Science Museum, London, as part of a new exhibition in the Wellcome Wing.

Table of Contents

List of Tables

List of Figures

Acknowledgements

I would like to take this opportunity to thank a number of people who have helped me during this project. They include: Professor Mike Cowling, my supervisor, for his guidance and support; Margaret Smith, for her assistance and technical support with experimental procedures and testing apparatus, and for her advice on chemical aspects in this work; Lynn Cullen, for her help with preparing this thesis; and the technicians who have helped build testing apparatus and assisted in experiments.

I would especially like to thank my wife, Fiona, for her continued support for me over the years and her patience while I was writing my thesis.

This research was supported by the Engineering and Physical Sciences Research Council (EPSRC), Grant No. GR/L 27022, administered through the Marine Technology Directorate (MTD). Such support is gratefully acknowledged.

Chapter 1 Introduction

The purpose of this project was to conduct research into the behaviour of 'smart' materials in an underwater environment, so that elements of these materials could be combined to form a hybrid device whose density and stiffness could be altered. The target application for this hybrid material was an element of variable buoyancy with uses in oceanographic surveying applications and in underwater operations in the oil and gas industry.

As the need for data acquisition in physical oceanography increases, unmanned autonomous underwater vehicles (AUVs) are required to undertake longer missions, involving frequent excursions between the surface and ocean depths for the relay of data [1]. The propulsive power of these autonomous underwater vehicles and packages is mainly confined to the onboard electric battery supply, in one form or the other. Buoyancy change in these devices is a major issue, since overcoming too little or too much inherent buoyancy by active propulsion requires substantial power reserves.

There are a number of ways that a vehicle's buoyancy might change, including a change in depth or salinity, the accumulation of biofouling, slow leaks, or the acquisition of samples [2]. It would be advantageous to make small compensating changes in the vehicle's buoyancy in the event of sudden gains or losses. Changing buoyancy can also be used as a means of propulsion, as seen in an underwater glider [3]. For the requirement of diving to a desired depth, the concept of neutral buoyancy in an underwater device at any depth is attractive from the point of view of energy conservation. This could be achievable if the

aggregate density of the device could be made to continuously match that of the surrounding seawater without the expenditure of much energy from the batteries [1].

Attempts to control buoyancy, to provide a neutral buoyancy at any depth, have been relatively crude and mechanically complex. Foam materials of differing densities are available and the major components for different densities are rigid hollow polymer spheres, embedded in a syntactic or polyurethane foam matrix [4]. Other solutions involve the pumping of water from chambers [5] or the inflation of flexible buoyancy elements [6].

The overall aim of the research was to demonstrate the application of smart materials as variable buoyancy elements in marine applications so as to be able to produce neutral buoyancy at any depth. The smart materials would be incorporated into a controllable device that would permit instantaneous volumetric/density changes, or changes in stiffness, which could impart the desired degree of buoyancy.

The science of 'smart' materials and structures has been developing over the past 10-15 years [7]. The definition of a smart structure is one "which has built-in or intrinsic sensors, actuators and control mechanisms, whereby it is capable of sensing a stimulus, responding to it in a predetermined manner and extent in an appropriate time, and reverting to its original state as soon as the stimulus is removed" [8]. The elements considered in this study included electrorheological (ER) and magnetorheological (MR) fluids, responsive polymers gels, shape memory alloys and shape memory polymers.

In Chapter 2, the numerous mechanisms of buoyancy control employed by marine animals and organisms are reviewed. These mechanisms are found to be diverse, but, apart from active swimming, they also produce only slow changes in depth (buoyancy). However, the form of buoyancy control employed by most organisms is passive, as opposed to active swimmers, who employ energy intensive mechanisms. The buoyancy mechanisms provide opportunities for functional biomimetics, i.e. the transferral to engineering analogues. Therefore, the natural buoyancy mechanisms are compared with those currently used in various underwater vehicles and devices. The attempts being made to mimic the mechanisms present in nature are also described.

A review of the current technology associated with various smart materials is undertaken in Chapter 3. Controllable fluids are detailed (electrorheological and magnetorheological fluids), whose stiffness or viscosity can be altered with the application of an electric (or magnetic) field. Shape memory materials are also described. These include alloys, polymers and ceramics that can change their shape and stiffness upon a change in temperature. Finally, an evaluation is conducted of responsive polymer gels, which also exhibit shape memory characteristics under the influence of temperature, electric fields, and solvent or pH changes. For all the materials outlined in the chapter, their potential for use in a marine environment is determined from their actuation and response properties and from a review of current applications of the materials in underwater vehicles and devices.

Chapter 4 describes extensive experiments conducted on polymer gels under the influence of various stimuli. These include the effect of d.c. electric fields on polyacrylamide gels, the influence of seawater solutions and temperature on the volume of polyacrylamide gels, and the effect of temperature on the volume and density of poly(*N*-isopropylacrylamide) gels immersed in solutions of distilled water and seawater. Experiments were also conducted on the mechanical properties of the two polymer gel systems, and also on the actuating power of the gels.

Experiments conducted on NiTi shape memory alloys are illustrated in Chapter 5. A concept design for an actuation/variable-volume system is proposed and built using helical coil springs made of the NiTi material. The device is tested and evaluated, providing valuable information for the future development of a variable-volume device, which could be used to change the overall density and buoyancy of an underwater vehicle or device.

Chapter 6 discusses the potential of smart materials as actuating elements in a buoyancy control system for underwater devices. The results of experiments conducted on shape memory alloys and polymer gels are discussed further in relation to buoyancy control. Finally, proposals for future work are described based on the work conducted in this project and also on advancements in the field by other researchers.

Conclusions on the work presented in this thesis are presented in Chapter 7. The subsequent appendices include relevant journal papers published, or accepted for publication (subject to minor corrections), drawn from this research [9-11].

1.1 References

1. Scrimshaw K.H. 1996. Aspects of buoyancy control and materials assessment applicable to deep submergence unmanned autonomous underwater vehicles (AUVs). *Oceanology International 1996* pp. 245-262.
2. McCanna J. and Rae G.J. 1997. Shape memory alloy buoyancy regulator for subsea robots. *10th international symposium on unmanned untethered submersible technology*. SPIE, pp. 206-216.
3. Kunzig R. 1996. A thousand diving robots. *Discover* **April**, pp. 60-71.
4. Balmoral hitec buoyancy 1989. *Buoyancy - in depth*. Balmoral Group Ltd.
5. Allmendinger E.E. (Ed.) 1990. *Submersible vehicle systems design*. The Society of Naval Architects and Marine Engineers.
6. Webb D.C., Simonetti P.J. 1999. The SLOCUM AUV: An environmentally propelled underwater glider. *11th international symposium on unmanned untethered submersible technology*. pp. 75-85.
7. Rogers C.A., Barker D.K., Jaeger C.A. 1989. Introduction to smart materials and structures. In: *Smart materials, structures and mathematical issues*. Rogers C.A. (Ed.), Technomic Publishers, pp. 17-28.
8. Ahmad I. 1989. Smart structures and materials. In: *Smart materials, structures and mathematical issues*. Rogers C.A. (Ed.), Technomic Publishers, pp. 13-16.
9. Molloy P.J., Cowling M.J. 2000. Buoyancy mechanisms of marine organisms: lessons from nature. *Underwater technology* **24**(2), pp. 41-49.

10. Molloy P.J., Smith M.J., Cowling M.J. 2000. The effects of salinity and temperature on the behaviour of polyacrylamide gels. *Materials and Design* **21**, pp. 169-174.

11. Molloy P.J., Cowling M.J. 2000. Volume and density changes in polymer gels in seawater environments. *Journal of materials: design and applications.* Accepted, subject to minor corrections. Resubmitted, May 2000.

Chapter 2 Buoyancy

Animals and plants, in order to survive in competition with each other, have evolved ways of living using the least amount of resources. This involves efficiency both in metabolism and optimal apportionment of energy between the various functions of life, including the control of buoyancy. A similar situation is often found in engineering, where cost is usually the most significant parameter. In the case of underwater devices, the more energy used in buoyancy control means more cost to a mission or survey. It seems likely, then, that ideas from nature, sometimes called biomimetics, could improve the energy efficiency of engineering at many levels. This chapter reviews how many pelagic organisms maintain their buoyancy in the ocean. These mechanisms are compared with those currently used in various underwater devices, and the attempts being made to mimic natural buoyancy mechanisms are described.

2.1 Buoyancy Mechanisms of Marine Organisms

2.1.1 Introduction

Thousands of pelagic organisms exist in the ocean, from the surface waters down to the deep sea floor. Each species lives within a certain range of depth and, as far as is known, the individuals of a species must keep to their particular environment in order to flourish [1]. The protein-based tissues and skeletal materials of many of these marine organisms

are considerably more dense than seawater, which has a density range of about 1.024 to 1.030g/cm^3 [2]. To compensate, these organisms employ a variety of methods in order to remain at their chosen depth in the water column. Table 1 summarises many of the mechanisms found in marine life.

Table 2.1 Buoyancy mechanisms in marine organisms.

Method	**Marine organisms**
Exclusion of heavy ions	Gelatinous marine animals, plankton
Increase in surface area	Plankton
Ammonium-rich body fluid	Some oceanic squid and crustaceans, plankton
Gas-filled shell	Some cephalopods (e.g. cuttlefish, *Nautilus*, and *spirula*)
Gas-filled swimbladder	Teleosts (e.g. cod and haddock)
Hydrocarbon squalene	Squaloid sharks
Low-density waxes	Deep-diving mammals (e.g. sperm whale)
None	Bottom dwellers (e.g. lobster, octopus), constant swimmers (e.g. some squid, mackerel, blue shark)

The Stokes' equation determines the sinking rate of small organisms [3]:

$$SR = \frac{2}{9}\frac{(\rho_1 - \rho_2)gr^2}{(V_W)(\phi)} \tag{2.1}$$

where SR = sinking rate; ρ_1 = density of the organism; ρ_2 = density of seawater; g = gravitational acceleration; r = radius of a sphere of identical volume; V_w = viscosity of seawater; and ϕ = form resistance, which expresses the effect of departure from the spherical form on sinking rate. Control of the local density or viscosity of seawater is beyond the capabilities of an organism, but either increasing its own form resistance

(departing as much from a spherical shape) or decreasing its density with respect to that of seawater can bring about a reduction in the sinking rate.

2.1.2 Plankton

The proteins, carbohydrates and skeletal structures that make up plankton usually have a density greater than that of seawater and, hence, plankton tend to sink in the water column. Therefore they must employ strategies to aid their buoyancy or reduce their rate of sinking.

Plankton have a number of ways of reducing their density, one such method being ionic replacement to reduce the density of body fluids. Seawater is a complex mixture of ions, of which sodium (Na^+), chloride (Cl^-), magnesium (Mg^{2+}) and sulphate (SO_4^{2-}) account for over 97% of the total ionic content [4]. Replacement of a heavy ion, such as sulphate, with a lighter ion, such as chloride, can reduce the density of the solution. Ions with negative partial molar volumes, such as magnesium, cause close packing of water molecules and therefore increase the density of the solution. Replacement of these with ions of positive partial molar volumes, such as sodium, induce a less regular structure and lower the solution's density [4].

Organisms such as ctenophores, salps and heteropods actively exclude heavy ions such as SO_4^{2-} from their bodies and replace them with osmotically similar but lighter Cl^- ions [5]. Newton & Potts [4] observed the exclusion of Mg^{2+} and SO_4^{2-} ions from the larval bodies

of *Hoarus vulgaris* (Arthropoda: Decapoda), *Asterias* (Echinodermata) and *Obelia*. Gross & Zeuthen [6] and Kahn & Swift [7] have found similar ion replacement mechanisms present in other plankton. One such organism is the dinoflagellate *Noctiluca*, whose internal fluid contains ammonium chloride (NH_4Cl) which is isosmotic with seawater but is less dense [5,7].

Some plankton use gas vesicles for buoyancy. Researchers [8,9] describe how freshwater and marine blue-green algae can change overall buoyancy by modifying the cellular carbohydrate content. The siphonophore colonies also use gas floats, e.g. the Portuguese man-of-war (*Physalia*) [5]. Another low-density strategy is the use of fats or oils that are less dense than water. Copepods and diatoms store oils that maintain their buoyancy, and which can also be used as food reserves [5].

If plankton cannot reduce their density then they must increase their form resistance. Smaller organisms have a slower sinking rate than their larger counterparts, as they have a greater surface area relative to volume [5]. By remaining small, plankton offer far more surface area of resistance to sinking per unit volume of living material, than if they were large. The other way of increasing the form resistance is to change the shape of the body or develop spines and body projections. These can add considerable resistance, but add little to the weight [10]. A few long spines increase drag more than a greater number of short spines. The species *Acanthometra* has projections, called myonemes, projecting out from the gelatinous body of the organism [2]. When the myonemes contract, the

gelatinous matrix is greatly expanded and the organism rises in the water. On relaxation of the myonemes, the matrix shrinks and is followed by sinking (Figure 2.1).

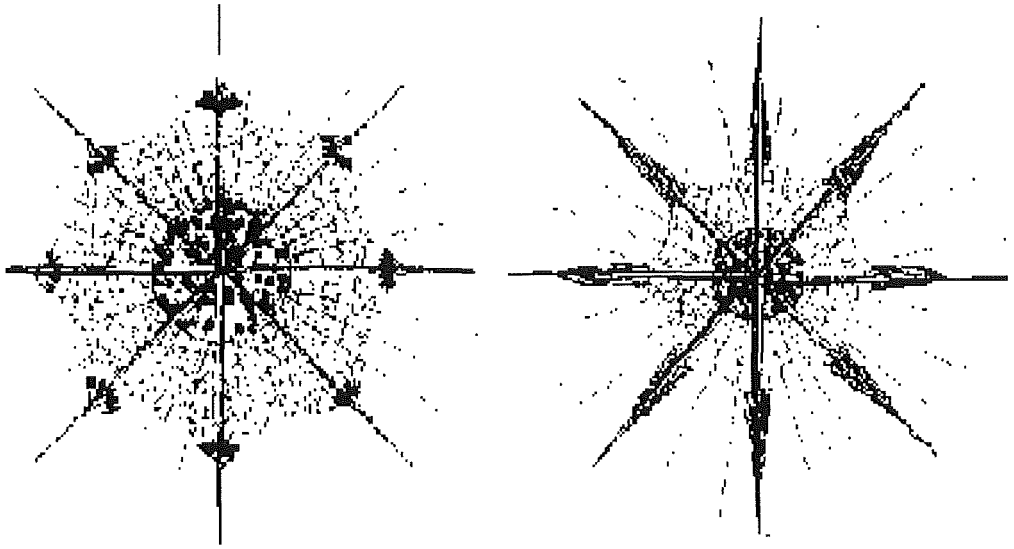

Figure 2.1 The acantharian radiolarion. Left, with outer cytoplasm expanded (myonemes contracted); right, with cytoplasm withdrawn (myonemes relaxed) [2].

Certain plankton can undergo vertical migrations to the depths and back up to shallow waters. For example, during a typical day, phytoplankton photosynthesise and accumulate carbohydrates, causing nitrogen supplies to become limited. This tips the balance of the cell from being positively buoyant to negatively buoyant and the cell begins to sink. Photosynthesis decreases and with it the production of carbohydrates. However, metabolic activity continues and internal NO_3^- pools accumulate in the cell with the expenditure of energy. These tip the balance back in favour of positive buoyancy and the cell begins to rise again. In this way the plankton oscillates between positive and negative buoyancy. Studies of the coastal marine diatom *Thalassiosira weissflogii* showed that the

density and sinking rate of the cell was affected by carbohydrate production, causing it to sink [11], although Fisher & Harrison [12] found no positive correlation between sinking rate and carbohydrate content for the organism. Moore & Villareal [13] studied the vertical migration of three oceanic diatoms of the genus *Rhizosolenia* and found carbohydrate ballasting can account for buoyancy changes. Whether as solitary cells or as aggregations (mats), *Rhizosolenia* migrate in this way to deep nutrient pools (below 80-100m) and then return to the surface for photosynthesis. This migration helps the transport of nitrate (new nitrogen) from depth into the surface waters and surface-derived carbon is respired at depth [14].

A number of hypotheses have been suggested for the vertical migration of zooplankton [5]. Mclaren [15] and Haney [16] suggest that zooplankton descend into the depths during the day to avoid predators in the upper lighted areas. Another hypothesis is that they are avoiding damage from light. Hardy [17] suggests that descent into the depths brings a fresh supply of food for the zooplankton. Currents at depth are generally slower than in the shallow waters, so while the zooplankton are at depth, the swifter upper currents bring along a fresh supply of phytoplankton. The zooplankton then rise to the surface to feed. A final reason for migration is that descent into the depths allows the production of phytoplankton. The hypothesis also suggests that less energy is needed for zooplankton to stay in cold, deep waters than trying to maintain themselves constantly in the warm, upper waters [15,18-20].

2.1.3 Cephalopods

There are some 700-800 species of modern cephalopod. They are mostly squids and a number of octopods, with a few sepioids of the cuttlefish group [2]. They employ a number of methods to achieve neutral buoyancy [21], including the use of gas-filled chambers of *Nautilus*, *Spirula* and *Sepia*, replacement of heavy ions as in some octopods, and the storage of low-density fats in the *Gonatidae* family of squids. However, the majority of cephalopods achieving neutral buoyancy are oceanic squids using ammonium-rich solutions isosmotic with seawater.

Ammonium storage was first discovered in cranchiid squid [22]. Since then thirteen families of oceanic squid have been documented, or suggested, to use ammoniacal buoyancy, as have genera in three of the fourteen otherwise non-ammoniacal, muscular families [21,23]. The cranchiid squids can hang almost motionless in the sea and possess a large, fluid-filled buoyancy chamber. The fluid is principally ammonium chloride and is isosmotic with seawater [2,22]. It has a specific gravity of about 1.010 to 1.012, so a relatively large volume of the ammoniacal fluid is required to make the squid neutrally buoyant. This could take up almost two-thirds of the animal's total weight, making it very cumbersome. The squid secretes nitrogen, from the breakdown of proteins, in the form of ammonia instead of urea. This ammonia is trapped in the coelomic cavity. Because of the high acidity, the ammonia diffuses from the bloodstream into the cavity and dissociates into ions. They remain in the cavity to reduce the density of the fluid. The coelomic cavity hardly leaves space for the development of a capacious mantle cavity. In fact, such

squid, though capable of rather quick escape reactions, are small-finned, unhurried swimmers. In larger and more active kinds of squid there is no single buoyancy chamber (e.g. Histioteuthis). Instead, there are many small vacuolar chambers over the body, particularly in the arms and mantle, which are filled with ammoniacal fluids very similar in composition to those of cranchiid squids [2,21,24-26]. Although ammoniacal buoyancy offers an advantage, in that it maintains function at high ambient pressure or regardless of rapid changes in depth [22], few ammoniacal squids appear to exploit this advantage by undergoing large vertical migrations [27].

Nautilus, the last surviving genus of externally-shelled cephalopod, maintains neutral buoyancy in the sea through the use of a gas and liquid-filled portion of the shell which serves to lower the specific gravity of the entire shell and enclosed tissue to approximately that of seawater [28]. The saline or cameral liquid that originally filled the chambers is removed by osmosis through the siphuncle, a thin strand of tissue that extends back from the *Nautilus*' body through each chamber. The space left is filled passively with gas by diffusion, and the pressures within these chambers are subatmospheric [29]. As the animal grows, producing new flesh and shell material, it becomes progressively denser. By removing liquid in small volumes each day, a *Nautilus* can counterbalance density increases [30]. The system can also be used if there is a sudden increase or decrease in the weight of the *Nautilus*, such as ingestion of food or following an attack by a predator, where a portion of the shell may have been broken off [31]. Studies have shown that when challenged with a sudden decrease in buoyancy, *Nautilus* can increase its chamber-emptying rate in a compensatory fashion [32]. When sections of shell were removed, or

when extra buoyancy was attached to the *Nautilus*, it shut off the pumps in the siphuncle, resulting in a slow refilling of the last several chambers with liquid until neutral buoyancy was again achieved [33]. This gave the animal time to grow new shell material. It was a popular misconception that the *Nautilus* was capable of rapidly adding or subtracting fluid in the shell for the purpose of quickly ascending or descending [34,35]. Chamber refilling or emptying takes days, not hours, preventing rapid buoyancy changes.

The more recently evolved cephalopods, *Sepia* (cuttlefish) and *Spirula*, also possess chambered shells that are used to achieve neutral buoyancy. The cuttlebone of the *Sepia* consists of a number of thin chambers laid down, one below the other, at the rate of about one or two a week as the animal grows [29]. Parallel sheets (lamellae) of calcium carbonate form the chambers, which are sealed from each other, but within any individual chamber gas or liquid can move freely [36]. Numerous pillars support each chamber, and these have a sigmoidal cross-section (Figure 2.2). Liquid can be pumped into or out of the cuttlebone to decrease or increase the gas volume. The gas is principally nitrogen and its pressure in the older chambers is only about four-fifths of an atmosphere, regardless of depth [29]. This is enough to give the bone an overall density of around 60% that of seawater, sufficient to counter the heavier tissues of the cuttlefish. As in the *Nautilus*, the presence of the gas is purely incidental, as it diffuses passively into the partially vacated space that develops due to the active pumping out of the entrained liquid.

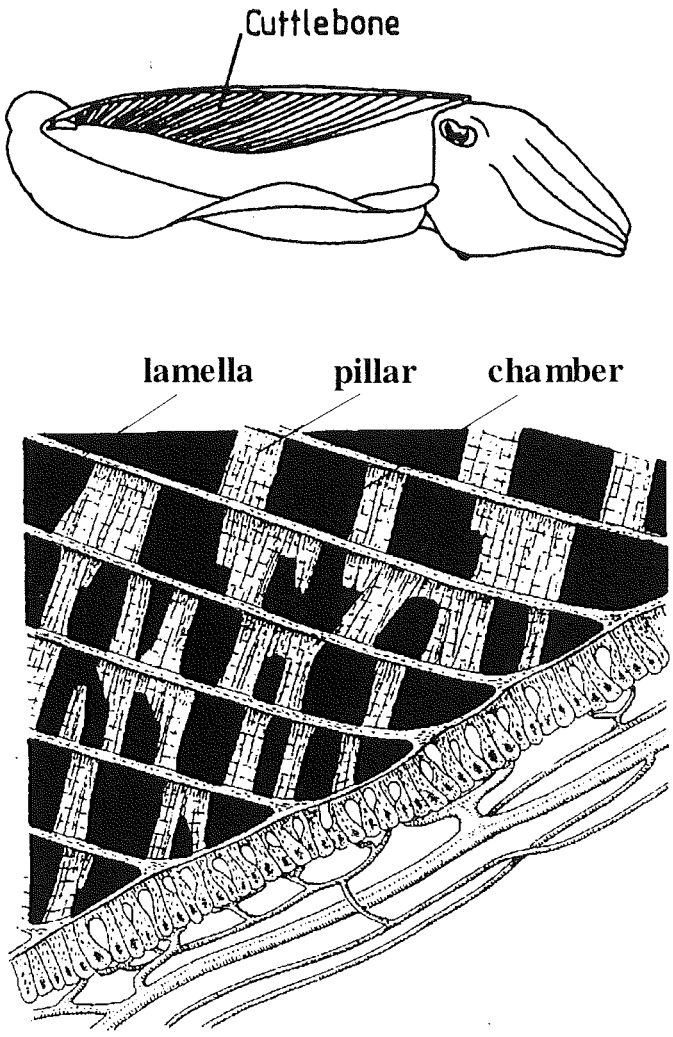

Figure 2.2 The position and microstructure of the cuttlebone [36].

This entrained liquid is primarily a sodium chloride solution, at a lower concentration than in the blood of the cuttlefish. This creates an osmotic pressure sufficient to balance hydrostatic pressure. The yellowish membrane at the back end of the cuttlebone has an ample blood supply that enables the membrane to pump salts from the liquid within the cuttlebone and into the blood. The effect of this is a flow of liquid from the cuttlebone into the bloodstream. Therefore, this salt pump can increase or decrease the osmotic pressure between the animal's blood and cuttlebone liquid in response to changes in hydrostatic pressure exerted by the sea.

Birchall & Thomas [36] found the cuttlebone matrix to have a mean crushing strength of 1.1MPa. Therefore, along with actively maintaining the buoyancy of the animal, the sealed chambers also provide a structure which combines high porosity (93%) and low specific gravity (0.19) with the ability to resist external pressures greater than 1MPa. Denton *et al* [37] reported that under hydrostatic pressure a whole cuttlebone withstood a pressure of 2.4MPa, (corresponding to a depth of 230m) before imploding. Failure of the shell was found to be progressive, not catastrophic [36]. The S-shaped cross-section of the pillars minimises any tendency for the pillars to buckle by maximising the second moment of area. Although cuttlefish can withstand pressures up to 24atm, they do not seem to live deeper than 150m, where the pressure is 16atm. *Nautilus* shells collapse at about 65atm, but they also remain at a safer depth of about 500m, where the pressure is at 51atm [38]. The same is true of the *Spirula*. Even though its shell implodes at pressures corresponding to a depth of 1700m, most *Spirula* are caught at depths of 600-700m during the day, and at 300-100m by night [39].

2.1.4 Teleost Fish

Teleosts are a large diverse group of bony fish. Many species, including the cod and haddock, are equipped with swimbladders that give them neutral buoyancy [2]. Typically, a swimbladder occupies around 5% of the total volume of a fish and the low density of the gases that inflate the bladder offset the higher density of the muscle and bone. However, the volume of the swimbladder can change with depth. As the fish swims downward,

pressure increases at one atmosphere every 10 metres. Therefore when a fish dives deeper, it must secrete more gas into the swimbladder, and reabsorb gas from the swimbladder when it wishes to rise. The rates of secretion or reabsorption are quite slow. Fish caught at depth and immediately brought to the surface nearly always die because their swimbladders expand rapidly as the pressure drops, thus crowding and rupturing their vital organs.

The gas pressure exerted in the swimbladder directly opposes the hydrostatic pressure of the sea. The proportion of oxygen found in swimbladders increases with depth. A fish living at a depth of 1000m has a partial pressure of oxygen in the swimbladder of 100atm, but only 0.2atm in the surrounding tissues, so somehow the swimbladder pressure must be maintained to resist the hydrostatic pressure [29]. This is partly achieved by having impermeable walls and also by the gas gland and its blood supply, the rete mirabile. The rete is made up of arterial and venous capillaries lying next to each other, forming a countercurrent system.

In the gas gland, lactic acid is produced from glycogen and diffuses into adjoining blood capillaries (Figure 2.3). This causes an increase in acidity that results in a rapid displacement of O_2 from haemoglobin [40]. Therefore there is an increase in the concentration of free (diffusible) oxygen molecules. The blood leaves the gas gland and enters the rete mirabile counter-current system. There is a progressive equilibration of diffusible substances between the ingoing and outgoing streams. Free oxygen molecules diffuse into the incoming blood and the acidity of the outgoing blood decreases [29].

Alkaline blood causes O_2 molecules to recombine with haemoglobin. However, the rate of combination is far slower than displacement from haemoglobin, and it is this difference in rates that brings about an excess of oxygen molecules available for secretion. The counter-current system allows the concentration of free O_2 molecules to build up within the gas gland until there is a net diffusion of gas from the gas gland into the lumen of the swimbladder, against the hydrostatic pressure of the sea.

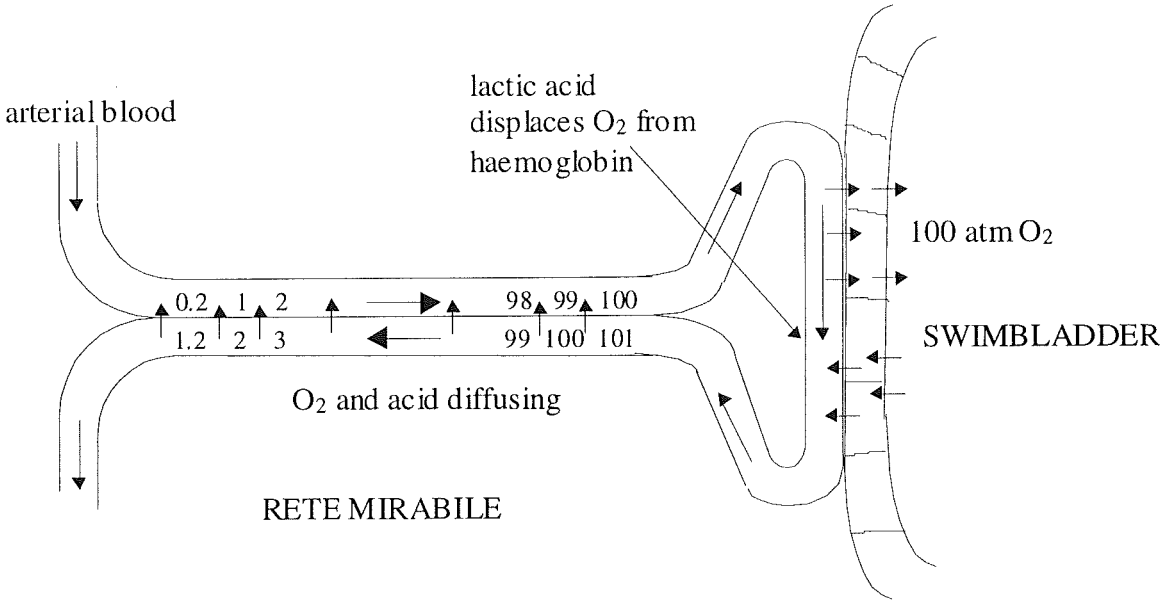

Figure 2.3 Diagram of mechanism whereby O_2 can be secreted into the swimbladder through the countercurrent circulation of the rete mirabile [29].

Gas reabsorption is carried out in one of two ways. Some fish have a valved duct leading to the oesophagus through which gas can escape [29]. Other fish have a closed system with a structure called an oval that acts like a sphincter to open or close some region of the swimbladder wall, so that the region is either exposed to or occluded from the gases. This region has its own blood supply not connected to a rete, so gases can dissolve into the blood and get carried away from the swimbladder.

2.1.5 Sharks

Deep-sea squaloid sharks have attained neutral buoyancy through the development of a large and oily liver. In most animals the liver is around 4-6% of the total weight, but in the shark it may be more than a quarter of the total weight [41]. The liver oil is mainly composed of hydrocarbon squalene, which has a specific gravity of 0.86 and is stored in such quantities that the uplift provided almost eliminates the shark's weight in seawater. It has been suggested that the mass of squalene would have to be controlled to within 1% in order to keep the animal within 0.1% of neutral buoyancy. The *Squalus acanthias* shark responds to changes in its weight by varying the less abundant lipid constituents of the liver oil, and not the amount of squalene [42]. When weights were attached to the shark, the presence of diacyl glyceryl ethers, which are less dense than the triglycerides in the liver oil, increased over two days. This increase in low-density lipids was sufficient to counter the weight increase.

2.1.6 Deep-diving Whales

Whales that dive deeply, like the sperm whale, have large amounts of low-density fats [29], much lower than the fats in shallow-diving whales. Clarke [43] advanced the theory that the spermaceti organ in the head of the sperm whale is used to regulate buoyancy by exploiting appreciable differences in density between the melted and unmelted forms of

the entrained waxes. The theory received much criticism [44-46], but the hypothesis was expanded to greater detail [47,48].

The spermaceti organ makes up the bulk of the head of the sperm whale, and it is filled with a liquid called spermaceti (Figure 2.4). It is a complex mixture containing some triglyceride fats like those found in other mammals and animals. However, spermaceti is composed chiefly (~73.5%) of waxes. These are the esters of fatty acids and monohydric alcohols, which have a much lower specific gravity than the triglyceride fats.

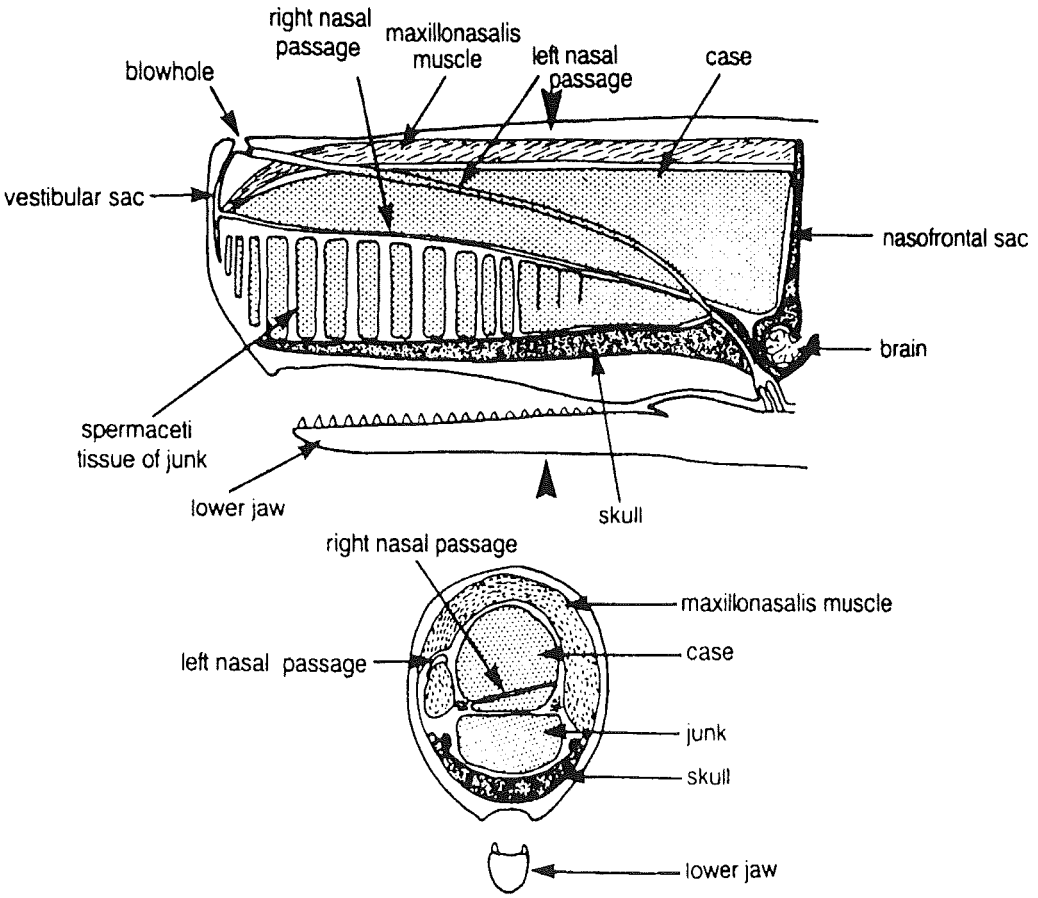

Figure 2.4 The structure of the head of the sperm whale [48].

Spermaceti is a clear, straw-coloured oil at about 30°C, but becomes cloudy if cooled and progressively solidifies and crystallises as the temperature drops. As it solidifies, it contracts and becomes denser. Clarke [47] found that the rate of density increase on cooling is greater at higher pressures. An increase in density of the spermaceti will result in a decrease in the buoyancy of the whale. If the sperm whale could control the temperature of the spermaceti organ and its oil, it could also control its density, and sink or rise with small expenditure in energy.

Clarke suggested that a mechanism might exist for flushing water through the right nasal passage, which, with its expanded sacs at the front and back of the spermaceti organ, would be well fitted to act as a useful heat-exchanger [47,48]. This would cool the spermaceti oil, increasing the specific gravity and causing the whale to become less buoyant. The lungs of the whale are isolated from the surface of the heat-exchanger by a sphincter muscle surrounding the right nasal passage where it joins the left, just before it enters the skull. Having isolated the right nasal passage, it can then be irrigated with water by the action of a larger block of muscle, the maxillonasalis, which can lift the forward end of the case, thus expanding the cavity within the right nasal passage. The cold seawater would cool the spermaceti organ near the passage. Blood flowing past the nasal passage would also be cooled, which could then cool the spermaceti oil further from the nasal passage. Using this method, and also from heat loss through the blubber and skin, the whale could achieve neutral buoyancy in three minutes while diving to a depth of 1000m.

To rise again, the whale would cease to circulate water through the nasal passages [47,48]. In addition, vaso-constriction at the skin surface would cease the loss of heat through the blubber. There would be enough muscle activity to cause heat to accumulate and be transferred to the spermaceti organ via the blood. The whale would then gently rise to the surface.

2.1.7 Seabed Dwellers and Active Swimmers

Although many organisms possess buoyancy devices, others do not and they must therefore remain on the bottom of the ocean or employ some form of muscular effort to maintain themselves at their particular depth. Lobsters, plaice (*Pleuronectes*), rays (*Raia*, selachians) and common octopus have no buoyancy organ so must live at the bottom of the sea [29].

Many organisms from plankton to certain species of shark must swim to keep themselves buoyant. Motile phytoplankton are capable of directed swimming and can control their position in the water column [11]. The barrel in which the amphipod *Phronima sedentaria* lives acts as a propulsion system with an entrance three times the area of the exit. This barrel greatly reduces the energy expended by the amphipod in maintaining its position [49]. This also occurs in individuals of the class Larvacea [50]. Having a foot with two lateral extensions, like wings, supports the spiral shell of the pteropod Limacina retroversa. Rhythmical flapping of the wings effects swimming [50]. The crustacean

Euphausia pacifica is the most negatively buoyant of the midwater crustaceans, and must swim constantly to avoid sinking [51].

Although many species of cephalopod possess buoyancy systems, some squid need to swim actively to prevent themselves from sinking [21]. The squid *Loligo forbesi* has fins at its posterior end that tend to tilt the squid nose down, but the thrust exerted by its jet from the funnel balances the moments. Active swimming is also a way of life for the Ommastrephidae, Enoploteuthidae, Brachioteuthidae and Ctenopterygidae species.

Fish that swim perpetually at high speeds tend to be denser than seawater. Mackerel and tuna never stop swimming, day or night. The bullet mackerel (*Auxis rochei*) swims at an average speed of 0.7m/s in order to generate enough lift from its fins [38]. Tunnies and sharks, such as the blue shark, swim with their pectoral fins extended with a positive angle of attack, so that upward lift acts on them. As these hydrofoils are anterior to the centre of mass, they tend to tilt the snout of the fish upwards. The forward thrust and uplift generated by the tail fin, called the heterocercal tail, balances the moments and allows the fish to swim horizontally. There is a minimum speed at which these fish can swim, under which stalling may occur. For a dogfish this is about 0.24m/s, and 0.6m/s for a skipjack tuna. In general, the more primitive fishes must rely on hydrofoils and propulsive power to maintain their buoyancy, whereas the more advanced organisms have evolved static or passive means to achieve a constant level in the water column [5]. Less energy is expended to obtain neutral buoyancy by these mechanisms than to have to move constantly to attain the required lift.

2.2 Buoyancy Mechanisms of Underwater Vehicles

Over the last century, mankind has attempted to emulate the ability of marine organisms to control their buoyancy and explore the ocean depths. The majority of submersible vehicles built in the 20th century have used a buoyancy system of making adjustments in weight by admitting or expelling seawater from variable ballast tanks [52]. The principle is similar to the rigid buoyancy chambers of the *Nautilus*, *spirula* and cuttlefish, by varying the gas and liquid contents. Mankind has managed to go one step further by being able to achieve rapid descents and ascents with the aid of sophisticated pumps. However, variable seawater ballast systems are restricted to shallow and mid-depth ranges because of the difficulty of pumping or blowing against high hydrostatic pressures [52]. Variable displacement systems using inflatable bladders are also unsuitable for deep ocean depths due to the high pressures. Increasing or decreasing the displacement of oil-inflatable/deflatable bladders makes adjustments in buoyancy. Again, active pumping is required to transfer a volume of liquid from an internal reservoir to an external bladder.

An inflatable bladder system was used in the submersible *Alvin* in the 1960's to finely control its buoyancy. It would dive and climb using three manoeuvrable propellers [53]. More recently, bladder systems have been used effectively in underwater profilers and gliders [54,55]. These relatively small torpedo-shaped floats periodically change their buoyancy by pumping fluid from an internal reservoir to an external bladder, thereby increasing float volume and buoyancy. Pumping requires energy from the onboard power

supply, thus limiting the duration that a float can stay in the ocean performing cyclical dives. Researchers [55] looked for ways of using the changes in temperature of seawater at the surface and at depth to somehow power the pump system. They opted for a system similar to that used by the sperm whale. By using a volume of pure hydrocarbon that was solid at deep ocean temperatures, but expanded when melted by surface temperatures [54], they were able to design a heat engine that could store enough energy to pump a volume of liquid to the external bladder of the float (Figure 2.5). The only internal power requirements were the control of the various valves of the pumping system.

Many forms of marine life use low-density materials to offset their more bulkier materials. For example, as explained earlier, many sharks have squalene in their livers that keep them buoyant, and some squid species use ammonium-based coelomic fluid to buoy themselves. Even tiny plankton employ some form of ion-exchange system to keep their internal body fluids light. In 1960 Auguste Piccard, in his bathyscaph *Trieste*, managed to dive into the Marianas Trench of the Pacific Ocean down to 10,916m, the deepest known depth on the earth [56]. It was a large vessel that could hold two men and was buoyed by a large float containing petrol. The fine adjustments to buoyancy were made by slowly releasing the petrol and by dropping weights to keep it just negatively buoyant as it descended.

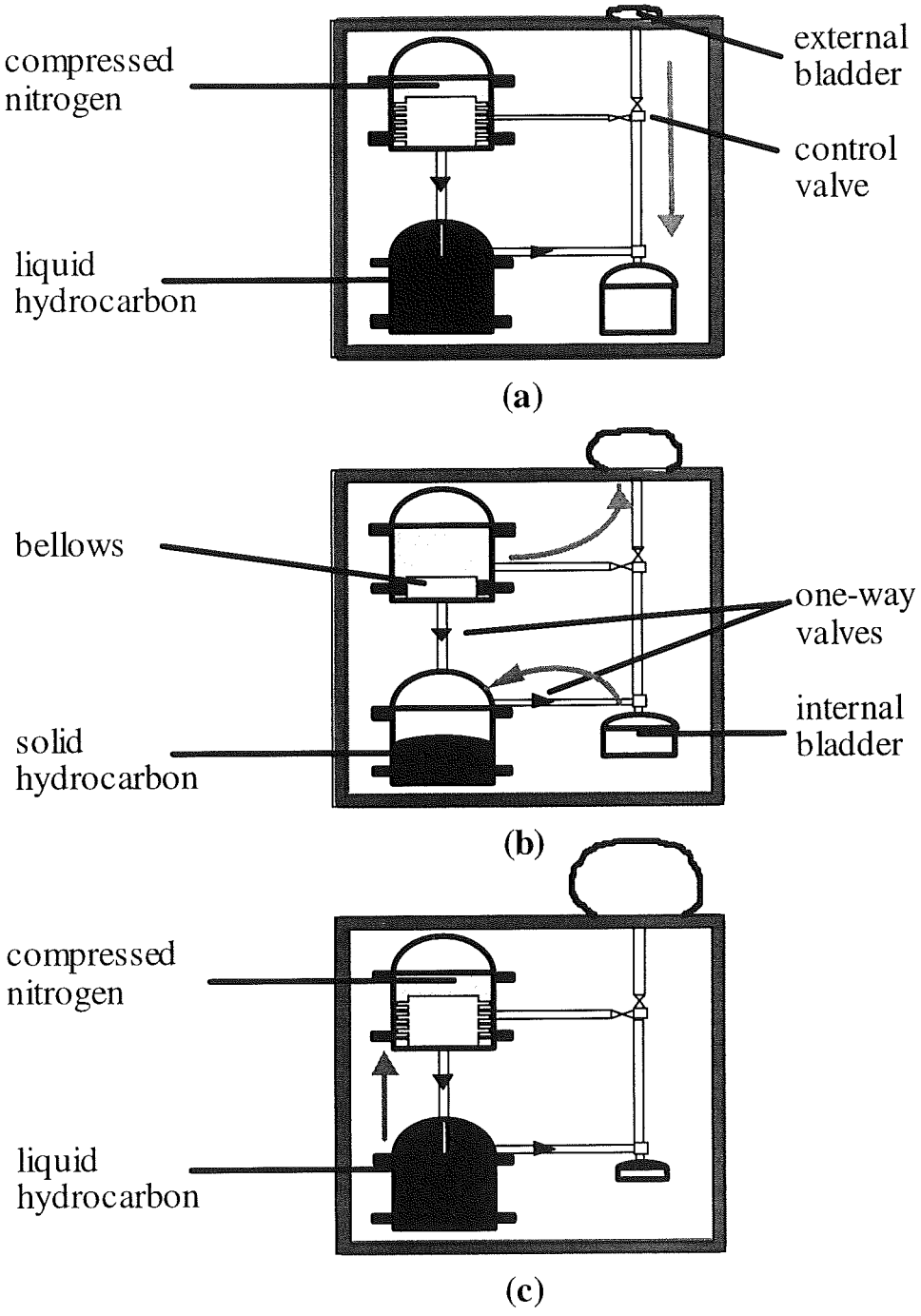

Figure 2.5 The thermal engine of the Slocum glider. (a) To dive, a 3-way control valve is closed, allowing glycol to flow into an internal bladder. (b) The cold temperatures at depth freeze the liquid hydrocarbon into a solid, creating a space that is filled by glycol from the internal bladder. To ascend, the control valve is closed the other way, and compressed nitrogen from the top tank pushes glycol out of a metal bellows into the external bladder. (c) The hydrocarbon melts again, pushing glycol back into the bellows, compressing the nitrogen and readying the glider for the next dive [55].

Also in the 1960's, foam composites and syntactic foams were developed which had low densities, high hydrostatic strength, a bulk modulus almost equal to seawater, and immunity to catastrophic failure. The foams could also be fabricated into irregular shapes and be used as a filler when "foamed-in-place". Since then they have been used in a wide variety of applications such as submersible vehicles, buoys, risers and floatation units [57]. However, the buoyancy provided by foams is passive and static, which is fine for floatation units and buoys, but inadequate for submersibles where other dynamic means are necessary for ascent and descent.

Hydrodynamic planes to facilitate vertical travel in the ocean are being utilised in gliders that use a fixed hydrofoil and the thermal engine described in Figure 2.5 [54]. At the surface the engine deflates the external bladder, giving the glider a negative buoyancy, which is sufficient to point the glider downwards. It sinks and gains speed, but the hydrofoil generates lift on the way and the glider eventually reaches a nadir point and begins to rise again. Meanwhile the thermal engine has been storing energy. The external bladder is inflated and provides a positive buoyancy to help the glider back to the surface.

With costs of running and maintaining large manned and unmanned submersibles remaining high, there is a trend towards the development of smaller, low-cost autonomous vehicles. Researchers are turning more and more to nature to try and mimic the characteristics of fish. One such project is the Robot Tuna and Robot Pike [58], small underwater robots that mimic the swimming actions of the tuna and pike. The buoyancy of these robots has been made neutral using light acetal structural elements. Another

project is concentrating on the swimming behaviour of the lamprey or eel [59]. The undulations of their tails are being imitated by using shape memory alloy wires.

It is the advent of smart materials such as shape memory alloys (SMA's) and polymer gels that could pave the way towards an intelligent buoyancy system for underwater vehicles. A small robotic fish, called MEFiR (Micro Electronic Fish Robot), is using shape memory alloy wires to control the tail movement, and the buoyancy of the device may be controlled by a water bladder utilising the contraction properties of a SMA piston [60]. Elsewhere, a variable buoyancy regulator is being tested using arrays of small hollow tubes ('straws') made of shape memory alloy, which can increase in volume when electrically heated [61]. The 'straws' can withstand hydrostatic pressures of 20 to 30 atmospheres. Another possible buoyancy system is a peristaltic pump using a compliant SMA-wrapped cylinder that would quietly and slowly pump a large volume of ballast seawater [62]. Finally, the great expansions and contractions found with certain polymer gels could be used as actuators to displace water and bring about a buoyancy change. The natural temperature and salinity gradients in the ocean could bring about the volumetric changes [63-64], thus providing a power source for actuation.

2.3 Conclusions

The review of marine organisms has shown that there is a large diversity of natural buoyancy control mechanisms. From the point of view of energy conservation, the more advanced creatures possess relatively passive forms of buoyancy control, but the rate of buoyancy change is quite slow for most of these creatures, sometimes taking days to overcome an excess or deficiency in buoyancy. The less advanced marine animals, the active swimmers, are very energy intensive, but can counteract depth changes relatively quickly. However, for most marine creatures, it is preferable for their survival to maintain a constant level in the oceans. Therefore, it can be difficult to obtain a specific analogue for use in a marine device designed to traverse through many environments and depths.

2.4 References

1. Marshall N. B. 1954. *Aspects of deep-sea biology,* Hutchinson, London.
2. Marshall N.B. 1979. *Developments in deep-sea biology,* Blandford Press, Poole.
3. Wiseman S.W., Reynolds C.S. 1981. Sinking rate and electrophoretic mobility of the fresh-water diatom *Asterionella Formosa*: an experimental investigation. *British phycol. journal* **16**(4), pp. 357-361.
4. Newton C., Potts W.T.W. 1993. Ionic regulation and buoyancy in some planktonic organisms. *Journal mar. biol. ass. U.K.* **73**(1), pp. 15-23.

5. Nybakken J.W. 1993. *Marine biology: an ecological approach* Third edition. Harper Collins College Publishers.

6. Gross F., Zeuthen E. 1948. The buoyancy of plankton diatoms: a problem of cell physiology. *Proceedings of the royal society B.* **135**(880), pp. 382-389.

7. Kahn N., Swift E. 1978. Positive buoyancy through ionic control in the nonmotile marine dinoflagellate *Pyrocystis noctiluca* Murray ex Schuett. *Limnol. oceanogr.* **23**, pp. 649-658.

8. Walsby A.E. 1978. The properties and buoyancy-providing role of gas vacuoles in *Trichodesmium* Ehrenberg. *British phycol. journal* **13**, pp. 103-116.

9. Walsby A.E., Reynolds C.S., Oliver R.L., Kromkamp J. 1989. The role of gas vacuoles and carbohydrate content in the buoyancy and vertical distribution of *Anabaena minutissima* in Lake Rotongaio, New Zealand. *Ergebn. limnol.* **32**, pp. 1-25.

10. Furbish D.JJ., Arnold A.J. 1997. Hydrodynamic strategies in the morphological evolution of spinose planktonic foraminifera. *Geological society of america bulletin* **109**(2), pp. 1055-1072.

11. Richardson T.L., Cullen J.J. 1995. Changes in buoyancy and chemical composition during growth in a coastal marine diatom: ecological and biogeochemical consequences. *Marine ecology progress series* **128**, pp. 77-90.

12. Fisher A.E., Harrison P.J. 1996. Does carbohydrate content affect the sinking rates of marine diatoms? *Journal of phycol.* **32**, pp. 360-365.

13. Moore J.K., Villareal T.A. 1996. Buoyancy and growth characteristics of three positively buoyant marine diatoms. *Marine ecology progress series* **132**, pp. 203-213.

14. Villareal T.A., Pilskain C., Brzezinski M., Lipschultz F., Dennett M., Gardner G.B. 1999. Upward transport of oceanic nitrate by migrating diatom mats. *Nature* **397**, pp. 423-425.

15. Mclaren I.A. 1963. Effects of temperature on growth of zooplankton and the adaptive value of vertical migration. *Journal fish. res. bd. Can.* **20**, pp. 685-727.

16. Haney J.F. 1988. Diel patterns of zooplankton behaviour. *Bull. mar. sci.* **43**(3), pp. 583-603.

17. Hardy A.C. 1953. Some problems of pelagic life, in: *Essays in marine biology (Richard Elmhurst memorial lectures).* Oliver and Boyd, Edinburgh, pp.101-121.

18. McAllister C.D. 1969. Aspects of estimating zooplankton production from phytoplankton production. *Journal fish. res. bd. Can.* **26**, pp. 199-220.

19. Enright J.T. 1977. Diurnal vertical migration: Adaptive significance and timing. Part I, selective advantage: a metabolic model. *Limnol. oceanog.* **22**, pp. 856-872.

20. Mclaren I.A. 1974. Demographic strategy of vertical migration by a marine copepod. *Amer. nat.* **108**, pp. 91-102.

21. Clarke M.R., Denton E.J., Gilpin-Brown J.B. 1979. On the use of ammonium for buoyancy in squids. *Journal mar. biol. ass. U.K.* **59**, pp. 259-276.

22. Denton E.J., Gilpin-Brown J.B., Shaw T.I. 1969. A buoyancy mechanism found in cranchiid squid. *Proc. roy. soc. Lond. B.* **174**, pp. 271-279.

23. Voight J.R., Portner H.O., Odor R.K. 1994. A review of ammonia-mediated buoyancy in squids (Cephalopoda Teuthoidea). *Marine and freshwater behaviour and physiology* **25**(1-3), pp. 193-203.

24. Clarke M.R., Denton E.J., Gilpin-Brown J.B. 1969. On the buoyancy of squid of the families Histioteuthidae, Octopoteuthidae, and Chiroteuthidae. *Proc. r. soc. Lond. B.* **174**, pp. 271-279.

25. Dilly P.N., Nixon M, Young J.Z. 1977. *Mastigoteuthis* – the whip-lash squid. *Journal zool. Lond.* **181**, pp. 527-559.

26. Roper C.F.E., Lu C.C. 1990. Comparative morphology and function of dermal structures in oceanic squids (Cephalopoda). *Smith. contrib. zool.* **493**, pp. 1-40.

27. Roper C.F.E., Young R.E. 1975. Vertical distribution of pelagic cephalopods. *Smith. contrib. zool.* **209**, pp. 1-51.

28. Denton E.J., Gilpin-Brown J.B. 1966. On the buoyancy of the pearly *Nautilus*. *Journal mar. biol. ass. U.K.* **46**, pp. 723-759.

29. Denton E.J. 1974. *Buoyancy in marine animals.* Oxford University Press, London.

30. Ward P.D. 1982. Have shell, will float. *Natural history* **91**(10), pp. 64-69.

31. Ward P.D. 1986. Rates and processes of compensatory buoyancy change in *Nautilus macromphalus*. *Veliger* **28**(4), pp. 356-368.

32. Greenwald L., Ward P.D., Greenwald O. 1980. Cameral liquid transport and buoyancy control in chambered nautilus (*Nautilus macromphalus*). *Nature* **286**, pp. 55-56.

33. Ward P.D., Greenwald L. 1982. Chamber refilling in *nautilus*. *Journal mar. biol. ass. U.K.* **62**, pp. 469-475.

34. Willey A. 1902. Contributions to the natural history of the pearly nautilus. in: *A. Willey's zoological results,* Cambridge University Press, part 6, pp. 691-830.

35. Heptonstall W. 1970. Buoyancy control in ammonoids. *Lethaia* **3**, pp. 317-328.

36. Birchall J.D., Thomas W.L. 1983. On the architecture and function of cuttlefish bone. *Journal of materials science* **18**, pp. 2081-2086.

37. Denton E.J., Gilpin-Brown J.B., Howarth J.V. 1961. *Journal mar. biol. ass. U.K.* **41**, pp. 351.

38. Alexander R. McNeill 1982. *In: Locomotion of animals*, Blackie, Glasgow, Chapter 3.

39. Clarke M.R. 1966. A review of the systematics and ecology of oceanic squids. *Advances in marine biology* **4**, pp. 91-300.

40. Steen J.B. 1970. The swimbladder as a hydrostatic organ. in: *Fish physiology,* Hoar W.S., Randall D.J. (Eds)., *Vol. IV*, Academic Press, New York and London.

41. Bone Q., Marshall N.B. 1982. *Biology of fishes,* Blackie and Sons, Glasgow.

42. Malins D.C., Barone A. 1970. Glycerol ether metabolism: regulation of buoyancy in dogfish *Squalus acanthias*. *Science* **167**, pp. 79-80.

43. Clarke M.R. 1970. The function of the spermaceti organ of the sperm whale. *Nature* **228**, pp. 873-874.

44. Ridgeway S.H. 1970. Buoyancy regulation in deep diving whales. *Nature* **232**, pp. 133-134.

45. Norris K.S., Harvey G.W. 1972. A theory for the function of the spermaceti organ of the sperm whale. in: *Animal orientation and navigation,* Galler S.R., Schmidt-Koenig K., Jacobs G.J., Belleville R.E. (Eds)., NASA Special Publication.

46. Schenkkan E.J., Purves P.E. 1973. The comparative anatomy of the nasal tract and the function of the spermaceti organ in the Physeteridae (Mammalia, Odontoceti). *Bijdragen tot de dierkunde* **43**, pp. 92-112.

47. Clarke M.R. 1978. *Journal mar. biol. ass. U.K.* **58**, pp. 1-71.

48. Bonner N. 1989. In: *Whales of the world*, Blandford, pp. 89-93.

49. Davenport J. 1994. Observations on the locomotion and buoyancy of *Phronima sedentariea* (Forskal 1775) (Crustacea, Amphipoda, Hyperiidea). *Journal of natural history* **28**(4), pp. 787-793.

50. Todd C.D., Laverack M.S., Boxshall G.A. 1996. *Coastal marine zooplankton. Second Edition.* Cambridge University Press.

51. Childress J.J., Nygaard M.H. 1974. The chemical composition of midwater crustaceans as a function of depth of occurrence off Southern California. *Marine biology* **27**, pp. 225-238.

52. Allmendinger E.E. (Ed.) 1990. *Submersible vehicle systems design.* The Society of Naval Architects and Marine Engineers.

53. MacDonald A.G. 1975. *Physiological aspects of deep sea biology.* Cambridge University Press, Cambridge, London, New York, Melbourne.

54. Kunzig R. 1996. A thousand diving robots. *Discover* **April**, pp. 60-71.

55. Webb D.C., Simonetti P.J. 1999. The SLOCUM AUV: An environmentally propelled underwater glider. *11th international symposium on unmanned untethered submersible technology.* pp. 75-85.

56. Gabler U. 1986. *Submarine design.* Bernard & Graefe Verlag, Koblenz.

57. Balmoral hitec buoyancy 1989. *Buoyancy - in depth.* Balmoral Group Ltd.

58. MIT department of ocean engineering, http://web.mit.edu/towtank/www/pike.

59. Jalbert J.C., Kasin S., Ayers J. 1995. Design considerations and experiments of a biologically based undulatory lamprey AUV. *9th international symposium on unmanned untethered submersible technology.* pp. 124-138.

60. Rose C.J., Myler H.R. 1996. A design for a microelectronic fish robot. *1996 Florida conference on recent advances in robotics.* IEEE.

61. McCanna J., Rae G.J. 1997. Shape memory alloy buoyancy regulator for subsea robots. *10th international symposium on unmanned untethered submersible technology.* pp. 206-216.

62. Mide technology corporation, Cambridge, MA 02141. Proposal of research to the Office of Naval Research phase I Awards - N96-161.

63. Molloy P.J., Smith M.J., Cowling M.J. 2000. The effects of salinity and temperature on the behaviour of polyacrylamide gels. *Materials and design* **21**(3), pp. 169-174.

64. Molloy P.J., Cowling M.J. 2000. Volume and density changes in polymer gels in seawater environments. *Journal of materials: design and applications.* Accepted, subject to minor corrections. Resubmitted, May 2000.

Chapter 3 Smart Materials

3.1 Introduction

Intelligent materials are rapidly becoming a focal point for ongoing research and development activities in many engineering applications due to distinct advantages these materials offer when compared to classical ones. Smart materials exhibit interesting behaviour in response to external stimuli, allowing a single piece of material to replace a more complicated device previously needed to perform the same function [1]. They can be defined in many different ways: materials functioning as both sensing and actuation; materials which have multiple responses to one stimulus, in a coordinated fashion; passively smart materials with self-repairing or stand-by characteristics to withstand sudden changes; actively smart materials utilising feedback to adjust their properties; smart materials and systems mimicking biological functions, sometimes in load bearing structural systems [2]. In fact, biological systems can provide significant guidance in the development of smart engineered materials and structures [3], as shown in Chapter 2.

Actuator materials should have the ability to change the shape, stiffness, position, natural frequency and/or other mechanical or physical characteristics of the structures in which they are incorporated, in response to changes in temperature, electric field, solvent composition, etc [4]. The most popular materials being used are controllable fluids, shape memory materials and polymer gels.

3.2 Controllable Fluids

3.2.1 Introduction

The essential characteristic of controllable fluids is their ability to reversibly change from a free-flowing, linear viscous fluid to a semi-solid in milliseconds when exposed to an applied electric or magnetic field [5]. Typically, this change is manifested when the fluids are sheared and a yield stress develops that is more or less proportional to the magnitude of the applied field. Interest in controllable fluids derives from their ability to provide simple, quiet, rapid-response interfaces between electronic controls and mechanical systems [6].

Electrorheological (ER) fluids are suspensions which experience reversible changes in rheological properties such as viscosity, plasticity and elasticity when subjected to electric fields. This is due to the controllable interaction between polarised micron-sized dielectric particles within the ER suspension [2]. Magnetorheological (MR) fluids are the magnetic analogs of ER fluids, consisting of micron-sized magnetically polarisable particles dispersed in a carrier medium such as mineral or silicone oil. An applied magnetic field causes particle chains to form and the fluid becomes a semi-solid which exhibits

viscoplastic behaviour similar to that of ER fluids [5]. Transition to rheological equilibrium for both materials can be achieved in a few milliseconds.

3.2.2 Electrorheological Fluids

Fluids that exhibit a property known as electrorheology were first reported by Winslow [7]. After lapping plate contacts in oil on a semiconductive solid to improve a relay, he discovered a large shear force was necessary to move one plate across the other when an electric field was applied to them. Research and interest continued into the 1960's, but dropped off due to the fluids' instability and lack of commercial applications. However, some researchers began developing applications for ER fluids in the 1980's, and it is now believed that ER materials hold tremendous potential in altering the design and performance of many hydraulic and mechanical devices, such as valves, actuators, damping devices and suspensions [8].

ER fluids contain fine particles, ranging in size from 1 to 100μm across, and are electrically non-conducting organic materials such as starch and cellulose, or inorganic materials such as ceramics, glass or polymers. The particles are suspended in a non-conducting oil, such as mineral oil, silicone oil, or chlorinated paraffin [8]. Producing the ER effect of changing the fluid from a liquid to a solid and back involves the application of an electrical field of between 1000 to 4000 Volts across two electrodes with, typically, a 1mm gap between them. Below 1kV/mm electric field, the ER fluid behaves much like the carrier fluid. Above this level, the particles begin to polarise and align into fibres or

chains that bridge from one electrode to the other. Application of the electric field causes the high-voltage electrode to acquire a net positive charge and the ground electrode to acquire a net negative charge. In response, the positive and negative charges on the particles separate, shifting the positive charge to the particle side nearest the negative electrode and the negative charge to the side nearest the positive electrode [9].

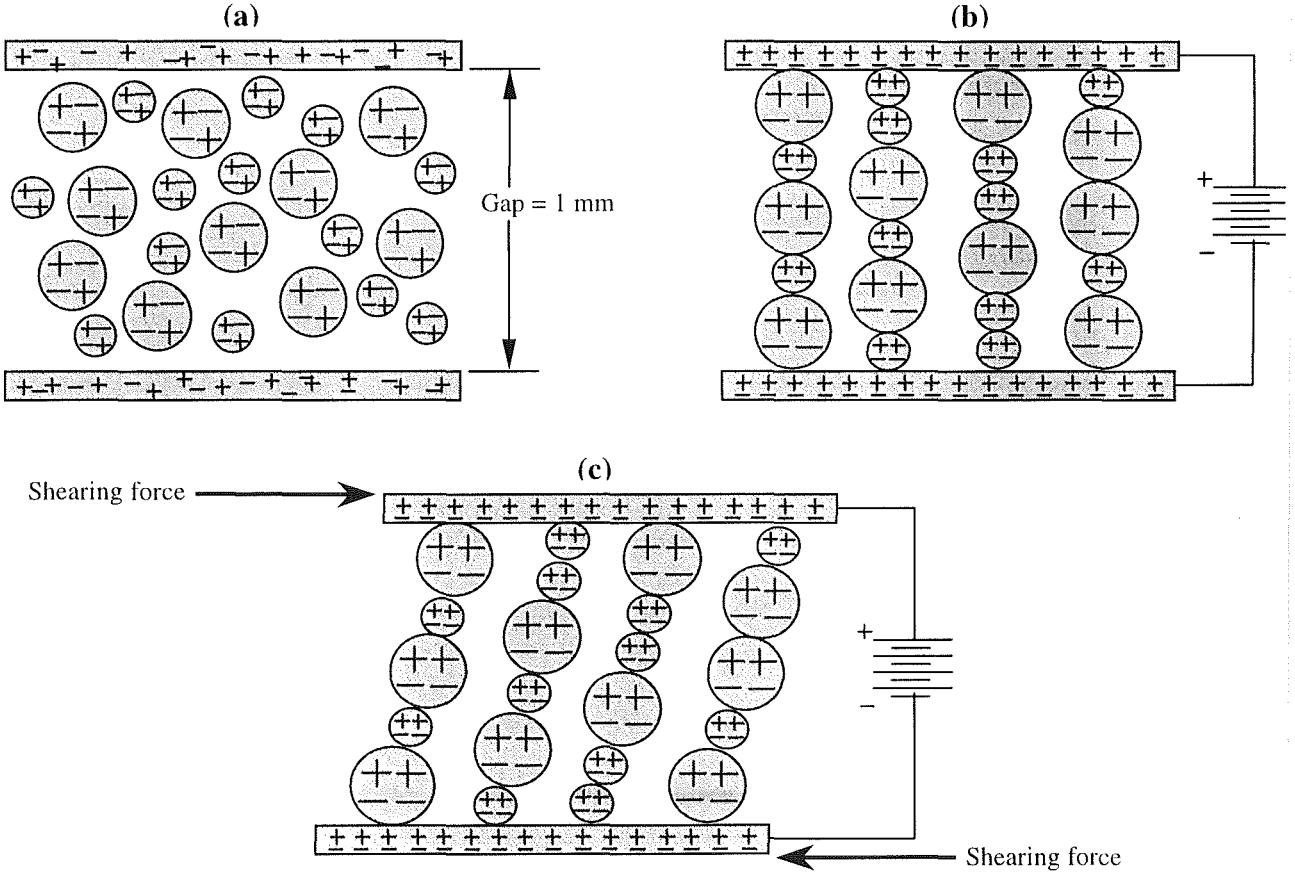

Figure 3.1 (a) Random particle structure in an ER fluid not subjected to an electric field. (b) Organised particle structure when an electric field is applied. (c) Shearing force applied to fibres. [8]

The particles then line up with their positive and negative ends touching in a chain-like formation within the liquid that extends from one electrode to the other (Figure 3.1) [8].

These newly-formed fibres inhibit flow within the liquid, which has now become a gel-like semi-solid between the electrodes. A small deflection of the medium can take place without having the chains fracture (Figure 3.1(c)). A greater force can cause the chains to break, but charges on the particles still attract, so they continually remake and break. The effect is fully reversible and virtually instantaneous. Once the applied field is switched off, the ER material reverts to liquid form (Figure 3.2) [10].

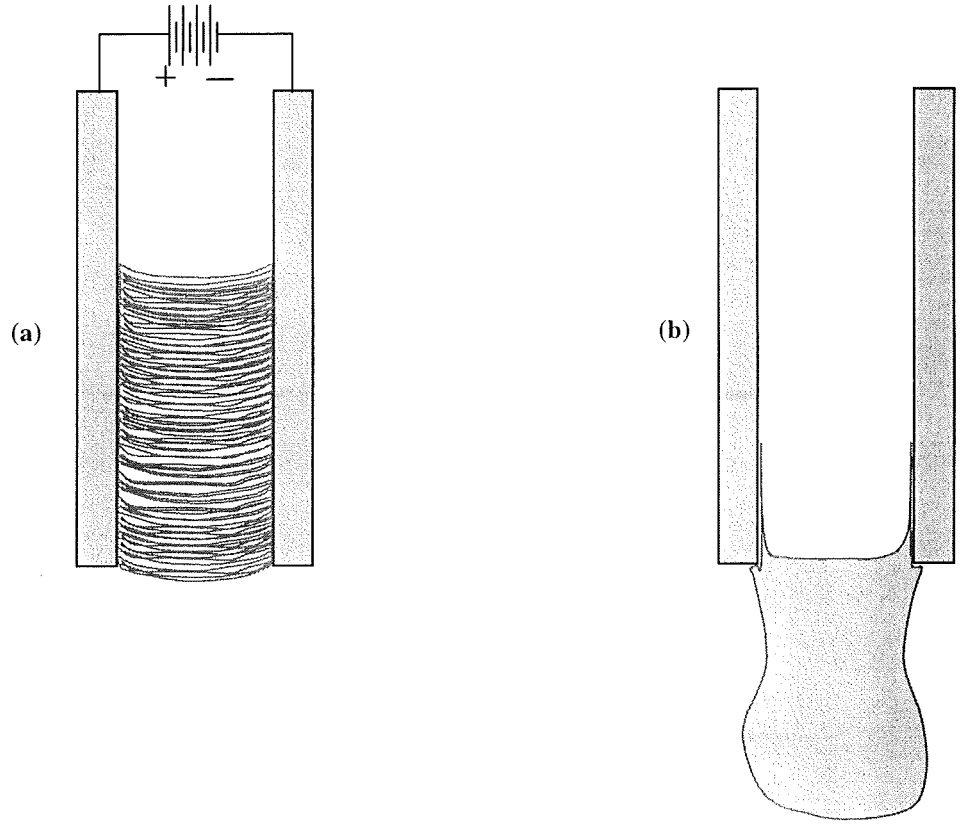

Figure 3.2 (a) ER fluid is retained against gravity when an electric field is applied. (b) ER fluid collapses immediately when the field is switched off. [10]

3.2.3 Magnetorheological Fluids

The initial discovery and development of magnetorheological fluids is credited to Jacob Rabinow [11] in the 1940s, almost concurrent with Winslow's ER fluid work. Dynamic yield strengths exhibited by ER fluids are in the range of 3 to 5 kPa for electric fields of 3 to 5 kV/mm. The maximum strength of the fluid is generally limited by the electrical breakdown strength of the fluid [6]. MR fluids routinely exhibit much greater dynamic yield strengths in the range of 50 to 100 kPa for applied magnetic fields of 150-250 kA/m. The ultimate strength of the fluids is limited by magnetic saturation. Table 3.1 compares ER and MR fluids.

Table 3.1 Comparison of properties of typical ER and MR fluids [6].

Property	ER Fluid	MR Fluid
Yield Strength (Field)	2 – 5 kPa (3 – 5 kV/mm) Field limited by breakdown	50 – 100 kPa (150 – 250 kA/m) Field limited by saturation
Viscosity (no field)	0.2 – 0.3 Pa-s @ 25°C	0.2 – 0.3 Pa-s @ 25°C
Operating Temperature	+10 to +90°C (ionic, DC) -25 to +125°C (non-ionic, AC)	-40 to +150°C limited by carrier fluid
Current Density	2 – 15 mA/cm^2 (4 kV/mm, 25°C) (x10 – x100 @ 90°C)	Can energise with permanent magnets
Specific Gravity	1 – 2.5	3 – 4
Ancillary Materials	Any (conductive surfaces)	Iron / Steel
Colour	Any, opaque or transparent	Brown, black, grey/opaque

MR fluids are stable suspensions of non-colloidal very fine ferromagnetic particles in an insulating carrying medium exhibiting controllable rheological behaviour in the presence of an applied magnetic field [12]. The dispersed ferromagnetic particles are spherical in

shape with a diameter size ranging from 1-10μm. Carbonyl iron powders are preferred and can constitute up to 50% of the total fluid volume. The carrying fluid is usually silicone oil, kerosene, or synthetic oil, which have viscosities in the range 0.01 – 1.0 Ns/m^2 at 40°C.

Operation of the magnetorheological effect is essentially similar to that for electrorheological fluids (Figure 3.3). ER fluids require thousands of volts for operation, while MR fluids operate under a much lower voltage, such as a car battery voltage. They therefore have distinct safety advantages over ER fluids. The generation of greater shear stresses, greater stability and less temperature dependence also shows how MR fluids can be much more favourable than ER fluids [12].

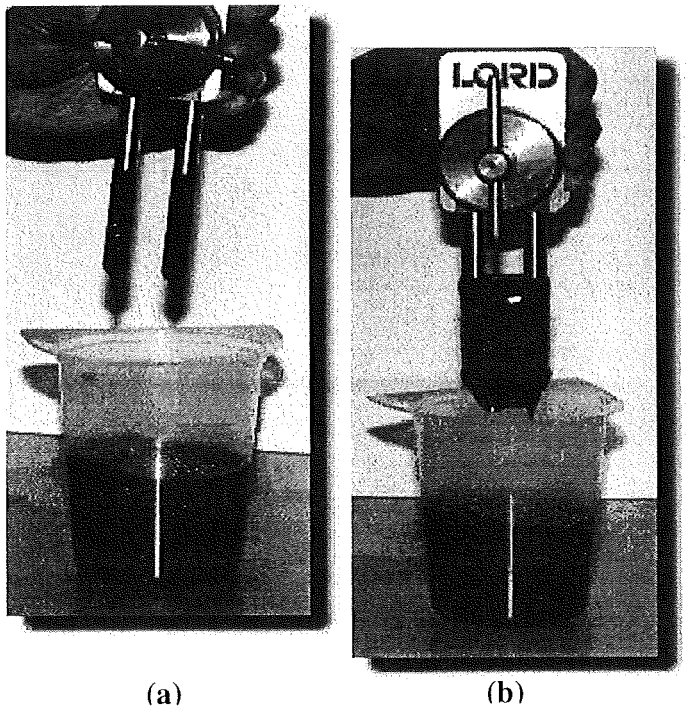

Figure 3.3 (a) When the two electrodes of a switchable permanent magnet are inserted into magnetorheological fluid with no magnetic field, there is no change in fluid properties. (b) The presence of a magnetic field causes the MR fluid to change from a liquid to a semi-solid between the electrodes [13].

3.2.4 ER and MR Applications and Actuators

There are four broad areas where ER and MR fluids have engineering uses: static situations, clutch-based devices, flow-based systems and applications involving damping [14]. Typical static devices include release mechanisms and load-programmable safety catches. The fluid is constrained in a cell made of two electrodes, one fixed and one moving. This offers a high resistance to movement when the applied field is applied. If the applied stress exceeds the yield stress of the fluid or the applied field is removed the 'solid' structure fails allowing an appropriate action to occur.

When controllable fluids are constrained between concentric cylinders or parallel plates, clutch and brake systems can be designed. They rely on the induced shear stress of the fluids to transmit a torque to begin or halt rotation. The MR fluid rotary brake, developed by Lord Corporation [6], is compact, smooth-acting, requires low-power to operate and is capable of high torque at low speed (Figure 3.4). These brakes are being incorporated into Nautilus exercise machines, allowing the users to vary the machines' resistance to accommodate their levels of fitness and desired workout intensity [15].

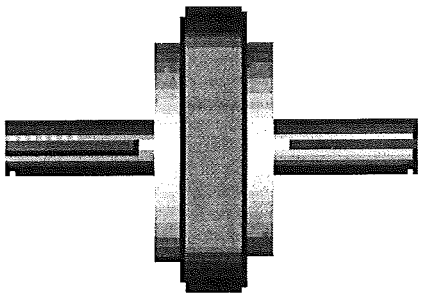

Figure 3.4 The MR fluid rotary brake [6].

Advanced Fluid Systems [16] have also developed a rotary torque device. The magnetic fluid rotary feedthrough is a device that transmits rotary motion into a vacuum vessel with minimal torque requirements. The main components are a magnetic circuit and precision bearings. The magnetic circuit comprises magnets, pole pieces, magnetic fluid, and a magnetically permeable toothed shaft.

In the valve flow mode the ER or MR fluid is pumped down a flow path and the applied field causes an increase in the pressure drop along the flow path [14]. This has applications in pump systems that are effectively valve-less, in that there are no traditional moving parts to regulate fluid flow.

ER and MR fluids are finding the majority of their use in damping and suspension applications. An example of an ER fluid shock absorber is shown in Figure 3.5 [17], using a duct-flow geometry. This configuration is the most common form of ER or MR fluid damper, but squeeze-film geometries (Figure 3.6) have also been designed [6]. These

dampers are being used as automobile suspensions, in engine mounts, and also as bicycle shock absorbers. Advanced Fluid Systems were able to overcome the main limitation of ER fluids, the low yield strength, to develop commercial car and bicycle suspensions [16].

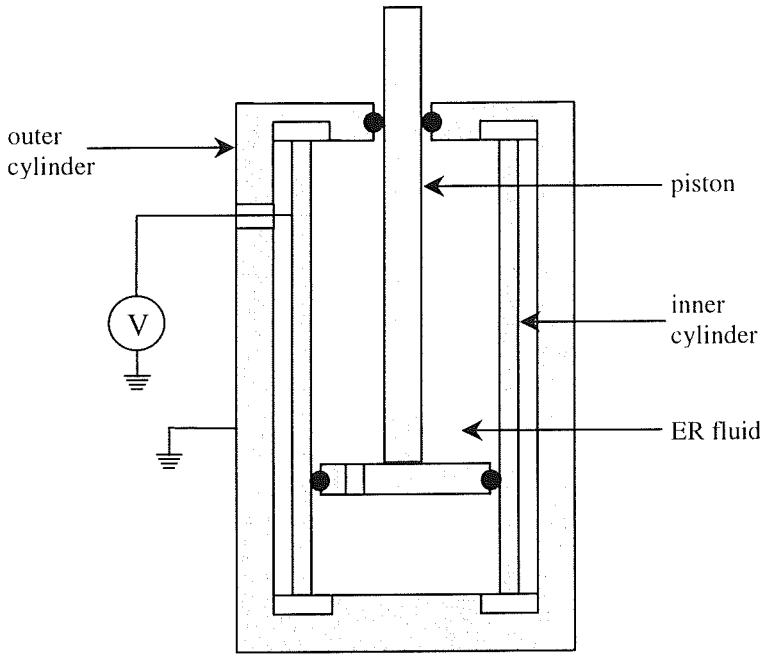

Figure 3.5 ER fluid-filled shock absorber [17].

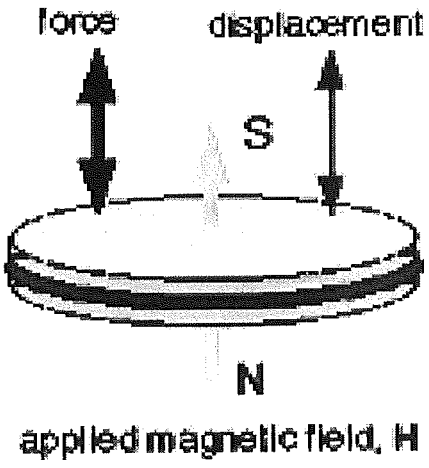

Figure 3.6 Squeeze-film mode using MR fluid [6].

Finally, controllable fluids can be used to control the vibration of cantilever beam arrangements, such as helicopter rotor blades and space structures. Researchers have

looked at ER fluid-filled beams, where the application of an electric field produces an almost linear increase in the fundamental resonance frequency and damping ratio. There are some drawbacks, however. The presence of fluid-filled cavities within a beam is not very desirable in terms of structural efficiency, sealing the fluid in place poses practical difficulties and the need for high voltages in the control loop would present a safety hazard in many environments [18].

3.2.5 Conclusions on Controllable Fluids

Electrorheological and magnetorheological fluids have much potential in controllable viscosity applications, such as the clutch and shock absorbers outlined earlier. They also have potential in variable stiffness elements, where the fluids could be embedded in suitably designed composites. Such elements could be used in underwater vehicles, where the vehicle would possess a hull of controllable compliance, capable of counteracting sea pressures and affecting the overall buoyancy. However, the target applications for this research are small autonomous underwater vehicles with limited power supplies. The large power requirements for activation of ER fluids make them unsuitable for an underwater environment. MR fluids may have more potential, but these also require substantial power supplies and cumbersome magnetic cores.

3.3 Shape Memory Materials

3.3.1 Introduction

Shape memory materials are becoming major elements in intelligent or smart systems and structures due to their unusual, but controllable, properties. These properties include the shape memory effect (SME), superelasticity, large recoverable stroke and high damping capacity. Shape memory materials may sense thermal, mechanical, magnetic or electrical stimuli and exhibit actuation or some pre-determined response, making it possible to tune some technical parameters such as shape, position, strain, stiffness, natural frequency, damping, friction and other static and dynamic characteristics of material systems in response to the environmental changes [19]. A variety of alloys, ceramics, polymers and gels have been found to exhibit SME behaviour. Polymer gels exhibit many other properties and will be examined in detail later in the chapter.

3.3.2 Shape Memory Alloys

Shape memory alloys (SMA's) have the ability to return to a predetermined shape when heated. When the SMA is cold, or below its transformation temperature, it has a very low yield strength and can be deformed quite easily into a new shape. When the material is heated above its transformation temperature it undergoes a change in crystal structure which causes it to return to its original shape. If the SMA encounters any resistance

during this transformation, it can generate extremely large forces, which leads them to be used as very effective actuators. The advantages of SMA's become more pronounced as the size of the application decreases. Large mechanisms may find solenoids, motors, and electromagnets more appropriate. But in applications where the larger actuators cannot be used, shape memory alloys provide an excellent alternative [20]. There are few actuating mechanisms which produce more useful work per unit volume than SMA's.

3.3.2.1 Mechanism of the Shape Memory Effect

In 1951, shape recovery abilities were observed on a bar of gold-cadmium [21], but the expense of gold and the toxicity of cadmium limited further research efforts [22]. A cheaper, non-toxic alloy was developed by the US Naval Ordnance Laboratory (NOL) in 1963 [23] that exhibited greater shape memory effect. The alloy was nickel-titanium and was named Nitinol, combining the alloy constituents and the discovering laboratory. Many other alloys were investigated in the subsequent years that exhibited the shape memory effect. Table 3.2 lists many of them and their transformation temperature and hysteresis [24]. Even so, nickel-titanium, along with copper-zinc-aluminium, remained the alloys of choice because of their strength, low cost and large shape-changing abilities.

Shape memory alloys undergo a change in their crystalline form or arrangement as they are cooled or heated through their characteristic transformation temperature (TTR). For NiTi alloys, this phase change is from an ordered cubic crystal form above its TTR, where

the alloy is in its austenitic form, to a monoclinic crystal phase below the transformation temperature, where the alloy is in its martensitic form [25].

Table 3.2 Alloys which have the shape memory effect [24].

Alloy	Composition	Transformation Temperature Range, °C	Transformation Hysteresis, °C
AgCd	44~49 at % Cd	-190~-50	~15
AuCd	46.5~50 at % Cd	30~100	~15
CuAlNi	14~14.5 wt% Al	-140~100	~35
	3~4.5 wt% Ni		
CuSn	~15 at % Sn	-120~30	
CuZn	38.5~41.5 wt% Zn	-180~-10	~10
CuZnX	**few wt% X**	**-180~200**	**~10**
(X=Si, Sn, Al)			
InTl	18-23 at % Tl	60~100	~4
NiAl	36~38 at % Al	-180~100	~10
NiTi	**49~51 at % Ni**	**-50~110**	**~30**
FePt	~25 at % Pt	~-130	~4
MnCu	5~35 at % Cu	-250~180	~25
FeMnSi	32 wt% Mn, 6 wt% Si	-200~150	~100

The shape memory effect is based on a variant of the 'martensitic' phase transformation of rapidly cooled austenitic steels. All martensitic transformations occur without atomic diffusion; i.e. there is no redistribution of atoms between phases. They are readily reversed when the alloy is reheated to an appropriate temperature [26]. Figure 3.7 shows the effect of a martensitic reaction on the electrical resistivity of steel [27]. As the temperature decreases a point, M_s, is reached at which a new phase begins to precipitate martensitically within the high temperature 'parent' phase. The transformation is complete by the time a slightly lower temperature, M_f, is reached. Upon reheating, the martensitic phase begins to transform back to the parent phase at point A_s, and the reverse

transformation is complete at a higher temperature, A_f. The same terminology is used when describing SMA's, even though the parent phase is not austenitic.

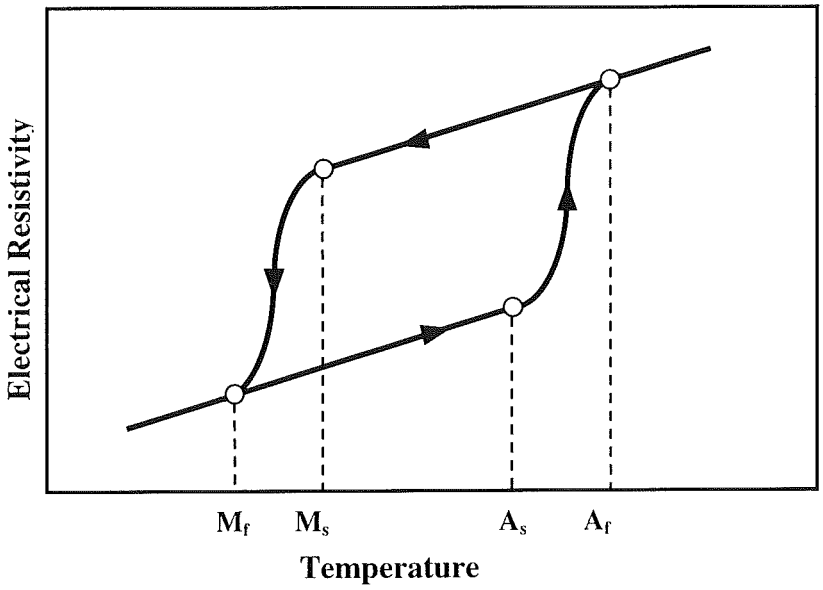

Figure 3.7 Resistivity-temperature curve for a typical martensitic phase transformation [27].

The A_s point occurs at a higher temperature than the M_s point, leading to a temperature hysteresis associated with the transformation. This is due to the need for super-cooling and super-heating to provide thermo-dynamic driving forces for the forward and reverse martensitic transformations respectively. In steels, the degree of hysteresis observed may be more than 200°C, but in SMA's the value typically lies in the range 5-30°C, as shown in Table 3.2.

When a shape memory alloy is deformed below its A_s temperature, it regains its original shape via a reverse transformation by heating the specimen above the A_f point [28]. In Figure 3.8, the mechanism of the shape memory effect is described for a single crystal parent phase (a), initially cooled (b) to a temperature below M_f. Martensites are formed in

a self-accommodating manner [29]. In this process, the shape of the specimen does not change as twins, or dislocations, are introduced to reduce any strain occurring during the formation of martensite. When an external stress is applied to the specimen, as in Figure 3.8(c), the twin boundaries move so as to accommodate the applied stress. If the stress is high enough, twins will align into a single variant of martensite (d) in a process known as twinning or detwinning. The shape memory effect occurs when the specimen is heated above the A_f temperature as each variant reverts to the parent phase in the original orientation. The thermodynamic driving force which causes the material to change to austenite upon heating is very strong – stronger than the yield strength of the alloy – and therefore the forces during shape recovery may be as high as the inherent strength of the austenite material [25].

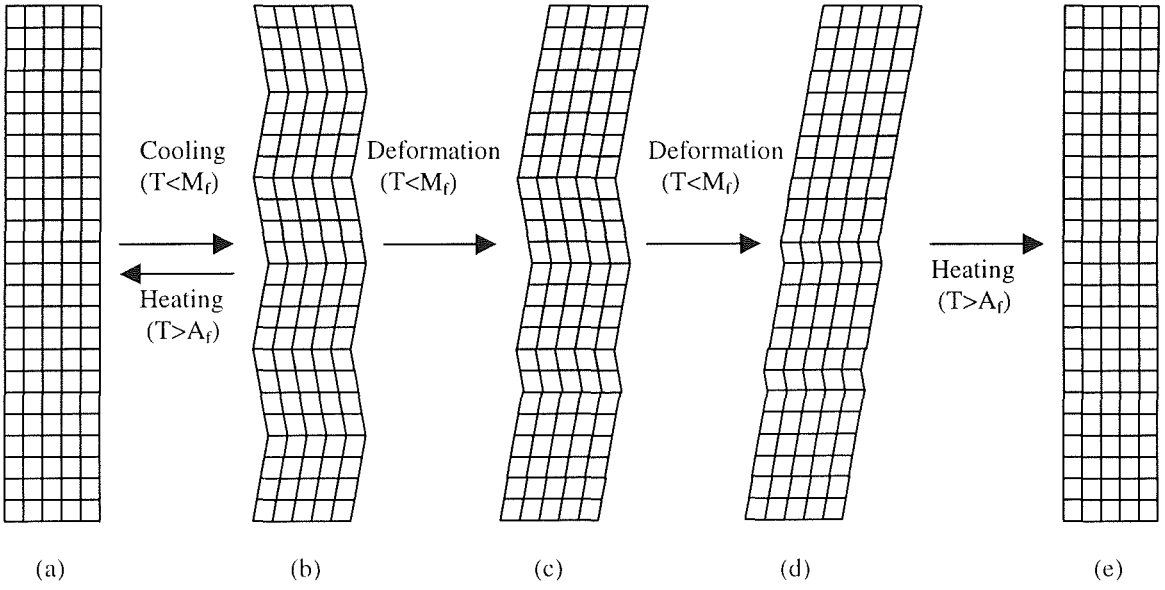

Figure 3.8 Mechanism of shape memory effect: (a) original parent single crystal, (b) self-accommodated martensite, (c-d) deformation in martensite proceeds by the growth of one variant at the expense of the other (i.e. twinning or detwinning), (e) upon heating to a temperature above A_f, each variant reverts to the parent phase in the original orientation by the reverse transformation [29].

The yield strength of the austenite phase of shape memory alloys is much greater than the stress required to deform the martensite phase. Thus, the work needed to deform SMA's at low temperature is much less than the work that can be extracted from them when they are heated. They can, therefore, make very effective actuators, either providing a one-off stroke, or cyclical motion [25].

3.3.2.2 Transformation Temperature

As stated earlier, the transformation temperature (TTR) of a shape memory alloy is the temperature at which the alloy changes from the higher temperature austenite to the lower temperature martensite or vice versa. However, the TTR for an alloy in heating is usually slightly higher than its TTR in cooling. In other words, there is a TTR hysteresis, a difference between the martensite to austenite and austenite to martensite transformation temperatures. Figure 3.9 illustrates this hysteresis for NiTi under constant load [25].

Total elongation and shape recovery during the cycle are represented as ΔL and T_1 is the amount of temperature hysteresis between martensite formation and austenite formation. The hysteresis is generally defined as the difference between the temperatures at which the material is 50% transformed to austenite upon heating and 50% transformed to martensite upon cooling [30].

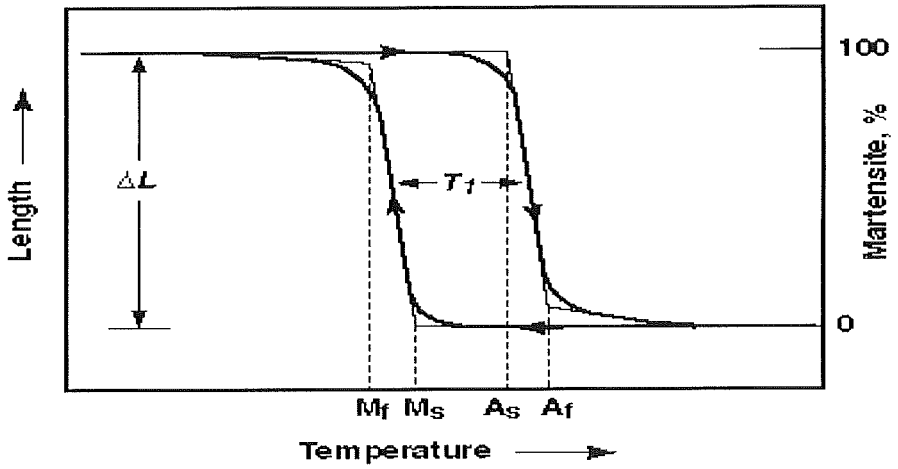

Figure 3.9 Typical transformation curve for NiTi showing elongation and recovery versus temperature under constant stress [25].

Alloy composition is the primary criterion which determines the TTR. For example, most commonly used shape memory alloys are NiTi. With slight changes in the amount of Ni (49-51%) in the alloy, the TTR can be adjusted over the range -50°C to +110°C (Table 3.2). The initial shape setting parameters also affect the TTR. Depending on the size of the NiTi sample, the heat treatment temperature can vary from 400°C to 500°C with times as short as 1-2 minutes up to 30 minutes. Higher heat treatment times and temperatures will increase the actuation temperature of the sample and often give a sharper thermal response (closer M_s-M_f and A_s-A_f values) [31]. However, there is a concurrent drop in peak force and ability for the NiTi element to resist permanent deformation.

Figure 3.9 showed the transformation curve for NiTi under a constant stress. It must be pointed out that the TTR of shape memory alloys is also influenced by applied stress. If a stress sufficient to deform the martensite in a sample is still imposed while the sample is heated, then shape recovery can only occur after enough extra heat energy to move the

sample against the imposed stress is supplied. As a result, the observed TTR increases with increasing applied stress [25]. Taking the example of cooling, martensite begins forming at M_s under no stress. When stress is applied, however, martensite can form above M_s and is called stress-induced martensite (SIM). Above M_s, the stress required to produce SIM increases with increasing temperature. In other words, an increase in applied stress can cause martensite to form closer to the austenitic phase temperatures, which can greatly affect the elongation and shape recovery characteristics, as can be seen in Figure 3.10.

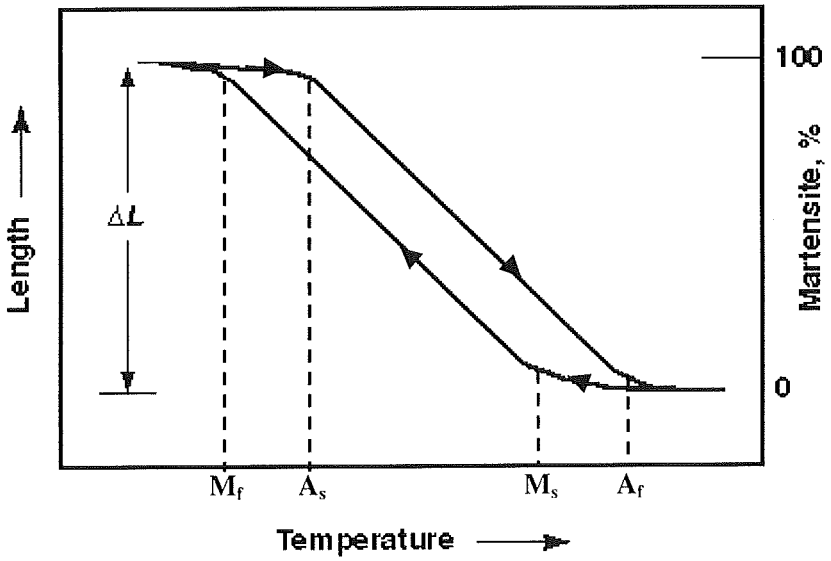

Figure 3.10 Motion versus temperature for NiTi element with increased applied stress, allowing a more gradual shape change with temperature and with improved control function response [32].

The advantages of stress-induced martensite can be utilised in proportional control of SMA devices. In the classic curve of motion versus temperature (Figure 3.9), a sharp shape change occurs over a small temperature range, thus requiring precise temperature control. By allowing the SMA element to work against a greater applied stress, the shape change is less severe, as in Figure 3.10, and a small temperature change results in a less drastic amount of motion from the SMA element [32]. There is a limit to the temperature

at which SIM can be induced, called M_d. This is the point where the applied stress permanently deforms the austenite.

3.3.2.3 Superelasticity

Superelasticity occurs when a shape memory alloy is deformed above A_f, but still below M_d. Stress-induced martensite will form, causing the alloy to strain. However, as soon as the stress is reduced, the alloy will revert back to austenite and recover all strain, again so long as the applied stress does not raise the martensite formation temperature above the critical M_d temperature. This process provides a very springy, 'rubberlike' elasticity in shape memory alloys, as can be seen in Figure 3.11. In the stress-strain curve, the superelastic SMA is seen to deform to large strains at a fairly constant stress and can exert uniform recovery forces over large amounts of springback [25,33].

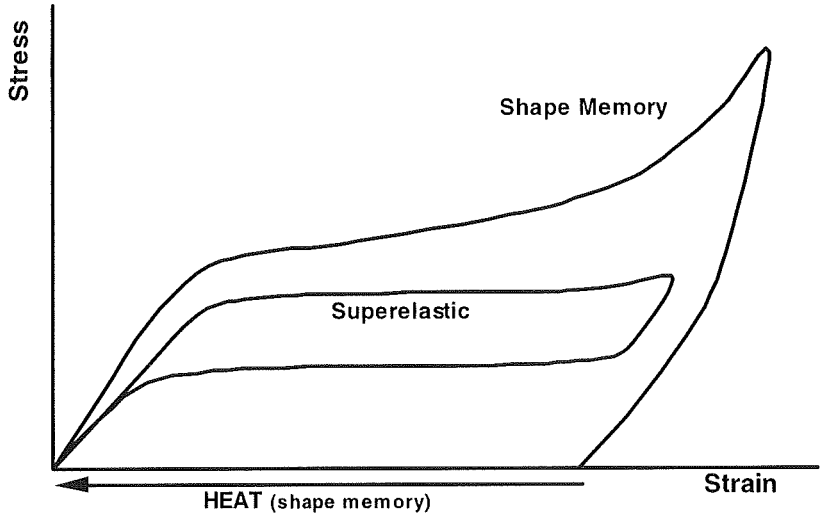

Figure 3.11 Superelastic alloys exhibit almost uniform stresses for large strains with the ability of recovering all strain once applied stress is removed. Shape memory alloys need the application of heat to recover strain [33].

3.3.2.4 Properties of NiTi SMA's

Table 3.3 details many of the properties of NiTi shape memory alloys [34].

Table 3.3 Selected properties of NiTi shape memory alloys [34].

Transformation Properties	
Transformation Temperature	-50 to +110 °C
Latent Heat of Transformation	5.78 cal/g
Transformation Strain	
for single cycle	max 8%
for 100 cycles	max 6%
for 10^5 cycles	max 4%
Hysteresis	15 to 50 °C
Physical and Electrical Properties	
Melting Point	1300 °C
Density	6.45 g/cm^3
Thermal Conductivity	
austenite	0.18 W/cm • °C
martensite	0.086 W/cm • °C
Coefficient of Thermal Expansion	
austenite	11 x 10^{-6} / °C
martensite	6 x 10^{-6} / °C
Resistivity	
austenite	approx. 100 μ-ohms • cm
martensite	approx. 80 μ-ohms • cm
Specific Heat	0.20 cal/g • °C
Corrosion Performance	excellent
Mechanical Properties	
Young's Modulus	
austenite	approx. 83 GPa
martensite	approx. 28 to 41 GPa
Yield Strength	
austenite	195 to 690 MPa
martensite	70 to 140 MPa
Ultimate Tensile Strength	
fully annealed	895 MPa
work hardened	1900 MPa
Poisson's Ratio	0.33
Elongation to Failure	
fully annealed	25 to 50%
work hardened	5 to 10%

The properties outlined in the Table 3.3 represent a broad range of NiTi shape memory alloys, as slight changes in composition, heat treatment temperatures and times, cycling or training history can significantly alter the properties. The transformation temperature is a prime example of this, as mentioned in section 3.3.2.1. The transformation strain for a single cycle of NiTi, 8%, is the maximum recovery strain to expect from a sample, especially in wire form. Most NiTi wires can perform only a few cycles at maximum deformation. The recommended recovery strain reduces to about 4% for applications requiring repeated performance. Some permanent strain (~1%) may occur in the alloy over its lifetime when it is cycled repeatedly, and memory strain may decrease by about 0.5% [25]. For this reason, SMA's for high-cycle devices are usually precycled a few hundred times to stabilise the performance. Otherwise, devices may need to be adjusted and reassembled in order to take up any irreversible deformation that may have occurred in the SMA elements.

The Young's modulus, yield strength and ultimate tensile strength of NiTi SMA's also vary greatly depending on alloy composition, thermal processing and training. Some properties are compared to those of stainless steel in Table 3.4 [35]. Of more interest, however, are the forces and stresses obtainable from shape memory alloys when they undergo their shape recovery with the application of temperature. A NiTi wire can exert up to a maximum of around 600 MPa when heated, but a figure of about one-third the maximum is usually recommended to protect and preserve the memory training [22]. SMA elements used in cycling devices usually need some form of biasing force to return

them to their original shape when cool. The recommended bias force is generally 5-10% of the maximum recovery stress, which is in the range 30 to 60 MPa for NiTi wire. Decreasing the transformation temperature of NiTi shape memory alloy can bring about an increase in the recovery stress obtainable. An alloy with a TTR of about 0°C can have a recovery stress that is double that for an alloy with a TTR of around 50°C or greater [25].

Table 3.4 Comparison of properties of NiTi and ferritic stainless steel [35].

Property	NiTi	Stainless Steel
Recovery Strain	8% max.	0.8%
Effective Modulus	approx. 48 GPa	193 GPa
Ultimate Tensile Strength	approx. 1240 MPa	approx. 760 MPa
Density	6.45 g/cm^3	8.03 g/cm^3
Magnetic	No	Yes
Coefficient of Thermal Expansion	6 to 11 x 10^{-6} / °C	17.3 x 10^{-6} / °C
Resistivity	80 to 100 μ-ohms • cm	72 μ-ohms • cm
Biocompatibility	Excellent	Fair
Torqueability	Excellent	Poor

3.3.2.5 One-way and Two-way Memory

Shape memory alloys need some form of bias force to help them return to their original shape and position after the recovery mechanism has taken place. This biasing can take many forms including springs, a constant force/weight, opposing shape memory alloys, magnets, etc., as long as the bias force is great enough to deform the martensite. Alloys of this nature are referred to as having *one-way memory*. Only the shape of the parent phase (austenite) is remembered.

It is possible for SMA's to also 'remember' the shape of the martensitic phase under certain conditions and exhibit *two-way memory*. It is necessary to ensure that the parent phase always transforms to give an unbalanced population of martensitic variants, even when no external force is applied [26]. The component will then assume a parent phase shape whenever it is at temperatures above A_f, and deform to a martensite phase shape whenever it is at temperatures below M_f. In the absence of an external force acting to distort the martensite variant population, it is necessary to rely on a suitable distribution of internal forces. These can be induced by employing a number of techniques [36]. With all of these techniques, sites of internal stress are created within the high-temperature parent phase, which is essentially homogeneous. Therefore, the alloy has the ability to recover its shape in the reverse transformation upon heating. In addition, these sites of internal stress control the martensitic transformation which is initiated by cooling.

Having an alloy that exhibits two-way memory may seem ideal, especially since biasing mechanisms can then be eliminated from the design of the device. However, two-way memory alloys do come with some limitations. The amount of recoverable strain obtainable from two-way memory is generally about 2%, or less, for high-cycle applications, which is approximately half of the recoverable strain from one-way memory (4%) [37]. When the alloy is cooling to martensite and returning to its original shape, the forces exerted are extremely low. In addition, the two-way memory training can be erased quite easily with a slight overheating of the alloy. Finally, the hysteresis observed in one-way alloys is also present in two-way alloys. For these reasons, it is preferable to make

use of one-way memory, with an incorporated biasing force to produce a two-way actuator. The device can, therefore, exhibit larger strains, higher forces in both heating and cooling, and have excellent long-term stability.

3.3.2.6 Design and Applications of SMA Actuators

Free and Constrained Recovery

When a shape memory alloy is deformed in its martensitic state and then heated to above its transformation temperature, it undergoes a free recovery if nothing interferes with the recovery process. There are few applications for this mechanism, as the alloys are most useful for generating actuation forces. However, some applications have successfully used free recovery, including self-erecting space antennae [38], spectacle frames that return to their prescribed shape when dipped in hot water [39], and blood clot filters [40] and vascular stents that open, once they are inserted, due to the body temperature of the patient [41].

The stress-strain curve of free recovery for NiTi is shown in Figure 3.12 [42]. The associated strain-temperature curve is shown in Figure 3.13. The shape memory alloy is deformed to a total strain, ε_t, at a temperature, T_d, which is below the transformation temperature. When the deformation stress is unloaded, there is a small amount of recovery to ε_p, the apparent plastic strain. The alloy then undergoes a strain recovery as it

is heated through its transformation temperature to a final strain of ε_f [42]. The strain has not returned fully to zero, due to some permanent strain. As mentioned earlier, up to 1% permanent strain may occur in NiTi alloys over the first few hundred cycles, along with some loss of memory strain.

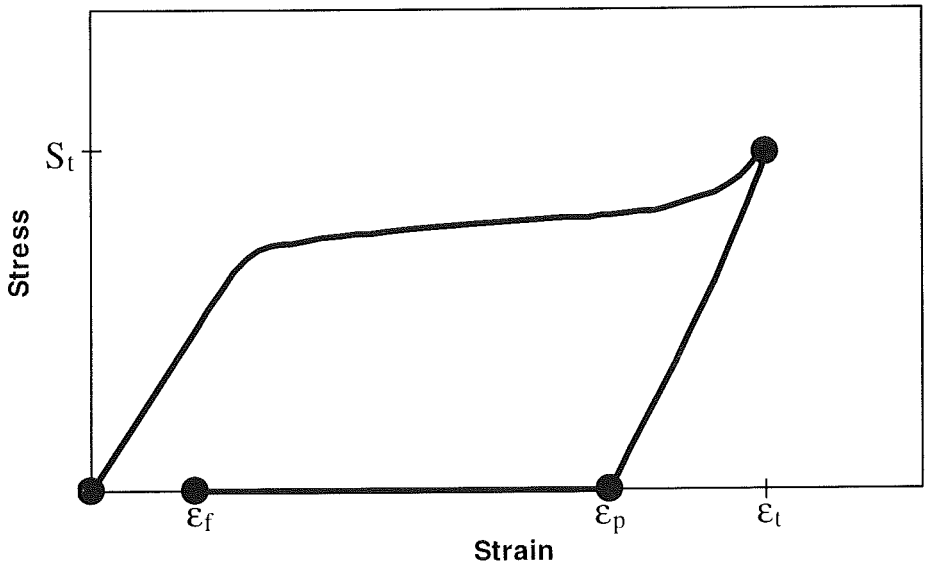

Figure 3.12 The stress-strain curve of free recovery for NiTi, showing deformation to ε_t, unloading to ε_p, and recovery to ε_f. [42].

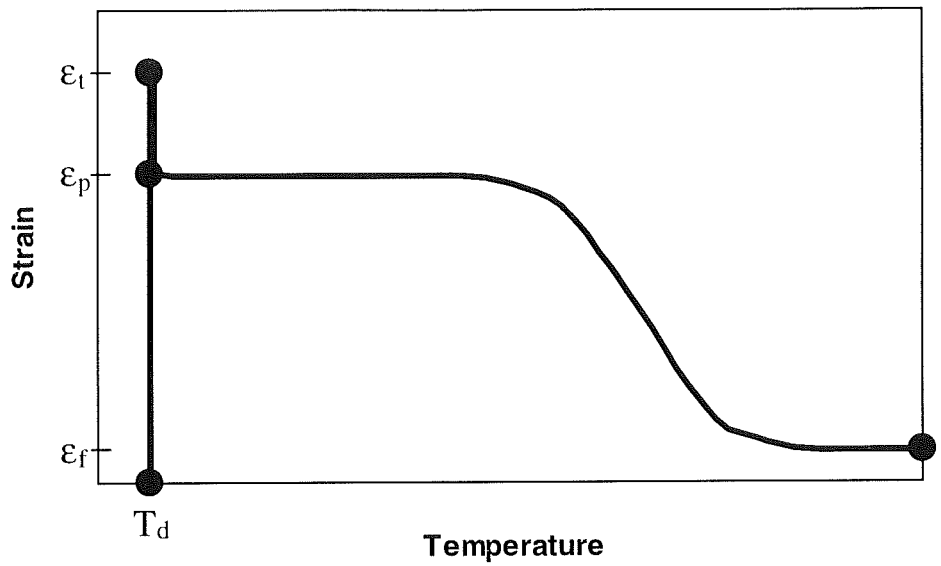

Figure 3.13 The strain-temperature curve of free recovery for NiTi, showing deformation, unloading, and then heating, with associated recovery to ε_f. [42].

The amount of recoverable strain, ε_r, defined as $(\varepsilon_p-\varepsilon_f)$, is influenced by the total strain, ε_t. As ε_t is increased, ε_p and ε_f also increase, but not at the same rate. The effect is that the recoverable strain, ε_r, increases as total strain is increased, but up to a maximum. It then decreases as permanent slip begins to impede the reversible deformation accommodated by twin boundary movement [42]. The maximum recoverable strain for NiTi alloys is around 8%.

A good example of constrained recovery is the Cryofit® hydraulic coupling ring made by Raychem [43, 44]. These couplings constitute the largest single use for shape memory alloy to date [25]. The NiTi alloy ring has a TTR of about -100°C and is expanded below this using liquid nitrogen to fit around the two tubes that are to be coupled. As the coupling ring warms to room temperature it recovers to a smaller diameter and holds the tubes tightly enough to form a high integrity seal at all temperatures above -75°C.

Figures 3.14 to 3.16 show the mechanism of constrained recovery in the form of stress-strain, strain-temperature and stress-temperature curves, respectively [42]. In this case the first parts of the curves are similar to free recovery in that the alloy is deformed below the TTR to a total strain of ε_t. As before, the alloy is unloaded to ε_p and heated to recover the strain. However, during strain recovery the alloy contacts a surface, such as the tubes being coupled by the Cryofit® rings, and no further recovery strain is possible. This point is denoted as ε_c, the contact strain point. There is, therefore, an unresolved recovery strain defined as $(\varepsilon_c-\varepsilon_f)$, the additional strain that could have been recovered if the recovery had been free [42]. A recovery stress is generated at the point of contact that reaches a maximum at σ_r.

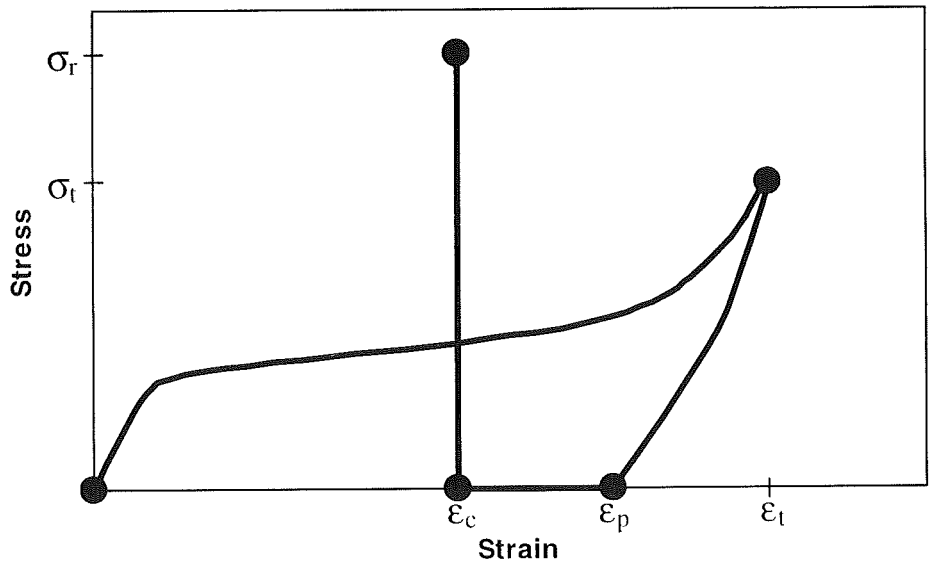

Figure 3.14 The stress-strain curve of constrained recovery for NiTi, showing deformation to ε_t, unloading to ε_p, and recovery until constraint at ε_c. A recovery stress is then generated that reaches a maximum at σ_r [42].

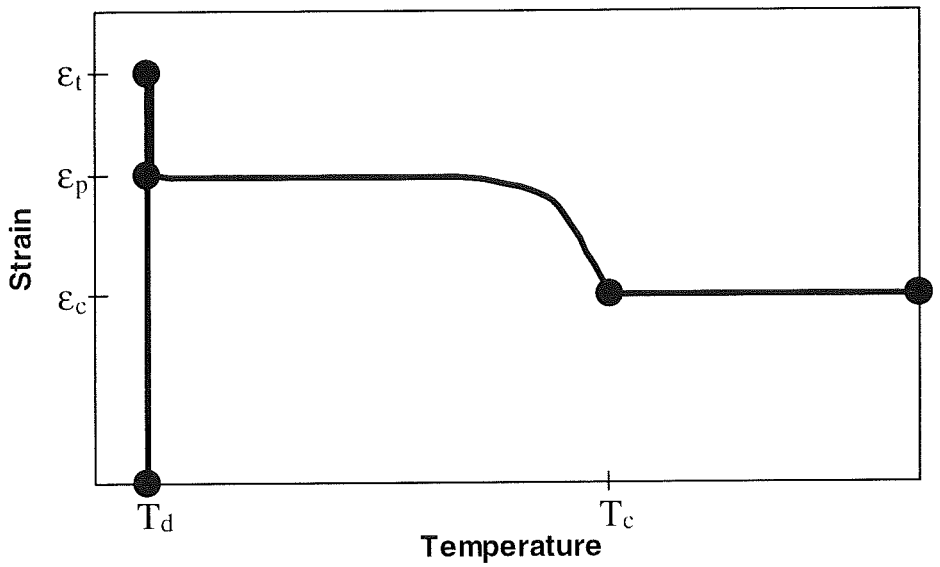

Figure 3.15 The strain-temperature curve of constrained recovery for NiTi, showing that recovery is prevented at the contact strain ε_c. [42].

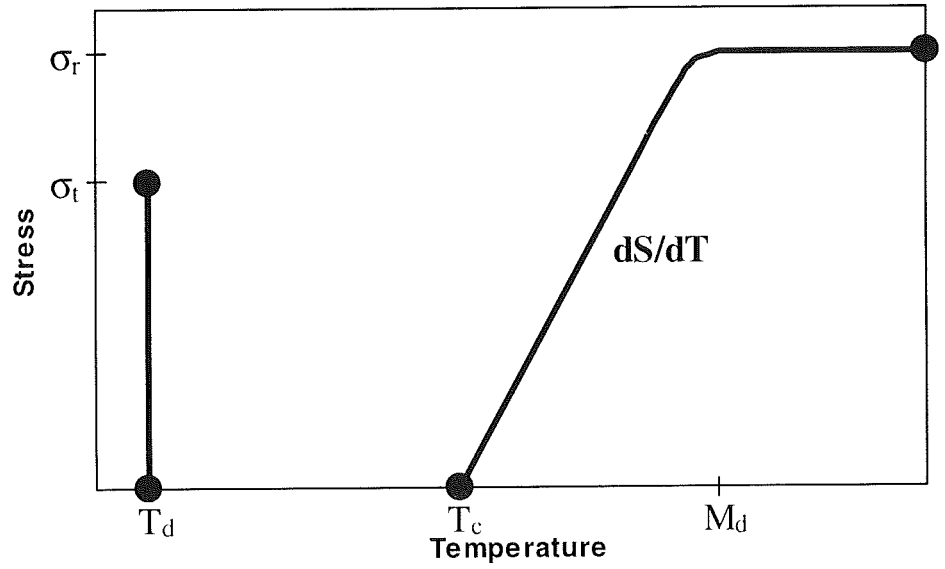

Figure 3.16 The stress-temperature curve of constrained recovery for NiTi, showing, initially, the deformation stress and unloading at T_d. At contact, the recovery stress increases linearly to a maximum, σ_r, at the M_d temperature [42].

With free recovery, there is a recovery strain but no recovery stress, and with constrained recovery, there is a recovery stress but no recovery strain. Work production devices incorporating SMA elements recover against a stress to do work, such as a NiTi wire or spring contracting to lift a mass. Therefore, there is a recovery stress and strain involved. When the alloy cools, the applied stress from the mass is usually enough to deform the wire or spring to return to the shape before heating. Figure 3.17 outlines many of the ways of creating effective bias force mechanisms against shape memory wires or springs [22].

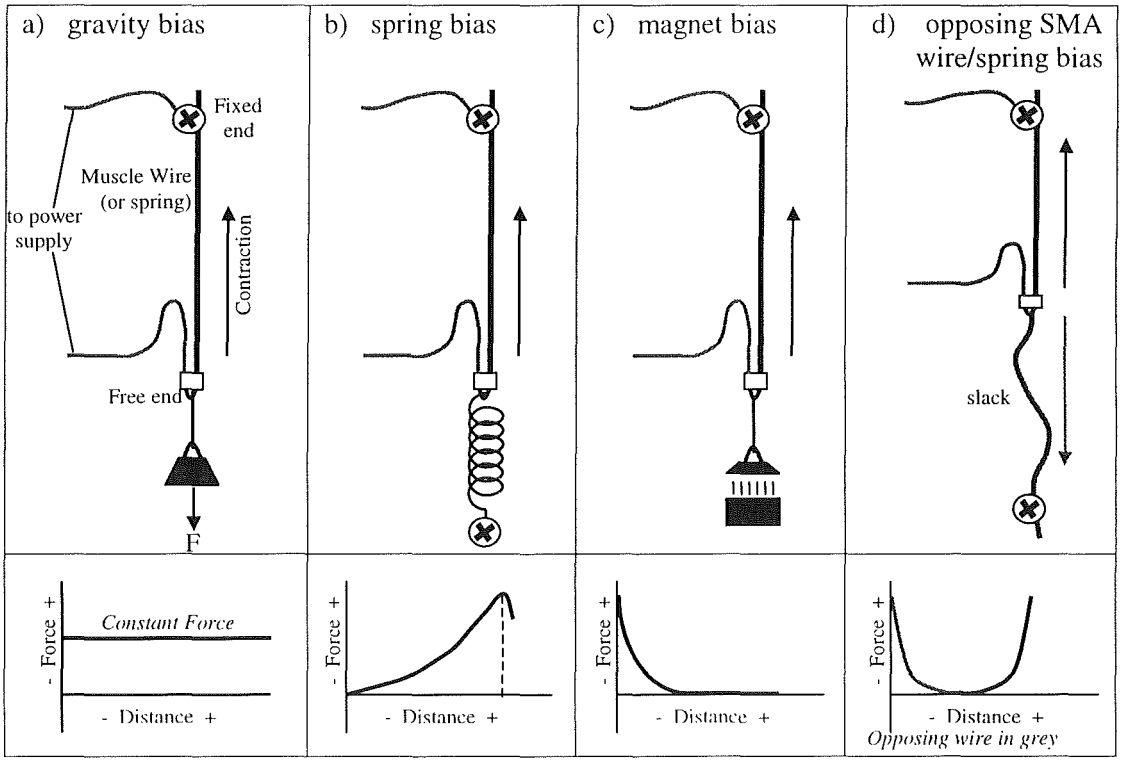

Figure 3.17 Bias force mechanisms for SMA wires and springs [22].

As with free and constrained recovery, there are characteristic stress-strain and strain-temperature profiles for work production using bias mechanisms (Figures 3.18 and 3.19) [45]. The shape memory alloy is initially deformed to ε_t, as with free and constrained recovery, and unloaded to ε_p. This time, however, a bias stress, σ_0, is then applied to the alloy to strain it to ε_m, denoted the martensitic strain. Heating causes the alloy to recover against the bias mechanism to an austenitic strain, ε_a. Cooling allows the bias mechanism to deform the alloy back to the point ε_m. Note that the bias mechanism in the figure is a constant force, hence no difference in stress in heating or cooling. The profile using a bias spring would have austenitic and martensitic stress points, σ_a and σ_m, forming a slope equal to the spring constant of the bias spring.

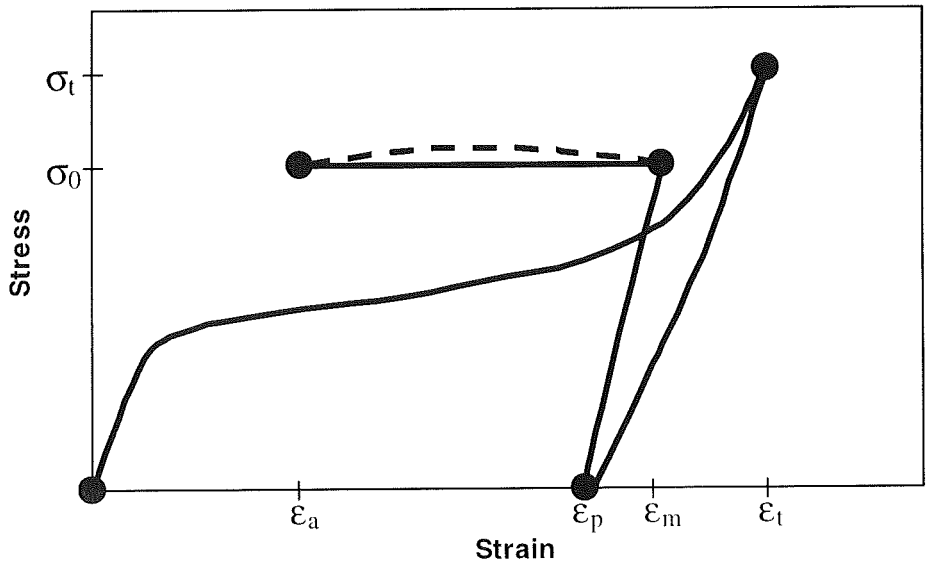

Figure 3.18 The strain-strain curve of work production of NiTi alloy, showing deformation, unloading, loading to the applied bias stress, and heating to recover to ε_a. Subsequent cooling (dashed line) returns the deformed shape, ε_m. [45]

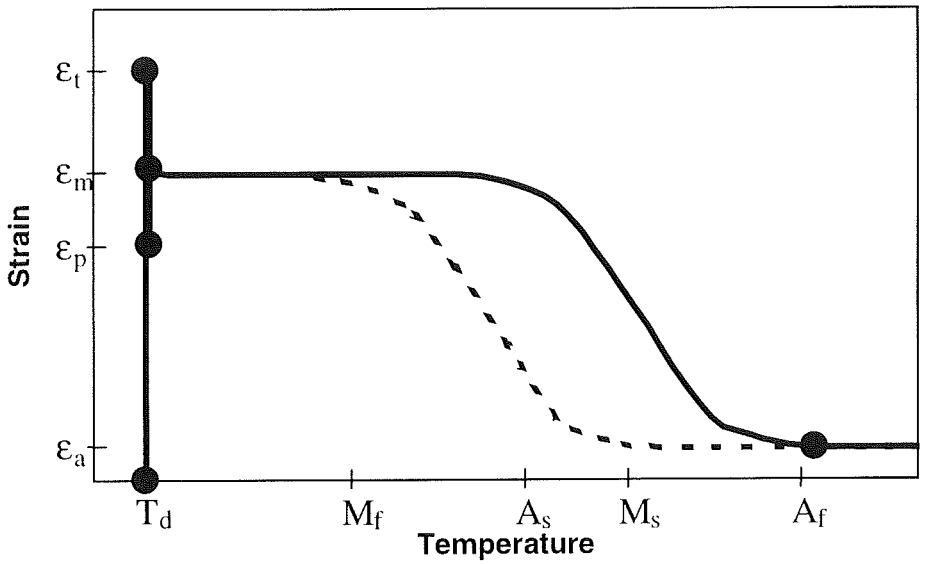

Figure 3.19 The strain-temperature curve of work production of NiTi alloy, showing the four transformation temperatures. [45]

With the possible exception of straight wire, the most popular and useful form of NiTi shape memory alloy for actuators is helical coil springs. Such springs can be used either in extension (tension) or compression, can provide an impressively large stroke, and may be designed to exert significant forces [46]. This can be illustrated by a comparison between the shape recovery of a straight wire and a spring whose closed length is the same as the wire. A straight wire of 30mm length and 1mm diameter exhibiting a 4% strain recovery has a stroke length of only 1.2mm, while an 8mm diameter helical coil, using 30 turns of 1mm wire, will have a stroke of 30mm [47]. This is because the SMA spring has an actual wire length of about 750mm. An SMA spring can, therefore, exhibit a greater stroke to length ratio. If the same 30mm wire was made into a spring of 2.5mm diameter, its closed length would be only about 6mm while exhibiting the same 1.2mm stroke. SMA springs, therefore, are useful where space is at a minimum.

An extension spring provides a pulling force by contracting when heated to the high-temperature austenitic state. When the spring is being trained for memory, it is constrained in its close-coiled position on a mandrel and given its heat treatment [48]. All deflections in both austenitic and martensitic states are measured with respect to this closed configuration (Figure 3.20). The same applies to SMA compression springs, which are trained to extend to an open configuration when heated. All deflections are measured with respect to this open (austenitic) state. As with NiTi wire, hysteresis is also present in NiTi springs, and is dependent on alloy composition and applied stress level.

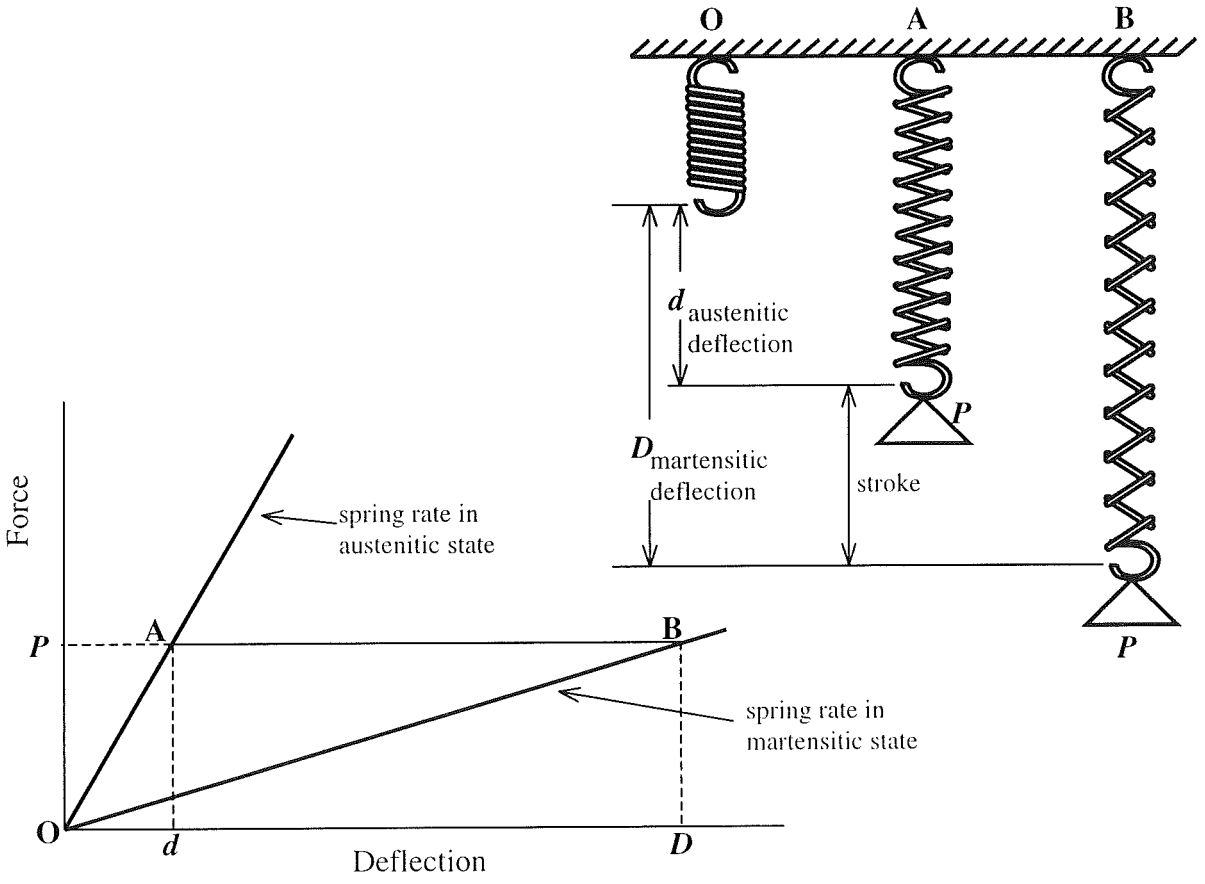

Figure 3.20 At low temperature, a NiTi spring is loaded along line ***OB***. At high temperature, the spring contracts to point ***A*** with a deflection ***d*** and a net motion or stroke of ***(D-d)***, thus performing work equal to ***P(D-d)***. When the spring is again martensitic, the load extends the spring to point ***B***, resetting it for another contraction. [48]

The formulae for conventional spring design are also used when designing shape memory alloy springs [49]. The effective shear modulus, however, is not constant. The change in shear modulus of NiTi springs going from the high temperature phase to the low temperature phase is approximately 300% [47]. In normal spring design, the only requirement is to obtain the relationship between load and deflection, whereas with SMA springs the change in deflection as a function of temperature must also be calculated. The following formulae are used [47]:

Spring deflection

$$\delta = \frac{8PD^3 n}{Gd^4} \qquad (3.1)$$

Shear strain

$$\gamma = \frac{\delta d}{\pi n D^2} \qquad (3.2)$$

Torsional Shear stress

$$\tau = \frac{8PD\kappa}{\pi d^3} \qquad (3.3)$$

Wahl stress correction factor

$$\kappa = \frac{4C-1}{4C-4} + \frac{0.615}{C} \qquad (3.4)$$

Shear modulus

$$G = \frac{\tau}{\gamma} \qquad (3.5)$$

Spring index

$$C = \frac{D}{d} \qquad (3.6)$$

Nomenclature

δ = deflection, mm

P = load, N

D = mean diameter of spring, mm

d = wire diameter, mm

n = active turns

G = shear modulus, MPa

γ = shear strain

κ = Wahl correction factor

C = spring index

τ = torsional shear stress, MPa

The other parameter to take into account when designing two-way actuators is the nature of the biasing mechanism. In Figure 3.20 this is a constant force applied by a mass, resulting in a stroke of zero slope. In most practical applications, however, a conventional steel spring is used to deform the SMA spring at low temperature. The SMA spring works against an ever increasing force from the bias spring (Figure 3.21) [47], which is shown with a negative slope as it is opposing the SMA spring. This mechanism, though very simple, has the problem that large operational strokes cannot be achieved. As the SMA spring extends, the recovery force available diminishes, while the bias force increases, leading to a rapid decrease in the effective force of the mechanism [50]. The SMA spring and bias spring are balanced in both high and low temperature states at point **A** and **B**, respectively. The two-way motion is observed as a stroke distance **D**. If the actuator operates against an external force, $\mathbf{P_1}$, the stroke is proportionally shortened to $\mathbf{D_1}$ at point **C** [47].

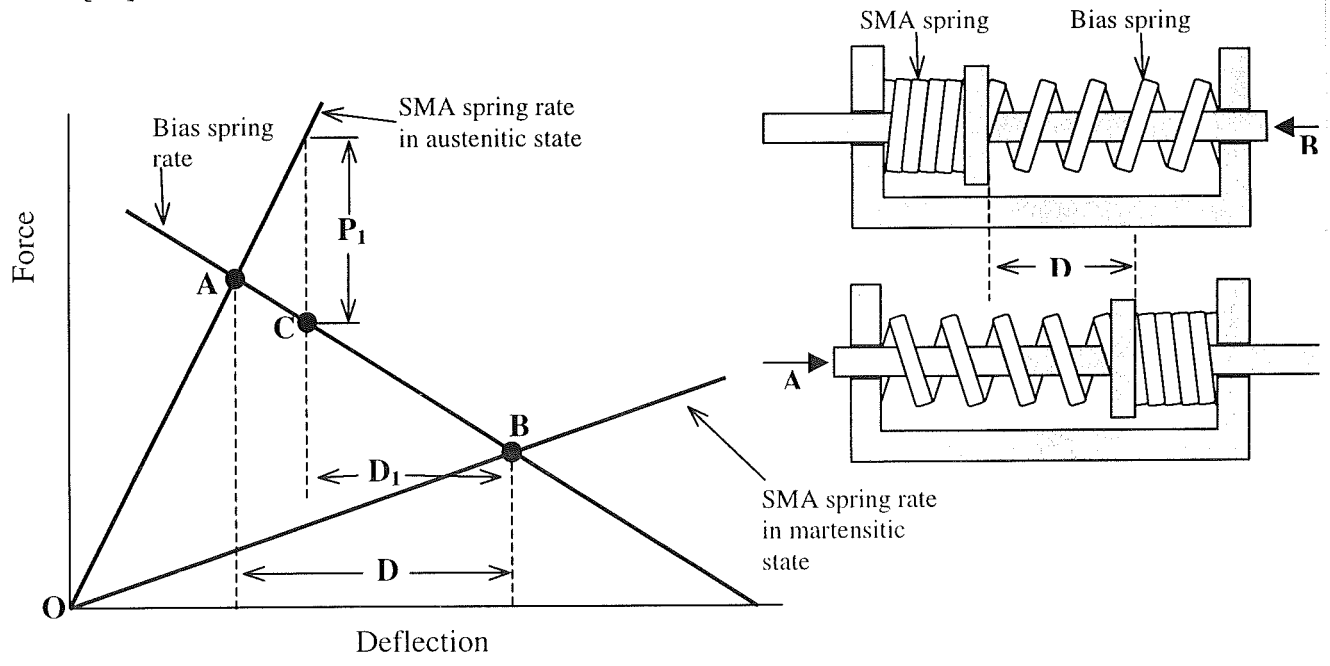

Figure 3.21 Two-way SMA actuator with a spring bias and associated force-deflection diagram. [47]

Some trial and error may be involved when determining the appropriate bias spring for a two-way actuator, to give the most effective force and stroke outputs This will depend on whether a high strain and low stress is desired, or a low strain and high stress. In general, the bias spring is initially chosen to have a spring constant roughly equal or slightly greater than the low-temperature SMA spring constant [47], just enough to reset the SMA spring and give the largest stroke possible. The effects of higher spring rates on stroke, output force, temperature response and hysteresis can then be determined.

Applications in Underwater Technology

Shape memory alloys are opening new horizons in underwater vehicles and actuators in terms of actuation simplicity, compactness and miniaturisation potential. They have some important advantages for use in underwater systems [51]:

- they can be rapidly cooled by the surrounding water, greatly decreasing their cycle time, although power input requirements are 20 times higher for SMA elements with no insulation [52];
- three-dimension movement is possible with suitable arrangement and activation of groups of SMA wires or springs;
- SMA springs can exhibit large deformations relative to their length;
- in well-designed configurations, the forces they generate may be distributed over a large surface area;
- they only require a thin electrical connection, allowing a greater degree of autonomy and relatively convenient control.

One area where SMA's are finding use is in the propulsion of small biomimetic vehicles, attempting to mimic the natural undulatory fin motion of fish. A simple hydrofoil consisting of forward and aft fibreglass sections connected by an elastomeric mid-section uses SMA wires to deflect the aft section (Figure 3.22) [53].

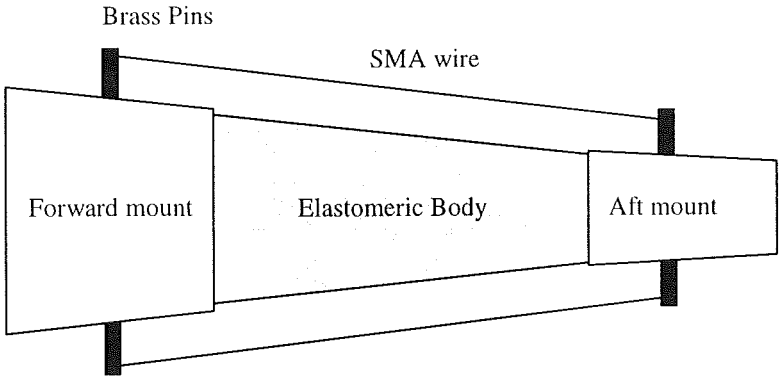

Figure 3.22 Side profile of hydrofoil with shape memory alloy wire actuators. [53]

Controlled heating and cooling of the SMA wires generates bi-directional bending of the elastomer, which in turn deflects or oscillates the trailing edge of the hydrofoil. The SMA actuators are able to deflect the trailing edge by ±5° at rates as high as 2 Hz. This is for full transformation of the SMA wires. When only partial transformation is used, the amount of fin displacement is reduced, but frequencies as high as 10 Hz may be attainable, which may give a greater thrust than slower, but larger tail actions [53].

Another configuration for a hydrofoil is shown in Figure 3.23 [54]. The linear actuators proposed for the system are SMA springs, because of their high stroke to length ratio. They would be arranged in opposing pairs connected to the corners of the foil, roughly perpendicular to the face, and also connected to the frame of the vehicle. The arrangement

and actuation of the various SMA elements can be used to pitch the foil forwards, or send it sideways. Reactive polymer gel actuators have also been proposed for the design.

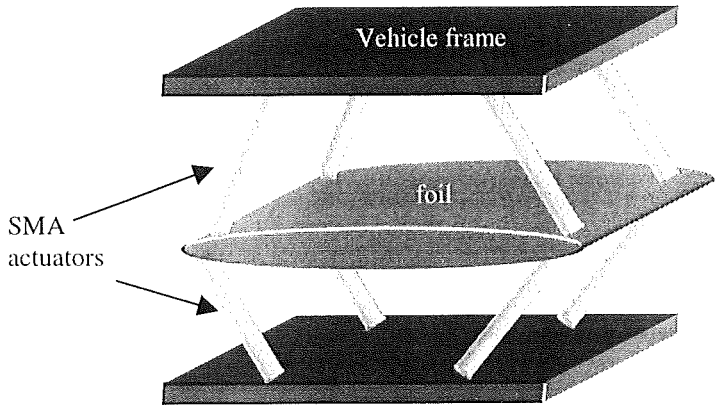

Figure 3.23 Configuration for two-dimensional thruster utilising SMA springs. [54]

The models introduced above can be taken to the next step in an attempt to design biomimetic fish robots [55-57] that are based largely on basic concepts of fish swimming and control mechanisms. One design is based on the movements of the lamprey or eel [55,56]. The inner body of the robot consists of a number of identical segments, each one a flexible polyurethane spinal chord with SMA wires attached along the length that are surrounded by a silicone oil (Figure 3.24). The oil has good electrical insulation and heat conduction properties, and also has a specific gravity of 0.91 - 0.92, which can provide some buoyancy for the system. The skeletal system is enclosed in a flexible membrane, which, coupled with the polyurethane backbone, has a stiffness roughly equal to the reset force for the NiTi wires. This eliminates the necessity for an external bias force. Activation of opposing SMA wire groups in successive segments mimic the undulatory movements of the lamprey or eel. Experiments carried out on four connected segments,

conducted in air, showed a cycle time of 1.7 seconds, which could be significantly reduced when the system is immersed in water [56].

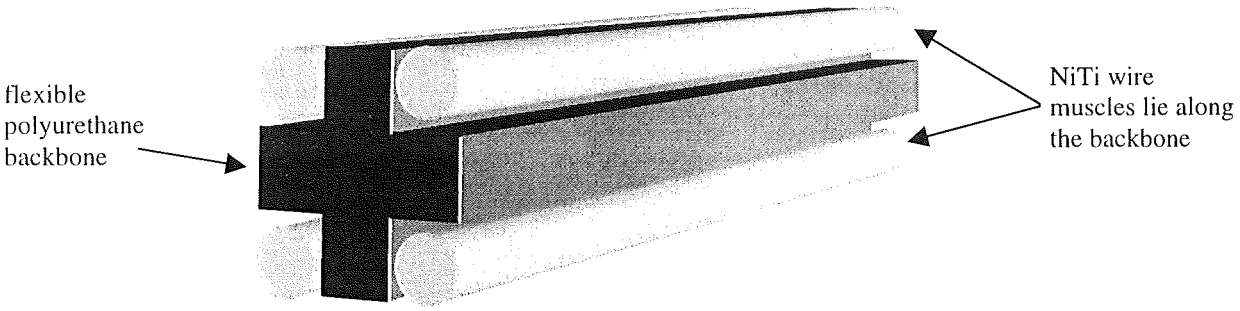

Figure 3.24 Segment of lamprey robot, with flexible polyurethane backbone and SMA wire actuators. Activation of opposing wire groups in successive segments causes the overall system to undulate like a lamprey or eel, e.g. activation of the left pair of SMA wires in one segment, along with the activation of the right pair in the next segment, and so on. [55]

A clearer picture of the SMA wire activation of a spined biomimetic fish robot is shown in Figure 3.25 [57]. Dashed and solid lines represent the actuators in the actuated and relaxed state, respectively. The configuration illustrated represents a half-cycle, the other cycle being the opposite state for each particular wire. Continuous cycling would cause the robot to mimic the swimming techniques of a fish.

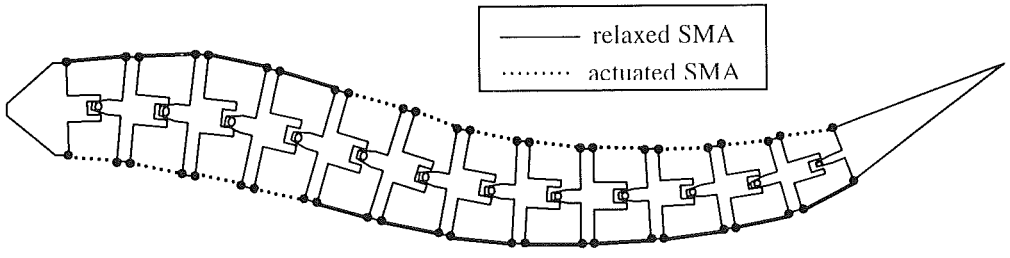

Figure 3.25 Conceptual design of an SMA-actuated underwater vehicle. [57]

Shape memory alloys are also being investigated for their use in buoyancy control of underwater robots and vehicles. For example, one company is developing a ballast-water pump system using SMA rings [58]. The rings fit around a flexible tube and contract inwards to force ballast water along the tube and outwith the vessel. The system also incorporates a one-way SMA valve to prevent back-flow.

Another buoyancy regulating design uses arrays of SMA tubes that are directly exposed to the sea [59]. Each hollow SMA straw is sealed and filled with air (Figure 3.26). They are trained to have a two-way shape memory effect so that they can change shape from a flattened straw at low temperature to a round cross-section when heated. They can, therefore, change their volume and displacement and, thus, their buoyancy. The straws can operate to a maximum depth of 1000 m, where they can still change to the austenite circular shape and bring about an increase in buoyancy to raise the vehicle.

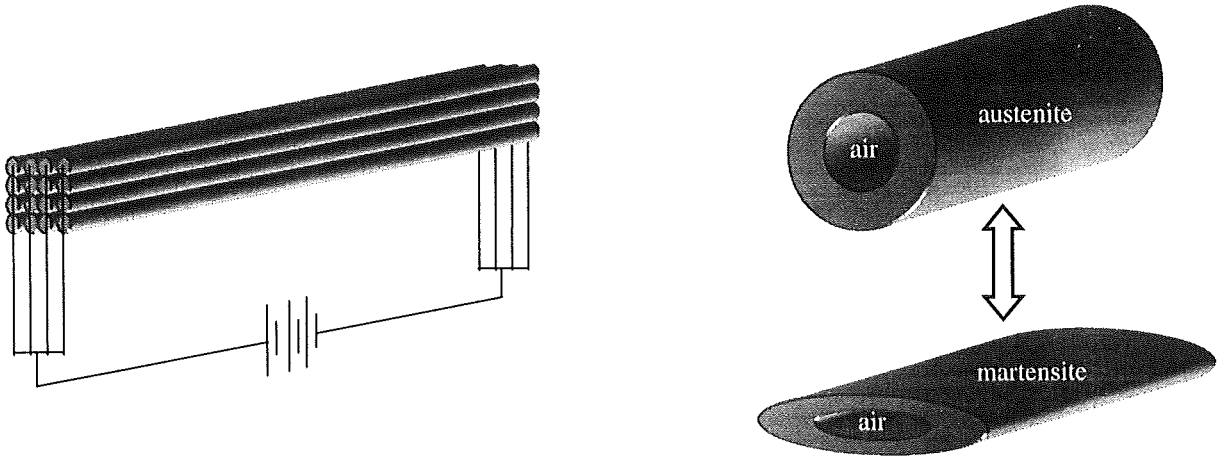

Figure 3.26 Array of NiTi straws which are flat when cool and expand to circular cross-section when heated. [59]

The effects of hydrostatic pressure must, of course, be taken into account when designing shape memory alloys for underwater applications. The increase in depth and corresponding increase in stress on the alloy can affect the transformation temperature, stroke length, hysteresis and recovery stress of the material. For example, transformation temperature increases with hydrostatic pressure at a rate of $7.1 \pm 2°C$/kbar [60].

3.3.2.7 Conclusions on Shape Memory Alloys

Shape memory alloys cannot be classed as very efficient materials. In fact, the process of feeding heat energy to the material, having that converted to mechanical work during the phase transformation, and using some form of energy to cool the element gives a practical efficiency of just 3-4% [25]. Efficiency is, however, just a ratio comparing input to output. The materials are better described in terms of their effectiveness, which involves the best use of resources without waste [61]. Shape memory alloys exhibit some of the best power output per amount of material known [25], about one watt per gram of alloy.

The ability of shape memory alloys to change shape while exerting significant forces, coupled with their capacity to function well underwater, makes them ideal candidates in the development of a novel buoyancy control system for small underwater robots and vehicles.

3.3.3 Shape Memory Polymers

Shape memory polymers (SMP's) are lightweight, low in density, high in shape recovery ability, easy to manipulate and economical as compared with shape memory alloys, and therefore their development is being actively promoted [62-66]. The SMP's which have demonstrated the best processibility and mechanical properties are the polyurethane-based thermoplastic polymers, developed by Mitsubishi Heavy Industry [67].

3.3.3.1 Mechanism of the Shape Memory Effect

Polyurethane SMP's, like most polymeric materials, change mechanical properties as shown in Figure 3.27 [65], going from fairly rigid structures below the T_g to softer materials as they are heated above the T_g. The slope at the T_g temperature is very steep, allowing a quick transition from hard to soft, and vice versa.

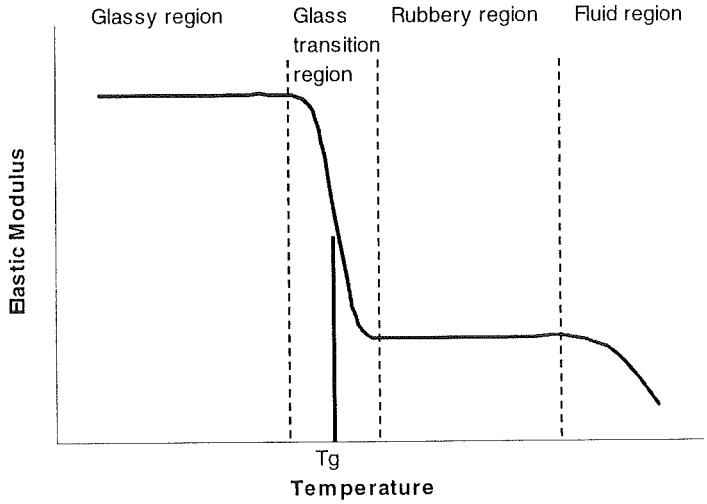

Figure 3.27 Temperature dependence of elastic modulus of polyurethane SMP's [65].

The change in elastic modulus can be as much as three orders of magnitude, from 1 MPa in the rubbery state to 1000 MPa in the glassy state [67]. Above T_g, the SMP can be easily deformed by the application of stress. By maintaining the stress whilst cooling the material, it will retain the new shape imposed on it. Upon heating again, the SMP will recover the original shape attained during the moulding process.

The basic properties of shape memory polymers are compared to shape memory alloys in Table 3.5 [64,68].

Table 3.5 Comparison of properties of NiTi SMA's and polyurethane SMP's [64,68].

Property	NiTi shape memory alloy	Shape memory polymer
Recovery Stress	200-400 MPa	1-3 MPa
Recovery Strain	8% max.	50-600%
Low Temperature Modulus	~ 48 GPa	~1000 MPa
High Temperature Modulus	~193 GPa	~1 MPa
Density	6.45 g/cm^3	1-1.3 g/cm^3
Phase Transformation	Martensitic	Glass Transition
Shaping	Difficult	Easy
Cost	Expensive	Cheap
Heat Conductivity	High	Low

3.3.3.2 Design and Applications of SMP Actuators

The elastic modulus and shape recovery properties of SMP's are being utilised mainly in automotive and medical fields. An automatic choke for internal combustion engines using SMP's has been developed [64]. When the engine is at rest, the polymer element remains rigid and is used to block off air. As the engine is warmed, the polymer element begins

bending, allowing a bias spring to open the air intake valve and permit the desired amount of combustion air.

In the medical world, polyurethane shape memory polymers are desirable because of their very low thrombogenicity and excellent biocompatibility. The materials are used as catheters which remain stiff at room temperature but soften once they are inserted into the body [69]. This allows the physician to push against a stiff section outside the body while the portion of catheter inside the body is pliable and easily guided along arterial passages resulting in less damage and discomfort for the patient.

Shape memory foams have also been developed [70]. Traditional foams are moulded to a particular shape and transported to the site of use. Their bulkiness can be a hindrance to their transportation from the moulding plant to the site. By using SMP's, the as-moulded foams can be compressed, below their T_g, to a fraction of their volume, transported with ease, and then heated above their T_g to return them to their as-moulded shape.

3.3.3.3 Conclusions on Shape Memory Polymers

Shape memory polymers have several distinct advantages compared to shape memory alloys [19], such as low density, high shape recovery (maximum strain recovery > 500%), easy processibility, and low cost. However, they have one major negative aspect, which is their low recovery force. With as little as 4 MPa of applied stress, any shape-recovery properties inherent in the material are lost. For this reason, SMP's are usually used in

cases where only free recovery or very low recovery force and mechanical strength are needed [19]. In underwater applications, especially in buoyancy control devices where water pressures are high, shape memory polymers clearly do not have a recovery stress great enough to be effective actuators. Research to improve their strength is in progress, including the incorporation of strengthening elements to form composites [63], which may lead to applications such as hulls of variable stiffness.

3.3.4 Shape Memory Ceramics

The mechanism of the shape memory effect in ceramics is outlined in Figure 3.28 [71]. The antiferroelectric (AFE) to ferroelectric (FE) transition can be induced by a large electric field and can generate strains [19]. The phase transition, which is caused by the switching or reorientation of the polarised domains, is accompanied by a lattice distortion leading to a linear and net volume expansion.

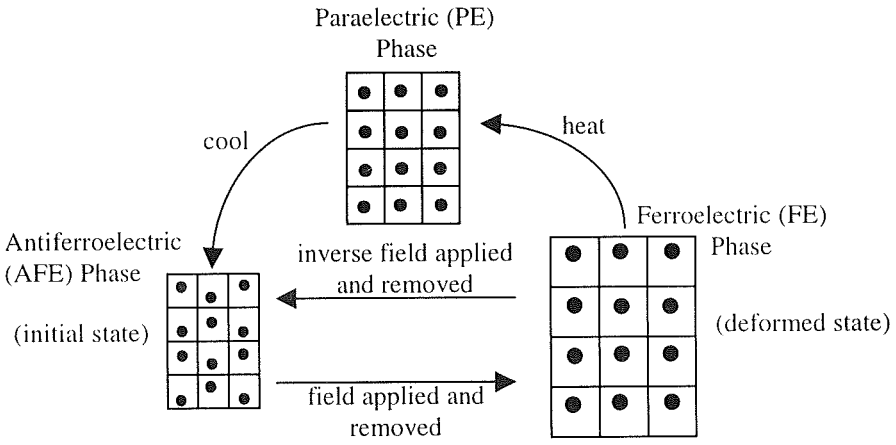

Figure 3.28 Shape memory effect in antiferroelectric ceramics [71].

Compared to shape memory alloys, the advantages of shape memory ceramics are fast response speed, good controllability by electric field to memorise and recover the shape, and low energy consumption (~1/100 of SMA) [71]. These are outlined in Table 3.6. Also evident from the table are the disadvantages, which far outweigh any advantages. A major downfall is that SMC's only exhibit recovery strains in the region 0.1%-0.7%. This is very limiting for actuating purposes, especially for a buoyancy control device, where larger strains and volumes are necessary.

Table 3.6 Comparison of properties of NiTi SMA's and antiferroelectric SMC's [71].

Property	NiTi shape memory alloy	Shape memory ceramic
Recovery Stress	~400 MPa	~100 MPa
Recovery Strain	8% max.	0.1-0.7%
Driving Power	heat (W ~ kW)	voltage (mW ~ W)
Response Speed	sec ~ min	msec
Durability	10^5 cycles	$>10^6$ cycles

3.4 Polymers Gels

3.4.1 Introduction

A gel is a form of matter intermediate between a liquid and a solid. It has two constituents; a crosslinked polymer network, and a solvent which fills up the pores in the network [72]. Polymer gels can respond to changes in their environment, such as pH [73], temperature [74], solvent composition [75], and applied voltage [76]. One response can be a change in size and shape [77], which could mean a conversion of chemical energy directly to mechanical work. The benefits of this conversion could be used wherever power for more conventional devices is limited or difficult to obtain, such as in an underwater environment.

The swelling behaviour of polymer gels was first explained by the Flory-Huggin's equation [78]. This led to the prediction of a discontinuous volume phase transition in gels [79], which was eventually observed (accidentally) by Tanaka [80,81]. He found that partially ionised polyacrylamide gels undergo a discontinuous volume change as a function of solvent composition. This discovery sparked considerable interest and research in the field, both theoretically and experimentally [72-82]. The large changes in volume exhibited by the gels has also encouraged research into their possible use in actuators and devices [83].

3.4.2 Phase Transition

The state of a polymer gel, such as a polyacrylamide gel, is affected by the solvent in which it is immersed. Depending on the solvent, the polymer molecules will either spread out or bunch together. In a poor solvent, the polymer segments will avoid solvent molecules and the polymer will coil up. In a good solvent, the polymer segments and solvent atoms attract each other causing an increase in the dimensions [77]. This expansion continues until the network has stretched enough so that the resulting elastic force counteracts the inflow of solvent molecules. The response velocity, or rate of swelling or shrinking, depends on the size of the gel. For a spherical gel, the response velocity is proportional to the square of the final radius of the gel [82]. Therefore, for a faster response, smaller gels are preferred.

The elastic force due to swelling depends on the degree of crosslinking of the polymer network. There is less swelling for strongly crosslinked gels [77]. Also, as the temperature decreases the polymer network loses its elasticity. At a critical temperature the modulus goes to zero and the gel becomes infinitely compressible.

Temperature is, therefore, an important factor in gel strength and phase transition. The temperature at which polymerisation of the network takes place also affects the structure and physical properties of the gel. It has been shown that polyacrylamide gels polymerised between 0-4°C are turbid (opaque), highly porous and unelastic [84]. Polymerisation above 60°C also gives unelastic gels with short chains. The best

temperatures are between 25-30°C. The resultant gels are transparent, with small pores, and are elastic. Hydrogen bonds among crosslinking molecules are stabilised at low temperatures, but are progressively broken down at higher temperatures. Opaque gels at low temperatures are regarded as 'faulty' gels, because the distribution of polymer chains within the matrix is non-homogenous, i.e. there are areas of high and low strand density. This leads to highly porous gels with low elasticity and low swelling rates in solvents.

The volume of a gel is influenced by osmotic pressure, π, which is the sum of three components illustrated by the following Flory-Huggin's [78] assumption:

$$\pi = \pi_{mix} + \pi_{el} + \pi_{ion} \tag{3.7}$$

where,

π_{mix} = polymer-polymer affinity
π_{el} = rubber elasticity
π_{ion} = hydrogen-ion pressure

3.4.2.1 Polymer-Polymer Affinity

The polymer-polymer affinity, π_{mix}, is due mainly to the van der Waals interaction between the polymer strands and the solvent [85]. Depending on the ions in the gel and solvent, this interaction is either attractive or repulsive. When there is an attraction, the polymer reduces its total energy by surrounding itself with solvent molecules. When there is repulsion, the solvent is excluded from the gel. For example, if a polyacrylamide gel is

immersed in an acetone/water mixture, the polymer strands have a greater affinity for the other strands than they do for the solvent molecules. Therefore the acetone/water molecules are excluded and the strands tend to coil up. This creates a negative pressure, π_{mix}, which causes a collapse in the gel [77].

The π_{mix} pressure is always negative. It depends on the solvent composition and is independent of temperature. It does, however, also depend on the volume of the gel and is stronger for smaller volumes. π_{mix} is a short-range force. It is fully effective only if two polymer segments are touching. The probability of direct contact between segments is inversely proportional to the square of the gel volume [77]. Therefore as the gel continues to contract, the π_{mix} pressure increases.

3.4.2.2 Rubber Elasticity

This force, π_{el}, relates to the elasticity of the individual polymer strands, i.e. their resistance to stretching or bunching [86]. A single strand is a chain of rigid segments that are freely-jointed together, and these segments are in constant motion because of their thermal energy. If the strand is held at both ends and extended to its full length, the thermal agitation of the segments causes a force tending to pull the ends inwards. Conversely, if the strand is held in a coiled position the random motion of the segments tend to push the ends apart. Between these two extremes there exists an optimum strand length where the segments are neither in tension or compression. This length equals the

square root of the number of segments in the strand multiplied by the length of the segments.

The strength of the rubber elasticity of a polyacrylamide gel depends on how actively the polymer segments are moving [77]. The motion is thermally induced, so the π_{el} strength is proportional to the temperature. The temperature, however, does not affect the direction of π_{el}, but only the magnitude of this force. Direction depends on the state of the gel. If it is swollen and the strands are stretched, then the π_{el} pressure tends to make the gel contract. If the gel is initially contracted and the strands are bunched together, the π_{el} pressure tends to swell the gel, which is denoted as swelling in the positive direction. An increase in temperature augments the relative π_{el} pressure, so that a rise in temperature increases the tendency for a collapsed gel to swell, and for a swollen gel to contract.

3.4.2.3 Hydrogen Ion Pressure

Immersing a polyacrylamide gel in a solvent such as N,N,N',N'-tetramethyl-ethylenediamine (TEMED) hydrolyses (or ionises) a portion of side chains in the polymer network [81]. The hydrogen ion pressure, π_{ion}, is associated with the degree of ionisation of the polymer network, which releases an abundance of positively charged hydrogen ions into the gel fluid. These positive ions are immersed in a sea of negative charges attached to the polymer network, so the gel remains electrically neutral. The background negative charges effectively screen the mutual repulsion of the hydrogen ions.

Hydrogen ions give rise to a positive pressure, π_{ion}, that is temperature dependent [87]. If the temperature of a polyacrylamide gel was increased, the π_{ion} pressure would also increase. The unrestricted gel would therefore expand, but doing this would reduce the effect of π_{ion}.

The magnitude and direction of the three components of osmotic pressure, π, in conjunction with each other govern whether a gel swells or shrinks [88]. At a fixed solvent composition and temperature the gel will adjust its volume so that the total osmotic pressure will be zero. If the osmotic pressure is positive, the gel will take up fluid and the volume will increase. If it is negative, the gel will expel fluid and the volume will decrease. This process continues until equilibrium is reached.

For example, consider a contracted polyacrylamide gel that is immersed in a low concentration of acetone at a high temperature. This state of contraction and high temperature influences the magnitude of the rubber elasticity. The π_{el} magnitude will be large and π_{el} will have a tendency towards positive swelling [77]. The high temperature also increases the hydrogen ion pressure, π_{ion}, which is always positive. The polymer-polymer affinity, π_{mix}, which is always negative, will be low because of the low acetone concentration. The net effect is a large positive osmotic pressure. Therefore the gel volume increases. But the hydrogen ion pressure abates as volume increases. Also, as the polymer strands increase in length, the positive π_{el} pressure becomes less and eventually negative as the strands 'overshoot' their optimum length. Eventually the volume expansion will cease as the osmotic pressure reaches zero [77].

The collapse of a polyacrylamide gel can also be brought on at constant temperature and constant solvent composition by changing the pH of the solution [81] or by adding a salt to it [89]. Both of these factors alter the effective ionisation of the polymer network. Adding acid reduces the pH and raises the concentration of hydrogen ions, inducing some of the ionised groups on the polymer to recombine with super-abundant hydrogen ions. Therefore, the π_{ion} pressure is reduced and the gel collapses at a higher temperature than it would in a neutral solution [77].

The positively-charged metal ions of salts, such as sodium chloride (NaCl) or magnesium chloride ($MgCl_2$), congregate around and, therefore, shield the negative charges on the polymer. The negative chloride ions neutralise the hydrogen ions in the solution. The result is an overall reduction in the π_{ion} pressure, bringing about a collapse. It was found that only half as many divalent Mg ions are needed to neutralise the network as monovalent sodium ions [81].

Phase transition has also been observed in partially hydrolysed polyacrylamide gels under the influence of an electric field of 2V/cm [76], while immersed in a 50% acetone/water mixture. The swollen gel shrank at the anode, which was interpreted as the electric field pushing and squeezing the anodic side of the gel (Figure 3.29). The collapse was later explained as a change in the osmotic pressure due to the ionic distribution inside and outside the gel under the influence of the electric field [90].

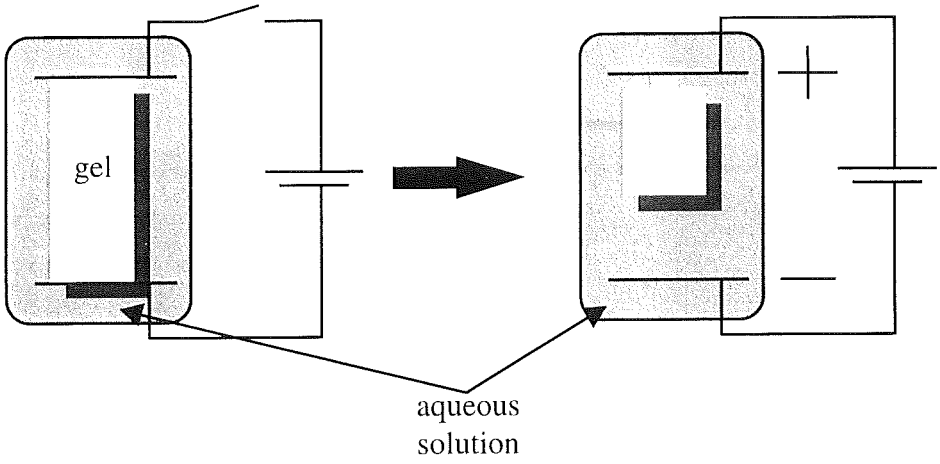

Figure 3.29 Collapse of polyacrylamide gel in 50% acetone/water, under the influence of an electric field [76].

When a polyacrylamide gel is placed in a high concentration of NaOH solution, it swells at the anode side instead of collapsing [90]. When the NaOH concentration is low, the gel shrinks at the anode. There is a change in the osmotic pressure based upon a difference in mobile ion concentrations between the inside and outside of the gel. When the NaOH concentration is high, the excess of Na^+ ions move to the anode side of the gel, causing the osmotic pressure to increase leading to a swelling [91]. With low NaOH concentrations, H^+ ions are produced by the electrolysis of water, and this suppresses the dissociation of carboxyl groups near the anode. As a result, π at the anode side decreases, leading to a shrinkage [90].

The observed swelling or shrinking is a differential deformation, so placing a rectangular gel parallel to the two electrodes causes it to bend towards the cathode under an electric field (Figure 3.30). Reversing the field causes the gel to straighten and bend in the

opposite direction. Typical field strength is about 10V/cm. There is a faster reaction time as the thickness of the gel is reduced [91].

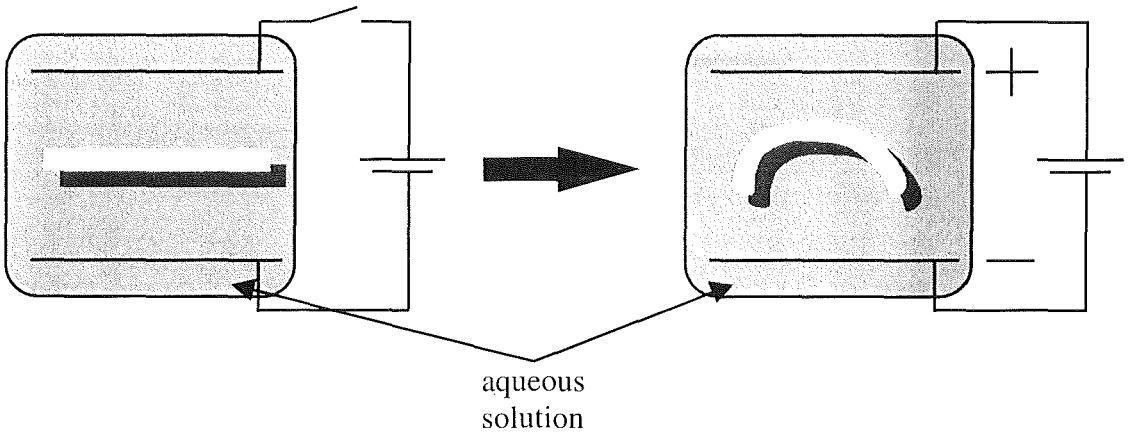

Figure 3.30 Bending motion of a polyacrylamide gel in an NaOH solution, under the influence of an electric field [90].

3.4.2.4 Hydrophobic Interaction

In an attempt to find a gel that undergoes a volume phase transition in pure water, rather than an acetone-water mixture, gels which had hydrophobic side groups were studied [85]. The behaviour of *N*-isopropylacrylamide (NIPA) gels when subjected to changes in solvent composition and temperature was found to be in contrast to polyacrylamide gels. At low temperatures NIPA gels swell in pure water, but at high temperatures the gels collapse. There is an 8-fold discontinuous volume transition at approximately 33.2°C [92]. The temperature dependence, which is opposite to the transition induced by van der Waals forces, is due to the hydrophobic interaction of the gel and water [85]. The water molecules in the vicinity of the hydrophobic polymer chains have more ordered structures, and thus a lower entropy, than those away from the polymer chains. At higher

temperatures the polymer network shrinks and becomes more ordered, but the water molecules are excluded from the polymer network, resulting in a collapse of the gel.

As a NIPA gel is heated, there is a phase coexistence in the form of swollen and shrunken phases [87,93]. If a cylindrical gel is heated to a temperature, T_1, 0.2°C above the phase transition temperature, a large portion of the gel is swollen, but the ends of the gel rod are collapsed. This state will remain unless the temperature is again raised to, for example, T_1+1.1°C. The high-temperature phase grows at the expense of the low-temperature phase, and the swollen regions disappear (Figure 3.31). The same behaviour is also observed during cooling of the NIPA gel. There is temperature hysteresis of approximately two degrees between heating and cooling [87]

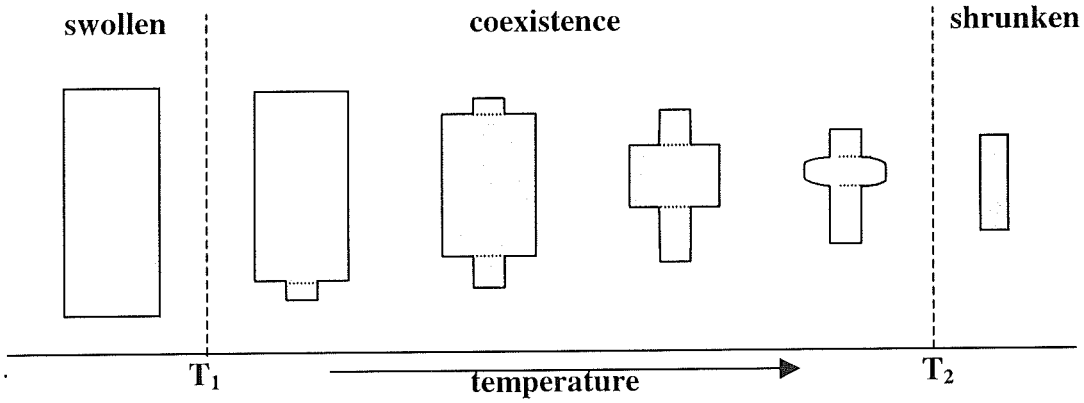

Figure 3.31 Process of phase transition in a NIPA gel rod on heating. Phase coexistence starts at T_1 and ends at T_2. Between these temperatures, the volume fraction of the shrunken phase increases with temperature [87].

The phase transition temperature of NIPA gels has been found to be stress and strain dependent [87,94-96], which is an important observation if the gels are to be used as functional devices with mechanical constraints. Under uniaxial stress, the transition

temperature increases by 1°C as strain is increased up to 400%. The transition temperature also increases with the application of hydrostatic pressure [87]. The hydrophobic interaction between the polymer segments and solvent are affected by the hydrostatic pressure, causing a change in the excess free energy. The result is that the swollen state of the gel is more stable at higher pressures and a higher temperature is needed to induce the phase transition [97].

3.4.3 Design and Applications of Gel Actuators

The major advantages of gel actuated devices are compactness, simplicity, modest weight, small power requirements and low material costs [98]. In principle, like shape memory alloys, there need only be one moving part. All that is required for electrically sensitive gels is the electric field or a method of heating and cooling for thermo-sensitive gels. Studies have been carried out on an energy-saving method of heating NIPA gels, swollen in NaCl solution, using electrodes inserted within both ends of the gel rods [99]. Gels that use an exchange of fluid medium to swell and contract, such as a pure water/salt water system, may require more complex periphery pumping mechanisms. This is one of the major disadvantages of polymer gels – the fact that they must be contained within a solvent bath. Another is that the response times of gels are often much longer than conventional actuator components [98].

There are a number of designs using polymer gels as actuators. They generally involve having the gel and solvent bath contained in either rigid or flexible containers [100]. One

such arrangement is a gel film acting as a belt of a pulley. When one 'arm' of the gel belt is actuated and contracts, the pulley is rotated in one direction. Deactivation of that side and activation of the other causes rotation in the opposite direction. Another configuration is a simple extension device, where a contracted gel in a flexible bellows is allowed to expand. A similar device is gel moulded into a doughnut shape, that can expand and be used as a sphincter valve mechanism [99].

There has also been some study of the uses of polymer gel actuators in underwater applications. The simple two-dimensional thruster outlined earlier in the SMA section (Figure 3.23) can also utilise gel as the fin actuators [54]. The researchers propose two gels: polyvinyl alcohol plus acrylic acid plus allylamine, which has an actuation strength of 0.3 MPa, an actuation strain of 45%, and a reaction time of 0.13 seconds; and poly-acrylonitrile, with an actuation strength of 2 MPa, an actuation strain of 95%, and a reaction time of 2 seconds. Another study uses polyacrylamide gels that undulate in electric fields to mimic fishtail motion [101-102].

3.4.4 Conclusions on Polymer Gels

Actuators exploiting the chemical/mechanical properties of polymer gels have great potential in applications where weight and size are at a premium, such as in underwater applications. The utility of such actuators depends on the design of appropriate containers, but in an underwater environment, the natural salinity variations could also be used

effectively to bring about the required shape changes, thus negating the need for complex solvent bath containers. Variations in the overall density of the gels as they are exposed to seawater could bring about a sufficient buoyancy change, if incorporated in a small underwater vehicle.

3.5 Summary of Smart Materials

Smart materials possess great potential for applications in the underwater exploration and surveying industry. Electrorheological and magnetorheological fluids have potential in variable stiffness elements, but the large power requirements for activation of the fluids make them unsuitable for an underwater environment. Shape memory alloys change shape while exerting significant forces, making them ideal candidates in the development of a novel buoyancy control system. Shape memory polymers also change shape, but do not have a recovery stress great enough to be effective actuators. Because of the wide range of external stimuli, and the resultant volumetric changes, of polymer gels, they may also prove to be suitable candidates as actuators in marine devices.

3.6 References

1. Fletcher R. 1996. Force transduction materials for human-technology interfaces. *IBM systems journal* **35**(3-4), pp. 630-638.
2. Shakeri C., Noori M.N., Hou Z. 1996. Smart materials and structures – a review. *Proceedings of the fourth materials engineering conference* **2**, pp. 863-876.
3. Srinivasan A.V. 1995. Smart biological systems as models for engineered structures. *Journal of materials science and engineering* **C99**, pp. 1-8.
4. Jain A.K., Sirkis J.S. 1994. Continuum damage mechanics in piezoelectric ceramics. *Adaptive structures and composite materials: analysis and application*, ASME International Mechanical Engineering Congress and Exposition, pp. 47-58.
5. Spencer B.F., Dyke S.J., Sain M.K., Carlson J.D. 1997. Phenomenological model of a magnetorheological damper. *ASCE journal of engineering mechanics* **123**, pp. 230-238.
6. Carlson J.D., Catanzarite D.M., St. Clair K.A. 1996. Commercial magnetorheological fluid devices. *Proceedings of the 5th international conference on electrorheological fluids, magnetorheological suspensions and associated technology*, World Scientific, pp. 2857-2865.
7. Winslow W. 1949. Induced fibration of suspensions. *Journal of applied physics* **20**, pp. 1137-1140.
8. Tolu-Honary A, Court M. 1994. Update on ER fluids. *Hydraulics and pneumatics* **January**, pp. 133-138.
9. Goldstein G. 1990. Electrorheological fluids: applications begin to gel. *Mechanical engineering* **October**, pp. 48-52.

10. Bullough W.A. 1991. Electrorheological fluids and the control of high-speed machines. *Endeavour* **15**(4), pp.165-169.

11. Rabinow J. 1948. The magnetic fluid clutch. *AIEE transactions* **67**, pp. 1308-1315.

12. Ashour O., Rogers C.A., Kordonsky W. 1996. Magnetorheological fluids: materials, characterisation, and devices. *Journal of intelligent material systems and structures* **7**(2), pp. 123-130.

13. Lord Corporation, 111 Lord Drive, PO Box 8012, Cary, NC 27511, USA. http://www.rheonetic.com.

14. Brooks D. 1989. Fluids get tough. *Physics world* **August**, pp. 35-42.

15. Paula G. 1997. Input output – exercise equipment puts on magnetorheological brakes. *Mechanical engineering* **May**, pp. 124.

16. Advanced Fluid Systems Ltd, Pensbury Industrial Estate, Pensbury Street, London SW8 4TJ, UK. http://www.a-f-s.com.

17. Havelka K.O., Pialet J.W. 1996. Electrorheological technology: the future is now. *Chemtech* **June**, pp. 36-45.

18. Ghandi M.V., Thompson B.S., Choi S.B. 1989. A new generation of innovative ultra-advanced intelligent composite materials featuring electrorheological fluids: an experimental investigation. *Journal of composite materials* **23**, pp. 1232-1255.

19. Wei Z.G., Sandström R., Miyazaki S. 1998. Shape-memory materials and hybrid composites for smart systems. Part I Shape-memory materials. *Journal of materials science* **33**, 3743-3762.

20. *Introduction to shape memory alloys.* TiNi Alloy Company. http://www.sma-mems.com.

21. Chang L.C., Read T.A. 1951. The gold-cadmium beta phase. *Transactions of the AIME* **191**, pp. 47.

22. Gilbertson R.G. 1992. *Muscle wires project book* Third edition. Mondo-tronics, San Anselmo, California.

23. Buehler W.J., Gilfrich J.V., Wiley R.C. 1963. Effect of low-temperature phase changes on the mechanical properties of alloys near composition NiTi. *Journal of applied physics* **34**(5), pp.1475-1477.

24. Shimizu K., Tadaki T. 1987. *Shape memory alloys.* Funakubo H.(Ed.), Gordon and Breach Science Publishers.

25. Hodgson D.E. 1988. *Using shape memory alloys.* Shape Memory Applications, Inc., Santa Clara, California.

26. Goddard N.D.R. 1992. *Smart materials: a review of the four key technologies and their likely industrial impact: final report.* ERA Technology Limited, Surrey, England.

27. Tong H.C., Wayman C.M. 1974. *Scripta metall* **8**, pp. 93.

28. Otsuka K., Wayman C.M. 1998. Mechanism of shape memory effect and superelasticity. In: *Shape memory materials.* Otsuka K., Wayman C.M. (Eds.), Cambridge University Press, pp. 27-48.

29. Otsuka K. 1985. Chapter 3 in: *Functional metallic materials.* Doyama M., Yamamoto R. (Eds.), pp. 56.

30. Transformation temperature hysteresis in NiTi alloys. *NiTi Smart Sheet #12.* Shape Memory Applications, Inc., Santa Clara, California, http://www.sma-inc.com.

31. Setting shapes in NiTi. *NiTi Smart Sheet #6.* Shape Memory Applications, Inc., Santa Clara, California, http://www.sma-inc.com.

32. Hodgeson D.E. 1990. Using shape memory for proportional control. In: *Engineering aspects of shape memory alloys.* Duerig T.W., Melton K.N., Stockel D, Wayman C.M. (Eds.), Butterworth-Heinemann, London, Boston, pp. 362-368.

33. Friend C.M., Morgan N.B. 1999. Shape-memory alloys in medicine – from new prosthetic devices to 'cuddly' instruments. In: *Medical applications for shape memory alloys (SMA).* IMechE, London.

34. Selected Properties of NiTi. *NiTi Smart Sheet #3.* Shape Memory Applications, Inc., Santa Clara, California, http://www.sma-inc.com.

35. Comparison of Properties of NiTi and Stainless Steel. *NiTi Smart Sheet #9.* Shape Memory Applications, Inc., Santa Clara, California, http://www.sma-inc.com.

36. Gandhi M.V., Thompson B.S. 1992. *Smart materials and structures.* Chapman and Hall, London, Glasgow, New York.

37. Two-way memory. *NiTi Smart Sheet #4.* Shape Memory Applications, Inc., Santa Clara, California, http://www.sma-inc.com.

38. Kisaichi M., Takahashi Y. 1989. Shape memory alloy and its uses. *The Sumitomo search no. 39* **Sept**, pp. 155-166.

39. Chute J.D., Hodgson D.E. 1988. *Proceedings from conference on engineering aspects of shape memory alloys.* Butterworth Scientific, Ltd.

40. Simon M., Kaplow R., Salzman E., Frieman D. 1977. A vena cava filter using thermal shape memory alloy. *Radiology* **125**(1), pp. 89-94.

41. Schwarzenburg H., Muller-Hulsbeck S., Gluer C.C., Wesner F., et al. *J. roentgenol* **170**, pp. 1181-1185.

42. Proft J.L., Duerig T.W. 1990. The mechanical aspects of constrained recovery. In: *Engineering aspects of shape memory alloys.* Duerig T.W., Melton K.N., Stockel D, Wayman C.M. (Eds.), Butterworth-Heinemann, London, Boston, pp. 115-129.

43. Harrison J.D., Hodgson D.E. 1975. *Shape memory effects in alloys.* Perkins J. (Ed.), Plenum Press, pp. 517.

44. Raychem Corp. 1977. US Patent No. 4035007.

45. Duerig T.W., Stockel D., Keeley A. 1990. Actuator and work production devices. In: *Engineering aspects of shape memory alloys.* Duerig T.W., Melton K.N., Stockel D, Wayman C.M. (Eds.), Butterworth-Heinemann, London, Boston, pp. 181-194.

46. Making shape memory springs. *NiTi Smart Sheet #7.* Shape Memory Applications, Inc., Santa Clara, California, http://www.sma-inc.com.

47. Ohkata I., Suzuki Y. 1998. The design of shape memory alloy actuators and their applications. In: *Shape memory materials.* Otsuka K., Wayman C.M. (Eds.), Cambridge University Press, pp. 240-266.

48. Giacommel J., Simpson J. 1995. Linear actuators from shape-memory alloys. *Machine design* **November 9**, pp. 99-100.

49. Wahl A.M. 1963. *Mechanical springs.* Second edition. McGraw-Hill, pp.235.

50. Tamura H., Suzuki Y. 1988. NiTi shape memory alloy springs and their applications. *Springs* **May**, pp. 19-23.

51. Vaidyanathan R., Chiel H.J., Quinn R.D. 2000. A hydrostatic robot for marine applications. *Robotics and autonomous systems* **30**, pp. 103-113.

52. Wright J.B.G. 1999. Investigation into shape memory alloys in relation to their application for use in autonomous underwater legged vehicles (AULV). *MSc. Thesis* Cranfield University.

53. Rediniotis O.K., Lagoudas D.C., Garner L.J., Wilson L.N. 1999. Development of a spined underwater biomimetic vehicle with SMA actuators. *Smart structures and integrated systems*. SPIE, Newport Beach, California, **3668**(Ch.93), 642-653.

54. McCanna J., Rae G.J. 1997. Simple two-dimensional thruster using intelligent materials. *10th International symposium on unmanned untethered submersible technology*. SPIE, pp. 196-205.

55. Adams A. 1998. Wiggling through the waves. *New scientist* **10 October**, pp. 32-35.

56. Jalbert J.C., Kasin S., Ayers J. 1995. Design considerations and experiments of a biologically based undulatory lamprey AUV. *9th International symposium on unmanned untethered submersible technology*. SPIE, pp. 124-138.

57. Webb G., Wilson L., Lagoudas D., Rediniotis O. 2000. Adaptive control of shape memory alloy actuators for underwater biomimetic applications. *AIAA journal* **38**(2), pp. 325-334.

58. Mide Technology Corporation, Cambridge, MA 02141. Proposal of research to the Office of Naval Research Phase I Awards - N96-161.

59. McCanna J. and Rae G.J. 1997. Shape memory alloy buoyancy regulator for subsea robots. *10th international symposium on unmanned untethered submersible technology*. SPIE, pp. 206-216.

60. Johari G.P., McAnanama J.G., Sartor G. 1996. Effect of hydrostatic pressure on the thermoelastic transformation of NiTi alloy and the entropy of transformation. *Philosophical magazine B* **74**(3), pp. 243-257.

61. De Bono E. 1979. Positive concepts. In: *Future positive*. Penguin Books, London, pp. 134-135.

62. Tobushi H., Hayashi S., Kojima S. 1992. Mechanical properties of shape memory polymer of polyurethane series - (basic characteristics of stress-strain-temperature relationship). *JSME international journal, series I* **35**(3), pp. 296-302.

63. Liang C., Rogers C.A., Malafeew E. 1997. Investigation of shape memory polymers and their hybrid composites. *Journal of intelligent material systems and structures* **8**(4), pp. 380-386.

64. Tobushi H., Hayashi S., Ikai A., Hara H. 1996. Thermomechanical properties of shape memory polymers of polyurethane series and their applications. *Journal de physique IV* **6**(C1), pp. 377-384.

65. Hayashi H. 1993. Properties and applications of polyurethane-series shape memory polymer. *International progress in urethanes* **6**, pp. 90-115.

66. Nagasawa H., Maeda M., Obuchi S., Toshima H., Shiba Y., Yokoyama I. 1997. Application of a shape memory polymer to ankle-foot-orthosis. *8th world congress of the international rehabilitation medicine association.* **1-2**(Ch.303), pp. 1311-1314.

67. Mitsubishi shape memory polymer. Mitsubishi Heavy Industries, Nagoya Research & Development Centre, Nagoya, Japan.

68. Irie M. 1998. Shape memory polymers. In: *Shape memory materials.* Otsuka K., Wayman C.M. (Eds.), Cambridge University Press, pp. 203-219.

69. Hayashi S. Properties and applications of polyurethane-bases shape memory polymer. Mitsubishi Heavy Industries.

70. Hayashi S., Fujimura H. 1991. Shape memory polymer foam. *U.S. Patent No. 5049591.*

71. Uchino K. 1998. Shape memory ceramics. In: *Shape memory materials.* Otsuka K., Wayman C.M. (Eds.), Cambridge University Press, pp. 184-202.

72. Li C. 1994. Scaling behaviours and mechanical properties of polymer gels. *PhD. Thesis* University of North Texas.

73. Katayama S, Hirokawa Y, Tanaka T. 1984. Reentrant phase-transition in acrylamide-derivative copolymer gels. *Macromolecules* **17**, pp. 2641-2643.

74. Hirokawa Y, Tanaka T. 1984. Volume phase transition in a nonionic gel. *Journal of chemical physics* **81**(12), pp. 6379-6380.

75. Zhang YQ, Tanaka T, Shibayama M. 1992. Super-absorbency and phase-transition of gels in physiological salt-solutions. *Nature* **360**, pp. 142-144.

76. Tanaka T, Nishio I, Sun ST, Ueno-Nishio S. 1982. Collapse of gels in an electric field. *Science* **218**, pp. 467-469.

77. Tanaka T. 1981. Gels. *Scientific American* **244**(Jan), pp. 110-123.

78. Flory P. 1953. *Principles of polymer chemistry.* Cornell University Press, Ithaca, New York, pp. 576.

79. Dusek K., Patterson D. 1968. Transition in swollen polymer networks induced by intramolecular condensation. *Journal of polymer science, Part A-2* **6**, pp. 1209-1216.

80. Tanaka T. 1978. Collapse of gels and the critical endpoint. *Physical review letters* **40**(12), pp. 820-823.

81. Tanaka T., Fillmore D., Sun S.T., Nishio I., Swislow G., Shah A. 1980. Phase transition in ionic gels. *Physical review letters* **45**(20), pp. 1636-1639.

82. Tanaka T., Fillmore D. 1979. Kinetics of swelling of gels. *Journal of chemical physics* **70**(3), pp. 1214-1218.

83. Osada Y., Gong J.P. 1999. Intelligent gels: their dynamism and functions. In: *SPIE Electroactive polymer actuators and devices.* Bar-Cohen Y. (Ed.), SPIE, **3669**, pp. 12-18.

84. Gelfi C, Righetti PG. 1981. Polymerisation kinetics of polyacrylamide gels II. Effect of temperature. *Electrophoresis* **2**, pp. 220-228.

85. Tanaka T. 1990. Phase transitions of gels. In: *Polyelectrolyte gels – properties, preparation, and applications.* Harland R.S., Prud'homme R.K. (Eds.), ACS Symposium Series, **480**(Ch.1), pp. 1-21.

86. Gehrke S.H., Lee P.I. 1990. Hydrogels for drug delivery systems. In: *Specialised drug delivery systems: manufacturing and production technology.* Tyle P. (Ed.), Drugs and pharmaceutical sciences, Marcel Dekker Inc., New York, **41**(Ch.8), pp. 333-392.

87. Hirotsu S. 1994. Static and time-dependent properties of polymer gels around the volume phase transition. *Phase transitions* **47**, pp. 183-240.

88. Hooper H.H., Baker J.P., Blanch H.W., Prausnitz J.M. 1990. Swelling equilibria for positively ionised polyacrylamide hydrogels. *Macromolecules* **23**, pp. 1096-1104.

89. Ohmine I., Tanaka T. 1982. Salt effects on the phase transition of ionic gels. *Journal of chemical physics* **77**, pp. 5725-5729.

90. Shiga T. 1997. Deformation and viscoelastic behaviour of polymer gels in electric fields. *Advances in polymer science* **134**, pp. 131-163.

91. Shiga T. 1998. Deformation and viscoelastic behaviour of polymer gels in electric fields. *Proc. japan acad.* **74**(B), pp. 6-11.

92. Hirokawa Y., Tanaka T. 1984. Volume phase transition in a nonionic gel. *Journal of chemical physics* **81**(12), pp. 6379-6380.

93. Hirose H., Shibayama M. 1998. Kinetics of volume phase transition in poly(*N*-isopropylacrylamide-*co*-acrylic acid) gels. *Macromolecules* **31**, pp. 5336-5342.

94. Suzuki A. 1993. Phase transition in gels of sub-millimetre size induced by interaction with stimuli. *Advances in polymer science* **110**, pp. 199-240.

95. Suzuki A. 1994. Phase transition in constrained polymer gels. *Journal of chemical physics* **101**(11), pp. 10003-10007.

96. Suzuki A., Sanda K., Omori Y. 1997. Phase transition in strongly stretched polymer gels. *Journal of chemical physics* **107**(13), pp. 5179-5185.

97. Kato E. 1997. Volume-phase transition of *N*-isopropylacrylamide gels induced by hydrostatic pressure. *Journal of chemical physics* **106**(9), pp. 3792-3797.

98. Segalman D.J., Witkowski W.R., Adolf D.B., Shahinpoor M. 1992. Theory and application of electrically controlled polymeric gels. *Smart materials and structures* **1**, pp. 95-100.

99. Kato N., Morito T., Takahashi F. 1998. An energy-saving method of heating for a chemomechanical poly(*N*-isopropylacrylamide) gel with Joule's heat. *Materials science and engineering C* **6**(1), pp. 27-31.

100. Adolf D.B., Shahinpoor M., Segalman D.J., Witkowski W.R. 1993. Electrically controlled polymeric gel actuators. *U.S. Patent No. 5250167.*

101. Shahinpoor M. 1992. Conceptual design, kinematics and dynamics of swimming robotic structures using ionic polymeric gel muscles. *Smart materials and structures* **1**, pp. 91-94.

102. Mojarrad M., Shahinpoor M. 1997. Biomimetic robotic propulsion using polymeric artificial muscles. *Proceedings of the IEEE international conference on robotic and automation* **3**, pp. 2152-2157.

Chapter 4 Polymer Gels — Experiments and Results

There is a need for small marine devices or vehicles that are able to take measurements throughout the water column, usually with limited power sources. Buoyancy control is important in these small underwater vehicles and sensor packages, to enable greater flexibility in measurements in the ocean. Gel systems might be used as the basis for actuators to control buoyancy in underwater applications.

Polymer gels can respond to changes in their environment, such as temperature [1], solvent composition [2], and applied voltage [3]. One response can be a change in size and shape [4], which could mean a conversion of chemical energy directly to mechanical work. The benefits of this conversion could be used wherever power for more conventional devices is limited or difficult to obtain, such as in an underwater environment. This chapter describes the work carried out on a number of polymer gel systems and how they responded to various stimuli, such as applied electric fields, seawater solutions, and temperature.

4.1 Electric Field Studies

The aim of this study was to see if polymer gels could prove useful as electrically driven actuators that provide a linear contraction or expansion. Two gel configurations were investigated: polymer gels responding to an electric field by expanding or contracting

along the length of the gel; and polymer gels bending under the influence of an applied electric field. Hydrolysed polyacrylamide gels were used in all electric field tests.

4.1.1 Experimental Details for Electric Field Studies

4.1.1.1 Gel Preparation

Polyacrylamide gels were prepared using an acylamide monomer and the crosslinking comonomer, *N'N*-methylene-bis-acrylamide. All chemicals were of reagent-grade quality and were used without further purification. Transparent rods of polyacrylamide gel were prepared based on a method described by Tanaka [5]. Doubling the amount of crosslinking agent and halving the amount of water altered the quantities, in order to produce a more mechanically robust gel. The gels were produced in polypropylene cylinders and cured at room temperature for one day. The gel rods so produced were 100mm long and had diameters of 8mm or 19mm. These were washed in distilled water to remove any residue monomers and the rods were then allowed to equalise in distilled water at room temperature for one week.

After equalising, the 8mm diameter rods were cut into rods of various lengths, and the 19mm rods were cut into discs of 8mm thickness. All components were soaked in a basic solution of 1.2% N,N,N',N'-tetramethyl-ethylenediamine (TEMED), for four weeks, allowing them to hydrolyse fully [6]. The effect of TEMED on the swelling characteristics of polymer gels was explained in Chapter 3, Section 3.4.2.3.

4.1.1.2 Test Method and Apparatus

A testing vessel was built, similar to those used in the literature [7-8]. It consisted of a rectangular Perspex dish, inside dimensions 45mm x 40mm x 35mm deep, with platinum plate electrodes, connected to a power supply (Figure 4.1). The electrode gap was 45mm, giving a maximum electric field of 6.67 V/cm. A variable d.c. voltage supply was used, where the voltage could be adjusted from 3V to 30V. Various solutions were used in the electric field tests, including seawater, 50% acetone/distilled water and NaOH solutions.

4.1.2 Results and Discussion on Electric Field Studies

A hydrolysed polyacrylamide gel was tested in a 50% acetone/distilled water mixture. The length of the gel was initially 30mm, with a diameter of 8mm. After 30 minutes at an electric field of 6.67 V/cm, the length of the gel increased to 33mm, and a portion of the diameter nearest the anode had increased to 11-12mm. This corresponded to, approximately, a 25% increase in volume. When the applied electric field was switched off, the gel returned almost to its original volume, but at a much slower rate (1.5 – 2 hours).

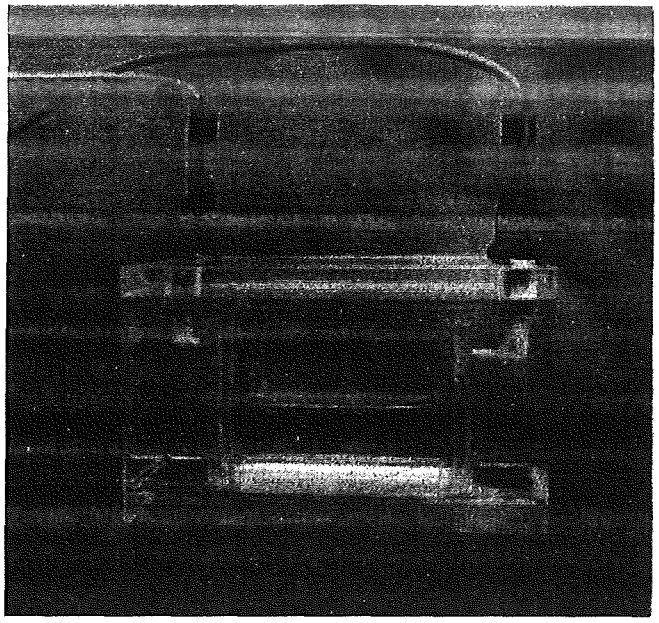

Figure 4.1 Gel testing bath with two platinum electrodes connected to a power supply.

The state of the gel after the increase in volume, produced from the electric field test, was irregular. The original swelling due to hydrolysis, when the polyacrylamide gel was soaked in 1.2% TEMED for 4 weeks, produced a weak, fluid-filled gel. The additional expansion at the anode side under the influence of an electric field caused small pieces of the gel to break off easily. This is illustrated in Figure 4.2.

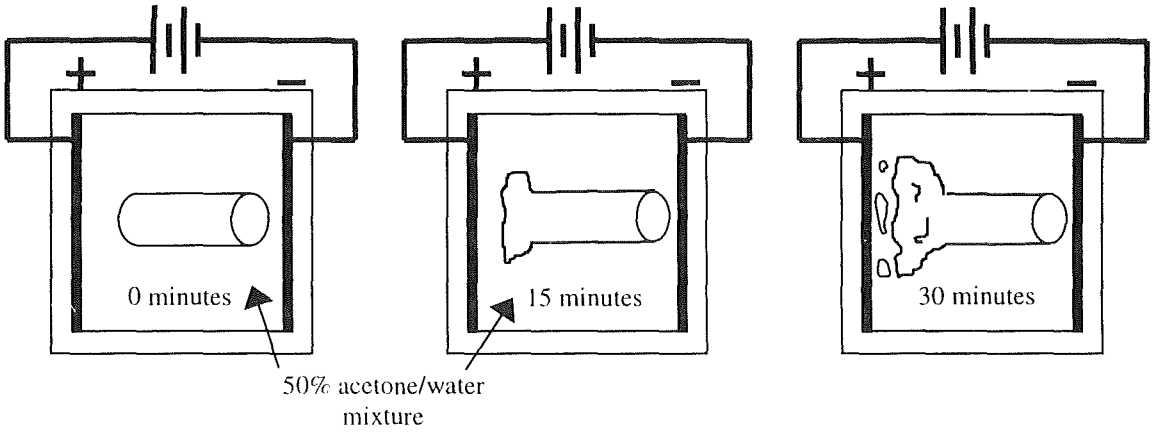

Figure 4.2 Appearance of polyacrylamide gel sample under the influence of an applied electric field of 6.67 V/cm.

When a polyacrylamide gel is immersed in seawater, the reaction to an electric field is vigorous. Because seawater is a strong electrolyte, a large current is drawn (85-90 mA), even in small electric fields of just 3V/cm. This results in an increase in the temperature of the seawater solution, which could be unsatisfactory for the state of the gel, although serious degradation of the gel does not occur until temperatures are in the range of 250°C to 300°C [9]. There is also much chlorine gas emitted during the electrolysis reaction, which may raise concerns about safety. The gel does exhibit an increase in volume at the anode side during the test, but not to the same degree as when gels are immersed in the acetone mixture. The high temperatures cause the swollen portion of the gel to split away.

The current drawn is quite low (15-20 mA) when a 0.02mol/L solution of NaOH is used, but much gas is still produced. However, the temperature of the solution does not increase significantly, making it useful as a medium for polyacrylamide gels. When a cylinder of gel of 8mm diameter was tested under the influence of a 3V/cm electric field, the length of the gel did not change after 1.5 hours. The diameter did increase, however, at the anode end, by approximately 38%, and along almost half the length of the gel. As the observed increase in volume was in the radial direction, another gel was tested with a diameter of 19mm and a length of 8mm. The applied electric field was 3V/cm. After 5 minutes, a lip developed at the anode side as it swelled slightly (Figure 4.3). The lip and swelling increased over the next 15 to 20 minutes, and a slight shrinkage became noticeable at the cathode end. After 45 minutes in the applied electric field, the gel had swelled so much in the radial direction at the anode side that it had lost balance and toppled over. The cathode

side diameter did not change much, but the anode side diameter had increased by about 30%. On examination of the gel, there was much splitting across the surface of the swollen side, similar to the weak, unstable nature of gels tested in acetone and seawater.

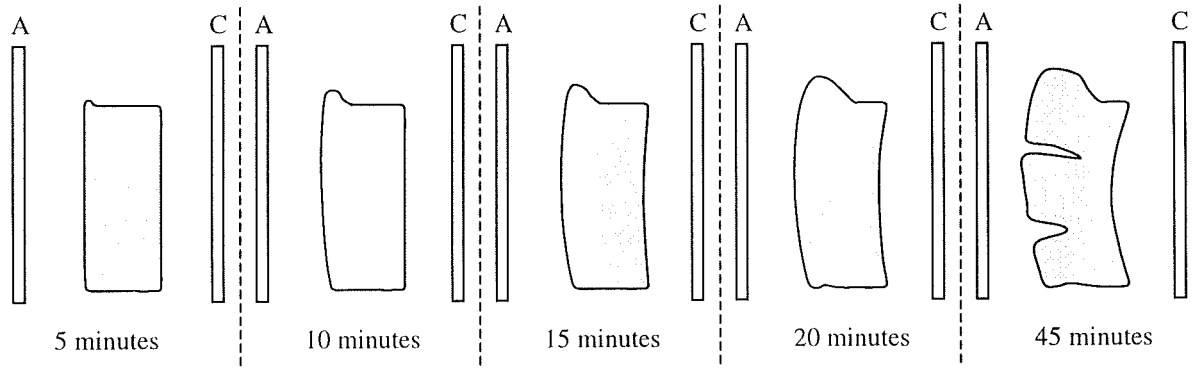

Figure 4.3 Swelling of polyacrylamide gel disc at the anode side, under the influence of an applied electric field of 3 V/cm.

Further tests were performed using the NaOH solution and smaller electric fields to see if the gels could remain intact whilst expanding in the field. It was found that electric fields of 1.5-2 V/cm, for periods over 2 hours, were necessary to bring about a similar amount of swelling. However, cracking on the surface of the gel always seemed to be a problem and would lead to the gels being unsatisfactory in a practical application.

The bending characteristics of hydrolysed polyacrylamide gels were also investigated by placing rods of gel parallel to the platinum electrodes. As before, the solutions used in the test bath were seawater, 50% acetone/water, and 0.02mol/L NaOH, the last-named eliciting the strongest reaction. Under the influence of an electric field of 6.67 V/cm, the gel rods were seen to bend (to as much as a semicircular shape) towards the cathode after

only 5 to 10 minutes, when immersed in NaOH. When the polarity of the electric field was reversed, the rods would straighten again and bend in the opposite direction. When one end of a gel rod was fixed, and the polarity of the electric field was changed periodically, the result was a pendulum motion in the gel. The time taken to complete one period, however, was slow at 15-20 minutes.

4.1.3 Conclusions on Electric Field Studies

There are noticeable changes in the shape of hydrolysed polyacrylamide gels when immersed in various solutions and subjected to an applied electric field. These shape changes were evident when the gel samples were placed with the largest axis perpendicular, or parallel, to the electrodes. Despite a reasonable amount of swelling being observed in a gel rod and disc placed perpendicular to electrodes, the region where the swelling takes place is weaker than the rest of the gel, with a tendency for the surface to split and shear away from the remainder of the gel. The problem of cracking is not observed in gels placed parallel to electrodes to generate a bending motion. However, the bending is unrestricted and the slightest constraint on the gel is enough to prevent any further motion.

Electrically activated polymers could still prove to be useful as actuators. A recent study has found that rapid a.c. voltage, instead of d.c. voltage, can significantly speed up the flow of ions through polymer gel tape, making the system's reaction and force output comparable to human muscle [10].

4.2 Seawater Studies

The effect of immersing hydrolysed polyacrylamide gels, i.e. ionic gels, in seawater of various salinity concentrations was studied in order to mimic realistic marine environments. Seawater is a solution of major and minor ions, gases and nutrients. Eleven major ions make up more than 99.99% of the dissolved material in deep ocean waters [11]. These major ions are listed in Table 4.1.

Table 4.1 Major ion composition of seawater [11].

Constituent	Symbol	Salinity, g/kg	Amount, %
Chloride	Cl^-	19.353	55.07
Sodium	Na^+	10.76	30.62
Sulphate	SO_4^-	2.712	7.72
Magnesium	Mg^{++}	1.294	3.68
Calcium	Ca^{++}	0.413	1.17
Potassium	K^+	0.387	1.10
Bicarbonate	HCO_3^-	0.142	0.40
Bromide	Br^-	0.067	0.19
Strontium	Sr^+	0.008	0.02
Boron	H_3BO_3	0.004	0.01
Fluoride	F^-	0.001	0.01
		~35.00	99.99

The effect of salt solutions on gels has been investigated [12-14], but not the effect of seawater of various salinities and at various temperatures, where the cocktail of numerous ions and salts can affect the behaviour of the gel. The varying salinities were used to emulate real environmental conditions in which these materials could be used, such as

oceans, coastal waters and estuaries. If gels are to be used in such marine environments, the effects of salinity and temperature are of significant interest.

4.2.1 Experimental Details for Salinity Studies

4.2.1.1 Gel Preparation

Polyacrylamide gels were prepared using an acrylamide monomer and the crosslinking comonomer, *N'N*-methylene-bis-acrylamide. All chemicals were of reagent-grade quality and were used without further purification. Transparent rods of gel were prepared based on a method described by Tanaka [5]. The quantities were altered by doubling the amount of crosslinking agent and halving the amount of water, in order to produce a more mechanically robust gel. The gels were produced in polypropylene cylinders and cured at room temperature. The gel rods so produced were 100mm long and had a diameter of 15mm. These were washed in distilled water to remove any residue monomers and the rods were then allowed to equalise in distilled water at room temperature for one week.

Using nomenclature introduced by Hjerten [15] to describe composition, the total monomer concentration, T, was found to be 10% and the percentage concentration of the crosslinking agent relative to the total concentration, C, was found to be 5%. Such gels were found to have an equilibrium water content (EWC) of approximately 90%.

After equalising, the rods were cut into discs and allowed to hydrolyse for three weeks by soaking in a 1.2% TEMED solution at room temperature. Assuming that the gels swell isotropically [16], the degree of swelling is calculated as a swelling ratio, V/V_0,

$$V/V_0 = (D/D_0)^3 \tag{4.1}$$

where V_0 and V are the volumes of the gel discs at preparation and after immersion in TEMED, respectively, and D_0 and D are the corresponding gel diameters. All gels used in the study were hydrolysed for a period of 21 days, resulting in a mean swelling ratio of $V/V_0 = 3.6 \pm 0.1$.

4.2.1.2 Salinity study

The salinity studies were carried out using seawater collected from the Largs Channel of the Firth of Clyde, Scotland. The seawater had a salinity of 35ppt when collected and it was filtered through Whatman glass microfibre filters, which removed any bacterial cultures. Solutions of 5ppt and 20ppt were prepared from seawater by diluting it with distilled water. The distilled water was produced by a Millipore-U10 system.

In order to investigate the effects of salinity on the hydrolysed gels, all the discs were weighed and their diameters were recorded using a Mitutoyo Profile Projector Type PJ-300. The discs were soaked in solutions (approximately 30ml) of distilled water, 5ppt saline, 20ppt saline or 35ppt saline (natural seawater).

All swelling experiments were carried out in triplicate. They were begun at 5°C and were taken through a temperature range in increments of 5°C up to 40°C. The solutions were kept at constant temperature using a Techne Flow Cooler FC-500 in conjunction with a Techne Circulator C-85D in a poly(methyl methacrylate) (PMMA) 10 litre tank of water.

After each 5°C temperature increment the gels were left for two days at this temperature to adjust. They were weighed and their diameters recorded each day. The solutions were changed daily during the experiment to simulate a larger body of water. The degree of swelling of the gels at each salinity concentration and temperature was found using equation 4.1.

The cyclical volumetric strain behaviour of the gels was also investigated by alternate exposure to distilled water and saline solutions of 5ppt, 20ppt or 35ppt seawater. The gels were allowed 2 days to equalise in the respective solution before being transferred to the alternate solution.

4.2.2 Results and Discussion on Seawater Studies

Figure 4.4 shows the degree of swelling of the gels with respect to temperature when immersed in one of the three saline concentrations. As mentioned previously, after hydrolysation in 1.2% TEMED for 21 days, the average degree of swelling of the gels was 3.6 ± 0.1. This will be referred to as the hydrolysation value. From Figure 4.4, it can be

seen that the degree of swelling of the gel discs decreases significantly from the above value when they are immersed in saline solutions, exhibiting a V/V_0 range between 1.1 and 1.4. The swelling degree for gels in 20ppt and 35ppt solutions are practically the same, with that for the 35ppt values being slightly lower than for the 20ppt solution. These values are significantly lower than the degree of swelling for the gels in the 5ppt solution.

The results are in line with what would be expected of such materials due to their polymer structure. Since the gels were hydrolysed before the salinity experiments, some of the $-CONH_2$ groups will have been converted to carboxyl groups, which spontaneously ionise leaving $-COO^-$ ions (Figure 4.5). This causes the gel to expand due to the repulsion of the ions. When the gel is then immersed in a saline solution the positive ions, such as the sodium and magnesium ions, shield the $-COO^-$ ions, negating the repulsion and resulting in a decrease in the degree of swelling. This effect is less pronounced in the low salinity as there are less ions available than at the higher salinities, i.e. 20ppt and 35ppt.

The effects of temperature play only a small part in the degree of swelling of the gels immersed in saline solutions. At all salinity concentrations there is a decrease in shrinkage from the hydrolysation value as the temperature increases, but only to a small extent. This is to be expected, as polyacrylamide gels are relatively insensitive to temperature [17]. As described in Chapter 3, Section 3.4.2, the hydrogen ion pressure, π_{ion}, and the rubber elasticity, π_{el}, are temperature dependent and this dependency will have a small effect on the magnitude of the swelling degree as the temperature increases [6].

Figure 4.6 shows the relationship between the degree of swelling and temperature for polyacrylamide gels in the salinity solutions investigated and also in distilled water. As in Figure 4.5, the degree of swelling of gels in seawater solutions is in the range of 1.1-1.4. In Figure 4.6, this range can be seen clearly in context with their original hydrolysation values of V/V_0 = 3.6. The figure shows the extent to which the gels have contracted in seawater solutions. There is also a great difference between gels in distilled water and those in seawater solutions. Distilled water gels have a swelling degree in the region of 4-5.5, which is higher than the hydrolysation value. This is due to the introduction of extra ions, O^- and H^+, into the gel network, therefore augmenting the existing repulsion that causes swelling.

These results demonstrate a possible use of hydrolysed polyacrylamide gels in a marine environment, utilising the significant differences in V/V_0 between gels in distilled water and gels in seawater, regardless of the salinity concentration. This was re-affirmed in a cyclic test (carried out at 40°C) where polyacrylamide gels were repeatedly transferred from distilled water to salinity solutions and back again. Figure 4.7 illustrates the significant swelling and contraction that can occur by changing the external solution from distilled water to seawater. The gels show good repeatability when contracted in seawater solutions. This shrinkage is reversible on transfer to distilled water. The changes in gel volume are not rigid or sudden. It takes approximately one hour at room temperature for a new solvent mixture to permeate a polyacrylamide gel by diffusion [6]. The shrinking or swelling that follows can take much longer to reach completion, perhaps several days [4]. This slow response is comparable to the speed that many marine organisms take to react to

a change in their buoyancy [18], as seen in Chapter 2. Microscopic plankton and many cephalopods, such as the *Nautilus*, can take two or three days to counteract sudden gains or losses to their desired depths. Although the gels prove to be biomimetic in relation to these organisms, the slow response is a major drawback if used in a marine device, where fast responses to changes in buoyancy are usually preferred.

4.2.3 Conclusions on Salinity Studies

The purpose of this study was to investigate polyacrylamide gels for their usefulness as possible actuators in marine applications, such as in buoyancy control of small vehicles and sensor packages. The work demonstrated that such gels contract in various seawater solutions and therefore, the use of polyacrylamide gels as actuators in marine applications might be considered. There was a significant reduction in the degree of swelling of the gels when transferred from TEMED to saline solutions, the most contraction occurring at the highest salinity concentration of 35ppt, corresponding to about a 50% reduction in volume. Slightly less contractions were observed for the lower salinities. All saline solutions promoted an increasing volume as the temperature increased. The significant differences in degree of swelling for gels in seawater and in distilled water also demonstrate their possible applications as actuators in marine applications, although the rate of volume change is quite slow.

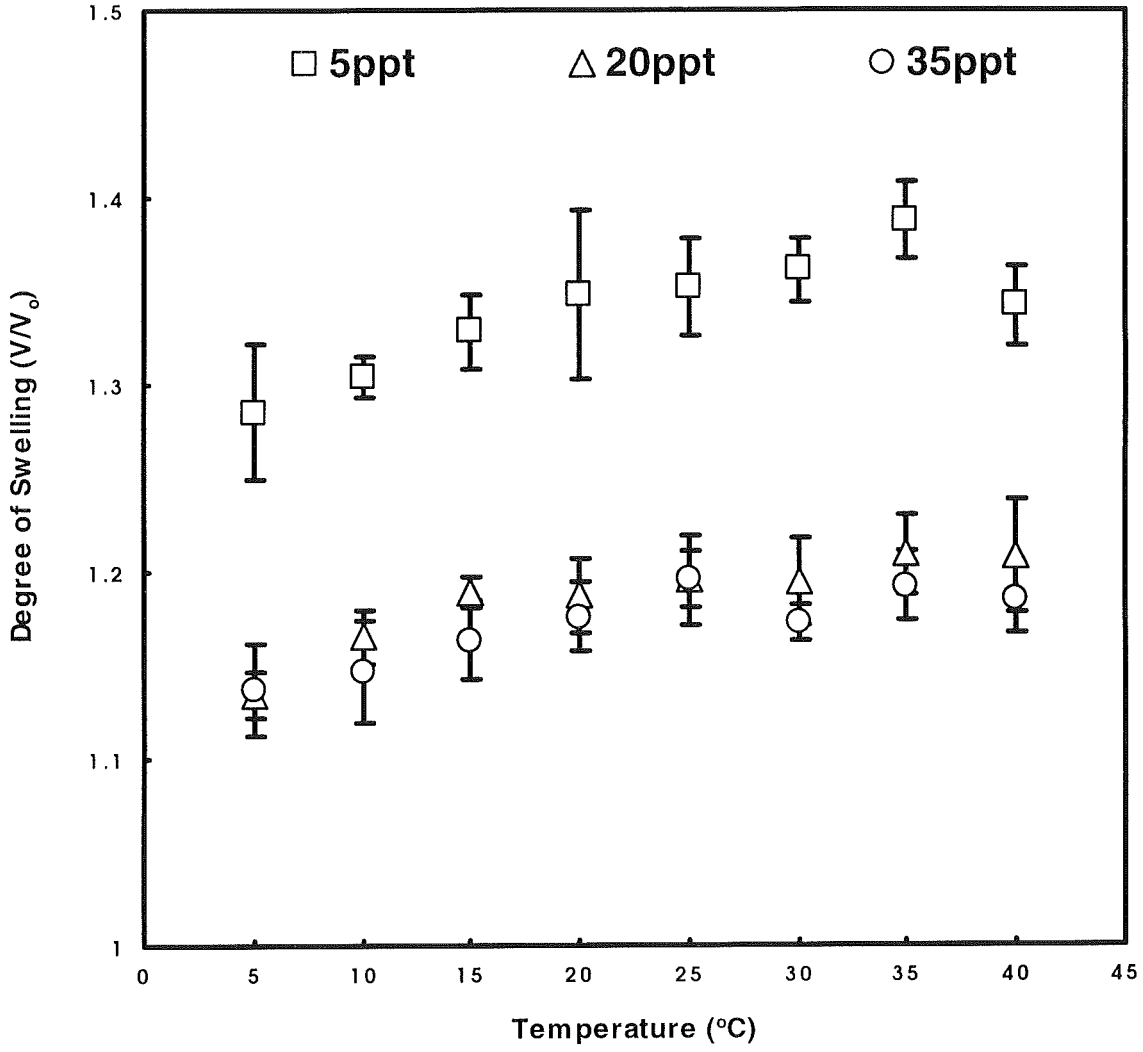

Figure 4.4 Degree of swelling of polyacrylamide gels with respect to temperature when immersed in one of the three saline concentrations.

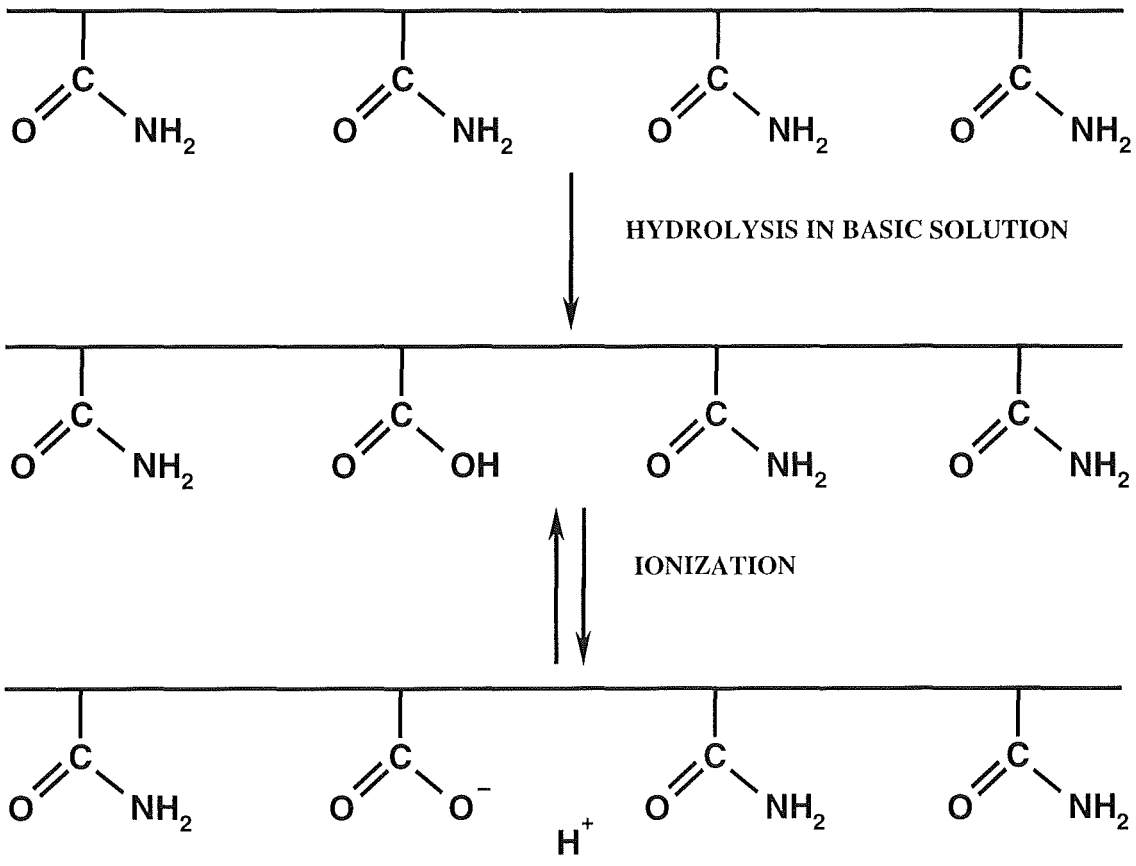

Figure 4.5 Hydrolysis of polyacrylamide gels [6].

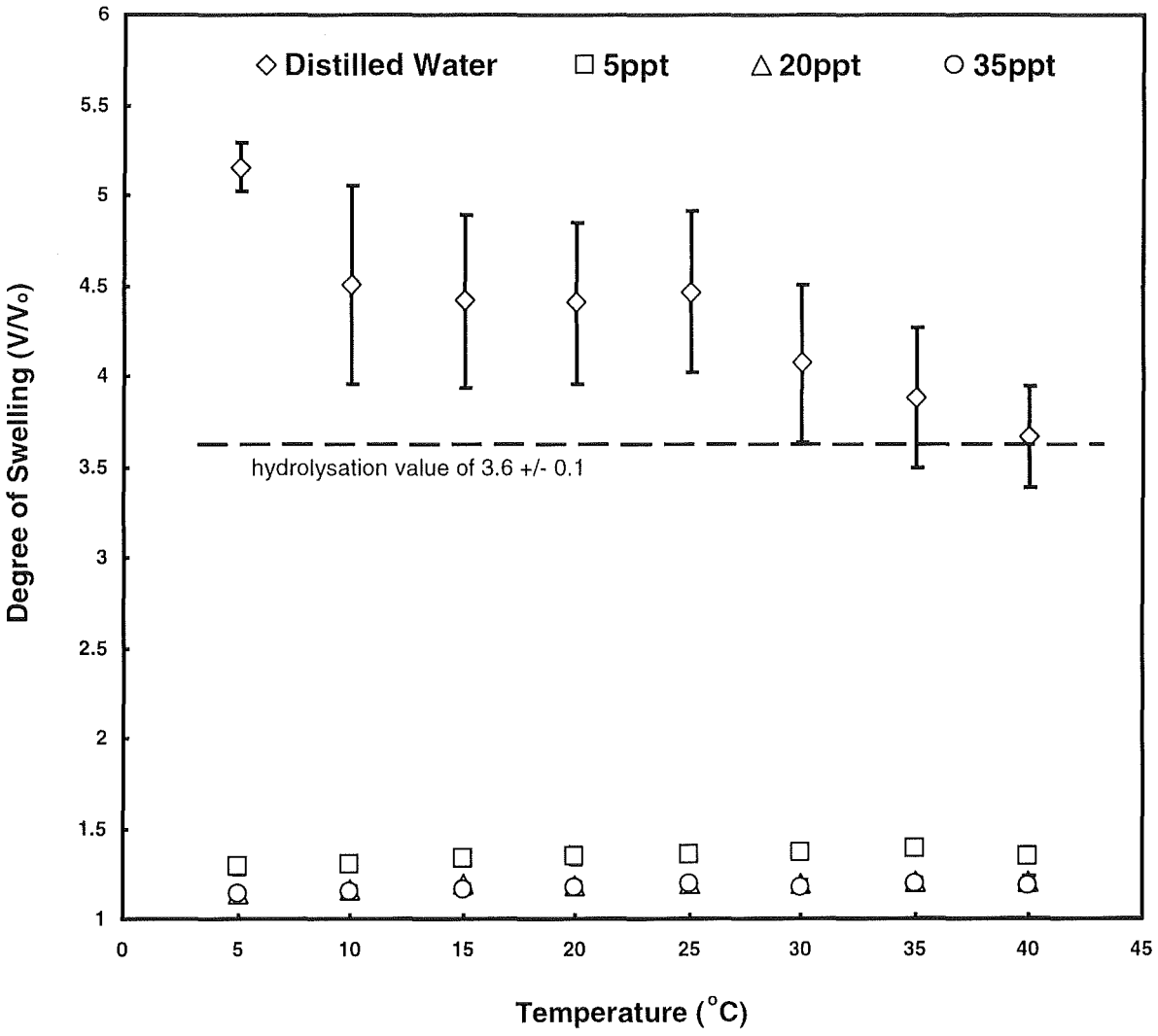

Figure 4.6 Degree of swelling of polyacrylamide gels with respect to temperature when immersed in one of the three saline concentrations and also in distilled water.

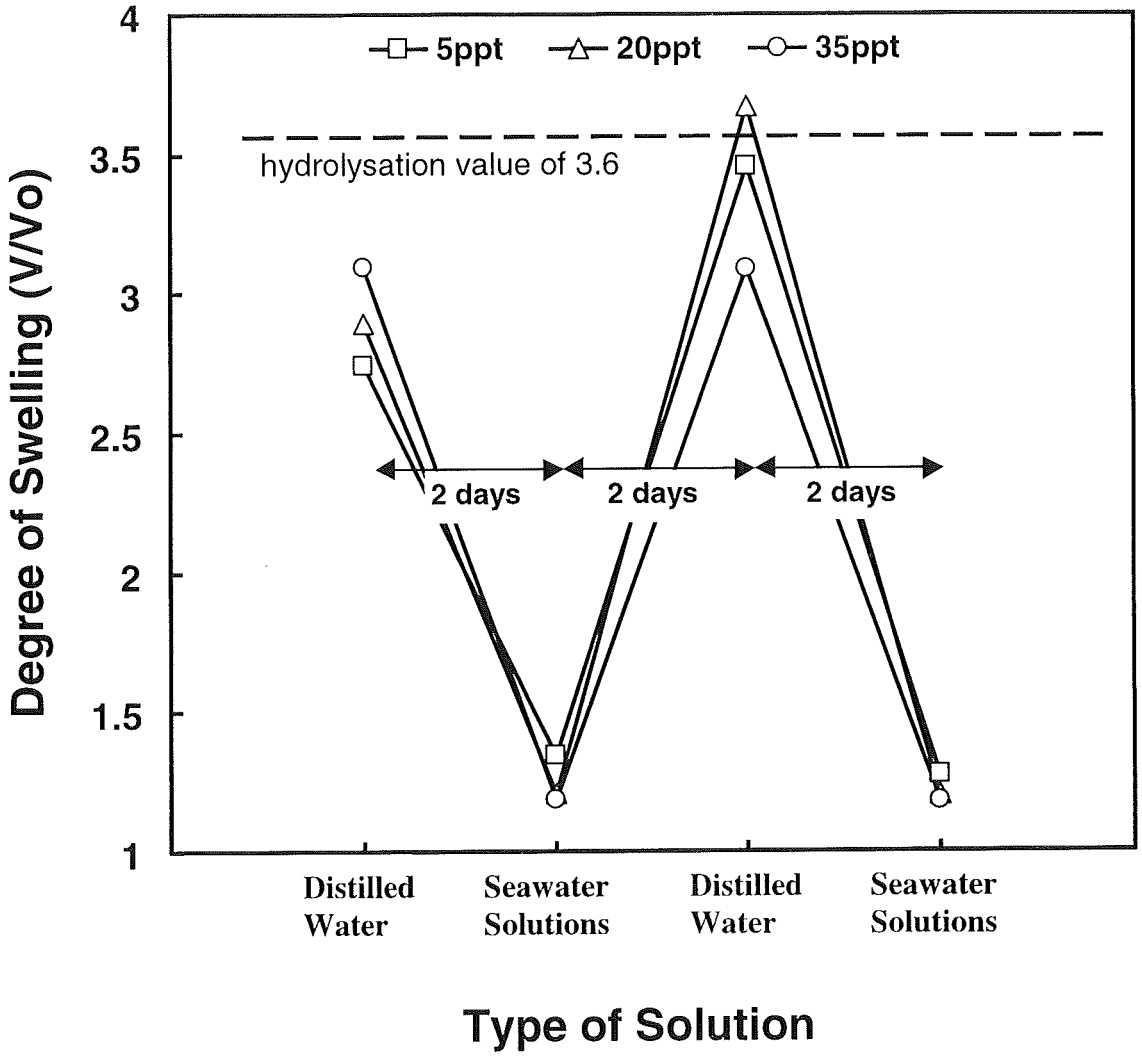

Figure 4.7 Cyclical volume contraction and expansion of polyacrylamide gels when transferred to and from solutions of seawater and distilled water.

4.3 Temperature Studies

In the previous section study, it was found that the salinity of seawater played a significant factor in gel volume of polyacrylamide gels, but the temperature sensitivity was minimal. This separate study concentrates on the behaviour of polymer gel systems that exhibit large volume changes when subjected to certain stimuli, such as temperature. A temperature sensitive gel, such as NIPA (*N*-isopropylacrylamide), has advantages over a solvent-sensitive gel in terms of easier control by onboard vehicle systems.

The volume phase transition of NIPA gels in distilled water has been extensively reported (see Chapter 3, Section 3.4.2.4), where the transition occurs at a temperature of approximately 34°C. The effect of seawater solutions on NIPA gels has not previously been studied. The aim of the current study was to investigate the suitability of NIPA gels as possible elements in underwater vehicles, especially in the area of buoyancy control.

4.3.1 Experimental Details for Temperature Studies

4.3.1.1 Gel Preparation

NIPA gels were prepared using an *N*-isopropylacrylamide monomer and the crosslinking comonomer, *N'N*-methylene-bis-acrylamide. All chemicals were of reagent-grade quality and were used without further purification. The distilled water was produced by a Millipore-U10 system. Transparent rods of gel were prepared based on a method

described by Tanaka [1]. The quantity of crosslinking agent was doubled and the amount of water was halved, in order to produce a more mechanically robust gel. The gels were produced in polypropylene cylinders of various diameters and cured at ambient temperatures for one day. The gel rods so produced were 100mm long and had diameters of 4.8mm, 12.8mm, 15.4mm or 20.4mm. These were washed in distilled water to remove any residue monomers and the rods were allowed to equalise in distilled water at ambient temperatures for one week.

4.3.1.2 Optimum Diameter Study

After equalising, the rods were cut to roughly equal lengths of approximately 30mm. The gel rods were then immersed in distilled water for one day at 34°C, which is 0.5°C above the known phase transition temperature for NIPA gels [19-21]. All gel samples remained cylindrical after the transition period, therefore, the degree of swelling, or contraction in this case, was calculated as a ratio, V_{GEL}/V_0,

$$V_{GEL}/V_0 = (D/D_0)^2 \bullet (L/L_0) \tag{4.2}$$

where V_0, D_0 and L_0 are the volume, diameter and length of the gel rod at preparation and V_{GEL}, D and L the subsequent respective dimensions after each temperature change. Equation 4.2 gives a more accurate indication of the volume ratio than equation 4.1. The gels were then transferred to distilled water at 30°C for one day to allow them to swell again. After this the above test was repeated, but this time the period of time at each

temperature was longer, at 6 days. All tests were carried out in triplicate. Gel dimensions were recorded using a Mitutoyo Profile Projector Type PJ-300, accurate to ±0.001mm.

4.3.1.3 Long-term Density Study

The gel samples used in this study had a diameter of 4.8mm and were roughly equal in length at 15mm. The density studies were carried out using distilled water or seawater collected from the Largs Channel in the Firth of Clyde, Scotland. The seawater had a salinity of 35ppt when collected and was filtered through Whatman glass microfibre filters (GF/C) to remove any bacterial cultures.

The density and volume of each NIPA gel was found using a density bottle (Figure 4.8) [22]. This consists of a pear-shaped flask and a ground glass stopper, which has a capillary hole through its centre, allowing liquid to escape. The volume contained in the density bottle can be determined to 0.001ml, which allows density measurements to be made with an accuracy of 0.01%.

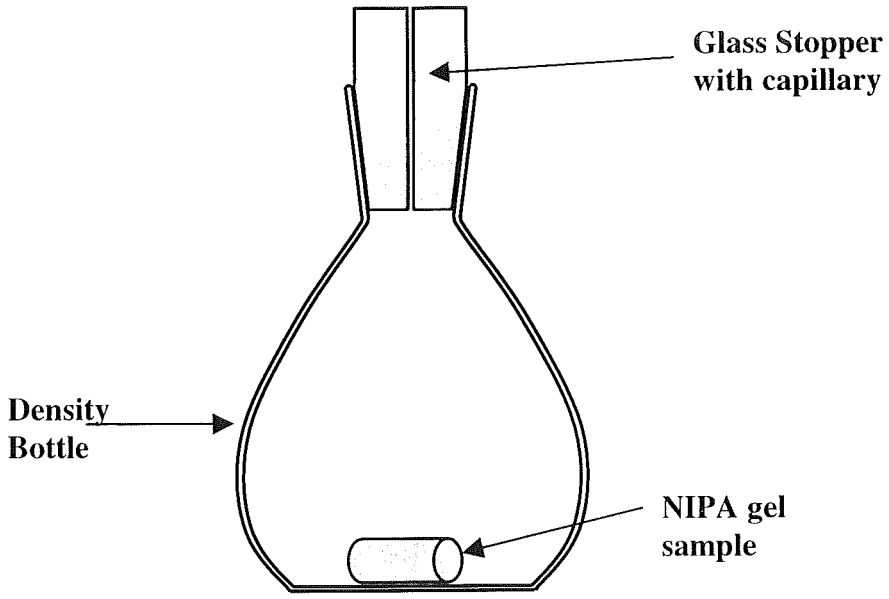

Figure 4.8 Density bottle used for measuring gel density and volume.

The empty density bottle is weighed, M_{DB}, and then re-weighed when filled with a liquid of known density and temperature, M_{DB+L}. The densities of distilled water and seawater are known at all temperatures [11,23]. Care was taken to ensure the exterior of the density bottle was dried of overflowed liquid before re-weighing. The internal volume of the density bottle, V_{DB}, was found from the equation,

$$V_{DB} = (M_{DB+L} - M_{DB}) / \rho_L \tag{4.3}$$

where ρ_L = density of liquid at known temperature. For a gel sample, the empty density bottle was weighed with the gel inside, M_{DB+GEL}, and re-weighed with the bottle filled with liquid, $M_{DB+GEL+L}$. The volume of liquid entrained, V_L, was calculated as $(M_{DB+GEL+L} - M_{DB+GEL}) / \rho_L$. The volume of the gel was then $V_{GEL} = V_{DB} - V_L$ and the density of the gel, ρ_{GEL}, was found from the equation

$$\rho_{GEL} = M_{GEL} / V_{GEL} = (M_{DB+GEL} - M_{DB}) / V_{GEL} \quad (4.4)$$

All experiments were carried out in triplicate. Tests began at 5°C and were taken through a temperature range up to 50°C. The temperature increments were 5°C, but were reduced to 2°C increments between the temperature range 28°C to 40°C. The solutions were kept at constant temperature using a Techne Flow Cooler FC-500 in conjunction with a Techne Circulator C-85D in a 10-litre polymethyl-methacrylate (PMMA) tank of water. After each temperature increase the gels were left to adjust for one day in the respective solution (distilled water or seawater). The solutions were changed daily during the experiments to simulate the dilution effects of a larger body of water. The volume and density of each gel was found as outlined above and these were used to determine the volume ratio at each temperature, V_{GEL} / V_0.

4.3.1.4 Short-term Density Study

NIPA gels in distilled water and seawater solutions were allowed to equalise at 25°C before being transferred to solutions at 50°C for a 12-hour period. As the gels shrank in size, the volumes and densities were recorded using a density bottle, with measurements taken every 2 hours. In a similar study, contracted gels, which had been equalised at 50°C, were transferred to distilled water and seawater solutions at 25°C for 12 hours and allowed to swell.

4.3.1.5 Mechanical Tests on NIPA gels

NIPA gels are known to have a transition temperature of approximately 34°C in distilled water, where a significant reduction in volume can occur over a period of time at that temperature. If the transparent gel is immersed in distilled water at higher temperatures than 34°C, the gel becomes opaque almost instantaneously and there is the possibility that the elastic modulus of the gel increases. The gel turns transparent again and the modulus possibly decreases when the temperature is reduced again.

Compression tests were performed on cylindrical samples (15.4mm diameter) of NIPA gel using a Lloyd L10000 materials testing machine (Figure 4.9). During the tests, the temperature of the gels was kept constant by immersing them in a volume of temperature-controlled distilled water. The distilled water was circulated and kept at a constant temperature using a Techne Circulator C-85D.

To determine the modulus of elasticity of the NIPA gels, they were subjected to a maximum strain of 10%, at the recommended rate of 50% strain per minute [24]. Crosshead displacement was measured using the internal extensometer of the Lloyds testing machine. Tests were carried out in triplicate through a temperature range of 30°C to 46°C, with 2°C increments. The failure stress of NIPA gels was also determined for a range of temperatures. Gel samples were loaded to failure at temperatures of 30°C, 35°C, 40°C and 45°C.

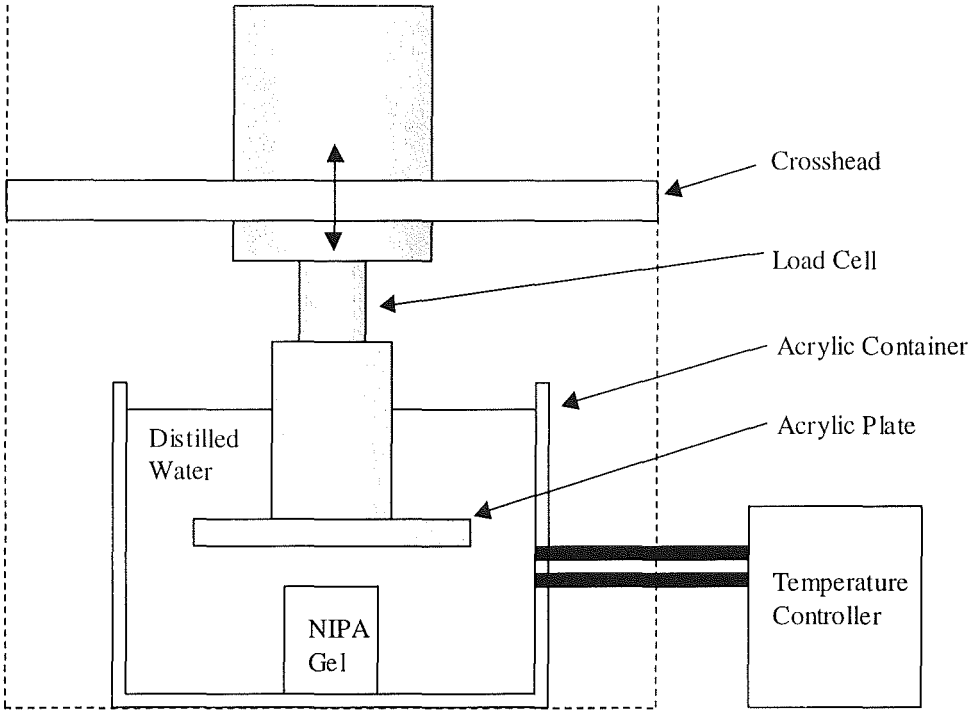

Figure 4.9 Compression test rig.

A series of tensile tests were also carried out on NIPA gel samples to determine the elastic modulus in tension. The main problem with testing in tension was in finding a suitable means of gripping the delicate samples. With conventional grips, it was difficult to maintain a force on the samples that was sufficient enough to prevent slippage of the gels in the grips, but also small enough not to damage the gel and affect the result. An initial attempt was to incorporate a polymer mesh in the tips of the tensile gel specimens, where they were to be gripped. Specially constructed grips with serrations gripped into the mesh to hold the specimen. To ensure that no undue stress was placed on the specimen, the deep serrations at the extreme end of the grips became progressively shallower towards the edge where the test took place. The grips were slightly tapered and the edges rounded to further reduce any stress. Helical springs and a nut and bolt provided the normal force on the mesh and gel.

In initial tests, the serrated grips were found to impart much stress on the samples, causing the samples to break at the mesh boundary. A redesign of the grips involved cutting a wedge-shaped groove into them, using a CNC machine. The wedge grip would hold specially moulded gel samples in place without imparting too much stress, as in Figure 4.10. Trial tests showed that no slippage or stress concentrations occurred at the grips.

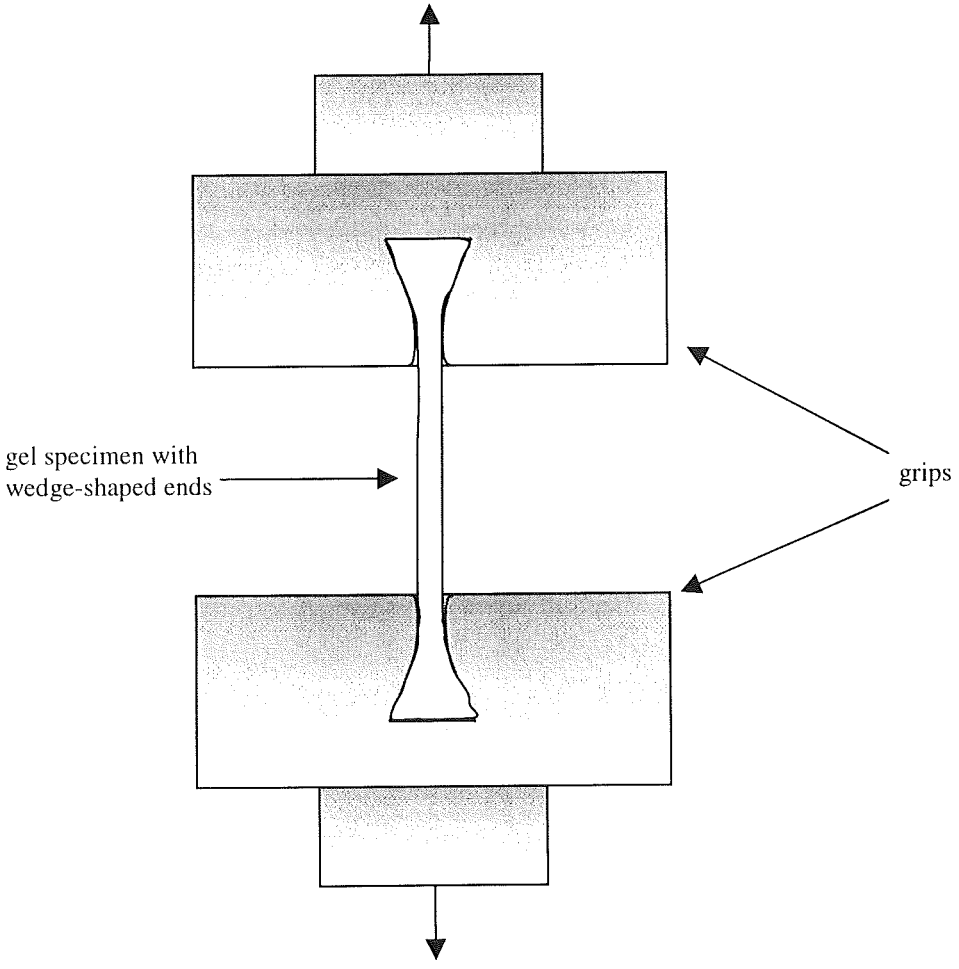

Figure 4.10 Tensile test rig using wedge-shaped grips and specimens.

Tests were carried out on the wedge-shaped tensile specimens of NIPA gel at temperatures ranging from 30°C to 47°C, using the Lloyds testing machine and internal extensometer. The specimens had a width of 3mm and a thickness of 4.5mm. The gauge length of the specimens was 35mm and a 10% strain was subjected to the gels at each temperature. Strain rate was set at the recommended 50% per minute. During the tests, the temperature of the gels was kept constant by immersing them in a volume of temperature-controlled distilled water.

4.3.2 Results and Observations on Temperature Studies

4.3.2.1 Optimum Diameter Study

The results of this study can be seen in Figure 4.11. After immersion at 34°C for one day, the volume change (contraction) increases as the gel diameter decreases. This is also true when the gels were immersed in solutions at 30°C for one day. Only the gel samples with the smallest diameter, 4.8mm, actually achieved a fully reversible volume change. Even after longer periods at respective temperatures, the larger diameter gels did not realise a volume transition comparable to smaller diameter samples. This is because the time needed for water diffusion into or out of the gel, to effect swelling and shrinking, is proportional to the square of the gel diameter [21]. In fact, most researchers now use gels of sub-millimetre size to speed up experiments [19]. If NIPA gels are to be used in

applications involving buoyancy control, these response characteristics need to be taken into account.

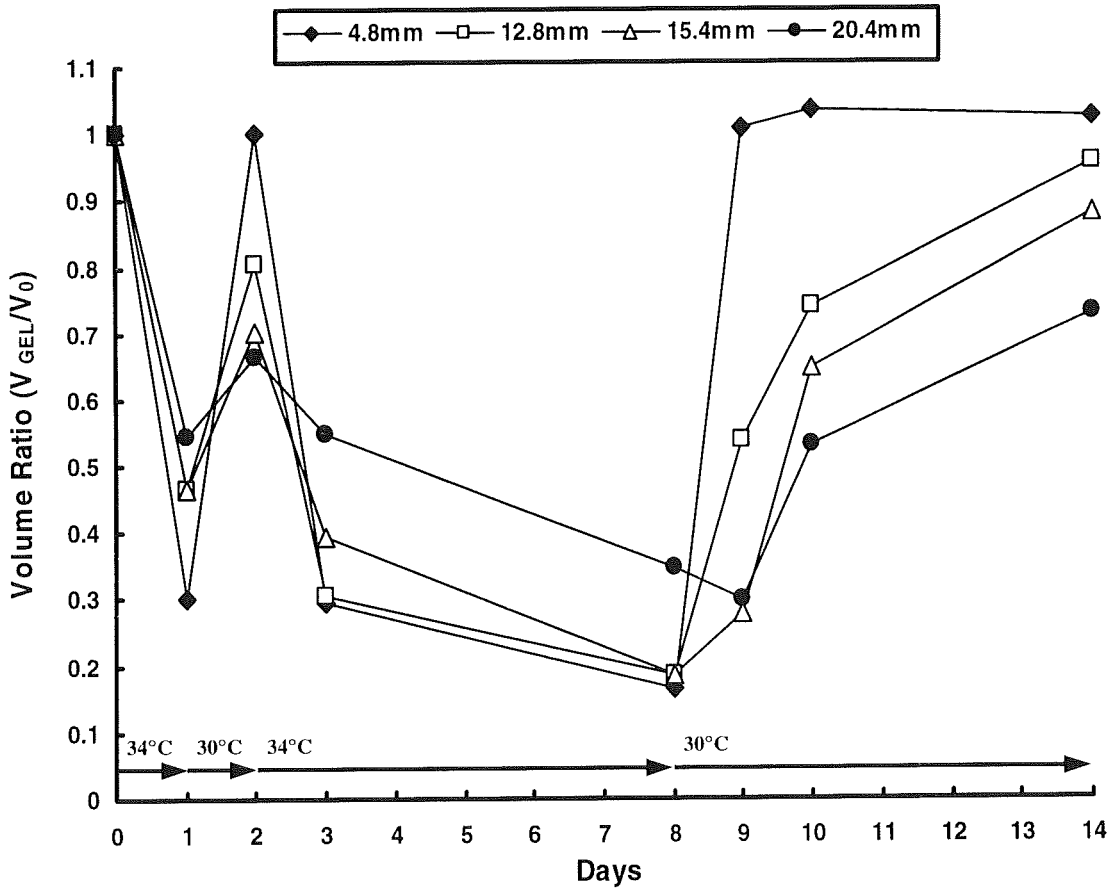

Figure 4.11 Dependence of gel volume on gel sample diameter and time in distilled water during temperature cycles.

4.3.2.2 Long-term Density Study

The volume ratios of NIPA gels, in both distilled water and seawater, as the temperature is increased slowly from 5°C to 50°C, are shown in Figure 4.12a. The volume phase transition temperature for NIPA gels in distilled water is known to be approximately 34°C [1] and the gels in this study do achieve full contraction at, or just above, this temperature. A surprising outcome for NIPA gels in seawater is that the transition temperature is significantly lower, in the range of 26 to 28°C. This is encouraging, as the power needed to heat the gels to this temperature would be less than if they were immersed in distilled water solutions. Saltwater effects on gel volume include polymer-polymer interactions and the combination of the three competitive interactions of polymer-water, polymer-ion and water-ion [19]. The polymer-water interaction is most important with respect to the shrinking force, as this depends on the association and release of structured water from the hydrophobic groups. The addition of salt affects the structures of the bound water, causing a shift in transition temperature to the lower temperature side.

In the swollen state, the NIPA networks are strongly bound to many water molecules and, further, loosely surrounded by many water molecules. As the temperature is increased, the hydrogen bonds among water molecules will gradually be destroyed because of vigorous thermal motions of molecules, leading to a loss of water molecules that are loosely bound [25]. The loss accompanies a decrease in the volume of the gel. The polymer network is now in closer contact and, thus strengthened, as are the polymer/water interactions, thus eventually leading to the collapsed state.

The corresponding densities of the gels as they shrink and undergo the phase transition are shown in Figure 4.12b. There is little change in density for gels in seawater or distilled water, below their respective transition temperatures. This, however, changes once the transition temperature is exceeded. For gels in distilled water, the density decreases by 15-25%. Gels in seawater exhibit the opposite effect after they exceed their transition point, in that they become denser (by as much 30-40%), before returning to their original densities at higher temperatures. The standard deviations tend to increase soon after the transition is reached. This may be due to the fact that the gels become a two-phase system during transition [20], with both shrunken and swollen phases in coexistence. As temperature increases, the shrunken phase becomes dominant due to the hydrophobic effect, but small pockets of swollen material may still exist which could affect the density of the gel.

The large change in density seen at approximately 34°C, coupled with the corresponding reduction in volume, could pave the way towards a variable volume/density device suitable for controlling the buoyancy of small underwater vehicles and sensor packages. This device could use the control of the temperature of a local volume of seawater from 25°C to 34°C, to bring about the density change, or a change of solution from seawater to distilled water at 34°C, where the density difference is most pronounced, at approximately 39%.

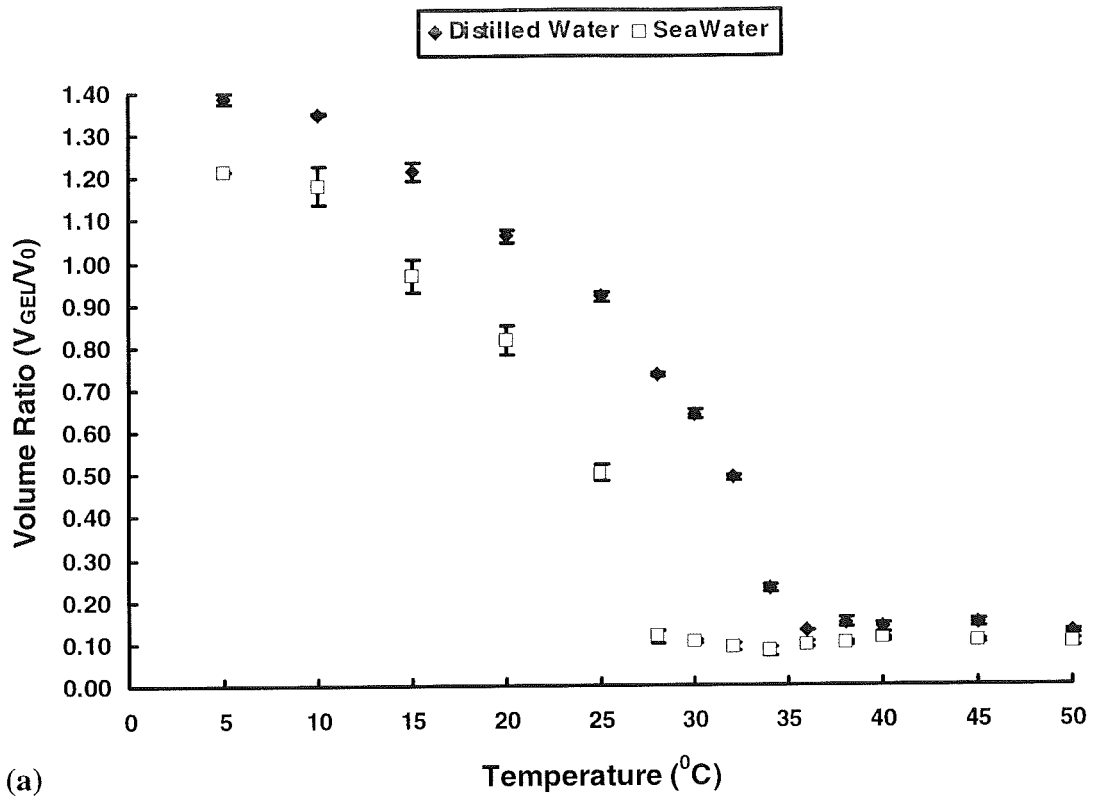

(a)

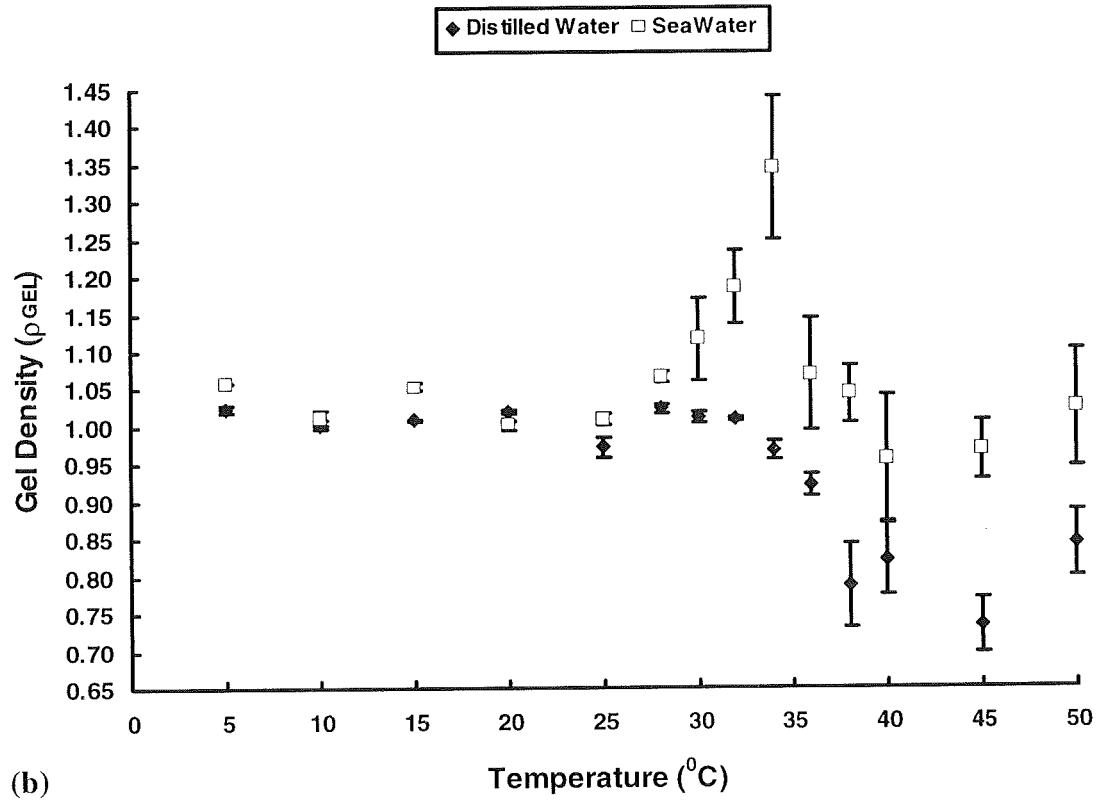

(b)

Figure 4.12 (a) Gel volume as a function of temperature for gels in distilled water or seawater. (b) Corresponding dependence of gel density on temperature.

4.3.2.3 Short-term Density Study

Having a gel system with a fast response time is of great interest in the field of buoyancy control. Figure 4.13a shows the reduction in volume of NIPA gels when immersed in distilled water and seawater at 50°C for a period of 12 hours. Figure 4.13b shows the corresponding density changes. After 6 hours the gels have shrunk to a volume ratio comparable to the long-term study. There is much fluctuation in density for both distilled water and seawater gels during this period, including a brief drop in density at the 4-hour mark. The phase coexistence is most pronounced at this point, as can be seen in Figure 4.14, and this presence of collapsed sections and hydrated swollen sections has possibly caused the gels to become less dense. After 6 hours, however, the gels are predominantly collapsed and, thus, increase in density again.

A study on the densities of the individual components of NIPA gels in distilled water, i.e. the polymer network and the solvent, revealed that the density of the polymer network in the swollen phase (T=30°C) was very low, at around 0.05 g/cm^3 [25]. The corresponding entrained solvent density was about 0.93 g/cm^3. At 34°C, the network density increased dramatically to 0.4014 g/cm^3, and the solvent density decreased suddenly to 0.6160 g/cm^3. As the temperature was increased to 50°C, a small steady increase was noted in the density of the network. The solvent density decreased slightly, but the decrease was not as steady, with slight increases noted. Therefore, the density fluctuations, observed in Figure 4.13b, could be a result of the density of the solvent component of the polymer gel and the presence of phase coexistence.

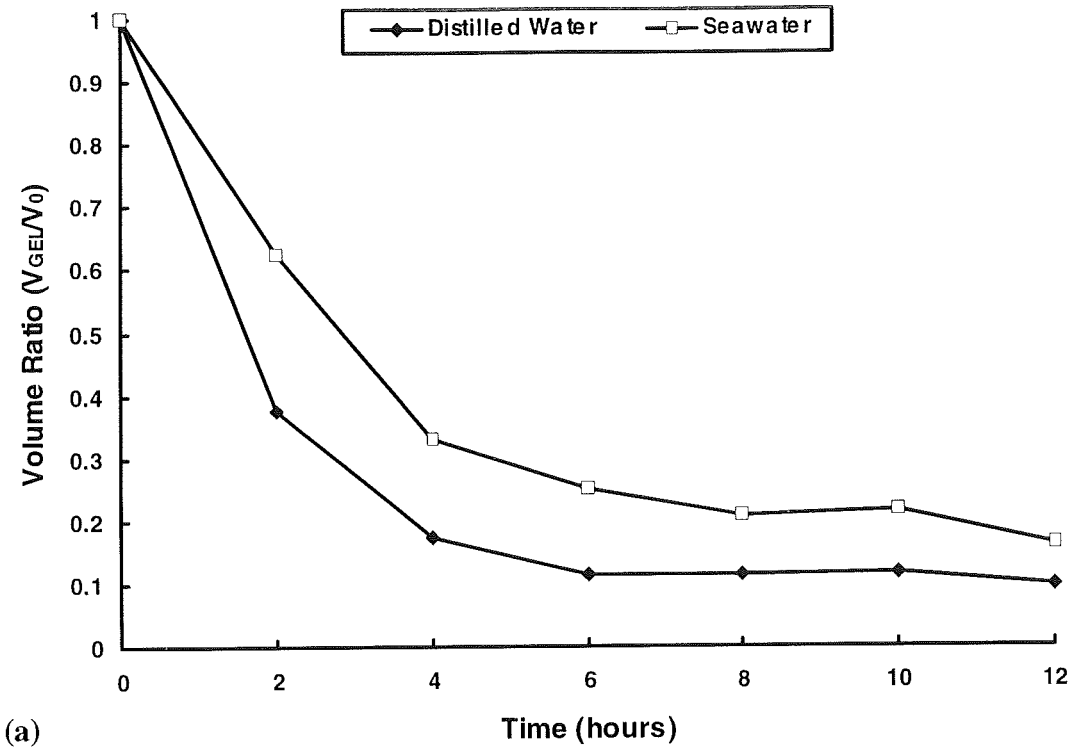

(a)

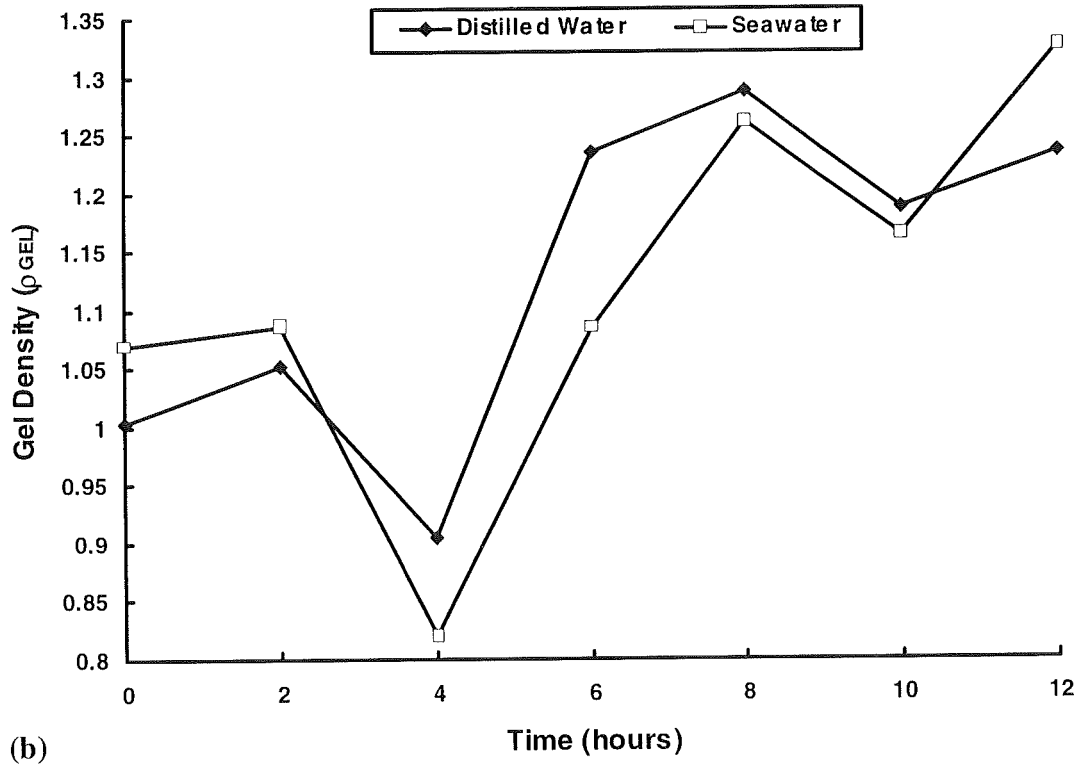

(b)

Figure 4.13 Short term effects on gels in distilled water or seawater immersed at 50°C for a period of 12 hours. (a) Gel volume; (b) Gel density.

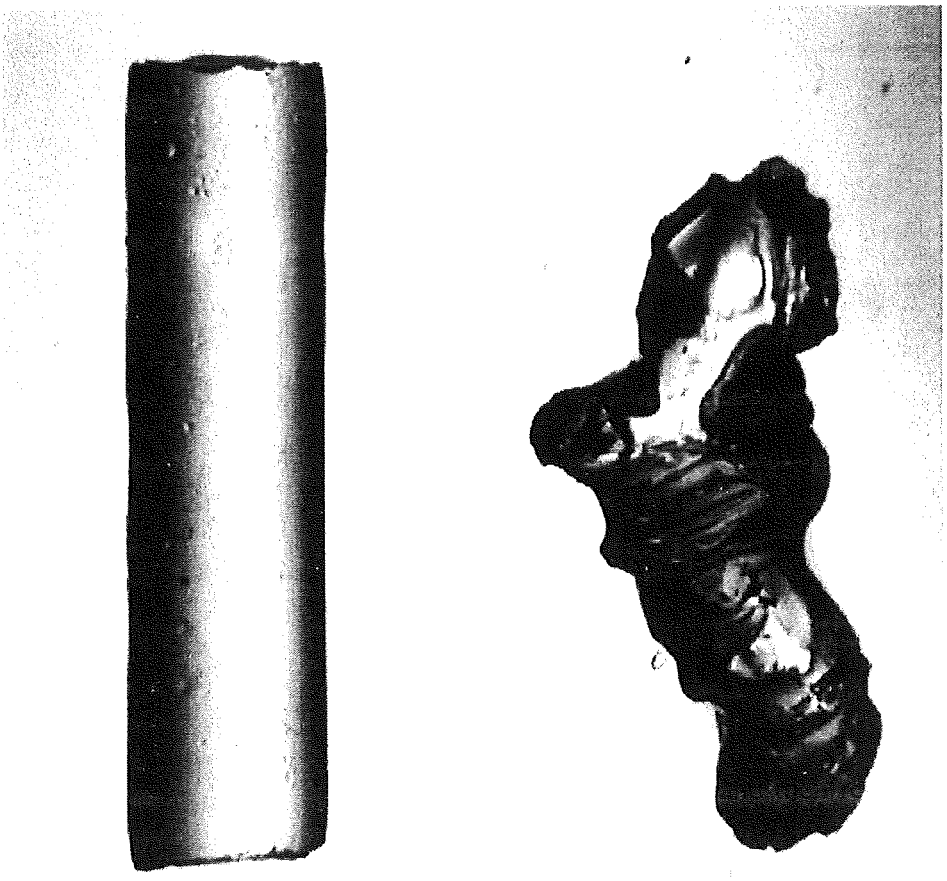

(a) (b)

Figure 4.14 (a) NIPA gel below the phase transition temperature. (b) Gel exhibiting phase co-existence as it contracts.

The collapsed gels from the previous study were allowed to reswell at 25°C. The change in volume from the collapsed phase to the swollen phase took place at a slower rate than when they were shrinking, as can be seen in Figure 4.15a. After 12 hours they still had not returned to their original volume and needed a full 24 hours to do so. This could simply be a thermodynamic reason, as the reswelling of the gel samples took place at a lower temperature than during the contraction phase.

The corresponding densities, in Figure 4.15b, fluctuate in the first 4 to 6 hours, where the coexistent phases are most prevalent and where the density of the solvent component of the polymer gel seems to be at its most erratic. During the following 6 hours of reswelling at 25°C, the overall densities of the NIPA gels settle into a smaller range. The density fluctuations are not as pronounced as the NIPA gels undergoing a collapse at 50°C, and, again, this could be due to the more relaxed thermodynamic state at 25°C.

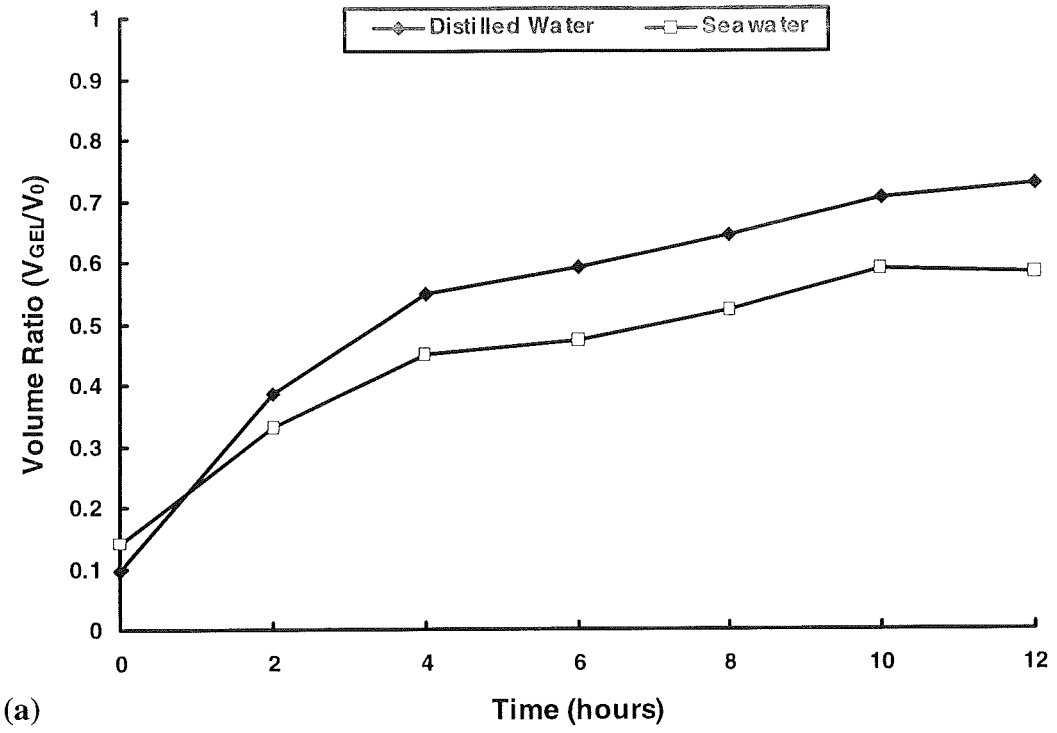

(a)

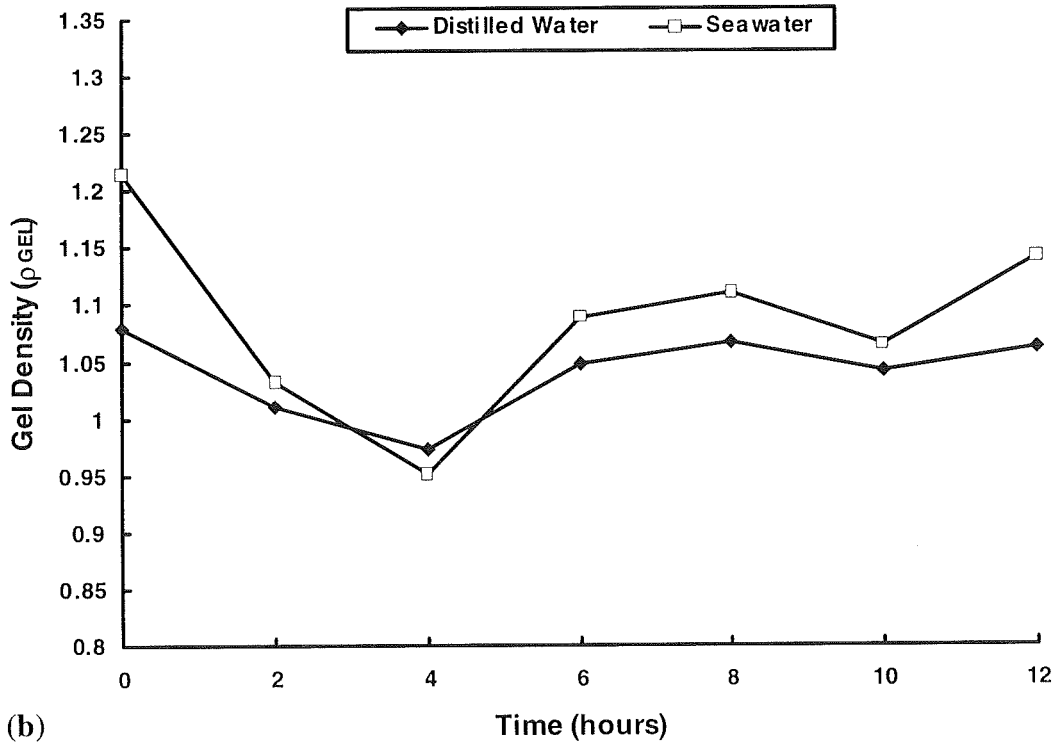

(b)

Figure 4.15 Short term effects on gels in distilled water or seawater immersed at 25°C for a period of 12 hours. (a) Gel volume; (b) Gel density.

4.3.2.4 Mechanical Tests on NIPA gels

Compression tests performed on NIPA gels in distilled water reveal that the mechanical properties also depend on the temperature of the gel and the volume phase transition temperature. These gel materials are very soft and mechanically quite weak. The elastic Young's modulus of NIPA gel at 30°C is 0.0152 MPa, which is approximately 5% of that of low modulus, acetoxy type silicone rubber sealant. The yield stress at 30°C is also very low (0.0395 MPa). Figure 4.16 shows the relationship between elastic modulus and temperature of NIPA gels. Up to 34°C there is hardly any change in elastic modulus. This is followed by a sharp increase in modulus as the temperature is raised from 34°C to 42°C. The elastic modulus levels off to a plateau at higher temperatures. There is a corresponding relationship between the transparency/opaqueness of the gel and the elastic modulus. Below 34°C the gel is relatively transparent, with just a slight cloudiness. At 36°C the gel becomes more opaque, turning white in colour. As the temperature is increased further, the gel becomes increasingly opaque. This indicates an inhomogeneity on the order of the wavelength of light develops, and the effective number of crosslinks increases as the result of the temperature increase [20]. It is interesting to note that an aqueous solution of NIPA also turns opaque with an abrupt increase in temperature, which is reversible. The corresponding viscosity of the solution has not been investigated, but an instantaneous increase in viscosity with temperature would be analogous to electro-rheological and magneto-rheological fluids, but with an easier and safer means of controlling the fluids.

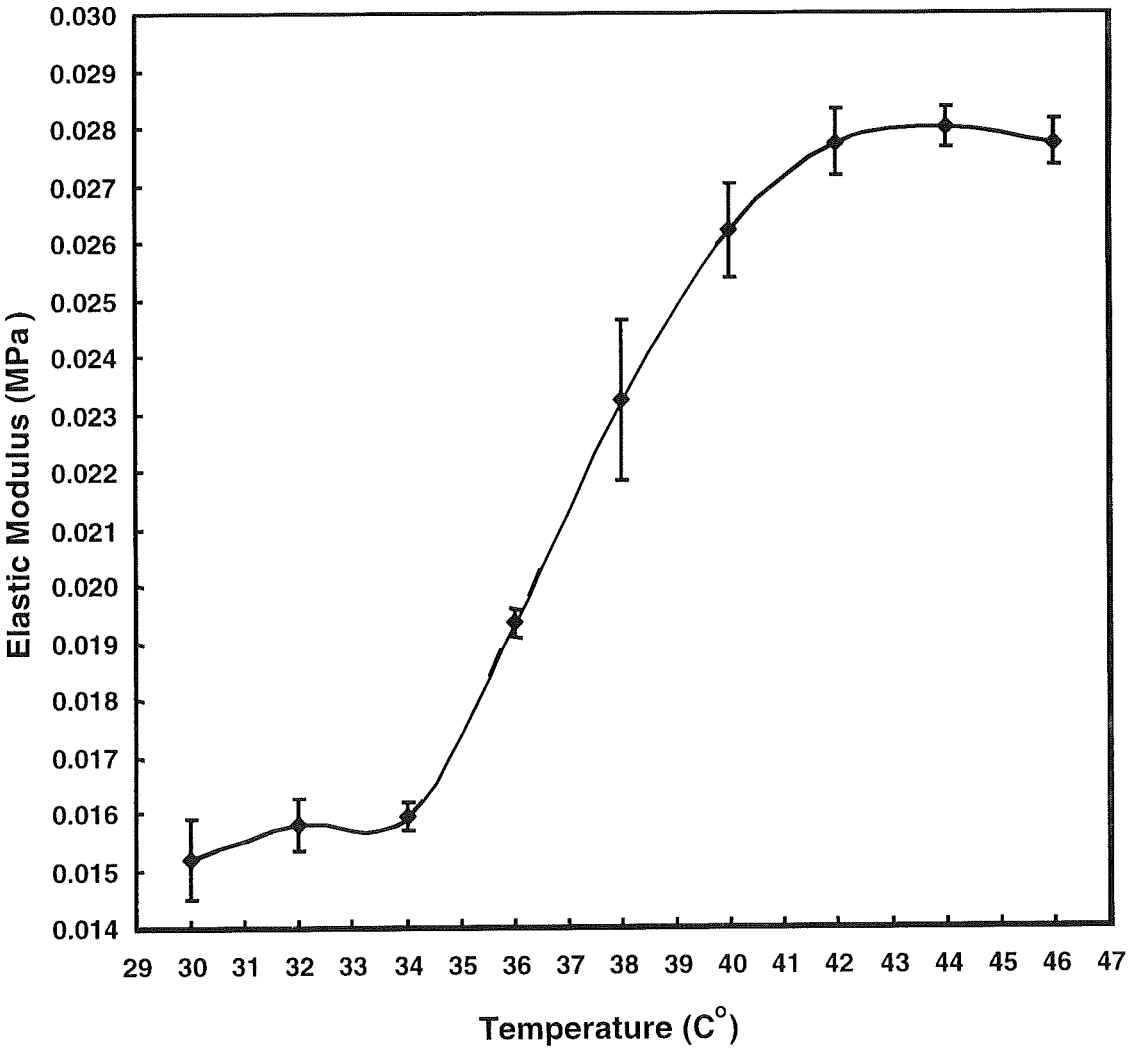

Figure 4.16 Compression elastic modulus as a function of temperature for NIPA gels tested in distilled water.

A corresponding increase is noted for the failure stress, as can be seen in Figure 4.17. There is a sharp, 4-fold, increase in failure stress as the temperature is raised from 35°C to 45°C. The nature of failure also depends on the temperature. A NIPA gel at 30°C is transparent and fails catastrophically at the yield point. The gel shatters into small

fragments and the load drops almost to zero, as can be seen in Figure 4.18. The subsequent increase in load is due to the compression of some of the smaller fragments.

A NIPA gel at 35°C is in an unstable condition, because it is so close to the critical transition temperature of 34°C. It is partly transparent and partly opaque. There are two types of strand densities present, microscopic bunched strands and large open strands. The gel fails catastrophically, but at a slightly lower stress and strain than the 30°C gel.

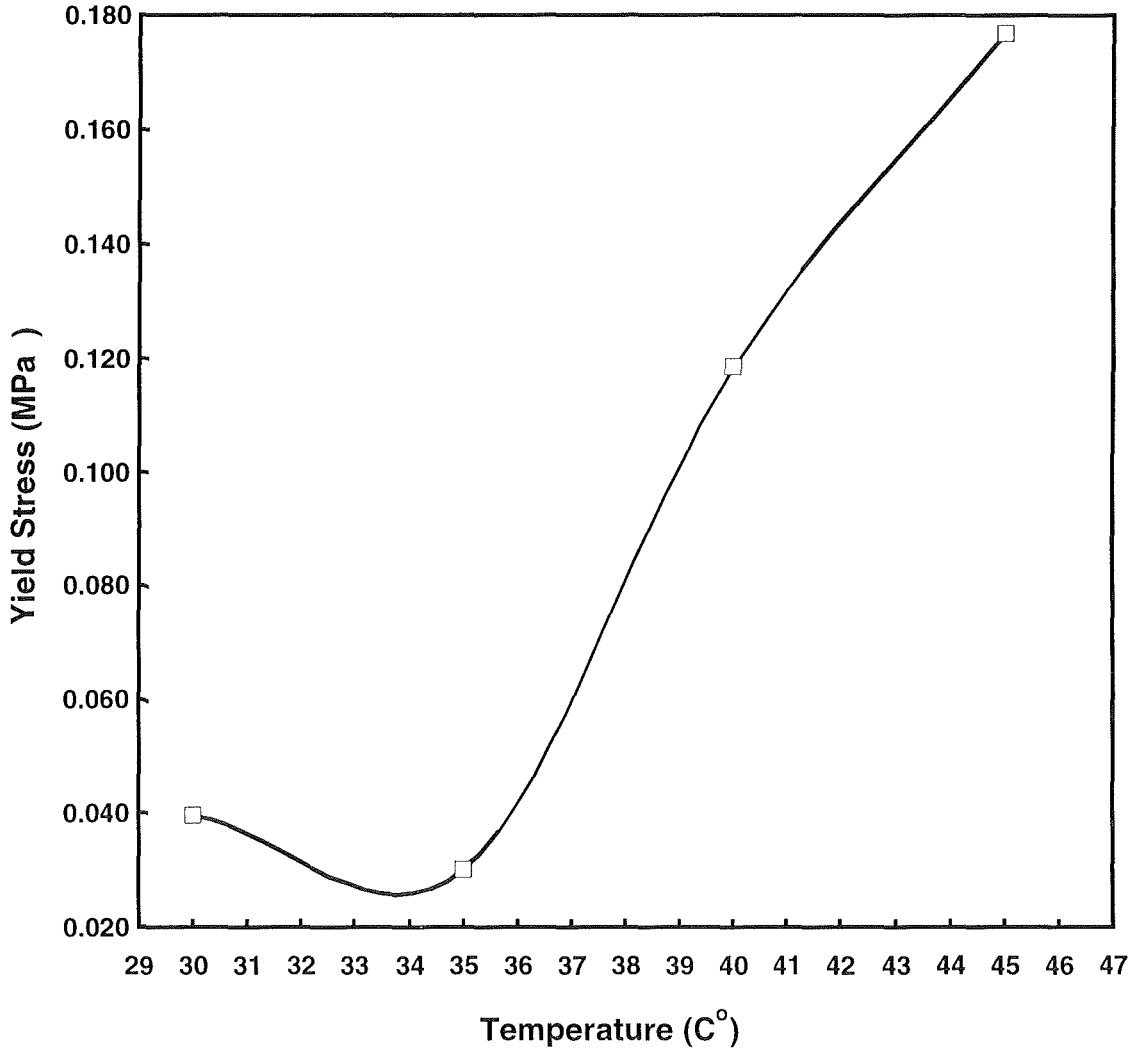

Figure 4.17 Failure stress as a function of temperature for NIPA gels tested in distilled water.

Gels at 40°C and 45 °C have become highly opaque and have a sponge-like property to them. There is no catastrophic failure present, just a yield point where the stress drops by about 20-25% before increasing again. Beyond this point the gel continues to be compressed between the two plates, and gets squeezed out the sides, much like a piece of plasticine. The development of opacity with temperature is reversible, and the rapid change shows that effective crosslinks are made through the association of segments which are already in close proximity with each other in the gel [20]. Few studies have been conducted on the opaque state of NIPA gels, but a preliminary study found that opaque gels exhibit significant viscoelasticity, and suggested that this may be due to the fact that the effective crosslink is not a permanent one but its position is changed by an external stress [20].

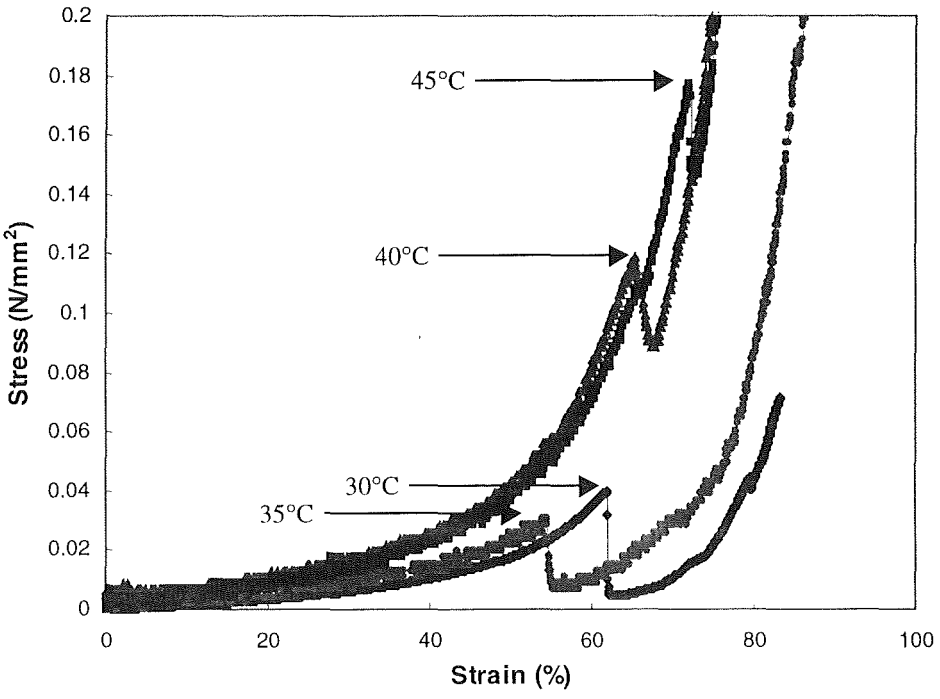

Figure 4.18 Stress-strain characteristics of NIPA gels tested to failure in distilled water at various temperatures. Arrows indicate failure point of the NIPA gels specimen at each temperature.

The results for NIPA gel specimens tested in tension are shown in Figure 4.19. Again, there is a marked increase in elastic modulus when the temperature of the NIPA specimen is increased. At 34°C, the magnitude of elastic modulus drops briefly, before increasing again. As 34°C is near the phase transition temperature, the mechanisms of phase coexistence could be influencing the result.

The modulus values obtained in both compression and tension were found to be quite low, even at high temperatures. The tensile modulus at high temperatures is similar in magnitude to the compression modulus. At low temperatures, however, the tensile modulus is about twice the magnitude of that recorded in compression. This could have been due to the sensitivity of the 50 Newton load cell. The recorded results for the tensile and compression moduli, at 30°C, were right at the sensitivity threshold of the Lloyds load cell. The manufacturers state that tests performed in compression output results with less of an error than the results from tests performed in tension. It can be assumed, then, that the compression results are more accurate than the tensile results, at 30°C, and, therefore, the results from the tensile modulus tests may, in fact, have been lower and similar to those in compression.

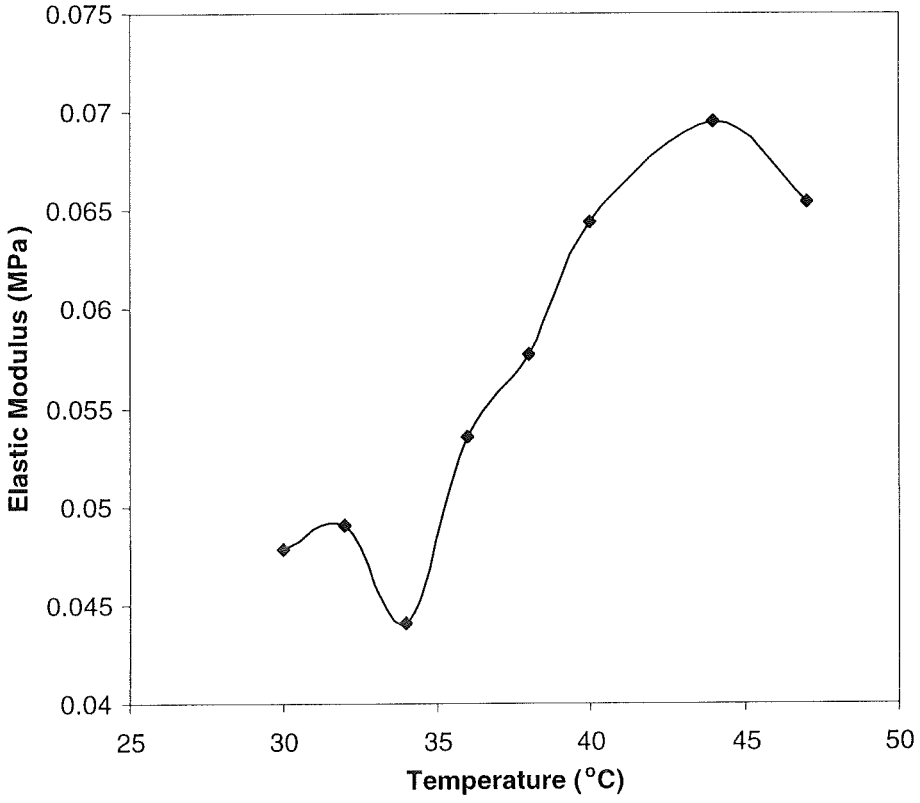

Figure 4.19 Tensile elastic modulus as a function of temperature for NIPA gels tested in distilled water.

4.3.2.5 Design Implications from Temperature Studies

The results of this study illustrate the possible uses of NIPA gels in the control of buoyancy in small, underwater vehicles. The significant change in compliance of the material could be exploited to create a passive or very low power, variable stiffness element, which could be controlled through a change in temperature, to counteract the

effects of seawater pressure. A change in compressibility could be enough to correct deviations from the neutral buoyancy position.

The differences in density of NIPA material in seawater, compared to its density in distilled water, could also be effectively used in buoyancy control. From Figure 2b, it can be seen that the density of the NIPA gel in seawater changes from a value very close to that of natural seawater (1.024 g/cm^3 at 20°C), to a maximum of 1.344 g/cm^3 at 34°C. A marine organism capable of changing its density by such a margin could increase or decrease its rate of sinking by almost 67% [18]. A small underwater device incorporating an element of the NIPA material could, with a suitable seawater or distilled water exchange system, bring about a substantial change in its overall density to control the buoyancy of the vehicle.

4.3.3 Conclusions on Temperature Studies

The purpose of this study was to investigate NIPA gels for their usefulness as possible actuators in marine applications, such as in the buoyancy control of small vehicles and sensor packages. The work demonstrated that for such gels there is a significant contraction in both distilled water and seawater solutions and that the volume phase transition temperature is lower for gels in seawater. The majority of contraction can occur within a couple of hours. The density of NIPA gels also changes above the transition temperature, increasing in seawater and decreasing in distilled water. The significant differences in mechanical properties, density and volume of NIPA gels, as temperature

and solvent medium is changed, demonstrate the possible use of NIPA materials as controllable actuators in specific marine applications, such as the control of buoyancy of small, autonomous marine devices.

4.4 Actuation Stresses and Strains of Polymer Gels

It has been shown that the mechanical properties of polymer gels can change under the influence of temperature. Studies have also shown that polyacrylamide and NIPA gels undergo substantial volume changes under the influence of stimuli such as salinity and temperature. These characteristics could prove very useful as actuator elements in marine environments, and the current study has attempted to quantify the actuation stresses and strains produced during the volume phase transition. Both the actuation stresses and strains produced due to swelling and contraction were measured.

4.4.1 Swelling Stresses and Strains – Experiments and Results

An experiment was set up where a cube of polyacrylamide gel (side length 18mm) was placed between two plastic plates, separated by extension springs, and allowed to swell against the springs of known stiffness. The polyacrylamide gel was prepared using the method described in previous sections [5], and cast in polypropylene cube trays of side 18mm and cured at room temperature for one day. The gel cubes were washed in distilled water to remove any residue monomers and the cubes were then allowed to equalise in distilled water at room temperature for one week.

The two plastic plates were set 18mm apart, separated by four extension springs, one at each corner, therefore imposing zero stress on the gel sample at the start of the test. This spring system had a stiffness of 0.33 N/mm. The cube of gel which was placed centrally between the plates, and the system was immersed for one week in a bath of 1.2% TEMED solution, which was kept at a temperature of 44°C by a hot plate. Preliminary studies had determined that the swelling process in 1.2% TEMED was accelerated at higher temperatures. A polysterene casing was placed around the bath to further maintain the temperature (Figure 4.20).

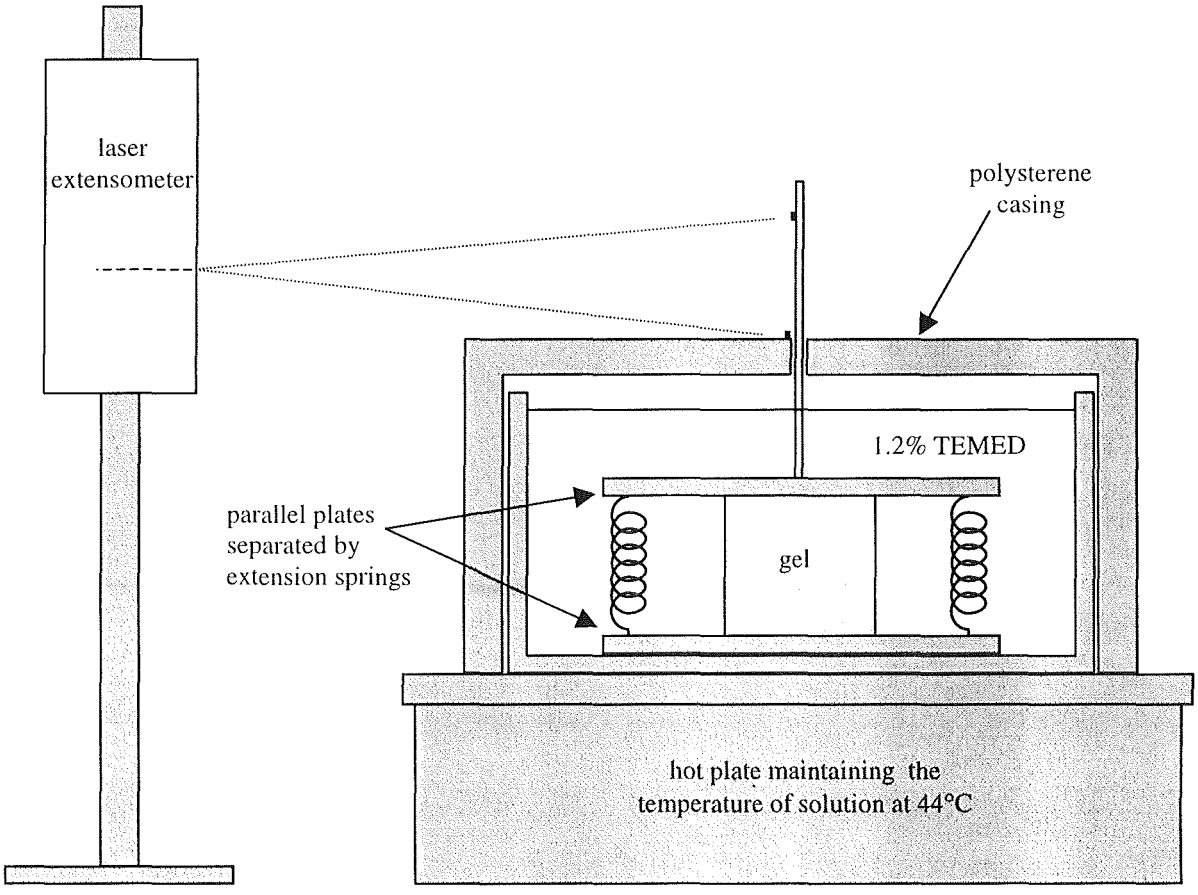

Figure 4.20 Test rig for measuring the swelling stresses of polyacrylamide gels immersed in 1.2% TEMED at 44°C.

A Lloyd's laser extensometer was used to record upper plate extension as the gel swelled in the TEMED solution. To do this a thin plastic strip rose vertically from the top plate through an opening in the polysterene. A relative displacement could be read from this strip. The actuation force exerted on the upper plate, due to the swelling of the gel cube, was calculated using the measured displacement and the stiffness of the spring system, 0.33 N/mm.

Figure 4.21 shows the actuation swelling forces exerted against the upper plate, as the polyacrylamide gel swelled in 1.2% TEMED at 44°C, over a period of 7 days. So as not to affect the test, the dimensions of the gel could not be measured as the cube was swelling. Therefore, the actuation stresses due to swelling could not be determined during the test period. The cross-section area of the cube at the end of the test was 23.5mm x 23.5mm, which corresponded to an actuation stress on the upper plate of 3.272×10^{-3} MPa, which is quite a low actuation stress.

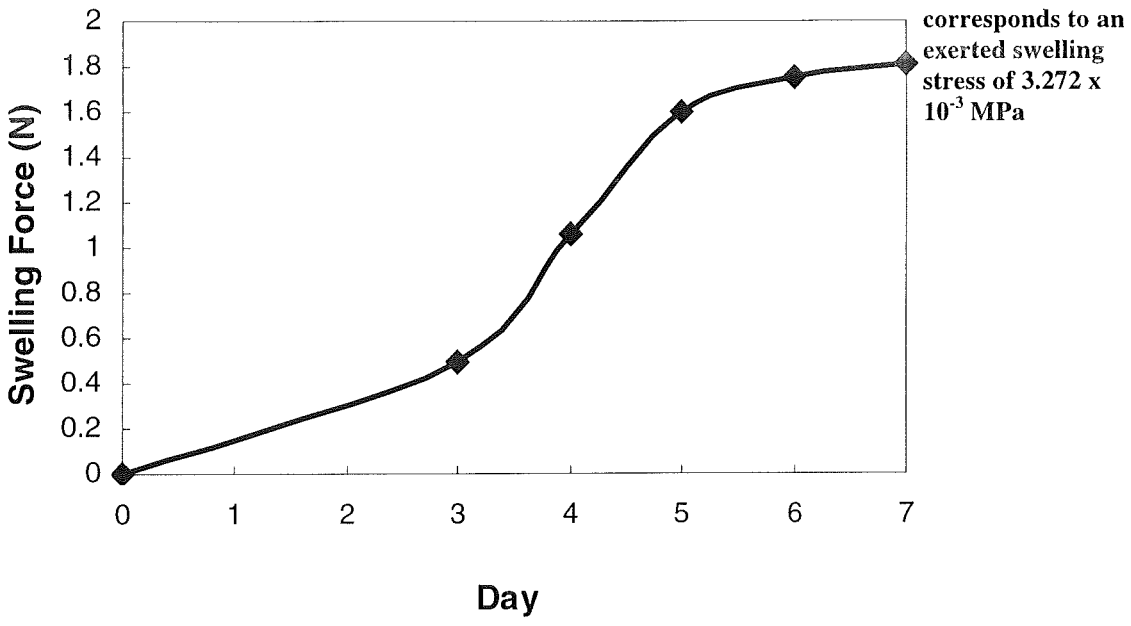

Figure 4.21 Actuation swelling forces of polyacrylamide gel immersed in 1.2% TEMED at 44°C for one week.

The gel sample in the above experiment swelled isotropically in the TEMED solution, i.e. swelling took place in all three axis directions. It is difficult to get an accurate measure of swelling pressure during the test, because the original dimensions change as the gel swells. The desired swelling for linear actuation is in one direction. Therefore, the test was modified to restrict swelling on the sides of a gel sample, leaving only one direction for the gel to swell. There were two advantages to this set-up: cross-sectional area of the gel sample would remain constant throughout the test, allowing ease of stress calculations without interfering with the test; and it was hoped that the 'restricted' swelling would be transferred to the free-swelling direction, thus augmenting the reaction in that direction.

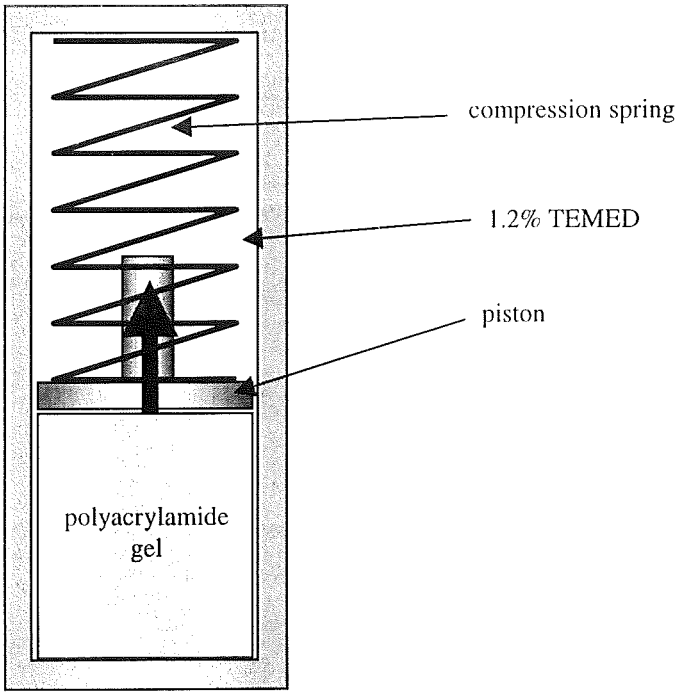

Figure 4.22 Test rig for measuring the swelling stresses and strains of polyacrylamide gels immersed in 1.2% TEMED at 44°C. Swelling has been restricted to just one direction.

A cylindrical polyacrylamide gel was prepared as before, using a polypropylene cylinder to cast the shape. The gel rod so produced was 100mm long and had a diameter of 12mm. It was washed in distilled water to remove any residue monomers and then allowed to equalise in distilled water at room temperature for one week. The gel rod was cut into a disc of height 22.8mm and placed in the bottom of a glass capsule, which had an inner diameter equal to the diameter of the gel, as in Figure 4.22. The capsule was filled with a solution of 1.2% TEMED and then sealed with a cap. The system was immersed in a water bath at 40°C and the gel was allowed to swell against a piston and compression spring connected to the top of the capsule. The compression spring had a stiffness of 0.23 N/mm. The displacement of the piston, caused by the swelling of the gel, was measured

daily using digital vernier callipers. As the cross-sectional area was kept constant, the actuation stresses due to swelling could be determined.

The results of the test are shown in Figure 4.23. Immediately obvious was the greater degree of swelling, compared to the previous experiment where the swelling directions were unrestricted. After just one day, the actuation swelling stress was 2.644×10^{-3} MPa. In the previous test, it had taken over six days to reach this value. There was a high rate of swelling in the first couple of days, with the rate decreasing steadily in subsequent days. After nine days, the actuation stress had reached a value of 13.259×10^{-3} MPa. This corresponded to an increase in the height of the gel disc by almost 30%. However, the length of the test, nine days, is impracticable in terms of using the materials as actuator elements in marine devices. Of much more importance is the actuation stress and strain after the first two days in TEMED at 40°C. Over 50% of the maximum stress and strain recorded occurred in the first two days.

The results of the test were ultimately governed by the strength of the spring used, and it remains to be seen if different spring constants would affect the strain rate and final strain. The test was essentially strain controlled, and it may be inferred that the final strain might have been greater with a weaker spring, or with none at all. A stronger spring may have actually fully constrained the gel, leading to an attempt at measuring the bulk modulus of the gel.

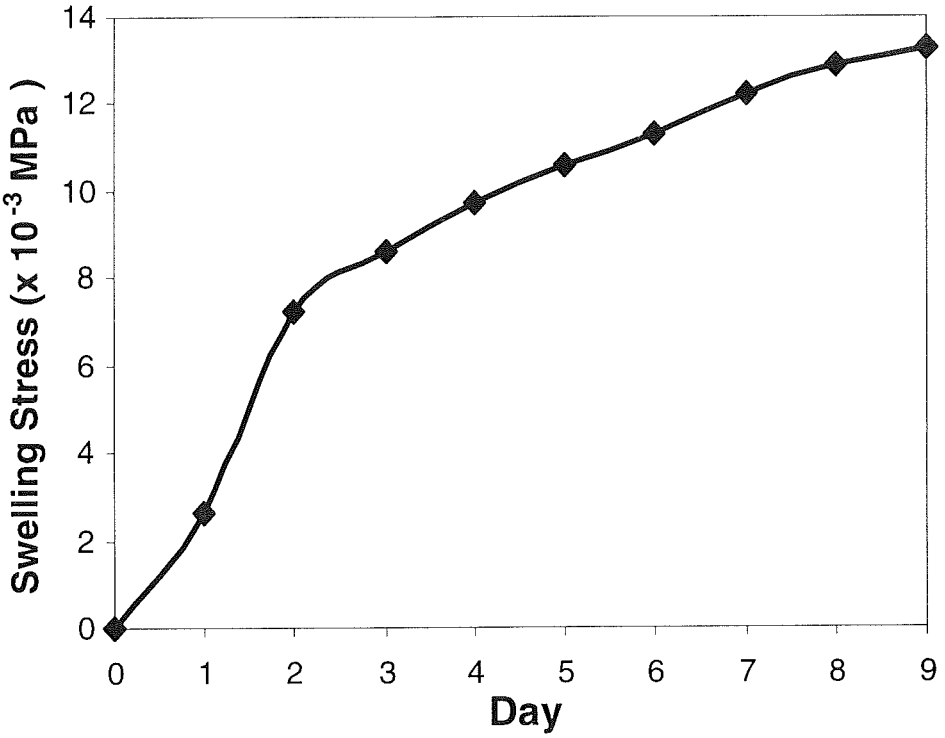

Figure 4.23 Actuation swelling stresses of polyacrylamide gel immersed in 1.2% TEMED at 40°C, where radial swelling is restricted.

Although a substantial increase in actuation stress and strain was observed for polyacrylamide gels restricted to swelling in one direction, it was felt that only the top edge of the gel disc was being exposed to the TEMED solution, thereby slowing down the diffusion of the solution through the gel. To realise a more pronounced swelling in this direction, the solution would need to penetrate at the sides of the gel disc as well as at the top, while radial swelling was still being restricted. Therefore, the tubing used to hold the gel disc would need to be permeable to the surrounding solution.

A study was carried out to investigate the swelling characteristics of polyacrylamide gels in semi-permeable Visking tubing, immersed in 1.2% TEMED at three temperatures:

20°C, 40°C, or 60°C. The diameters of the gel discs and the tubing were 16mm. The heights of the gel discs were also 16mm. Glass capsules were used to contain the TEMED solution, Visking tubing and gel discs (Figure 4.24). Water baths were used to maintain the solution temperatures at 20°C, 40°C, or 60°C. All tests were carried out in triplicate.

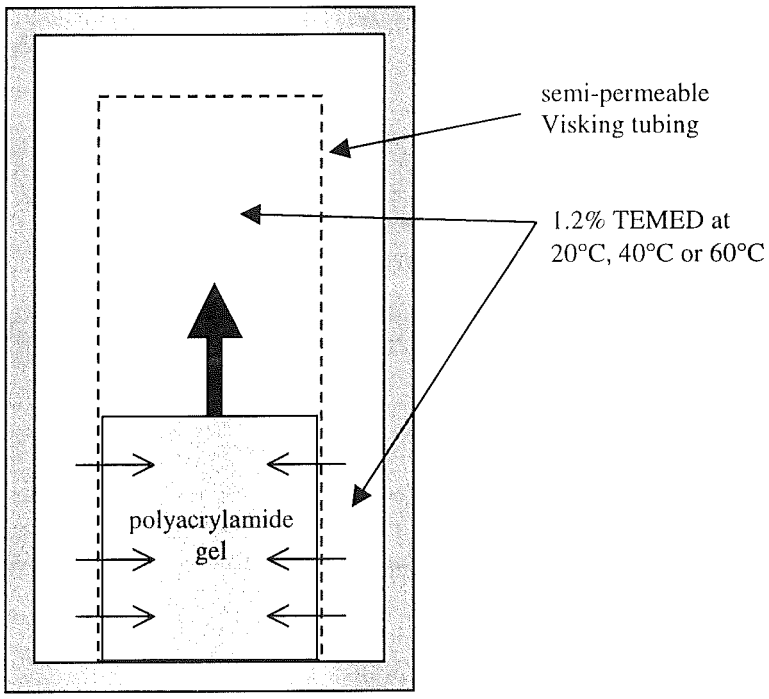

Figure 4.24 Test rig for measuring the actuation swelling strains of polyacrylamide gels immersed in 1.2% TEMED at 20°C, 40°C or 60°C. Swelling has been restricted to just one direction by using semi-permeable Visking tubing, but allowing TEMED to penetrate the sides of the gels, as well as the top.

The actuation strains for the polyacrylamide gels swelling in Visking tubing are outlined in Figure 4.25. All gels swelled in the Visking tubing, and the tubing restricted swelling in the radial direction. The gels also appeared to be stronger when handled, due to the tubing support. The most significant results were for the gels in the TEMED solution at 60°C, due to the extra thermodynamic energy. However, after two days at 60°C the gels began to distort in the tubing and fracture. This is noted with the large standard deviations in the

graph. There was clearly little actuation strain for gels at 20°C, but the strain at 40°C increased steadily. It took three days for gels at 40°C to achieve an actuation strain equivalent to that after just one day for gels at 60°C. However, the gels remained intact, with no sign of fracture.

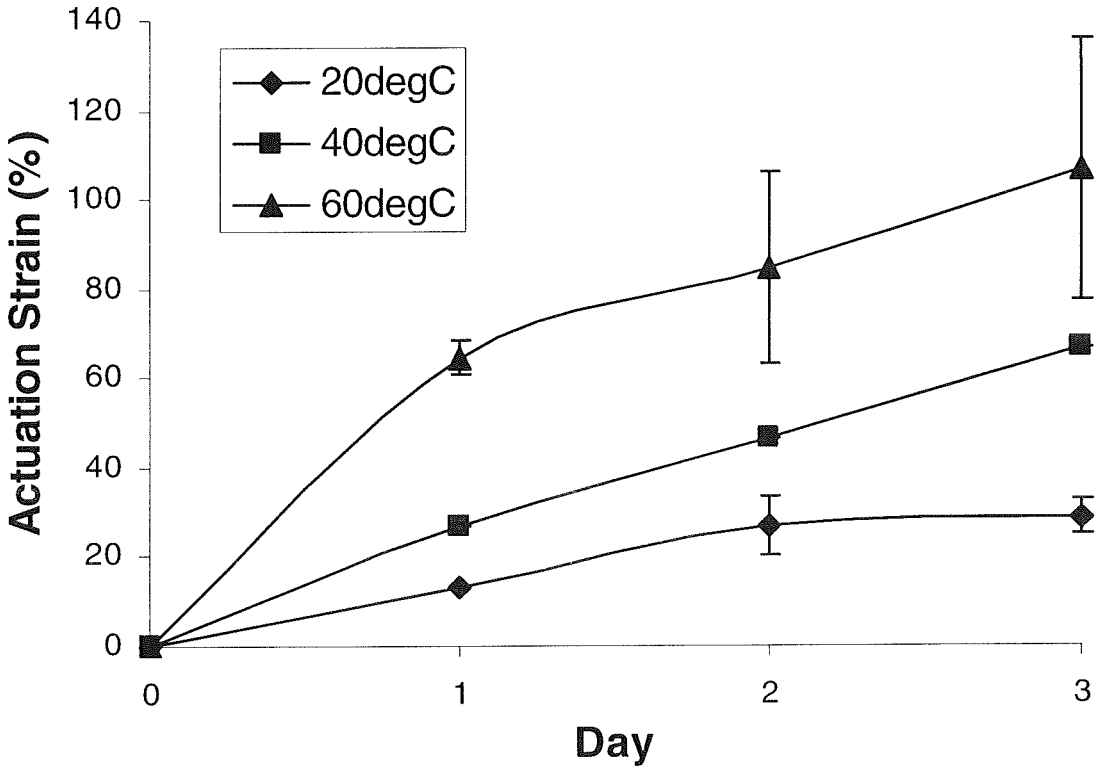

Figure 4.25 Actuation swelling strains of polyacrylamide gels immersed in 1.2% TEMED at 20°C, 40°C or 60°C. Swelling has been restricted to just one direction by using semi-permeable Visking tubing, but allowing TEMED to penetrate the sides of the gels, as well as the top.

From Figure 4.25 a number of recommendations can be made for the application of polyacrylamide gels as actuator elements. If a short-term actuation strain is required then swelling a polyacrylamide gel in 1.2% TEMED at 60°C is the best option. Swelling for more than one day will cause distortions and fracture in the gel, however. For longer

periods it may be better to swell a gel in 40°C TEMED to achieve a steadier increase in actuation strain and volume and to keep the gel in good condition.

4.4.2 Contraction Stresses – Experiments and Results

A series of tests were performed on wedge-ended polyacrylamide gel strips, using the specially constructed grips illustrated in Figure 4.10. The gel strips were produced using the method described earlier [5], cured for one day at room temperature and equalised in distilled water for one week. The strips so produced had gauge lengths of 35mm and a thickness of 1.5mm. Four widths of gel strip were tested: 5mm, 10mm, 15mm, and 20mm. The grips and gel strips were fitted to a Lloyds 10000 materials testing machine, and immersed in a solution bath also fitted to the testing machine. While the crosshead of the machine was fixed, the gel samples were allowed to contract in a bath of 50% acetone and distilled water at room temperature, thus recording a contraction force on the load cell.

It was not easy to determine the actuation stresses during the contraction of the gels, because of the difficulty of measuring the cross-sectional area. The rig set-up impaired direct measurement, and an accurate measure would have involved interrupting the test. For this reason, only the final dimensions could be measured, after the test was stopped. The tests were, typically, of a duration of between 90 and 110 minutes. Tests were stopped only when there was no apparent increase or decrease in the recorded load. Figure 4.26 shows the behaviour of the final actuation stress, as a function of the initial widths of the gel strips.

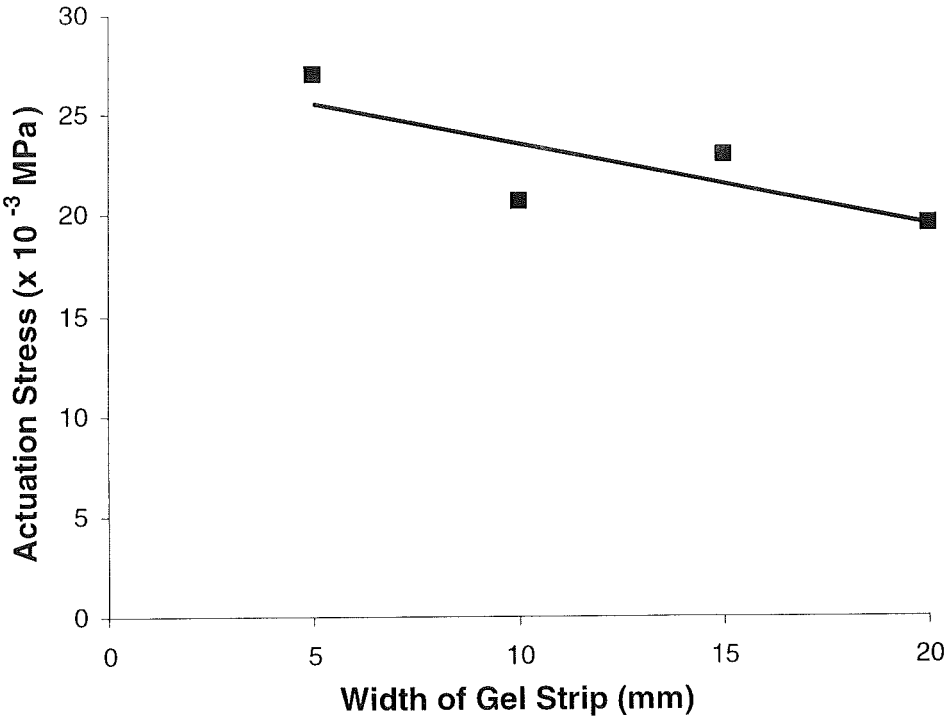

Figure 4.26 Final actuation stresses due to the contraction of polyacrylamide gel strips, of widths from 5mm to 20mm, immersed in 50% acetone and distilled water at room temperature. Fixing the position of the crosshead restricted strain.

As can be seen from the figure above, there is a slight decrease in contraction stress as the width of the strip is increased. A similar observation was noted earlier in Section 4.3.2.1, where the optimum diameter of NIPA gel was determined. The time needed for solvent diffusion into or out of a polymer gel, whether it is polyacrylamide or NIPA, is proportional to the square of the gel diameter [21]. The same is true for gels in the form of strips. The larger the gel, the longer is the distance for solvent to penetrate and, thus, the longer it takes for the solvent to permeate through. It takes approximately 30 minutes for a new acetone mixture to thoroughly permeate a centimetre long gel by diffusion [6]. The contraction that follows can take much longer to reach completion, perhaps days. From the graph, the fastest diffusion and subsequent contraction occurs with the gel strip of the

smallest dimensions, as this gel has exhibited the greatest contraction stress. The decrease in maximum stress is small, as the gel width increases, which could indicate that the bulk modulus of the gels is quite low. However, there are advantages to using the smaller gel samples, in terms of compactness, weight, greater actuation force to volume ratio, etc. There would probably be a greater power output per unit volume if the gels were even smaller, such as in the form of fibres, and an array of such gel fibres could be used to exert a significant force.

4.4.3 Conclusions on Actuation Stresses of Polymer Gels

Polyacrylamide gels have been found to be very soft and have a low strength. The swelling stresses measured were also quite low, in the range of 6-8 x 10^{-3} MPa. The results are similar to an alternative study [26], which had used the formation of Newton's rings, as the gel swelled against a glass plate, to determine the pressures exerted. Contraction stresses determined were also low, but about three times the magnitude of swelling stresses. Polymer gels designed for contraction have the advantage of miniaturisation to augment their actuation potential. This could be a problem for gels designed for swelling, which would need a diameter to height ratio great enough to avoid possible buckling problems due to their compression.

4.5 Conclusions on Polymer Gel Studies

Although the conclusions on electric field studies were not very positive, electrically activated polymers could still prove to be useful as actuators. Overall, polymer gels can exhibit useful changes in volume and density to facilitate a possible buoyancy change in an underwater device. They also exhibit controllable mechanical properties, and can apply actuation stresses and strains to facilitate work production. Although these actuation properties are quite small in magnitude, the miniaturisation of the materials may enhance the actuation capabilities.

4.6 References

1. Hirokawa Y., Tanaka T. 1984. Volume phase transition in a nonionic gel. *Journal of chemical physics* **81**(12), pp. 6379-6380.
2. Ohmine I., Tanaka T. 1982. Salt effects on the phase transition of ionic gels. *Journal of chemical physics* **77**, pp. 5725-5729.
3. Tanaka T, Nishio I, Sun ST, Ueno-Nishio S. 1982. Collapse of gels in an electric field. *Science* **218**, pp. 467-469.
4. Molloy P.J., Smith M.J., Cowling M.J. 2000. The effects of salinity and temperature on the behaviour of polyacrylamide gels. *Materials and Design* **21**, pp. 169-174.
5. Tanaka T., Fillmore D., Sun S.T., Nishio I., Swislow G., Shah A. 1980. Phase transitions in ionic gels. *Physical review letters* **45**, pp. 1636-1639.
6. Tanaka T. 1981. Gels. *Scientific American* **244**(Jan), pp. 110-123.
7. Okuzaki H., Osada Y. 1994. Electro-driven chemochemical polymer gels an intelligent soft material. *Journal of biomaterials science – polymer edition* **5**(5), pp. 485-496.
8. Shiga T. 1998. Deformation and viscoelastic behaviour of polymer gels in electric fields. *Proc. japan acad.* **74**(B), pp. 6-11.
9. Sansiñena J. M. Jet Propulsion Laboratory, 4800 Oak Grove Drive, Pasadena, CA 91109-8099, http://eis.jpl.nasa.gov/ndeaa/nasa-nde/nde-aa-l/nde-aa-l.htm. *Personal communication.*
10. Mullins J. 2000. Electric muscles up to pace. *New Scientist* **3rd June**.

11. Bretschneider C.L., Corcoran E.F., Jung G.H., McAllister R.F., Vine A.C., Zetler B.D. 1969. Basic oceanography. In: *Handbook of ocean and underwater engineering*. Myers J.J., Holm C.H., McAllister R.F. (Eds.), McGraw-Hill, London, San Francisco, Toronto, London, Sydney.

12. Ricka J., Tanaka T. 1984. Swelling of Ionic Gels: Quantitative performance of the Donnan theory. *Macromolecules* **17**, pp. 2916-2921.

13. Hooper H.H., Baker J.P., Blanch H.W., Prausnitz J.M. 1990. Swelling equilibria for positively ionised polyacrylamide hydrogels. *Macromolecules* **23**, pp. 1096-1104.

14. Baker J.P., Stephens D.R., Blanch H.W., Prausnitz J.M. 1992. Swelling equilibria of acrylamide-based polyampholyte hydrogels. *Macromolecules* **25**, pp. 1955-1958.

15. Hjerten S. 1962. *Arch. biochem. biophys. suppl 1.* pp. 147.

16. Ilavsky M. 1982. Phase transition in swollen gels. 2. Effect of charge concentration on the collapse and mechanical behaviour of polyacrylamide networks. *Macromolecules* **15**, pp. 782-788.

17. Chunfang L. 1994. Scaling behaviours and mechanical properties of polymer gels. *Ph.D. dissertation*, Denton, Texas.

18. Molloy P.J., Cowling M.J. 2000. Buoyancy mechanisms of marine organisms: lessons from nature. *Underwater technology* **24**(2), pp. 41-49.

19. Suzuki A. 1993. Phase transition in gels of sub-millimetre size induced by interaction with stimuli. *Advances in polymer science* **110**, pp. 199-240.

20. Hirotsu S. 1994. Static and time-dependent properties of polymer gels around the volume phase transition. *Phase transitions* **47**, pp. 183-240.

21. Suzuki A., Yoshikawa S., Bai G. 1999. Shrinking pattern and phase transition velocity of poly(*N*-isopropylacrylamide) gel. *Journal of chemical physics* **111**(1), pp. 360-367.

22. Molloy P.J., Cowling M.J. 2000. Volume and density changes in polymer gels in seawater environments. *Journal of materials: design and applications.* Accepted, subject to minor corrections. Resubmitted, May 2000.

23. Duxbury A.B., Duxbury A.C. 1993. *Fundamentals of oceanography, 2nd ed.* Wm. C. Brown, Boston, London, Sydney, pp. 92.

24. Anseth K.S., Bowman C.N., Brannon-Peppas L. 1996. Mechanical properties of hydrogels and their experimental determination. *Biomaterials* **17**, pp. 1647-1657.

25. Tokuhiro T. 1999. Temperature dependence of density of polymer gels 1. A pycnometry method applied to poly(*N*-isopropylacrylamide) – water system. *Journal of physical chemistry B* **103**, pp. 7097-7101.

26. Lagutina M.A., Dubrovskii S.A. 1996. The swelling pressure of weakly ionic acrylamide gels. *Polymer science, series A* **38**(9), pp. 1059-1064.

Chapter 5 Shape Memory Alloys — Experiments and Results

Shape memory alloys (SMA's) might be used as the basis for actuators to control buoyancy in underwater applications. As described in Chapter 3, Section 3.3.2.7, shape memory alloys exhibit some of the best power output per amount of material known [1]. This quality, coupled with their shape changing and actuating abilities, could prove very useful characteristics in the development of a novel buoyancy control system.

5.1 Development of Thought

The purpose of this study was to investigate shape memory alloys as possible actuators to control the buoyancy of underwater devices. The key was to find an effective means of controlling the volume expansion and contraction of an actuator element, whereby the effective density of the element can be changed. As shown in Chapter 3, Section 3.3.2.6, "Applications in Underwater Technology", tubular SMA elements have been considered for this application [2]. However, other solutions using shape memory alloys are worth consideration. SMA helical coil springs may provide the answer, as they are elements that can expand or contract considerably when heated, but without the need of great amounts of power. A SMA extension spring provides a tensile force by contracting when heated to the high-temperature austenitic state. By contrast, a SMA compression spring will extend when heated, providing a compressive force.

Obviously, any expansion or contraction of SMA springs would not, by itself, bring about a volume change, as any surrounding fluid would be free to flow through the spring coils. However, if the springs were enclosed in a deformable membrane, or other form of extendable enclosure, an overall change in volume and density would occur as the springs either expanded or contracted, when they were heated above their respective transition temperatures. It is preferable to have small SMA springs with diameters less than 10-15mm, wire diameters less than 2mm, and lengths of a few centimetres or less. Although larger springs are made and used, they require much more power to bring them to their transition temperatures, thus negating any advantages of using shape memory alloys in the first place. They also have a smaller surface area to weight ratio, which results in poorer cooling times [3]. Therefore, the volume and density changes produced from these small SMA springs would only be useful for small underwater devices. Larger devices would require a large number of the spring systems to obtain an effective density change. Again, in an autonomous underwater system, the advantages of SMA springs would be lost as their numbers increase, as more onboard power would be required to heat them.

A larger system could be built using the small SMA springs, possibly in a pusher-plate configuration, that would, effectively, output a similar percentage volume change, but with fewer spring elements. Such a system would need to be able to expand or contract, so there would be a combination of biasing (return) springs and NiTi springs, which could be controlled to bring about the required amount of volume change necessary.

SMA springs provide an actuation stroke when they are heated from below their transition temperature to just above their final transformation temperature. This essentially gives an on/off configuration, but for accurate buoyancy control, it would be necessary to have proportional control of the actuation stroke. This should be feasible as the change in length of SMA springs occurs over a temperature range. A desired stroke can be achieved by interrupting the progress of the transformation at a particular temperature. The problem with using SMA elements is the large amount of shape change that occurs over a reasonably small transition temperature range. The length change characteristics of a SMA tension spring are shown in Figure 5.1a.

A more gradual change in spring extension could be achieved by having a SMA spring work against a stiff bias spring, thus strongly increasing the opposing force as the SMA spring attempts to accomplish its shape recovery. Because of the stress sensitivity of the recovery temperature, this would force the shape recovery to occur over a wider temperature range [4]. This is illustrated in Figure 5.1b for a SMA tension spring. The figure also illustrates that hysteresis must still be taken into account. Even small changes in the desired SMA spring position means that one must move across the temperature hysteresis gap. If the SMA spring was being cooled to position 'a', and a new spring position was desired at 'b', the spring would need to be heated through the hysteresis gap, and along the transformation curve to the desired position.

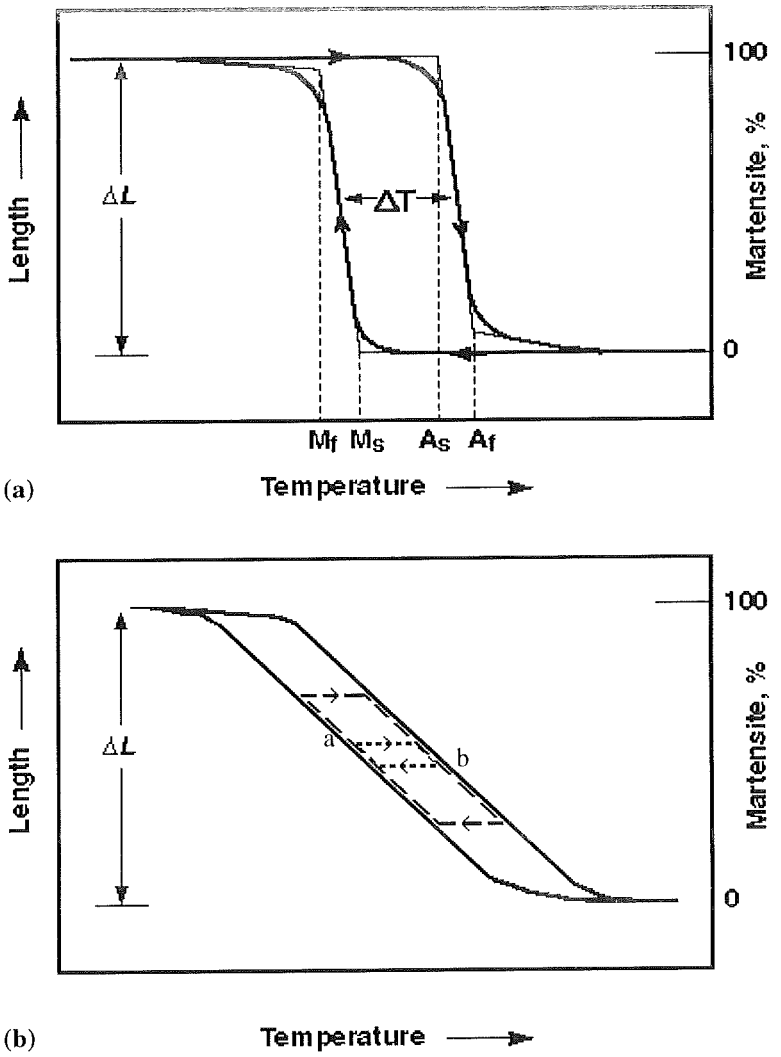

Figure 5.1 (a) Spring Extension vs Temperature for SMA tension spring under normal conditions. (b) Greater control of shape change with temperature due to an increased bias stress [4].

5.2 Experimental Details

5.2.1 Preliminary Volume/Density Tests

A number of preliminary volume/density experiments were performed using NiTi compression and tension springs, supplied by Mondo-tronics [5]. The 50:50 NiTi shape memory alloy compression springs had a wire diameter of 0.95mm, a spring diameter of 8mm, and 17 turns (Figure 5.2). They could be compressed down to 16mm in length when cooled below their transformation temperature, which is in the range 55°C to 65°C, according to the suppliers [5]. When heated electrically with 3 Amps (Ω = 1ohm), the SMA compression springs extended, unrestricted, to approximately 40mm, a percentage extension of 150%. If extension is restricted, the springs can exert a pressure of up to 0.16 MPa, based on the spring diameter [5].

The NiTi tension springs had a wire diameter of 0.75mm, a spring diameter of 6mm, and 19 turns (Figure 5.3). The overall closed length of the springs was 29mm and they could be extended by up to 775% when cool [5]. When heated above the transformation temperature of 45°C to 55°C, all deformation was recovered, if the springs were unrestricted. When a load of 3.5 N is exerted on a NiTi spring, corresponding to a shear stress of 150 MPa on the spring, it can contract from an extension of 152% to an extension of 48%, when heated with 2 Amps (Ω = 1.2ohms) [5].

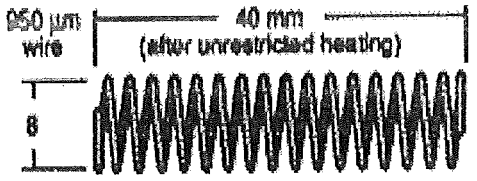

Figure 5.2 Austenitic (hot) form of a NiTi shape memory alloy compression spring [5].

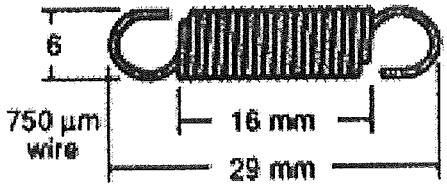

Figure 5.3 Austenitic (hot) form of a NiTi shape memory alloy tension spring [5].

The volume/density experiments were performed by enclosing a NiTi spring in a deformable membrane, which was made of latex rubber. Firstly, the latex rubber was stretched over the NiTi compression spring and sealed to make the system watertight. The latex rubber had a sufficient stiffness to compress the spring. The initial volume of the compression spring and sealed membrane was approximately 2.25 cm^3, and the density was approximately 1.06 g/cm^3. The spring/membrane system was then placed in a Techne Circulator C-85D water bath using tap water, $\rho \cong 1.000$ g/cm^3. The system was then heated above the final transition temperature of the SMA compression spring, 65°C.

The above experiment was repeated for the NiTi tension spring, which was extended to 70mm, or 140% extension. The spring was enclosed in the latex rubber membrane, but

this time the membrane was under no tension to compress the spring. The initial volume of the tension spring and sealed membrane was approximately 1.98 cm^3. The spring/membrane system was then placed in the water bath using tap water, and heated above the final transition temperature of the SMA tension spring, 55°C.

5.2.2 Design and Testing of SMA Spring Actuator Device

A parallel-plate device was constructed, as detailed in Figure 5.4, linked by four NiTi compression springs. The SMA compression springs were supplied by Mondo-tronics [5], and were of the same composition, dimensions, force output and stroke as those used in the preliminary tests (see Figure 5.2). The basic design of the rig was four NiTi compression springs between two circular fibreglass epoxy panels of diameter 100mm and 2mm thickness. A steel extension spring was positioned at the centre of the plates to provide enough biasing force to return the SMA compression springs to their original length, but not enough to restrict the actuation power of the SMA springs. Two aluminium guide bars ensured the rig remained stable during the actuation and return phase.

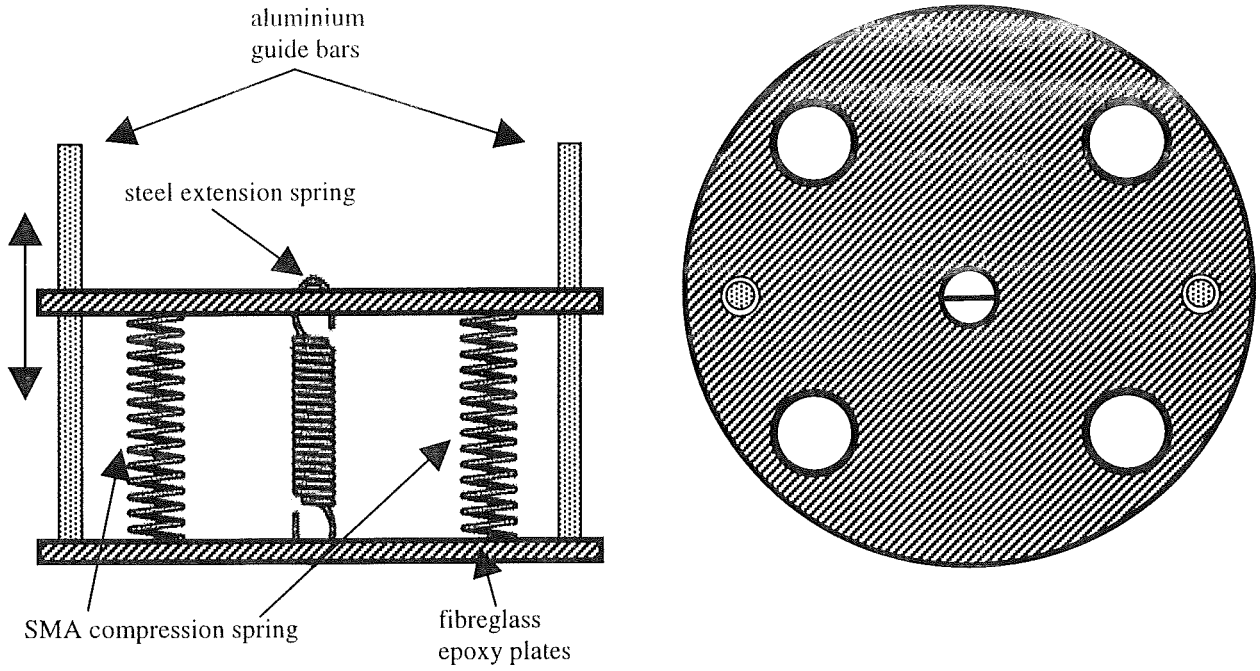

Figure 5.4 Actuator design to provide a volume change, incorporating four SMA compression springs and a centre extension spring, used as a biasing element.

Initially, the steel biasing extension spring was omitted, so that tests could be carried out to determine the influence of constant external loads on the plate separation. It is difficult to spot-weld or solder NiTi shape memory alloys, therefore the four SMA compression springs were attached to the contact pads on the parallel plates using conductive epoxy adhesive. They were electrically linked in series and connected to a temperature controller. A thermocouple was attached to one of the springs, using the conductive epoxy, and was also connected to the temperature controller.

Constant load tests were performed by placing weights, corresponding to loads of 1N to 12N, on the top plate of the SMA spring device. The increase in plate separation distance

was recorded for each load as the temperature of the springs was increased from 35°C to 70°C, and back again to 35°C (Figure 5.5).

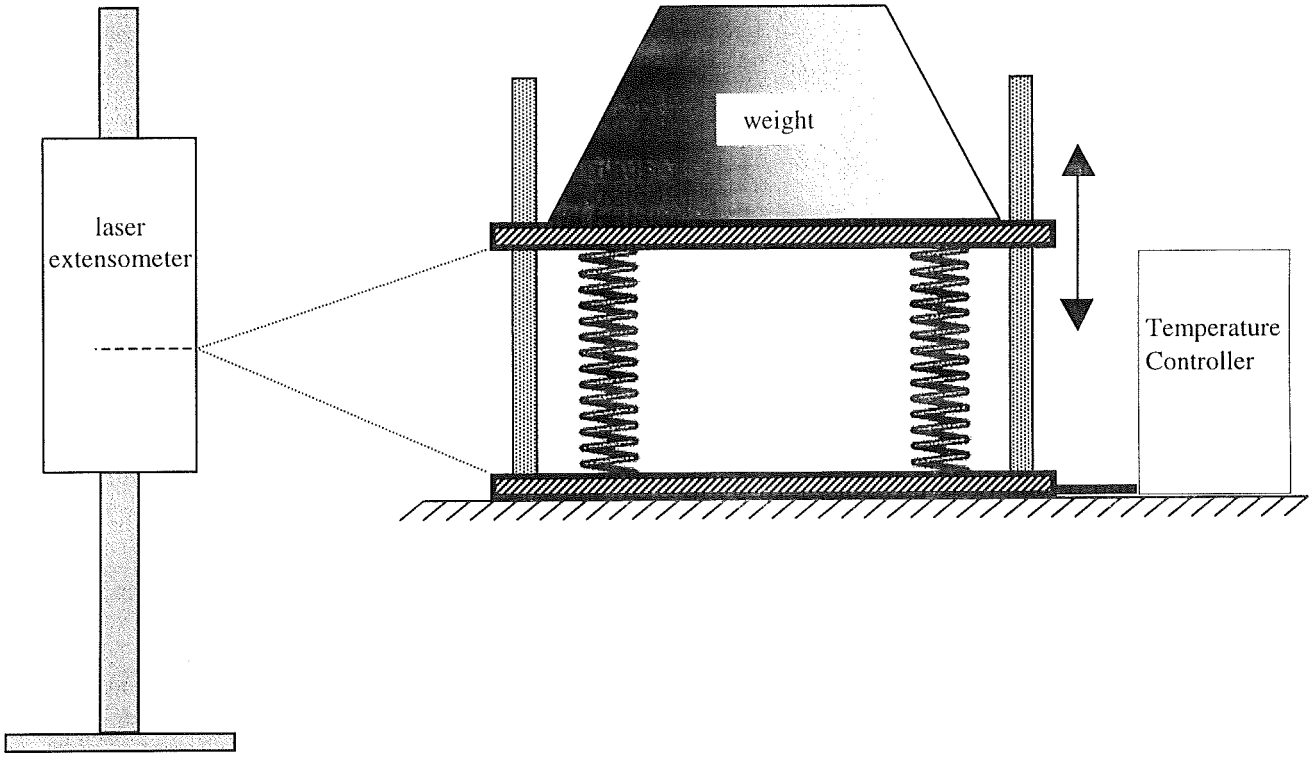

Figure 5.5 Experimental set-up for SMA spring device under constant load.

Before the application of each load, the plate separation distance was set at approximately 32mm, which involved compressing the springs and allowing them to naturally recover under no external stress. The placing of weights obviously compressed the springs further, and the new separation was denoted the initial plate separation (IPS) for that external load. A Lloyds extensometer recorded the plate separation, using reflective strips on the edges of the two plates (Figure 5.5).

Tests were also carried out to determine the influence of spring temperature on the elastic modulus of the device as a system, i.e. modulus values were calculated using the device area of 7854mm^2 (plate diameter = 100mm). The actuator device was heated to a set temperature using the temperature controller. While the temperature was held constant, a compression test was conducted using a Lloyds L10000 materials testing machine (Figure 5.6). The resultant slope from the compression test was used to find the elastic modulus of the device for that temperature. This was repeated for temperatures ranging from 30°C to 65°C.

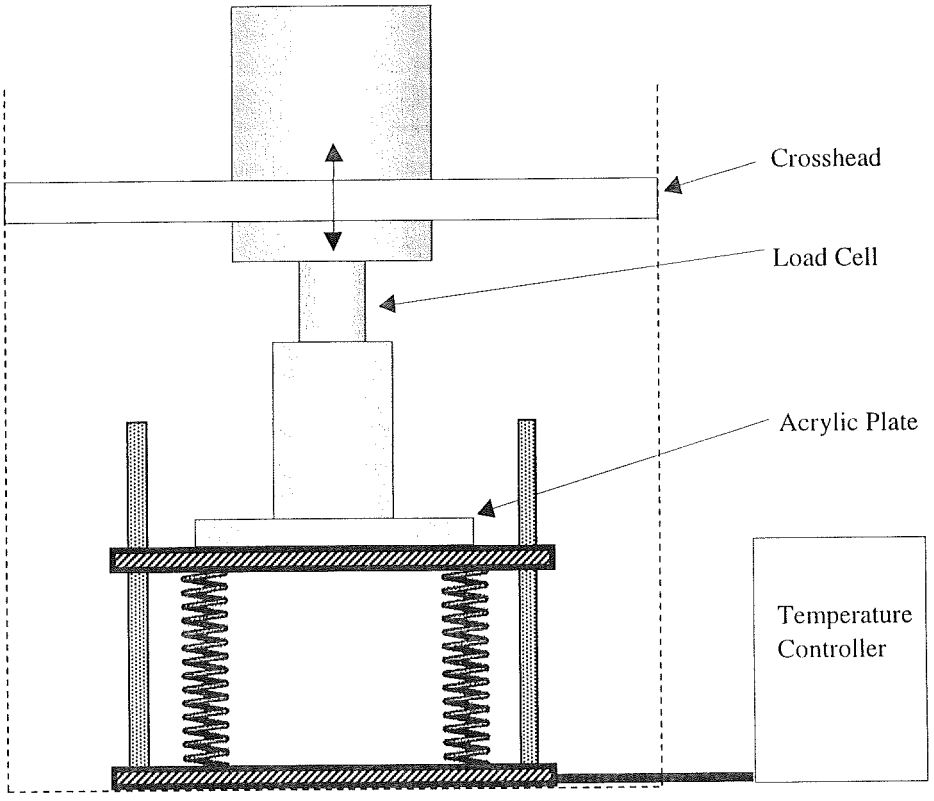

Figure 5.6 Experimental set-up for testing the elastic modulus SMA spring device at various temperatures.

5.3 Results and Discussion

5.3.1 Preliminary Volume/Density Results

The maximum volume increase the SMA compression spring is capable of is approximately 150%, if enclosed in an ideal membrane. For the experiments, the extensibility of the latex membrane prevented the spring from being compressed to its closed length, and the stiffness of the membrane also prevented maximum austenitic extension. The resultant volume increase would be much less than 150%. The initial volume of the SMA compression spring and sealed membrane was approximately 2.25 cm^3, and the density was approximately 1.06 g/cm^3, 6% greater than the density of the tap water in the water bath. Therefore, upon immersion in the water bath the compression spring immediately sank to the bottom. As the SMA compression spring was heated to 65°C, it expanded against the flexible latex rubber membrane and the overall volume changed by approximately 25%. This was a sufficient increase in volume to reduce the system density to $0.88g/cm^3$ and cause the spring to rise to the surface. When taken out of the bath, the spring system cooled in air, and the extended rubber membrane had a sufficient stiffness to compress the spring back and restore the original volume of the spring/membrane system.

Initially, for the SMA tension spring enclosed in the flexible latex rubber membrane, the system was extended by 140%,. The initial density of the system was less than the density of tap water in the water bath, causing the system to float. When the spring contracted due

to heating, it decreased in volume by approximately 50% and increased in density, causing it to sink to the bottom of the tank. The problem with this SMA tension spring system was that there was no biasing force present to return the tension spring to its original length.

There was a lack of control inherent in these initial experiments. They were basically on/off experiments using the low-temperature and high-temperature spring system volumes to bring about a change in density. A more precise control of temperature could have produced the exact volume required to produce neutral buoyancy of the system. For example, in the SMA compression spring experiment, a total volume increase of 25% occurred when the temperature was raised from below to above the transition temperature range. If the temperature of the spring had been known, which would have produced a percentage volume increase of just 6%, the system could have achieved neutral buoyancy.

5.3.2 SMA Spring Actuator Device Results and Discussion

The dependence of plate separation distance on temperature and constant external loads is shown in Figure 5.7. The corresponding shear stress on each compression spring, due to the external load, is also included, so as to determine the point when the springs start to become overstressed. As can be seen from the figure, the initial plate separation (IPS), at the beginning of each test, steadily decreased as the external load increased. The plate separation at zero load was 31.55mm and this decreased by 27% to 23.05mm with the application of a shear stress of 63.43 MPa (12N) on each SMA compression spring. This corresponded to a (cold) system spring stiffness of 1.41 N/mm.

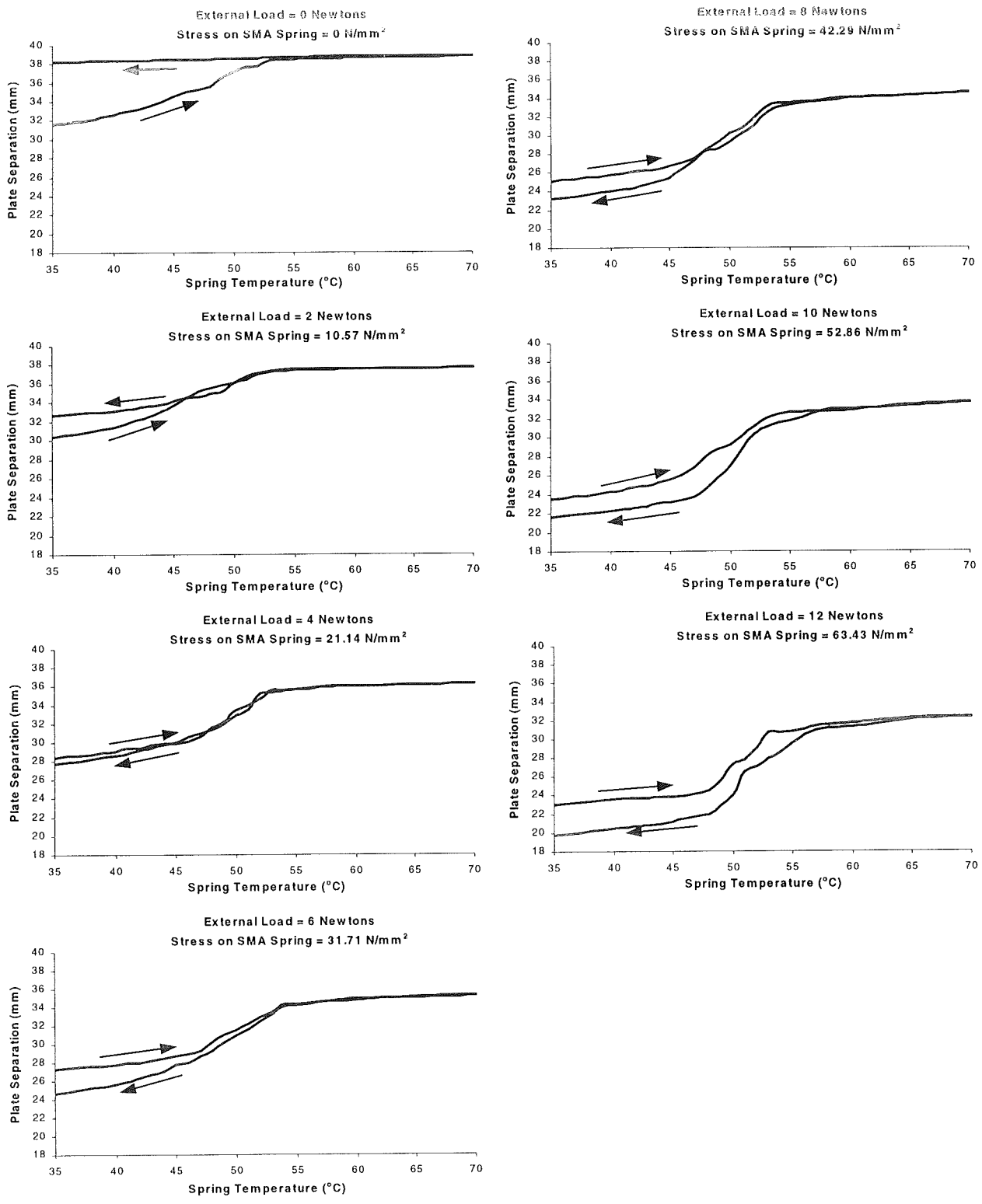

Figure 5.7 Relationship between the temperature of the SMA springs and the separation of the plates of the device. Shear stresses ranging from 0 to 63.43 MPa were imposed on each SMA spring during the tests. (1 N/mm^2 = 1 MPa)

As the SMA springs in the device exhibited only one-way shape change with temperature, an external load is essential for returning the springs and plate to their initial position, but the external load has to be sufficient to overcome the natural (cold) spring forces. Therefore, as can be seen from Figures 5.7, loads of 2N or less were insufficient to return the plates back near their initial position. This corresponded to a shear stress on each SMA spring of 10.57 MPa or less. With greater shear stresses, the final plate separation (FPS) may actually sink below the initial separation. For example, a shear stress of 63.43 MPa (12N) on each SMA spring caused an initial plate separation of 23.05mm. After the temperature cycle was completed, the FPS was 13.7% lower than the IPS, at 19.9mm. For control reasons, a similar initial and final separation would be preferred, and a simple stop mechanism incorporated into the device would ensure there was no excess travel. The stop mechanism would also prevent over stressing of the SMA springs.

The application of external loads also affected the plate separation distance when the SMA compression springs were hot, i.e. when they had been heated into their austenitic state. With no external stress, the plates reached a maximum separation of 38.8mm, but this decreased steadily by nearly 17% to 32.3mm, when each spring was subjected to a shear stress of 63.43 MPa (12N). This corresponded to a (hot) system spring stiffness of 1.85 N/mm, a 31% increase from the cold state of the device.

For all plots in Figure 5.7, the phase transition began at a temperature of approximately 45°C and ended at around 55°C. Transition from austenite back to the martensitic phase occurred at about 53-55°C and ended around 45°C. These transition temperatures are, in

actual fact, about 10°C lower than the stated transition temperatures from the suppliers. There is very little hysteresis evident from the plots in Figure 5.7. This is encouraging, as a device with as little hysteresis as possible is the most desirable from a control point of view. Up to a shear stress of 52.86 MPa (10N) on each spring, the temperature hysteresis was very small. At the higher shear stresses, however, there was a difference of nearly 5°C in temperature between the fully heated spring temperature, A_f, and when it started to cool (i.e. the point when the plate started to return). Transformation temperatures are certainly dependent on the stress level, with the effect of raising the M_f and A_f temperatures with increasing stress [6]. By association, the hysteresis range also increases with increasing stress. An interesting observation is that the plate began to return at a temperature higher than the A_f temperature. This is in contrast to classical hysteresis behaviour of shape memory alloys [7], where return movement normally starts at a temperature lower than the A_f temperature, giving a typical hysteresis of around 10-15°C.

The influence of external shear stresses on plate separation can be seen more clearly in Figure 5.8. The graph illustrates the decrease in initial plate separation (IPS) and austenitic plate separation (APS) as shear stress was increased. The position of the plate upon completion of the temperature cycle is also shown. As stated earlier, for shear stresses greater than 10.57 MPa (2N), the final plate separation decreased below the IPS. This did not become a significant problem until the external shear stress on each spring exceeded 42.29 MPa (8N). The actuation stroke of the device, denoted APS – IPS in Figure 5.8, increased with external shear stress to a maximum at 52.86 MPa (10N), after which the stroke began to suffer due to the severity of the imposed stresses. Figure 5.9

shows more clearly the actuation stroke of each SMA spring as a function of the external shear stress.

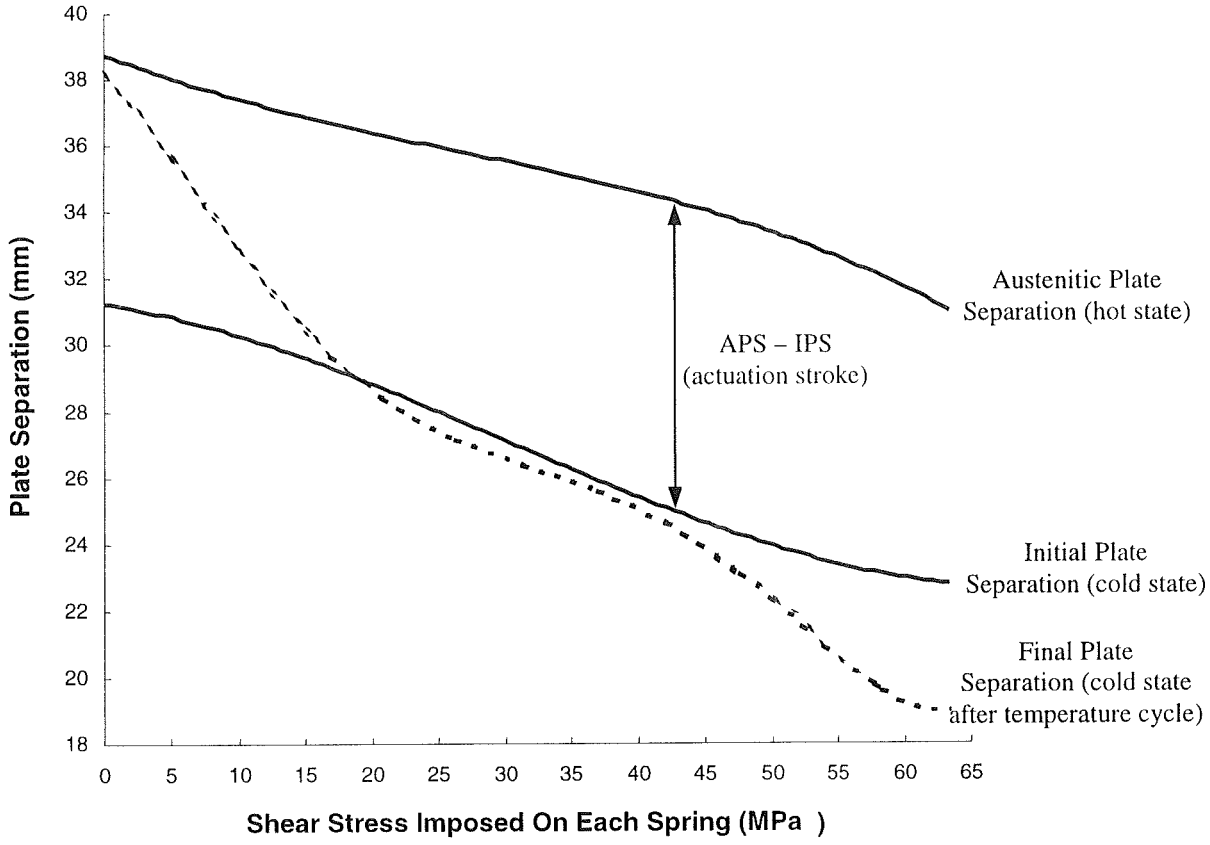

Figure 5.8 Relationship between the device plate separation and external load imposed on the device.

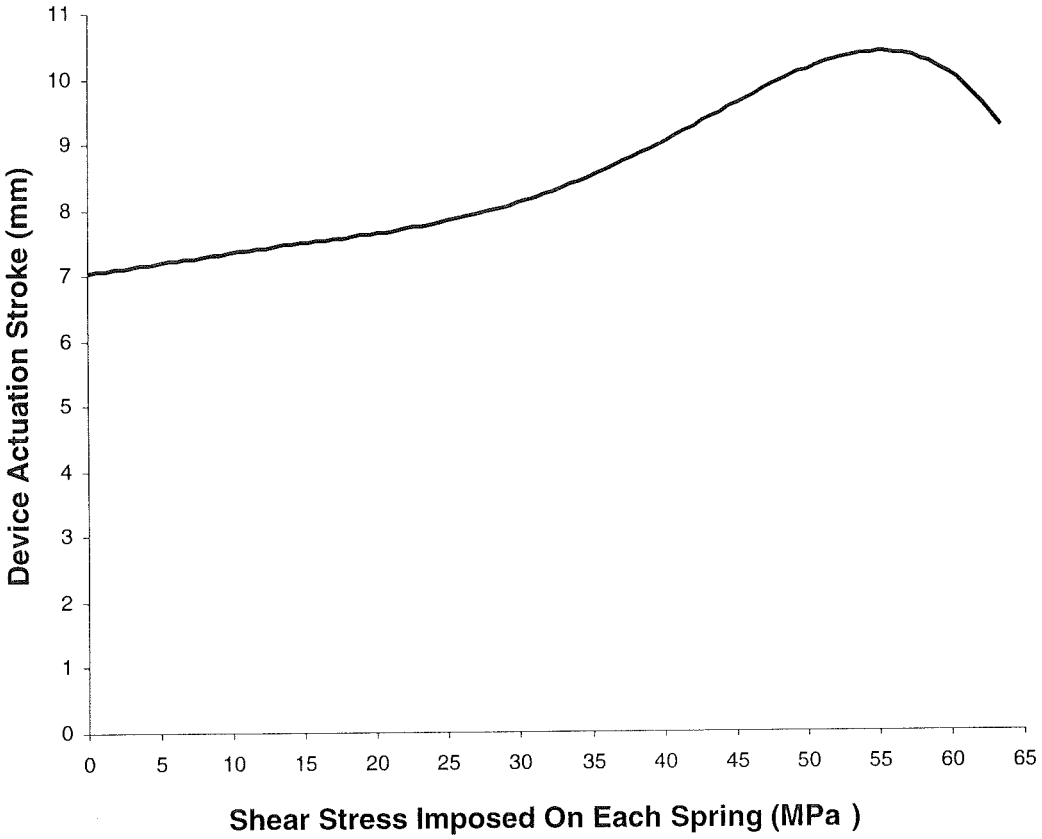

Figure 5.9 Relationship between the device actuation stroke and external shear stress imposed on each shape memory alloy compression spring.

Tests were also carried out to determine the influence of spring temperature on the elastic modulus of the device as a system. Figure 5.10 shows the change in modulus for the device as the temperature of the shape memory alloy springs was increased from 30°C to 65°C. The modulus behaviour as spring temperature was returned from 65°C to 30°C is also shown in the figure.

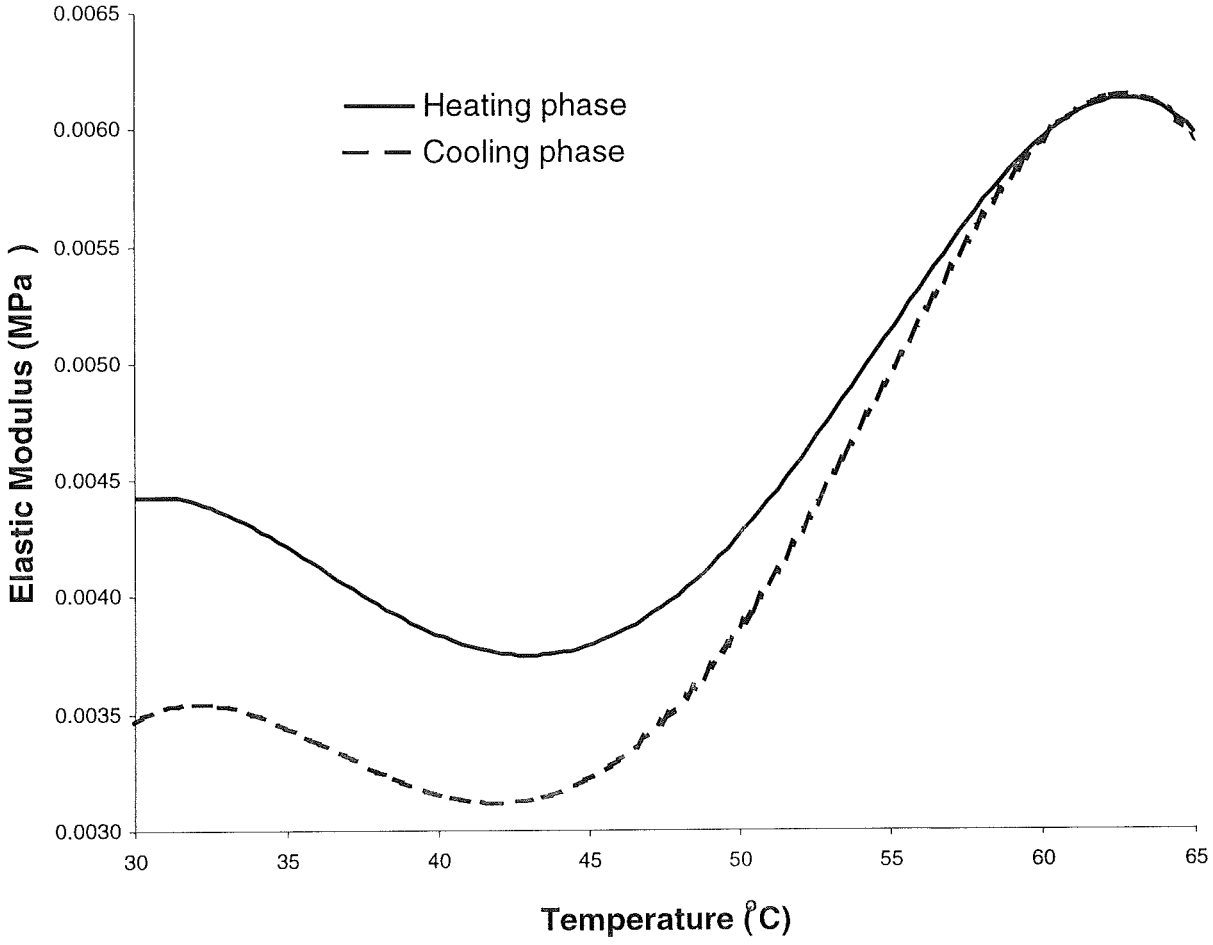

Figure 5.10 Relationship between the elastic modulus of the device as the temperature of the SMA springs was increased and decreased.

As can be seen from the above figure, the elastic modulus of the device during the heating phase initially decreased, as the temperature was increased from 30 to 45°C. The modulus then increased significantly as the springs were heated through their transition temperatures, from 45 to 55°C. The modulus reached a maximum at a temperature just higher than the final austenitic temperature, which is an increase in elastic modulus of approximately 60% from the value at 43°C. Further heating caused a slight decrease in

elastic modulus. The presence of the minimum in both the heating and cooling curves occurs close to the M_s and M_f temperature values. The slight decreases in elastic moduli may be due to the formation of self-accommodation in the crystal lattice of the NiTi alloy. The lattice changes from the ordered austenite configuration to a twinned lattice, which are more mobile, with low energy interfaces. Direct comparison with previously published work is difficult, as the design and configuration of the device is unique to this study. However, similar increases in elastic modulus of shape memory alloys have been observed. The modulus of NiTi wire increases from 27600 MPa to about 70000 MPa with the application of temperature [8]. The shear modulus of a 5.25mm diameter NiTi tension spring increases from 2700 MPa to 24500 MPa [9].

As the temperature was decreased from 65°C to 30°C, the modulus behaviour followed a similar trend to that observed during the heating phase curve. There was a sharp decrease in modulus as the springs were cooled to below their final martensitic temperature at 45°C. The magnitude of the modulus was lower at this point than in the heating phase, and remained lower during the remainder of the cooling phase to 30°C.

5.4 Further Development of SMA Spring Actuator Device

In the state used in the previous experiments, the SMA spring actuator device provided a useful actuation force output and stroke. For the purposes of producing appropriate volumetric changes, however, the device would need to be contained in a watertight casing if it is to be used underwater. This casing would have to have the ability to deform to

accommodate the expanding and contracting springs, and resist the direct or indirect effects of the surrounding water pressure.

The actuator device was modified slightly by reducing the diameter of the parallel fibreglass epoxy plates from 100mm to 60mm. The two aluminium guide bars were also modified so they could be contained between the two plates. This was achieved by using a piston system. The new guide bar system also provided a suitable stop mechanism to prevent over stressing of the SMA springs. A steel extension bias spring was also fitted to the device to act as a bias when the shape memory alloy springs were cool. The spring constant for the bias spring was 1.5 N/mm, which was approximately 10% greater than the spring constant of the actuator system. This would provide enough bias to return the SMA springs to their original positions, but low enough to have little effect on the high-temperature actuation stroke. The new actuator system was then enclosed in a two-piece sliding assembly, with the use of o-rings and lubricant to create an effective seal. The assembly can be seen in Figure 5.11. The two-piece casing was made from aluminium alloy of 4mm thickness, with access holes to accommodate the supply wires and thermocouple wire. The inner diameter of the base section was 61mm and the inner height was 30mm to accommodate the SMA spring actuator. The inner diameter of the top section was 72mm, to create an effective sliding seal with the base section and o-rings.

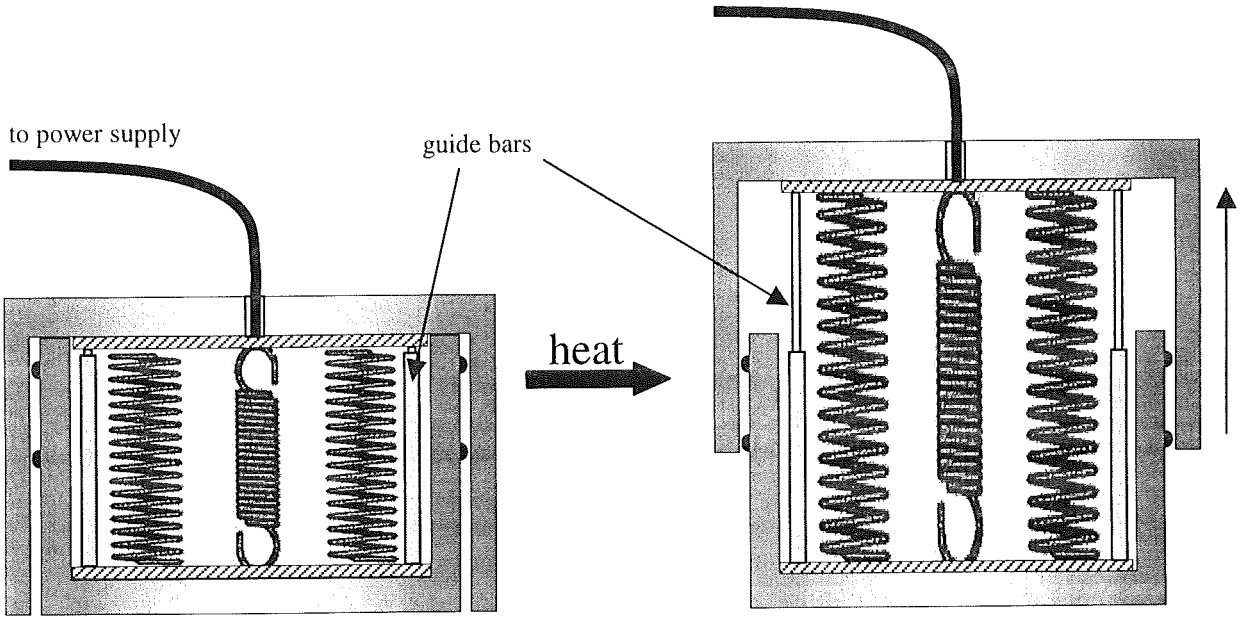

Figure 5.11 Actuator design to provide a volume change, enclosed in a two-piece aluminium assembly using o-rings to provide an effective seal.

Upon testing the new system, a number of problems became evident. The main problem was associated with how the assembly was sealed, and the associated friction caused by the two o-rings, even with a lubricant, such as vacuum grease. The casing was found to be too tight, causing it to greatly restrict movement. The actuation force of the SMA springs could not overcome the friction. The wall if the casing was thinned slightly, which allowed it to move somewhat under spring force while maintaining a watertight seal. The vacuum grease was found to be too viscous and it also greatly restricted a smooth sliding motion as the springs expanded. In fact, very often there would be no movement at all until the springs had heated to their final transformation temperature, thereby exerting

their greatest force. A sudden motion would then occur as the strength of the springs overcame the friction.

Various alternatives to the vacuum grease were tested, and a combination of silicone oil and petroleum jelly was found to improve the motion of the aluminium caps while still maintaining the seal. However, there was still a degree of friction evident from the o-rings.

Another problem, associated with the friction of the casing, was that the biasing force of the steel spring was now insufficient to reset the position of the SMA springs after they had cooled. The bias spring had to be replaced with one of greater stiffness, nearer to the stiffness of the system at high temperature, 1.85 N/mm. The advantages of having a greater bias force were outlined earlier in Figure 5.1, allowing a more accurate control of spring extension with temperature. The downside, however, is an overall reduction in maximum stroke output of the springs, due to the increased load on them.

A further problem was the air enclosure for the springs. Even with a stiffer bias spring, the system would take a long time to return to the original position after the temperature cycle. This was due to inefficient cooling inside the enclosure, causing the springs to cool slowly. Under the conditions, the heating phase took just 20-30 seconds, but the cooling phase took extremely longer at 5-10 minutes.

Due to the problems outlined earlier, the results of tests on the system were less than encouraging. Under constant external loads, because of the friction present in the system, the spring temperature had to be around 55°C or higher to record any significant movement of the device. At most, a 3mm stroke was recorded, corresponding to just 5% volumetric increase. This stroke was recorded only at lower loads. External loads greater than 6N were too high for the springs to work against. It was difficult to determine the shear stresses imposed on the SMA springs. Apart from the known applied loads, the sliding friction from the two-piece assembly could not be determined.

The tests carried out on the two-piece actuator design showed that the sliding seal greatly restricted a smooth stroke as the springs expanded upon heating. Therefore, the two-piece assembly was abandoned. The current proposal is to return to a one-piece assembly. The simplest and most effective solution is to enclose the actuation device in a flexible membrane, such as latex rubber, as was done previously for individual SMA springs. Expansion of the actuation device could bring about an increase in volume and, hence, a decrease in density that could be sufficient enough to cause it to rise in a water column. Latex rubber is flexible and would stretch as the device expanded, and the membrane could also serve as an effective bias force to return the springs to their original position, negating the use of a bias spring.

5.5 Conclusions of Shape Memory Alloy Studies

NiTi shape memory alloys show great potential for being used as effective actuators to output substantial axial stresses and strains. This could lead to a device, enclosed in a suitable enclosure, which utilises the controllable mechanical properties of the alloys to bring about volumetric changes. The SMA spring actuator device constructed and tested for this study has been donated to the Science Museum, London, minus a flexible membrane. The device, shown in Figure 5.12, will be part of the 'Innovations' exhibition in the Wellcome Wing.

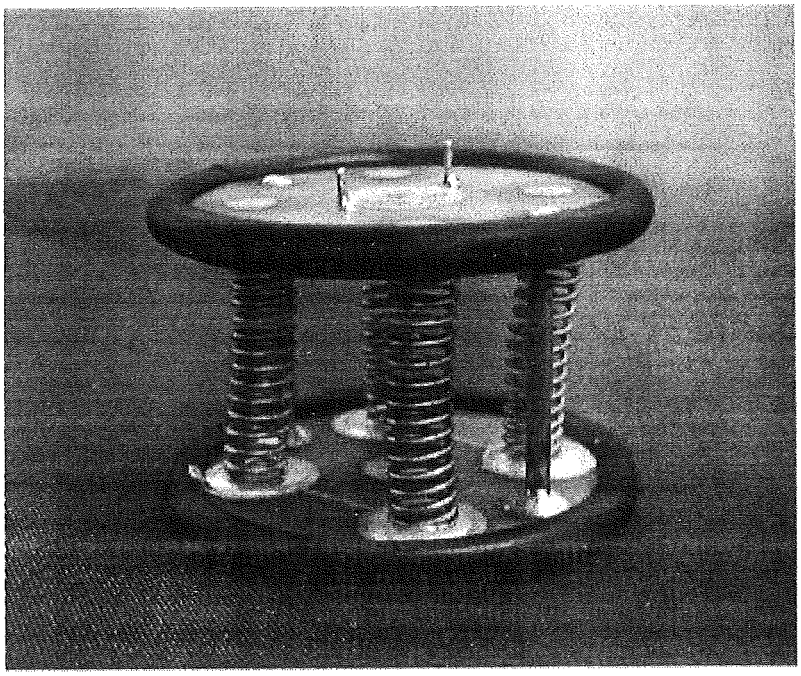

Figure 5.12 SMA spring actuator design, minus flexible enclosure.

5.7 References

1. Hodgson D.E. 1988. *Using shape memory alloys.* Shape Memory Applications, Inc., Santa Clara, California.
2. McCanna J. and Rae G.J. 1997. Shape memory alloy buoyancy regulator for subsea robots. *10th international symposium on unmanned untethered submersible technology.* SPIE, pp. 206-216.
3. Ohkata I., Suzuki Y. 1998. The design of shape memory alloy actuators and their applications. In: *Shape memory materials.* Otsuka K., Wayman C.M. (Eds.), Cambridge University Press, pp. 240-266.
4. Hodgson D.E. 1990. Using shape memory for proportional control. In: *Engineering aspects of shape memory alloys.* Duerig T.W., Melton K.N., Stockel D, Wayman C.M. (Eds.), Butterworth-Heinemann, London, Boston, pp. 362-368.
5. Mondo-tronics, San Anselmo, California. www.robotstore.com.
6. Waram T. 1990. Design principles for NiTi actuators. In: *Engineering aspects of shape memory alloys.* Duerig T.W., Melton K.N., Stockel D, Wayman C.M. (Eds.), Butterworth-Heinemann, London, Boston, pp. 234-244.
7. Transformation temperature hysteresis in NiTi alloys. *NiTi Smart Sheet #12.* Shape Memory Applications, Inc., Santa Clara, California, http://www.sma-inc.com.
8. Gandhi M.V., Thompson B.S. 1992. *Smart materials and structures.* Chapman and Hall, London, Glasgow, New York.
9. Giacommel J., Simpson J. 1995. Linear actuators from shape-memory alloys. *Machine design* **November 9**, pp. 99-100.

Chapter 6 Overall Discussion and Future Work

The target application of this project was an element of variable buoyancy with uses in oceanographic surveys and in other underwater operations. For this purpose, research was conducted into the behaviour of 'smart' materials in an underwater environment, such as responsive polymer gel systems and shape memory alloys. Much attention was also focused on the diverse buoyancy mechanisms present in nature, in the hope of finding a viable analogue that could be transferred to the engineering world.

As described in Chapter 2, Stoke's equation stated that a marine organism's position in the water column is determined by its form, or hydrodynamic, resistance, and its density relative to the density of the surrounding seawater [1-2]. In most cases, marine creatures attempt to change their density, rather than their form resistance, to control their buoyancy, as the transferral and replacement of heavy fluids and ions with lighter ones results in less expenditure of energy. Either a change in mass or a change in volume can control density, and practically all organisms use a change in mass. The exception is the sperm whale, which can solidify a quantity of hydrocarbon oil, causing its volume to contract and reduce the volume exposed to the sea [3]. The whale can then dive to great depths with less propulsive power required from its tail fin.

The review identified a number of engineering analogues to natural buoyancy methods. For example, flexible bladders, which are vital for the maintenance of depth for teleost fish, are used in a number of survey floats [4-5]. The purpose is slightly different, though.

Whereas a fish swimbladder helps to maintain a constant depth, the bladder in a float is inflated to assist the float to the surface so that it can transmit its data. This system is quite efficient in terms of energy conservation. There is no need for thruster power to rise or fall in the ocean. The only power required is for a quick transferral of liquid or gas to or from the bladder. Once the volume change is completed, the physical forces due to the change in density are sufficient to raise or sink the device.

The above example shows how difficult it is to obtain an ideal biomimetic solution to the control of buoyancy. Most marine creatures are quite happy to stay within their small range of depth, but underwater vehicles are often required for a variety of missions involving various depth changes. However, many of the natural buoyancy methods could form the basis for specific applications in buoyancy control of underwater vehicles, such as in the fine control of neutral buoyancy.

There is scope for much future work in this area. Existing biomimetic solutions can always be refined to improve efficiency, and new ideas may be obtained by looking at some of the less obvious natural buoyancy mechanisms. For example, many species of plankton and some cephalopods exclude the presence of heavy ions from their body fluids and replace them with lighter ions. The emergence of responsive polymer gels could serve as effective engineering analogues for this exclusion of ions. It has already been shown in Chapter 4 how the major seawater ions affect the volume of polyacrylamide gels. Similar gels are also finding many applications in drug release systems, where the gels are 'programmed' to slowly release an enclosed drug to the body system [6]. The advantage

of this system in an underwater environment would be its passivity, not drawing on the onboard battery supply. It would remain to be seen if such a release of light ions to an entrained solution would output an appreciable change in weight and density. In nature, many organisms using this method need to have large amounts of fluid compared to their overall body volume, making them quite cumbersome [7]. This was also evident with the vessel, *Trieste*, containing large amounts of low-density petrol [8].

It may also be worthwhile investigating the other terms of Stoke's equation, such as the density of seawater and the viscosity of seawater. Such terms are regarded as constant and unchangeable for a particular depth in the ocean, and certainly they remain so for marine organisms. However, there may be ways of manipulating these values immediately local to a vessel, maybe with the application of electric or magnetic fields, or through the release of substances from polymer gel systems, as mentioned above. If such a method existed, it would still need to be weighed against the power drawn from batteries to create the effect.

Polymer gel systems exhibit good properties contributing to their suitability for use in marine applications. As was seen in Chapter 4, NIPA gels have a density close to that of seawater. However, this density value can also be changed with the application of temperature, thus giving a buoyancy control mechanism closely paralleling the mechanism found in sperm whales. Although the density changes found with NIPA gels are not very appreciable, especially when used in conjunction with a possibly larger vehicle or device,

the manipulation of this density may prove to be of great benefit in the fine control of neutral buoyancy.

To achieve neutral buoyancy, the aggregate density of a vehicle would need to continuously match that of the surrounding seawater. The density of seawater increases by approximately 0.45% for every change in depth of 1000m [9], and the overall density change of an underwater device would have to match this increase. The study of the density of NIPA gels showed a marked increase in density of 30-40%, just above their transition temperature of 28°C to 30°C. This is well above the requirements for neutral buoyancy as depth is increased. These gels would form only a small fraction of the total volume of a device or vehicle, allowing an array of such gel systems to be activated at will to produce the required change in density to bring about the neutral buoyancy.

If the density changes of NIPA gels were to be used in buoyancy control systems, the effects of hydrostatic pressure would need to be taken into account. The phase transition temperature of NIPA gels has been found to be stress and strain dependent, with corresponding increases in transition temperature evident with the application of hydrostatic pressure [10]. The swollen state of NIPA gel is more stable at higher pressures, resulting in higher temperatures being needed to induce the phase transition [11]. There are also some complex gel-volume profiles, depending on solution temperature, as hydrostatic pressure is increased up to 250 MPa [11]. The effects on gel density are currently unknown for these parameters. The density experiments conducted in this study were performed under negligible hydrostatic pressures. Clearly the present

results need to be expanded to include the effects of hydrostatic pressures on the density and volume of NIPA (and polyacrylamide) gels.

Polymer gel systems, particularly NIPA gels, were seen to provide excellent changes in elastic modulus, as temperature was increased above the transition temperature. Such a property has great potential in an element of variable stiffness. This may be possible by embedding the gel in some hybrid material, which would be capable of adjusting its compressibility to match that of seawater. Traditional compressees consist of a hollow, pressure resistant cylinder containing a spring element, such as a steel spring or gas-charged hydraulic accumulator [9]. Descent to depths greater than 1000m are not very feasible, however, as cylinder wall thicknesses need to be substantial to withstand sea pressures. Polymer gel materials may have the advantage of being in the form of a membrane, directly exposed to the sea pressure. Further work would need to be conducted on the suitability of such materials as compressee spring elements by determining the strain energy, or modulus of resilience, of polymer gels at different external pressures, temperatures and salinities.

The actuation capabilities of polymer gels were found to be quite low. In comparison, the contractile force generated from a single fibre ($5mm^2$ cross-section) of polyvinyl alcohol-polyacrylic acid (PVA-PAA) gel was 1.45N, equivalent to 0.29 MPa [12]. This is over 10 times greater than the contractile response of polyacrylamide gels found in this study. It is also close to the actuating capabilities of human muscle, which is approximately 0.35 MPa [13]. Other polymer-based materials, such as conducting polypyrole actuators are capable

of active stresses that are at least 10 times greater than human muscle [13], or over 100 times greater than the active stresses measured in this study. For the advancement of polymer actuators in underwater applications, research may need to be concentrated on these new polypyrole actuators.

Much work is still needed on the use of shape memory alloys in a practicable variable volume device. The experiments conducted in Chapter 5 have shown the potential of these materials for producing effective and reproducible strains, with the application of significant stresses. However, the design for enclosing the SMA spring device was less than satisfactory and much improvement needs to be made in this area. Enclosing the device in a deformable and flexible membrane may prove to be useful, but the concerns for this configuration would be the maximum workable depth for the device. Enclosures need to be capable of withstanding hydrostatic pressures, and the strength of a flexible membrane may not be sufficient, thus limiting the device to shallow depths.

The following are a few ideas for more pressure-resistant enclosures.

(1) Buckling Plate Design:

- SMA actuator is enclosed in a pressure-resistant casing
- ends are capped with saucer-shaped plates, which are initially concave when the actuator device is in its cold contracted position
- end plates are designed to buckle between concave shape and a convex shape

- when the SMA actuator is heated, it expands and pushes against the plates, causing them to buckle outwards, thus increasing the volume of the system
- bias springs (not shown) will return the SMA actuator to its original position
- stop bars attached to the plates will pull the plates back to the concave shape as the actuator is contracting

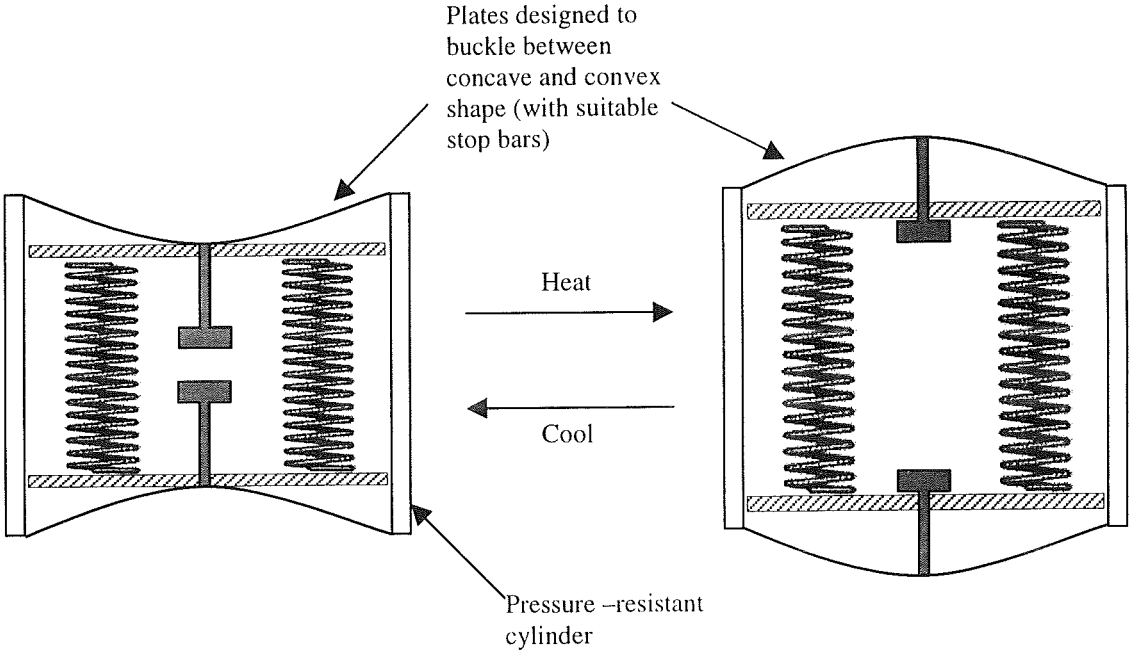

(2) Reinforced Bellows Design:

- SMA actuator is enclosed in reinforced flexible ducting or a mechanical bellows, with pressure-resistant end caps
- metal bellows have the advantage of working at greater depths
- heating the actuator will expand the system against hydrostatic pressure

- the spring resistance of the flexible ducting or mechanical bellow will provide sufficient bias to return the system to the initial position and volume

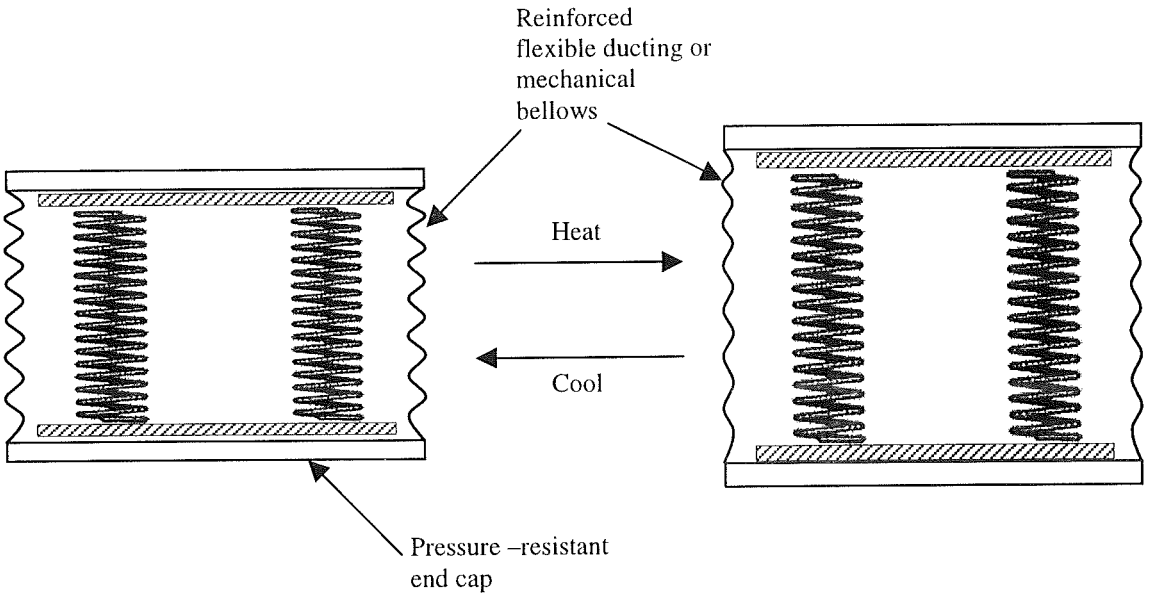

(3) Inflatable Bladder Designs:

- SMA actuator is enclosed in pressure-resistant casing with opening exposed to sea pressures
- Actuator works against a fixed volume of liquid in a flexible rubber bladder

- As actuator expands, the bladder is pushed out of the opening, thus increasing the volume of the system
- Bias springs or sea pressure will return the system to the original position and volume

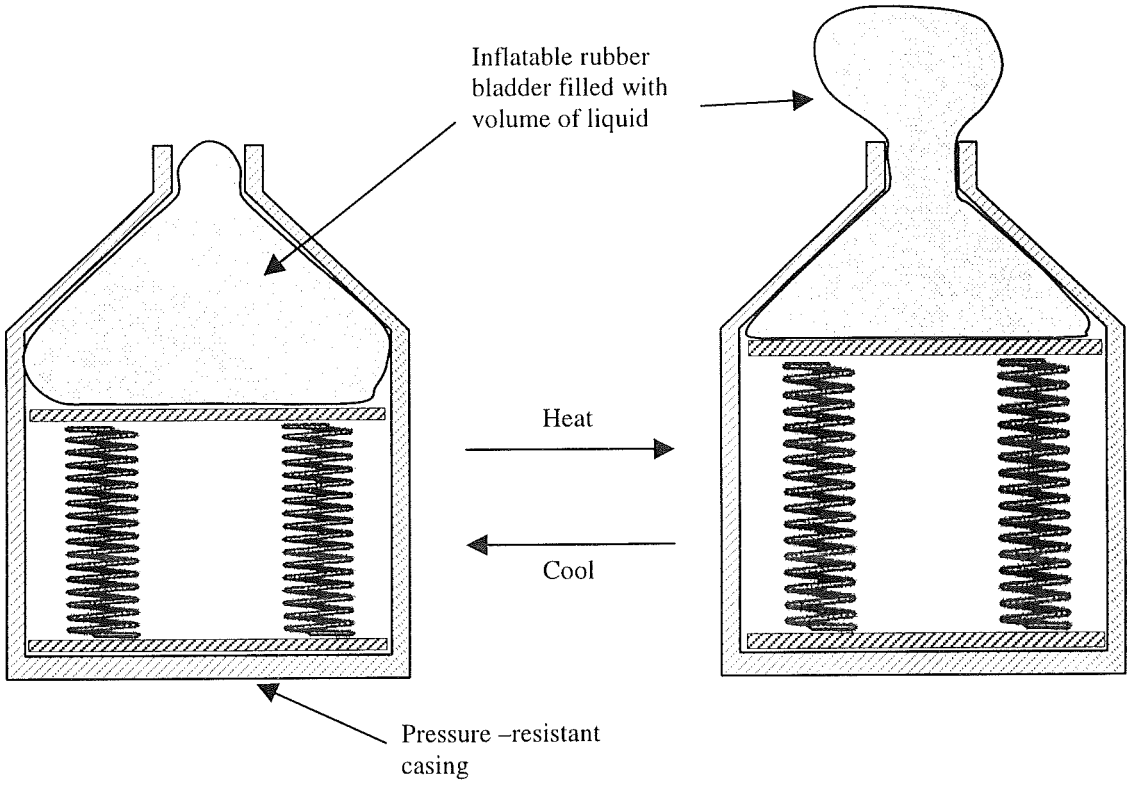

- SMA actuator works as part of a larger system in a pressure-resistant casing to expand or deflate an external bladder filled with oil
- When contracted, the space vacated by the SMA actuator fills with oil from the internal bladder
- The actuator forces the oil up to expand a mechanical bellows, which in turn compresses a volume of nitrogen gas.

- Upon the opening of a valve, the pressurised nitrogen forces the oil out of the bellow and into the external bladder, causing the overall volume to increase and reduce the density if the system
- To increase density again, a valve allows oil from the external bladder to the internal bladder
- The SMA actuator contracts again and the cycle can be repeated.

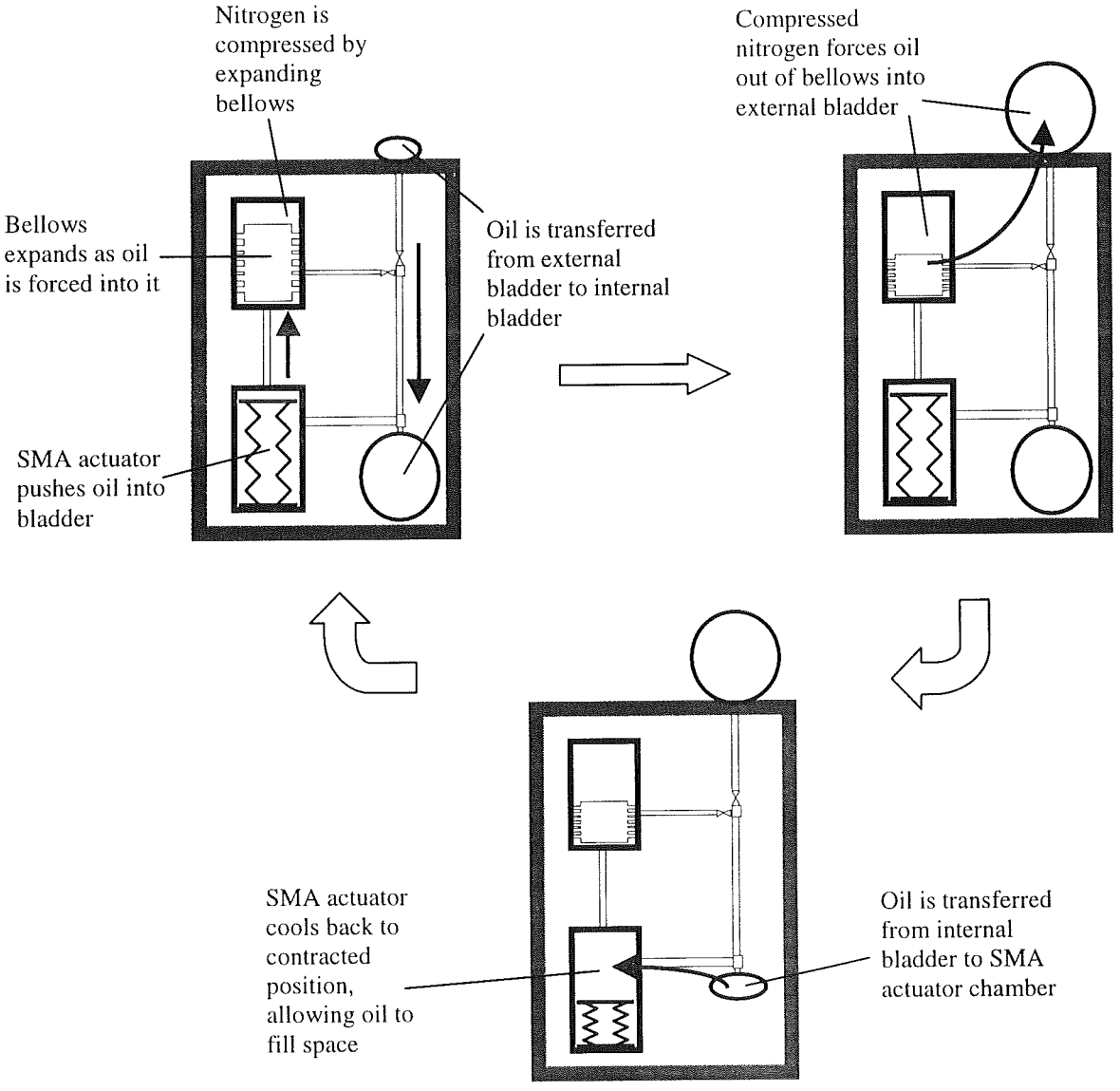

Future work in this area may diverge from the SMA spring assembly. The NiTi springs used in the study show appreciable increases in stiffness as their temperatures are increased. As suggested for polymer gels, these properties could be used as a variable stiffness element, if incorporated in a suitable membrane or laminate. To be effective, however, it may be better to use SMA wires, which have a superior work output per unit of material to SMA springs. SMA wires have also been proposed for an alternative buoyancy control method, as mentioned in Chapter 2. The design uses a compliant cylinder wrapped with SMA wires that contract to quietly and slowly pump a volume of ballast seawater from the vessel [14]. Another effective method uses arrays of small hollow tubes ('straws') made of shape memory alloy, which can increase in volume when electrically heated [15]. The 'straws' are limited to depths of less than 1000m.

There are clearly a number of avenues of future research which require to be pursued to achieve the objective of an effective and versatile buoyancy change device.

6.1 References

1. Wiseman S.W., Reynolds C.S. 1981. Sinking rate and electrophoretic mobility of the fresh-water diatom *Asterionella Formosa*: an experimental investigation. *British phycol. journal* **16**(4), pp. 357-361.
2. Nybakken J.W. 1993. *Marine biology: an ecological approach* Third edition. Harper Collins College Publishers.
3. Clarke M.R. 1978. *Journal mar. biol. ass. U.K.* **58**, pp. 1-71.
4. Webb D.C., Simonetti P.J. 1999. The SLOCUM AUV: An environmentally propelled underwater glider. *11th international symposium on unmanned untethered submersible technology*. pp. 75-85.
5. Davis R.E., Webb D.C., Regier L.A., Dufour J. 1992. The autonomous lagrangian circulation explorer (ALACE). *Journal of atmospheric and oceanic technology* **9**(3), pp. 264-285.
6. Gehrke S.H., Lee P.I. 1990. Hydrogels for drug delivery systems. *Specialised drug delivery systems, manufacturing and production technology*. Tyle P. (Ed.), Marcel Dekker, Inc., pp. 333-392.
7. Denton E.J., Gilpin-Brown J.B., Shaw T.I. 1969. A buoyancy mechanism found in cranchiid squid. *Proc. roy. soc. Lond. B.* **174**, pp. 271-279.
8. Gabler U. 1986. *Submarine design*. Bernard & Graefe Verlag, Koblenz.
9. Scrimshaw K.H. 1996. Aspects of buoyancy control and materials assessment applicable to deep submergence unmanned autonomous underwater vehicles (AUVs). *Oceanology International 1996* pp. 245-262.

10. Hirotsu S. 1994. Static and time-dependent properties of polymer gels around the volume phase transition. *Phase transitions* **47**, pp. 183-240.

11. Kato E. 1997. Volume-phase transition of *N*-isopropylacrylamide gels induced by hydrostatic pressure. *Journal of chemical physics* **106**(9), pp. 3792-3797.

12. Caldwell D.G., Tsagarakis N., Medrano-Cerda G.A. 2000. Bio-mimetic actuators: polymeric pseudo muscular actuators and pneumatic muscle actuators for biological emulation. *Mechatronics* **10**, pp. 499-530.

13. Madden J.D., Cush R.A., Kanigan T.S., Hunter I.W. 2000. Fast contracting polypyrole actuators. *Synthetic metals* **113**, pp. 185-192.

14. Mide technology corporation, Cambridge, MA 02141. Proposal of research to the Office of Naval Research phase I Awards - N96-161.

15. McCanna J., Rae G.J. 1997. Shape memory alloy buoyancy regulator for subsea robots. *10th international symposium on unmanned untethered submersible technology*. pp. 206-216.

Chapter 7 Conclusions

The general conclusions from this body of work are outlined as follows:

1. There is a need for a low power method of controlling the buoyancy of small autonomous underwater vehicles and devices.
2. There are a variety of natural buoyancy mechanisms, including the exclusion of heavy ions to create a less dense liquid, increasing or decreasing the surface area, the use of gas chambers, low-density waxes and oils, and hydrodynamic planes.
3. No clear biomimetic solution was obtained from the buoyancy mechanisms present in nature. However, many of them provide inspiration for engineering analogues.
4. Of the many smart materials currently available, responsive polymer gels and shape memory alloys appear to be the most suitable candidates for use as actuators in an underwater environment.
5. Polymer gels can be manipulated to output a change in volume, stiffness and density that can be used in the control of neutral buoyancy of a vehicle. However, there is still room for research and improvement, such as determining the effects of hydrostatic pressure on the density and volume of gels, and investigating alternative polymer actuators capable of outputting greater power ratios.
6. Shape memory alloys have great potential for providing actuation forces, but much work needs to be done to improve that knowledge and to design an effective buoyancy control device.

APPENDIX A

ELSEVIER

Materials and Design 21 (2000) 169–174

Materials & Design

The effects of salinity and temperature on the behaviour of polyacrylamide gels

P.J. Molloy*, M.J. Smith, M.J. Cowling

Glasgow Marine Technology Centre, University of Glasgow, Glasgow G12 8QQ, UK

Received 9 August 1999; accepted 27 September 1999

Abstract

Polymer gels are capable of undergoing large volume changes under the influence of solvent composition and temperature. Studies have been conducted on the effects of salinity and temperature on hydrolysed polyacrylamide gels. Three salinities were investigated from 5 parts per thousand (ppt) to 35 ppt, which is approximately the salinity of natural seawater in temperate waters. For each of the salinities, the effect of temperature from 5°C to 40°C with 5°C increments was investigated. It was found that hydrolysed polyacrylamide gels shrank in all the solutions, this effect being most pronounced at the high salinity (35 ppt), with a smaller volume decrease noted in 20 ppt and 5 ppt salinities, respectively. The effect of temperature was minimal, with all solutions promoting a decreasing volume change as the temperature increased. The polyacrylamide gels remained whole in the experiments with no visible signs of degradation. The cyclical volumetric strain behaviour of the gels was also investigated by alternate exposure to saline solutions and distilled water. Cyclical swelling and deswelling of the gels was observed which, in some cases, was fully reversible.

Keywords: Polyacrylamide gels; Seawater

1. Introduction

There is a need for marine devices which are able to take measurements throughout the water column, usually with limited power sources. Buoyancy control is important in these small, underwater vehicles and sensor packages to enable greater flexibility in measurements in the ocean. This paper has concentrated on the behaviour of polymer gel systems which exhibit large volume changes when subjected to certain stimuli. Such gel systems might be used as the basis for actuators to control buoyancy in underwater applications.

Polymer gels can respond to changes in their environment, such as pH [1], temperature [2], solvent composition [3], and applied voltage [4]. One response can be a change in size and shape [5], which could mean a conversion of chemical energy directly to mechanical work. The benefits of this conversion could be used wherever power for more conventional devices is limited or difficult to obtain, such as in an underwater environment.

This paper studies the effect of immersing hydrolysed polyacrylamide gels, i.e. ionic gels, in seawater of various salinity concentrations in order to mimic realistic marine environments. Seawater is effectively a solution of major and minor ions, gases and nutrients. Eleven major ions make up more than 99.99% of the dissolved material in the sea [6]. These major ions are listed in Table 1.

The effect of salt solutions on gels has been investigated [7–10], but not the effect of seawater of various

*Corresponding author. Tel.: +44-141-330-4361; fax: +44-141-330-4015.
E-mail address: pmolloy@mech.gla.ac.uk (P.J. Molloy).

0261-3069/00/$ - see front matter
PII: S0261-3069(99)00063-4

Table 1
Major ion composition of seawater

Common name	Chemical form	Amount (%)
Chloride	Cl^-	19.353
Sodium	Na^+	10.76
Sulphate	SO_4^{2-}	2.712
Magnesium	Mg^{2+}	1.294
Calcium	Ca^{2+}	0.413
Potassium	K^+	0.387
Bicarbonate	HCO_3^-	0.142
Bromide	Br^-	0.067
Strontium	Sr^{2+}	0.008
Boron	H_3BO_3	0.004
Fluoride	F^-	0.001

salinities and at various temperatures, where the cocktail of numerous ions and salts can affect the behaviour of the gel. The varying salinities were used to emulate real environmental conditions in which these materials could be used, such as oceans, coastal waters and estuaries. If gels are to be used in such marine environments, the effects of salinity and temperature are of significant interest.

Polymer gels consist of two components: a liquid phase and a network of long-chain molecules. The network of polymer molecules holds the liquid in place, and the liquid prevents the network from collapsing into a compact mass. The volume of a gel is influenced by osmotic pressure, π, which is the sum of three components illustrated by the following Flory–Rehner [11] assumption:

$$\pi = \pi_{mix} + \pi_{el} + \pi_{ion}, \quad (1)$$

where π_{mix} is polymer–polymer affinity, which relates to the interaction between the polymer strands and the solvent. The π_{mix} pressure is always negative. Its value depends on the solvent composition and is independent of temperature. π_{el} is rubber elasticity, the pressure which relates to the elasticity of the individual polymer strands, i.e. their resistance to stretching or bunching. The strength of the rubber elasticity of a gel is proportional to the temperature. The temperature, however, does not affect the direction of the π_{el} pressure, but only the magnitude of this force. Direction depends on the state of the gel. When the gel is swelling the π_{el} pressure is considered positive. π_{ion} is the hydrogen ion pressure, which is associated with the degree of ionisation of the polymer network. Ionisation releases an abundance of positively charged hydrogen ions into the gel fluid. Hydrogen ions give rise to a positive pressure that is temperature-dependent and tends to cause swelling in such gels.

The magnitude and direction of the three components of π in conjunction with each other governs whether a gel swells or shrinks. At a fixed solvent composition and temperature the gel will adjust its volume so that the total osmotic pressure will be zero. If the osmotic pressure is positive, the gel will take up fluid and the volume will increase. If it is negative, the gel will expel fluid and the volume will decrease. This process continues until equilibrium is reached.

The elastic force due to swelling depends on the degree of crosslinking of the polymer network. There is less swelling for strongly crosslinked gels. Also, as the temperature of the gel decreases the polymer network loses its elasticity. At a critical temperature the elasticity goes to zero and the gel becomes infinitely compressible.

Temperature is thus an important factor in gel strength and phase transition. The temperature at which polymerisation of the network takes place also affects the structure and physical properties of the gel. Gelfi et al. [12] have shown that gels polymerised between 0 and 4°C are turbid (opaque), highly porous and unelastic. These opaque gels are regarded as 'faulty' gels, because the distribution of polyacrylamide chains within the matrix is non-homogenous, i.e. there are areas of high and low strand density. This leads to low swellability in solvents. The optimum polymerisation temperatures are between 25 and 30°C. The resultant gels are transparent, with small pores, and are compliant. Polymerisation above 60°C results in gels with short polymer coils, which are slightly more porous and less compliant [12].

2. Experimental

2.1. Gel preparation

Polyacrylamide gels were prepared using an acrylamide monomer (Sigma) and the crosslinking comonomer, *N'N*-methylene-bis-acrylamide (Fluka). All chemicals were of reagent-grade quality and were used without further purification. Transparent rods of gel were prepared based on a method described by Tanaka [13]. Doubling the amount of crosslinking agent and halving the amount of water altered the quantities, in order to produce a more mechanically robust gel. The gels were produced in polypropylene cylinders and cured at room temperature. The gel rods so produced were 100 mm long and had a diameter of 15 mm. These were washed in distilled water to remove any residue monomers and the rods were then allowed to equalise in distilled water for 1 week.

Using nomenclature introduced by Hjerten [14] to describe composition, the total monomer concentration T was found to be 10% and the percentage concentration of the crosslinking agent relative to the total concentration C was found to be 5%. Such gels were

found to have an equilibrium water content (EWC) of approximately 90%.

After equalising, the rods were cut into discs and allowed to hydrolyse for 3 weeks by soaking in 1.2% *N,N,N',N'*-tetramethyl-ethylenediamine (TEMED), a basic solution. Assuming that the gels swell isotropically [15], the degree of swelling is calculated as a swelling ratio, V/V_0,

$$V/V_0 = (D/D_0)^3, \quad (2)$$

where V_0 and V are the volumes of the gel discs at preparation and after immersion in TEMED, respectively, and D_0 and D are the corresponding gel diameters. All gels used in the study were hydrolysed for a period of 21 days, resulting in a mean swelling ratio of $V/V_0 = 3.585 \pm 0.095$.

2.2. Salinity study

The salinity studies were carried out using seawater collected from the Largs Channel of the Firth of Clyde, Scotland. The seawater had a salinity of 35 ppt when collected and it was filtered through Whatman glass microfibre filters, which removed any bacterial cultures. Solutions of 5 ppt and 20 ppt were prepared from seawater by diluting it with distilled water. The distilled water was produced by a Millipore-U10 system.

In order to investigate the effects of salinity on the hydrolysed gels, all the discs were weighed and their diameters were recorded using a Mitutoyo Profile Projector Type PJ-300. The discs were soaked in solutions (approximately 30 ml) of distilled water, 5 ppt saline, 20 ppt saline or 35 ppt saline (natural seawater).

All swelling experiments were carried out in triplicate. They were begun at 5°C and were taken through a temperature range in increments of 5°C up to 40°C. The solutions were kept at constant temperature using a Techne Flow Cooler FC-500 in conjunction with a Techne Circulator C-85D in a poly-(methyl methacrylate) (PMMA) 10 L tank of water.

After each 5°C temperature increment the gels were left for 2 days at this temperature to adjust. They were weighed and their diameters recorded each day. The solutions were changed daily during the experiment to simulate a larger body of water. The degree of swelling of the gels at each salinity concentration and temperature was found using Eq. (2).

The cyclical volumetric strain behaviour of the gels was also investigated by alternate exposure to distilled water and saline solutions of 5 ppt, 20 ppt or 35 ppt seawater. The gels were allowed 2 days to equalise in the respective solution before being transferred to the alternate solution.

3. Results and discussion

Fig. 1 shows the degree of swelling of the gels with respect to temperature when immersed in one of the three saline concentrations. As mentioned previously, after hydrolysation in 1.2% TEMED for 21 days, the average degree of swelling of the gels was 3.585 ± 0.095. This will be referred to as the hydrolysation value.

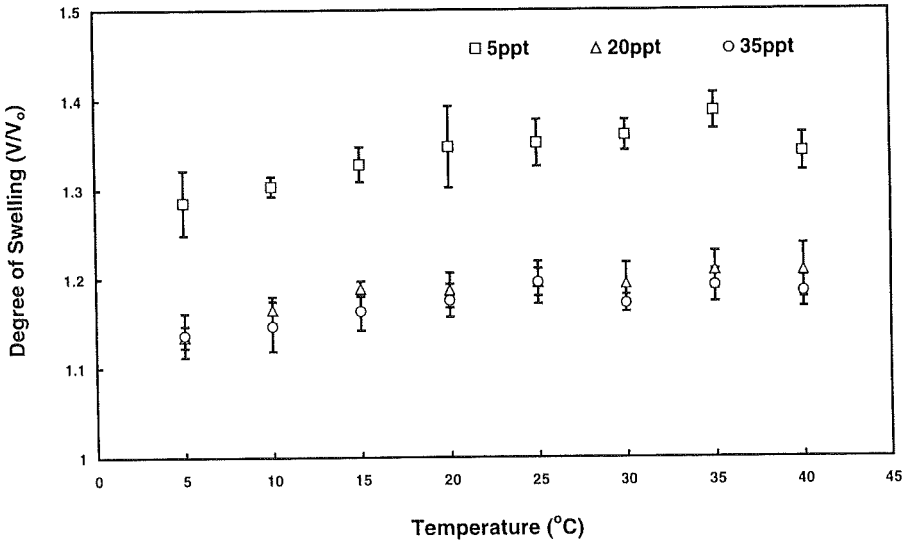

Fig. 1. Degree of swelling of polyacrylamide gels with respect to temperature when immersed in one of the three saline concentrations.

From Fig. 1, it can be seen that the degree of swelling of the gel discs decreases significantly from the above value when they are immersed in saline solutions, exhibiting a V/V_0 range between 1.1 and 1.4. The swelling degree for gels in 20 ppt and 35 ppt solutions are practically the same, with that for the 35 ppt values being slightly lower than for the 20 ppt solution. These values are significantly lower than the swelling degree for the gels in the 5 ppt solution. The results are in line with what would be expected of such materials due to their polymer structure.

Since the gels were hydrolysed before the salinity experiments, some of the $-CONH_2$ groups will have been converted to carboxyl groups, which spontaneously ionise leaving $-COO^-$ ions (Fig. 2). This causes the gel to expand due to the repulsion of the ions. When the gel is then immersed in a saline solution the positive ions, such as the sodium and magnesium ions, shield the $-COO^-$ ions, negating the repulsion and resulting in a decrease in the degree of swelling. This effect is less pronounced in the low salinity as there are less ions available than at the higher salinities, i.e. 20 ppt and 35 ppt.

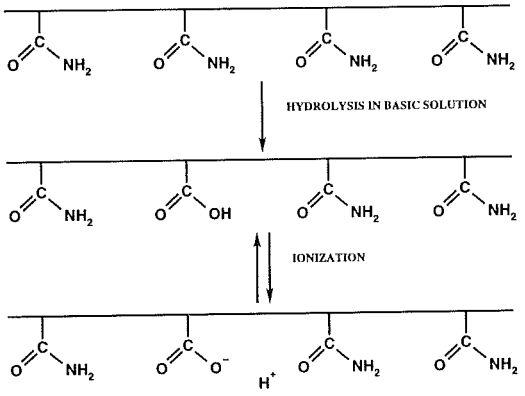

Fig. 2. Hydrolysis of polyacrylamide gels.

The effects of temperature play only a small part in the degree of swelling of the gels immersed in saline solutions. At all salinity concentrations there is less shrinkage from the hydrolysation value as the temperature increases, but only to a small extent. This is to be expected as polyacrylamide gels are relatively insensitive to temperature [16]. The hydrogen ion pressure, π_{ion}, and the rubber elasticity, π_{el}, are temperature-dependent and, thus, this dependency will have a small effect on the magnitude of the swelling degree as the temperature increases [5].

Fig. 3 shows the relationship between the degree of swelling and temperature for gels in the salinity solutions investigated and also in distilled water. There is a great difference between gels in distilled water and those in seawater solutions. Distilled water gels have a swelling degree in the region of 4–5.5, which is higher than the hydrolysation value. This is due to the introduction of extra ions, O^- and H^+, into the gel network and augmenting the existing repulsion that causes swelling. The gels in saline solutions, on the other hand, have contracted to a V/V_0 range of 1–1.5.

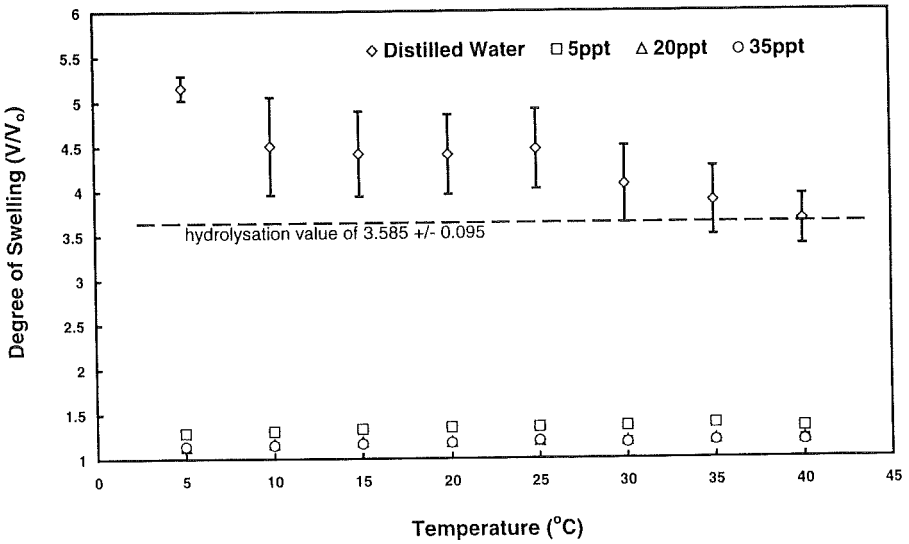

Fig. 3. Degree of swelling of polyacrylamide gels with respect to temperature when immersed in one of the three saline concentrations and also in distilled water.

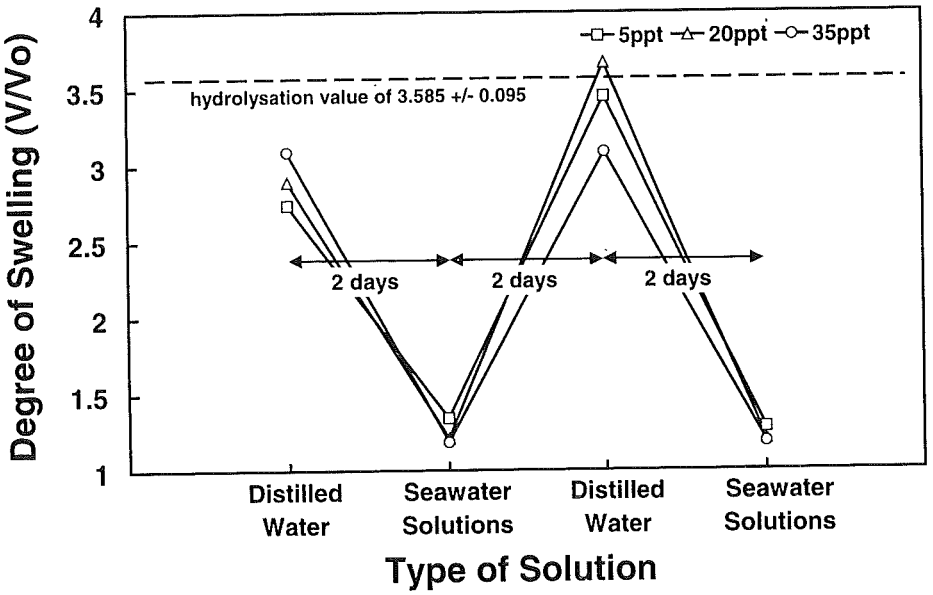

Fig. 4. Cyclical volume contraction and expansion of polyacrylamide gels when transferred to and from solutions of seawater and distilled water.

These results demonstrate a possible use of hydrolysed polyacrylamide gels in a seawater environment. There is a significant contraction of gels when immersed in seawater, regardless of the salinity concentration. This was re-affirmed in a cyclic test (carried out at 40°C) where polyacrylamide gels were repeatedly transferred from distilled water to salinity solutions and back again. Fig. 4 illustrates the significant swelling and contraction that can occur by changing the external solution from distilled water to seawater. The gels show good repeatability when contracted in seawater solutions. This shrinkage is reversible on transfer to distilled water. The changes in gel volume are not rigid or sudden. It takes approximately 1 h for a new solvent mixture to permeate the gel by diffusion [5]. The shrinking and swelling that follows can take much longer to reach completion, perhaps several days.

4. Conclusions

The purpose of this study was to investigate polyacrylamide gels for their usefulness as possible actuators in marine applications, such as in buoyancy control of small vehicles and sensor packages. The work demonstrated that such gels contract in various seawater solutions and therefore, the use of polyacrylamide gels as actuators in marine applications may be considered. There was a significant reduction in the degree of swelling of the gels when transferred from TEMED to saline solutions, the most contraction occurring at the highest salinity concentration of 35 ppt, with less contraction for the lower salinities. All saline solutions promoted an increasing volume as the temperature increased. The significant differences in degree of swelling for gels in seawater and in distilled water also demonstrates their possible applications as actuators in marine applications.

Acknowledgements

This research was supported by the Engineering and Physical Sciences Research Council (EPSRC), Grant No. GR/L 27022, administered through the Marine Technology Directorate (MTD). Such support is gratefully acknowledged.

References

[1] Katayama S, Hirokawa Y, Tanaka T. Reentrant phase-transition in acrylamide-derivative copolymer gels. Macromolecules 1984;17:2641–2643.
[2] Hirokawa Y, Tanaka T. Volume phase transition in a nonionic gel. J Chem Phys 1984;81(12):6379–6380.
[3] Zhang YQ, Tanaka T, Shibayama M. Super-absorbency and phase-transition of gels in physiological salt-solutions. Nature 1992;360:142–144.
[4] Tanaka T, Nishio I, Sun ST, Ueno-Nishio S. Collapse of gels in an electric field. Science 1982;218:467–469.
[5] Tanaka T. Gels Sci Am 1981;244:110–123.

[6] Bretschneider CL, Corcoran EF, Jung GH, McAllister RF, Vine AC, Zetler BD. Basic oceanography. In: Myers JJ, Holm CH, McAllister RF, editors. Handbook of Ocean and Underwater Engineering. London, San Francisco, Toronto, London, Sydney: McGraw-Hill, 1969.
[7] Ohmine I, Tanaka T. Salt effects on the phase transition of ionic gels. J Chem Phys 1982;77:5725–5729.
[8] Ricka J, Tanaka T. Swelling of ionic gels: quantitative performance of the Donnan theory. Macromolecules 1984;17: 2916–2921.
[9] Hooper HH, Baker JP, Blanch HW, Prausnitz JM. Swelling equilibria for positively ionized polyacrylamide hydrogels. Macromolecules 1990;23:1096–1104.
[10] Baker JP, Stephens DR, Blanch HW, Prausnitz JM. Swelling equilibria of acrylamide-based polyampholyte hydrogels. Macromolecules 1992;25:1955–1958.
[11] Flory PJ, Rehner J. J Chem Phys 1943;11:521.
[12] Gelfi C, Righetti PG. Polymerisation kinetics of polyacrylamide gels II. Effect of temperature. Electrophoresis 1981;2:220–228.
[13] Tanaka T, Fillmore D, Sun ST, Nishio I, Swislow G, Shah A. Phase transitions in ionic gels. Phys Rev Lett 1980;45: 1636–1639.
[14] Hjerten S. Arch Biochem Biophys Suppl 1962;1:147.
[15] Ilavsky M. Phase transition in swollen gels. 2. Effect of charge concentration on the collapse and mechanical behaviour of polyacrylamide networks. Macromolecules 1982;15:782–788.
[16] Chunfang L. Scaling behaviours and mechanical properties of polymer gels. Ph.D. dissertation, Denton, Texas, 1994.

APPENDIX B

ISSN 0141-0814. Journal of the Society for Underwater Technology, Vol. 25, No. 2, pp. 41–49, 1999/2000

Buoyancy Mechanisms of Marine Organisms: Lessons from Nature

P. J. MOLLOY and M. J. COWLING

Glasgow Marine Technology Centre, University of Glasgow, Glasgow G12 8QQ, UK

Abstract

This paper reviews how many pelagic organisms maintain their buoyancy in the ocean. Although there are thousands of different species of marine organisms, ranging in size from microscopic plankton to squid, shark and the large whales, the mechanisms they use to avoid sinking are not as varied. These mechanisms include: the exclusion of heavy ions to create a less dense liquid; enlarging the surface area of the organism to increase drag; the use of gas chambers; the use of low-density waxes and oils; and hydrodynamic planes. Natural buoyancy systems are compared with those currently used in various underwater vehicles; in addition, the attempts being made to mimic the mechanisms present in nature are described.

1. Introduction

Thousands of pelagic organisms exist in the ocean, from the surface waters down to the deep sea floor. Each species lives within a certain range of depth and, as far as is known, the individuals of a species must keep to their particular environment in order to flourish [1]. The protein-based tissues and skeletal materials of many of these marine organisms are considerably more dense than seawater, which has a density range of about 1.024–1.030 g/cm^3 [2]. To compensate, these organisms employ a variety of methods in order to remain at their chosen depth in the water column. Table 1 summarizes many of the mechanisms found in marine life. The Stokes' equation determines the sinking rate of an organism [3]:

$$SR = \frac{2}{9}\frac{(\rho_1 - \rho_2)gr^2}{(V_W)(\phi)}$$

where SR = sinking rate, ρ_1 = density of the organism, ρ_2 = density of seawater, g = gravitational acceleration; r = radius of a sphere of identical volume; V_W = viscosity of water; and ϕ = form resistance, which expresses the effect of departure from the spherical form on sinking rate. Control of the local density or viscosity of seawater is beyond the capabilities of an organism, but either increasing its own hydrodynamic resistance or decreasing its density with respect to that of seawater can bring about a reduction in the sinking rate.

2. Plankton

The proteins, carbohydrates and skeletal structures that make up plankton usually have a density greater than that of seawater and, hence, plankton tend to sink in the water column. Therefore they must employ strategies to aid their buoyancy or reduce their rate of sinking.

Plankton have a number of ways of reducing their density, one such method being ionic replacement to reduce the density of body fluids. Seawater is a complex mixture of ions, of which sodium (Na^+), chloride (Cl^-), magnesium (Mg^{2+}) and sulphate (SO_4^{2-}) account for over 97% of the total ionic content [4]. Replacement of a heavy ion, such as sulphate, with a lighter ion, such as chloride, can reduce the density of the solution. Ions with negative partial molar volumes, such as magnesium, cause close packing of water molecules and therefore increase the density of the solution. Replacement of these with ions of positive partial molar volumes, such as sodium, induce a less regular structure and lower the solution's density [4].

Organisms such as ctenophores, salps and heteropods actively exclude heavy ions such as SO_4^{2-} from their bodies and replace them with osmotically similar but lighter Cl^- ions [3]. Newton and Potts [4] observed the exclusion of Mg^{2+} and

Table 1 Buoyancy mechanisms in marine organisms

Method	Marine organisms
Exclusion of heavy ions	Gelatinous marine animals, plankton
Increase in surface area	Plankton
Ammonium-rich body fluid	Some oceanic squid and crustaceans, plankton
Gas-filled shell	Some cephalopods (e.g. cuttlefish, *Nautilus* and *Spirula*)
Gas-filled swimbladder	Teleosts (e.g. cod and haddock)
Hydrocarbon squalene	Squaloid sharks
Low-density waxes	Deep-diving mammals (e.g. sperm whale)
None	Bottom dwellers (e.g. lobster, octopus), constant swimmers (e.g. some squid, mackerel, blue shark)

SO_4^{2-} ions from the larval bodies of *Hoarus vulgaris* (Arthropoda: Decapoda), *Asterias* (Echinodermata) and *Obelia*. Gross and Zeuthen [5] and Kahn and Swift [6] have found similar ion replacement mechanisms present in other plankton. One such organism is the dinoflagellate *Noctiluca*, whose internal fluid contains ammonium chloride (NH_4Cl) which is isosmotic with seawater but is less dense [3, 6].

Some plankton use gas vesicles for buoyancy. Researchers [7, 8] describe how freshwater and marine blue-green algae can change overall buoyancy by modifying the cellular carbohydrate content. The siphonophore colonies also use gas floats, e.g. the Portuguese man-of-war (*Physalia*) [3]. Another low-density strategy is the use of fats or oils that are less dense than water. Copepods and diatoms store oils that maintain their buoyancy, and which can also be used as food reserves [3].

If plankton cannot reduce their density, then they must increase their hydrodynamic resistance. The smaller an organism is, the greater is its surface area relative to volume [3]. By remaining small, plankton offer far more surface area of resistance to sinking per unit volume of living material than if they were large. The other way of increasing the hydrodynamic resistance is to change the shape of the body or develop spines and body projections. These can add considerable resistance, but add little to the weight [9]. A few long spines increase drag more than a greater number of short spines. The species *Acanthometra* has projections, called myonemes, projecting out from the gelatinous body of the organism [2]. When the myonemes contract, the gelatinous matrix is greatly expanded and the organism rises in the water. On relaxation of the myonemes, the matrix shrinks and is followed by sinking (Figure 1).

Certain plankton can undergo vertical migrations to the depths and back up to shallow waters. For example, during a typical day, phytoplankton photosynthesize and accumulate carbohydrates, causing nitrogen supplies to become limited. This tips the balance of the cell from being positively buoyant to negatively buoyant and the cell begins to sink. Photosynthesis decreases and with it the production of carbohydrates. However, metabolic activity continues and internal NO_3^- pools accumulate in the cell with the expenditure of energy. These tip the balance back in favour of positive buoyancy and the cell begins to rise again. In this way the plankton oscillates between positive and negative buoyancy. Studies of the coastal marine diatom *Thalassiosira weissflogii* showed that the density and sinking rate of the cell was affected by carbohydrate production, causing it to sink [10], although Fisher and Harrison [11] found no positive correlation between sinking rate and carbohydrate content for the organism. Moore and Villareal [12] studied the vertical migration of three oceanic diatoms of the genus *Rhizosolenia* and found that carbohydrate ballasting can account for buoyancy changes. Whether as solitary cells or as aggregations (mats), *Rhizosolenia* migrate in this way to keep nutrient pools (below 80–100 m) and then return to the surface for photosynthesis. This migration helps the transport of nitrate (new nitrogen) from depth into the surface waters, and surface-derived carbon is respired at depth [13].

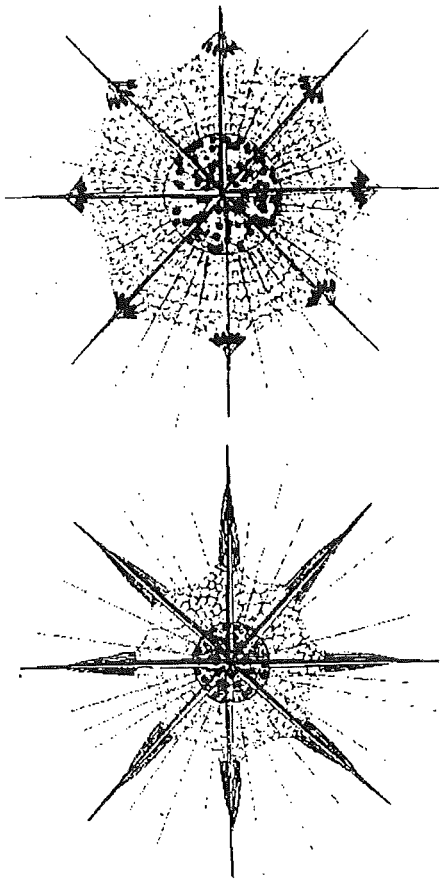

Figure 1 The acantharian radiolarion. Above, with outer cytoplasm expanded (myonemes contracted); below, with cytoplasm withdrawn (myonemes relaxed) [2].

A number of hypotheses have been suggested for the vertical migration of zooplankton [3]. Mclaren [14] and Haney [15] suggest that zooplankton descend into the depths during the day to avoid predators in the upper lighted areas. Another hypothesis is that they are avoiding damage from light. Hardy [16] suggests that descent into the depths brings a fresh supply of food for the zooplankton. Currents at depth are generally slower than in the shallow waters, so while the zooplankton are at depth, the swifter upper currents bring along a fresh supply of phyto-

plankton. The zooplankton then rise to the surface to feed. A final reason for migration is that descent into the depths allows the production of phytoplankton. The hypothesis also suggests that less energy is needed for zooplankton to stay in cold, deep waters than trying to maintain themselves constantly in the warm, upper waters [14, 17–19].

3. Cephalopods

There are some 700–800 species of modern cephalopod. They are mostly squids and a number of octopods, with a few sepioids of the cuttlefish group [2]. They employ a number of methods to achieve neutral buoyancy [20], including the use of gas-filled chambers of *Nautilus*, *Spirula* and *Sepia*, replacement of heavy ions as in some octopods, and the storage of low-density fats in the Gonatidae family of squids. However, the majority of cephalopods achieving neutral buoyancy are oceanic squids using ammonium-rich solutions isosmotic with seawater.

Ammonium storage was first discovered in cranchiid squids [21]. Since then, thirteen families of oceanic squid have been documented, or suggested, to use ammoniacal buoyancy, as have genera in three of the fourteen otherwise non-ammoniacal, muscular families [20, 22]. The cranchiid squids can hang almost motionless in the sea and possess a large, fluid-filled buoyancy chamber. The fluid is principally ammonium chloride and is isosmotic with seawater [2, 21]. It has a specific gravity of about 1.010–1.012, so a relatively large volume of the ammoniacal fluid is required to make the squid neutrally buoyant. This could take up almost two-thirds of the animal's total weight, making it very cumbersome. The squid secretes nitrogen from the breakdown of proteins in the form of ammonia instead of urea. This ammonia is trapped in the coelomic cavity. Because the acidity is high, the ammonia diffuses from the bloodstream into the cavity and dissociates into ions. They remain in the cavity to reduce the density of the fluid. The coelomic cavity hardly leaves space for the development of a capacious mantle cavity. In fact, such squid, though capable of rather quick escape reactions, are small-finned, unhurried swimmers. In larger and more active kinds of squid there is no single buoyancy chamber (e.g. *Histioteuthis*). Instead, there are many small vacuolar chambers over the body, particularly in the arms and mantle, that are filled with ammoniacal fluids very similar in composition to those of cranchiid squids [2, 20, 23–25]. Although ammoniacal buoyancy offers an advantage, in that it maintains function at high ambient pressure or regardless of rapid changes in depth [21], few ammoniacal squids appear to exploit this advantage by undergoing large vertical migrations [26].

Nautilus, the last surviving genus of externally shelled cephalopod, maintains neutral buoyancy in the sea through the use of a gas- and liquid-filled portion of the shell which serves to lower the specific gravity of the entire shell and enclosed tissue to approximately that of seawater [27]. The saline or cameral liquid that originally filled the chambers is removed by osmosis through the siphuncle, a thin strand of tissue that extends back from the body of *Nautilus* through each chamber. The space left is filled passively with gas by diffusion, and the pressures within these chambers are subatmospheric [28]. As the animal grows, producing new flesh and shell material, it becomes progressively denser. By removing liquid in small volumes each day, a *Nautilus* can counterbalance density increases [29]. The system can also be used if there is a sudden increase or decrease in the weight of the *Nautilus*, such as ingestion of food or following an attack by a predator, where a portion of the shell may have been broken off [30]. Studies have shown that, when challenged with a sudden decrease in buoyancy, *Nautilus* can increase its chamber emptying rate in a compensatory fashion [31]. When sections of shell were removed, or when extra buoyancy was attached to the *Nautilus*, it shut off the pumps in the siphuncle, resulting in a slow refilling of the last several chambers with liquid until neutral buoyancy was again achieved [32]. This gave the animal time to grow new shell material. It was a popular misconception that the *Nautilus* was capable of rapidly adding or subtracting water in the shell for the purpose of quickly ascending or descending [33, 34]. Chamber refilling or emptying takes days, not hours, preventing rapid buoyancy changes.

The more recently evolved cephalopods, *Sepia* (cuttlefish) and *Spirula*, also have chambered shells that are used to achieve neutral buoyancy. The cuttlebone of the *Sepia* consists of a number of thin chambers laid down, one below the other, at the rate of about one or two a week as the animal grows [28]. Parallel sheets (lamellae) of calcium carbonate form the chambers which are sealed from each other, but within any individual chamber gas or liquid can move freely [35]. Numerous pillars support each chamber, and these have a sigmoidal cross-section (Figure 2). Liquid can be pumped into or out of the cuttlebone to decrease or increase the gas volume. The gas is principally nitrogen and its pressure in the older chambers is only about four-fifths of an atmosphere, regardless of depth [28]. This is enough to give the bone an overall density of around 60% that of seawater, sufficient to counter the heavier tissues of the cuttlefish. As in the *Nautilus*, the presence of the gas is purely incidental as it diffuses passively into the partially vacated space that develops due to the active pumping out of the entrained liquid.

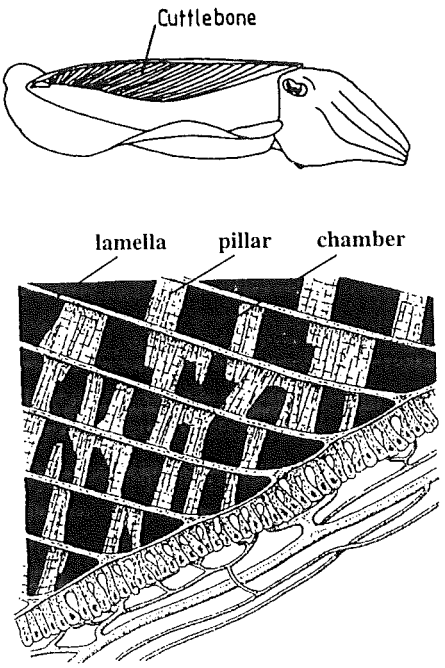

Figure 2 The position and microstructure of the cuttlebone [35].

This entrained liquid is primarily a sodium chloride solution, at a lower concentration than in the blood of the cuttlefish. This creates an osmotic pressure sufficient to balance hydrostatic pressure. The yellowish membrane at the back end of the cuttlebone has an ample blood supply that enables the membrane to pump salts from the liquid within the cuttlebone and into the blood. The effect of this is a flow of liquid from the cuttlebone into the bloodstream. Therefore, this salt pump can increase or decrease the osmotic pressure between the animal's blood and cuttlebone liquid in response to changes in hydrostatic pressure exerted by the sea.

Birchall and Thomas [35] found the cuttlebone matrix to have a mean crushing strength of 1.1 MPa. Therefore, along with actively maintaining the buoyancy of the animal, the sealed chambers also provide a structure which combines high porosity (93%) and low specific gravity (0.19) with the ability to resist external pressures greater than 1 MPa. Denton *et al.* [36] reported that under hydrostatic pressure a whole cuttlebone withstood a pressure of 2.4 MPa (corresponding to a depth of 230 m) before imploding. Failure of the shell was found to be progressive, not catastrophic [35]. The S-shaped cross-section of the pillars minimizes any tendency for the pillars to buckle by maximizing the second moment of area. Although cuttlefish can withstand pressures up to 24 atm, they do not seem to live deeper than 150 m, where the pressure is 16 atm. *Nautilus* shells collapse at about 65 atm, but they also remain at a safer depth of about 500 m, where the pressure is at 51 atm [37]. The same is true of the *Spirula*. Even though its shell implodes at pressures corresponding to a depth of 1700 m, most *Spirula* are caught at depths of 600–700 m during the day, and at 300–100 m by night [38].

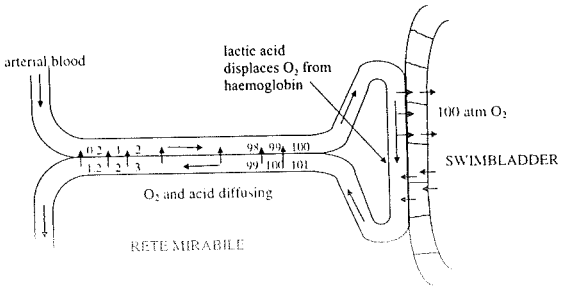

Figure 3 Diagram of mechanism whereby O_2 can be secreted into the swimbladder through the countercurrent circulation of the rete mirabile [28].

4. Teleost Fish

Teleosts are a large diverse group of bony fish. Many species, including the cod and haddock, are equipped with swimbladders that give them neutral buoyancy [2]. Typically, a swimbladder occupies around 5% of the total volume of a fish, and the low density of the gases that inflate the bladder offset the higher density of the muscle and bone. However, the volume of the swimbladder can change with depth. As the fish swims downward, pressure increases at one atmosphere every 10 m. Therefore, when a fish dives deeper, it must secrete more gas into the swimbladder, and reabsorb gas from the swimbladder when it wishes to rise. The rates of secretion or reabsorption are quite slow. Fish caught at depth and immediately brought to the surface nearly always die because their swimbladders expand rapidly as the pressure drops, thus crowding and rupturing their vital organs.

The gas pressure exerted in the swimbladder directly opposes the hydrostatic pressure of the sea. The proportion of oxygen found in swimbladders increases with depth. A fish living at a depth of 1000 m has a partial pressure of oxygen in the swimbladder of 100 atm, but only 0.2 atm in the surrounding tissues, so somehow the swimbladder pressure must be maintained to resist the hydrostatic pressure [28]. This is partly achieved by having impermeable walls and also by the gas gland and its blood supply, the rete mirabile. The rete is made up of arterial and venous capillaries lying next to each other, forming a countercurrent system.

In the gas gland, lactic acid is produced from glycogen and diffuses into adjointing blood capillaries (Figure 3). This causes an increase in acidity that results in a rapid displacement of O_2 from

haemoglobin [39]. Therefore there is an increase in the concentration of free (diffusible) oxygen molecules. The blood leaves the gas gland and enters the rete mirabile countercurrent system. There is a progressive equilibration of diffusible substances between the ingoing and outgoing streams. Free oxygen molecules diffuse into the incoming blood and the acidity of the outgoing blood decreases [28]. Alkaline blood causes O_2 molecules to recombine with haemoglobin. However, the rate of combination is far slower than displacement from haemoglobin, and it is this difference in rates that brings about an excess of oxygen molecules available for secretion. The countercurrent system allows the concentration of free O_2 molecules to build up within the gas gland until there is a net diffusion of gas from the gas gland into the lumen of the swimbladder, against the hydrostatic pressure of the sea.

Gas reabsorption is carried out in one of two ways. Some fish have a valved duct leading to the oesaphagus through which gas can escape [28]. Other fish have a closed system with a structure called an oval that acts like a sphincter to open or close some region of the swimbladder wall, so that the region is either exposed to or occluded from the gases. This region has its own blood supply not connected to a rete, so gases can dissolve into the blood and get carried away from the swimbladder.

5. Sharks

Deep-sea squaloid sharks have attained neutral buoyancy through the development of a large and oily liver. In most animals the liver is around 4–6% of the total weight, but in the shark it may be more than a quarter of the total weight [40]. The liver oil is mainly composed of hydrocarbon squalene, which has a specific gravity of 0.86 and is stored in such quantities that the uplift provided almost eliminates the shark's weight in seawater. It has been suggested that the mass of squalene would have to be controlled to within 1% in order to keep the animal within 0.1% of neutral buoyancy. The *Squalus acanthias* shark responds to changes in its weight by varying the less abundant lipid constituents of the liver oil, and not the amount of squalene [41]. When weights were attached to the shark, the presence of diacyl glyceryl ethers, which are less dense than the triglycerides in the liver oil, increased over two days. This increase in the low-density lipids was sufficient to counter the weight increase.

6. Deep-Diving Whales

Whales that dive deeply, like the sperm whale, have huge amounts of low-density fats [28], much lower than the fats in shallow-diving

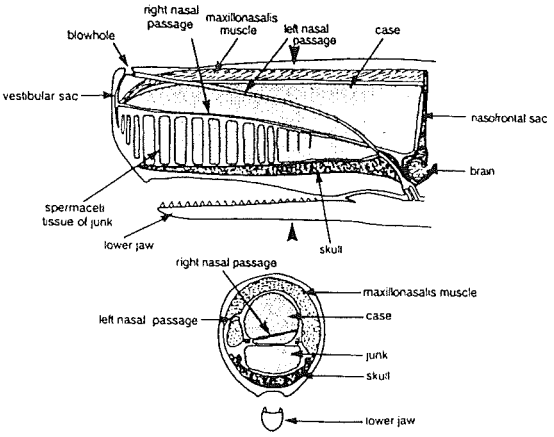

Figure 4 The structure of the head of the sperm whale [47].

whales. Clarke [42] advanced the theory that the spermaceti organ in the head of the sperm whale is used to regulate buoyancy by exploiting appreciable differences in density between the melted and unmelted forms of the entrained waxes. The theory received much criticism [43–45], but the hypothesis was expanded to greater detail [46, 47].

The spermaceti organ makes up the bulk of the head of the sperm whale, and it is filled with a liquid called spermaceti (Figure 4). It is a complex mixture containing some triglyceride fats like those found in other mammals and animals. However, spermaceti is composed chiefly (~73.5%) of waxes. These are the esters of fatty acids and monohydric alcohols, which have a much lower specific gravity than the triglyceride fats. Spermaceti is a clear straw-coloured oil at about 30°C, but becomes cloudy if cooled and progressively solidifies and crystallizes as the temperature drops. As it solidifies, it contract and becomes denser. Clarke [46] found that the rate of density increase on cooling is greater at higher pressures. An increase in density of the spermaceti will result in a decrease in the buoyancy of the whale. If the sperm whale could control the temperature of the spermaceti organ and its oil, it could also control its density, and sink or rise with small expenditure in energy.

Clarke suggested that a mechanism might exist for flushing water through the right nasal passage, which, with its expanded sacs at the front and back of the spermaceti organ, would be well fitted to act as a useful heat-exchanger [46, 47]. This would cool the spermaceti oil, increasing the specific gravity and causing the whale to become less buoyant. The lungs of the whale are isolated from the surface of the heat-exchanger by a sphincter muscle surrounding the right nasal passage where it joins the left, just before it enters the skull. Having isolated the right nasal passage, it can then be irrigated with water by the action of a larger block of muscle, the maxillona-

salis, which can lift the forward end of the case, thus expanding the cavity within the right nasal passage. The cold seawater would cool the spermaceti organ near the passage. Blood flowing past the nasal passage would also be cooled, which could then cool the spermaceti oil further from the nasal passage. Using this method, and also from heat loss through the blubber and skin, the whale could achieve neutral buoyancy in 3 minutes while diving to a depth of 1000 m.

To rise again, the whale would cease to circulate water through the nasal passages [46, 47]. In addition, vasoconstriction at the skin surface would cease the loss of heat through the blubber. There would be enough muscle activity to cause heat to accumulate and be transferred to the spermaceti organ via the blood. The whale would then gently rise to the surface.

7. Seabed Dwellers and Active Swimmers

Although many organisms possess buoyancy devices, others do not and they must therefore remain on the bottom of the ocean or employ some form of muscular effort to maintain themselves at their particular depth. Lobsters, plaice (*Pleuronectes*), rays (*Raia*, selachians) and common octopus have no buoyancy organ so must live at the bottom of the sea [28].

Many organisms from plankton to certain species of shark must swim to keep themselves buoyant. Motile phytoplankton are capable of directed swimming and can control their position in the water column [10]. The barrel in which the amphipod *Phronima sedentaria* lives acts as a propulsion system with an entrance three times the area of the exit. This barrel greatly reduces the energy expended by the amphipod in maintaining its position [48]. This also occurs in individuals of the class Larvacea [49]. The spiral shell of the pteropod *Limacina retroversa* is supported by having a foot with two lateral extensions, like wings. Rhythmical flapping of the wings effects swimming [49]. The crustacean *Euphausia pacifica* is the most negatively buoyant of the midwater crustaceans, and must swim constantly to avoid sinking [50].

Although many species of cephalopod possess buoyancy systems, some squid need to swim actively to prevent themselves from sinking [20]. The squid *Loligo forbesi* has fins at its posterior end that tend to tilt its nose down, but the thrust exerted by its jet from the funnel balances the moments. Active swimming is also a way of life for the Ommastrephidae, Enoploteuthidae, Brachioteuthidae and Ctenopterygidae species.

Fish which swim perpetually at high speeds tend to be denser than seawater. Mackerel and tuna never stop swimming day or night. The bullet mackerel (*Auxis rochei*) swims at an average speed of 0.7 m/s in order to generate enough lift from its fins [37]. Tunnies and sharks, such as the blue shark, swim with their pectoral fins extended with a positive angle of attack, so that upward lift acts on them. As these hydrofoils are anterior to the centre of mass, they tend to tilt the snout of the fish upwards. The forward thrust and uplift generated by the tail fin, called the heterocercal tail, balances the moments and allows the fish to swim horizontally. There is a minimum speed at which these fish can swim, under which stalling may occur. For a dogfish this is about 0.24 m/s, and 0.6 m/s for a skipjack tuna. In general, the more primitive fishes must rely on hydrofoils and propulsive power to maintain their buoyancy, whereas the more advanced organisms have evolved static or passive means to achieve a constant level in the water column [3]. Less energy is expended to obtain neutral buoyancy by these mechanisms than to have to move constantly to attain the required lift.

8. The Buoyancy of Underwater Vehicles: Learning from Nature?

Over the last century, mankind has attempted to emulate the ability of marine organisms to control their buoyancy and explore the ocean depths. The majority of submersible vehicles built in the twentieth century have used a buoyancy system of making adjustments in weight by admitting or expelling seawater from variable ballast tanks [51]. The principle is similar to the rigid buoyancy chambers of the *Nautilus*, *Spirula* and cuttlefish, by varying the gas and liquid contents. Mankind has managed to go one step further by being able to achieve rapid descents and ascents with the aid of sophisticated pumps. However, variable seawater ballast systems are restricted to shallow and mid-depth ranges because of the difficulty of pumping or blowing against high hydrostatic pressures [51]. Variable displacement systems using inflatable bladders are also unsuitable for deep ocean depths due to the high pressures. Adjustments in buoyancy are made by increasing or decreasing the displacement of oil-inflatable/deflatable bladders. Again, active pumping is required to transfer a volume of liquid from an internal reservoir to an external bladder.

An inflatable bladder system was used in the submersible *Alvin* in the 1960s to control its buoyancy finely. It would dive and climb using three manoeuvrable propellers [52]. More recently, bladder systems have been used effectively in underwater profilers and gliders [53, 54]. These relatively small torpedo-shaped floats periodically change their buoyancy by pumping fluid from an internal reservoir to an external bladder, thereby increasing float volume and buoyancy. Pumping requires energy from the onboard power supply, thus limiting the duration that a float can stay in the ocean performing cyclical dives. Researchers

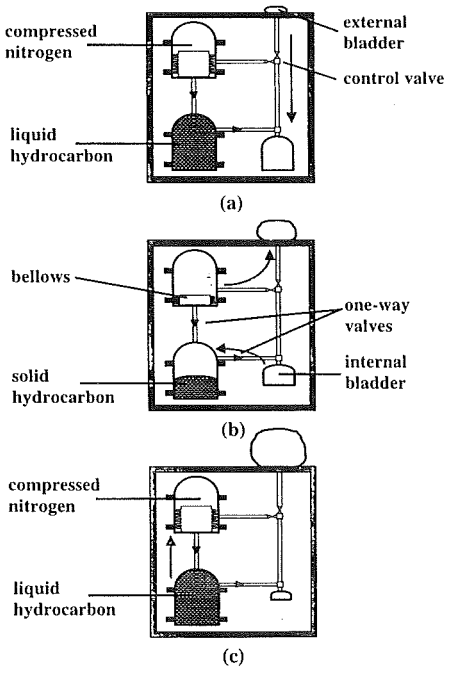

Figure 5 The thermal engine of the Slocum glider. (a) To dive, a three-way control valve is closed, allowing glycol to flow into an internal bladder. (b) The cold temperatures at depth freeze the liquid hydrocarbon into a solid, creating a space that is filled by glycol from the internal bladder. To ascend, the control valve is closed the other way, and compressed nitrogen from the top tank pushes glycol out of a metal bellows into the external bladder. (c) The hydrocarbon melts again, pushing glycol back into the bellows, compressing the nitrogen and readying the glider for the next dive [54].

[54] looked for ways of using the changes in temperature of seawater at the surface and at depth somehow to power the pump system. They opted for a system similar to that used by the sperm whale. By using a volume of pure hydrocarbon that was solid at deep ocean temperatures, but expanded when melted by surface temperatures [53], they were able to design a heat engine that could store enough energy to pump a volume of liquid to the external bladder of the float (Figure 5). The only internal power requirements were the control of the various valves of the pumping system.

Many forms of marine life use low-density materials to offset their bulkier materials. For example, as explained earlier, many sharks have squalene in their livers that keeps them buoyant, and some squid species use ammonium-based coelomic fluid to buoy themselves. Even tiny plankton employ some form of ion-exchange system to keep their internal body fluids light. In 1960 Auguste Piccard, in his bathyscaph *Trieste*, managed to dive into the Marianas Trench of the Pacific Ocean down to 10 916 m, the deepest known depth on the earth [55]. It was a large vessel that could hold two men and was buoyed by a large float containing petrol. The fine adjustments to buoyancy were made by slowly releasing the petrol and by dropping weights to keep it just negatively buoyant as it descended.

Also in the 1960s, foam composites and syntactic foams were developed which had low densities, high hydrostatic strength, a bulk modulus almost equal to seawater, and immunity to catastrophic failure. The foams could also be fabricated into irregular shapes and be used as a filler when 'foamed-in-place'. Since then they have been used in a wide variety of applications such as submersible vehicles, buoys, risers and flotation units [56]. However, the buoyancy provided by foams is passive and static, which is fine for flotation units and buoys, but inadequate for submersibles where other dynamic means are necessary for ascent and descent.

Hydrodynamic planes to facilitate vertical travel in the ocean are being utilized in gliders that use a fixed hydrofoil and the thermal engine described in Figure 5 [53]. At the surface the engine deflates the external bladder, giving the glider a negative buoyancy, which is sufficient to point the glider downwards. It sinks and gains speed, but the hydrofoil generates lift on the way and the glider eventually reaches a nadir point and begins to rise again. Meanwhile the thermal engine has been storing energy. The external bladder is inflated and provides a positive buoyancy to help the glider back to the surface.

With costs of running and maintaining large manned and unmanned submersibles remaining high, there is a trend towards the development of smaller, low-cost autonomous vehicles. Researchers are turning more and more to nature to try and mimic the characteristics of fish. One such project is the Robot Tuna and Robot Pike [57], small underwater robots that mimic the swimming actions of the tuna and pike. The buoyancy of these robots has been made neutral using light acetal structural elements. Another project is concentrating on the swimming behaviour of the lamprey or eel [58]. The undulations of their tails are being imitated by using shape memory alloy wires.

It is the advent of smart materials such as shape memory alloys (SMAs) and polymer gels that could pave the way towards an intelligent buoyancy system for underwater vehicles. A small robotic fish, called MEFiR (Micro Electronic Fish Robot), is using shape memory alloy wires to control the tail movement, and the buoyancy of the device may be controlled by a water bladder utilizing the contraction properties of an SMA piston [59]. Elsewhere, a variable buoyancy regulator is being tested using arrays of small hollow tubes ('straws') made of shape memory alloy that can increase in volume when electrically heated [60]. The 'straws' can with-

stand hydrostatic pressures of 20–30 atm. Another possible buoyancy system is a peristaltic pump using a compliant SMA-wrapped cylinder that would quietly and slowly pump a large volume of ballast seawater [61]. Finally, the great expansions and contractions found with certain polymer gels could be used as actuators to displace water and bring about a buoyancy change. The volumetric changes could be brought about by the natural temperature and salinity gradients in the ocean [62], thus providing a power source for actuation.

Acknowledgements

This research was supported by the Engineering and Physical Sciences Research Council (EPSRC), Grant No. GR/L 27022, administered through the Marine Technology Directorate (MTD). Such support is gratefully acknowledged.

References

1. Marshall, N.B., 1954, *Aspects of Deep-Sea Biology*, Hutchinson, London.
2. Marshall, N.B., 1979, *Developments in Deep-Sea Biology*, Blandford Press, Poole.
3. Wiseman, S.W., and Reynolds, C.S., 1981, Sinking rate and electrophoretic mobility of fresh-water diatom *Asterionella formosa*: an experimental investigation. *Br. Phycol. J.*, **16**(4), pp. 357–361.
4. Newton, C., and Potts, W.T.W., 1993, Ionic regulation and buoyancy in some planktonic organisms. *J. Mar. Biol. Ass. U.K.*, **73**(1), pp. 15–23.
5. Gross, F., and Zeuthen, E., 1948, The buoyancy of plankton diatoms: a problem of cell physiology. *Proc. Roy. Soc. Lond. B*, **135**(880), pp. 382–389.
6. Kahn, N., and Swift, E., 1978, Positive buoyancy through ionic control in the nonmotile marine dinoflagellate *Pyrocystis noctiluca* Murray ex Schuett. *Limnol. Oceanogr.*, **23**, pp. 649–658.
7. Walsby, A. E., 1978, The properties and buoyancy-providing role of gas vacuoles in *Trichodesmium* Ehrenberg. *Br. Phycol. J.*, **13**, pp. 103–116.
8. Walsby, A.E., Reynolds, C.S., Oliver, R.L., and Kromkamp, J., 1989, The role of gas vacuoles and carbohydrate content in the buoyancy and vertical distribution of *Anabaena minutissima* in Lake Rotongaio, New Zealand. *Ergebn. Limnol.*, **32**, pp. 1–25.
9. Furbish, D.J., and Arnold, A.J., 1997, Hydrodynamic strategies in the morphological evolution of spinose planktonic foraminifera. *Geol. Soc. Am. Bull.*, **109**(2), pp. 1055–1072.
10. Richardson, T.L., and Cullen, J.J., 1995, Changes in buoyancy and chemical composition during growth in a coastal marine diatom: ecological and biogeochemical consequences. *Marine Ecol. Progr. Ser.*, 128, pp. 77–90.
11. Fisher, A.E., and Harrison, P.J., 1996, Does carbohydrate content affect the sinking rates of marine diatoms? *J. Phycol.*, 32, pp. 360–365.
12. Moore, J.K., and Villareal, T.A., 1996, Buoyancy and growth characteristics of three positively buoyant marine diatoms. *Marine Ecol. Progr. Ser.*, **132**, pp. 203–213.
13. Villareal, T.A., Pilskain, C., Brzezinski, M., Lipschultz, F., Dennett, M., and Gardner, G.B., 1999, Upward transport of oceanic nitrate by migrating diatom mats. *Nature*, **397**, pp. 423–425.
14. Mclaren, I.A., 1963, Effects of temperature on growth of zooplankton and the adaptive value of vertical migration. *J. Fish. Res. Bd. Can.*, **20**, pp. 685–727.
15. Haney, J.F., 1988, Diel patterns of zooplankton behaviour. *Bull. Mar. Sci.*, **43**(3), pp. 583–603.
16. Hardy, A.C., 1953, Some problems of pelagic life. In *Essays in Marine Biology* (*Richard Elmhurst Memorial Lectures*). Oliver and Boyd, Edinburgh, pp. 101–121.
17. McAllister, C.D., 1969, Aspects of estimating zooplankton production from phytoplankton production. *J. Fish. Res. Bd. Can.*, **26**, pp. 199–220.
18. Enright, J.T., 1977, Diurnal vertical migration: adaptive significance and timing. Part I. Selective advantage: a metabolic model. *Limnol. Oceanogr.*, **22**, pp. 856–872.
19. Mclaren, I.A., 1974, Demographic strategy of vertical migration by a marine copepod. *Amer. Nat.*, **108**, pp. 91–102.
20. Clarke, M.R., Denton, E.J., and Gilpin-Brown, J.B., 1979, On the use of ammonium for buoyancy in squids. *J. Mar. Biol. Ass. U.K.*, **59**, pp. 259–276.
21. Denton, E.J., Gilpin-Brown, J.B., and Shaw, T.I., 1969, A buoyancy mechanism found in cranchiid squid. *Proc. Roy. Soc. Lond. B*, **174**, pp. 271–279.
22. Voight, J.R., Portner, H.O., and Odor, R.K., 1994, A review of ammonia-mediated buoyancy in squids (Cephalopoda Teuthoidea). *Mar. Freshwater Behav. Physiol.*, **25**(1–3), pp. 193–203.
23. Clarke, M.R., Denton, E.J., and Gilpin-Brown, J.B., 1969, On the buoyancy of squid of the families Histioteuthidae, Octopoteuthidae, and Chiroteuthidae. *Proc. R. Soc. Lond. B*, **174**, pp. 271–279.
24. Dilly, P.N., Nixon, M., and Young, J.Z., 1977, *Mastigoteuthis*—the whip-lash squid. *J. Zool. Lond.*, **181**, pp. 527–559.
25. Roper, C.F.E., and Lu, C.C., 1990, Comparative morphology and function of dermal structures in oceanic squids (Cephalopoda). *Smith. Contrib. Zool.*, **493**, pp. 1–40.
26. Roper, C.F.E., and Young, R.E., 1975, Vertical distribution of pelagic cephalopods. *Smith. Contrib. Zool.*, **209**, pp. 1–51.
27. Denton, E.J., and Gilpin-Brown, J.B., 1966, On the buoyancy of the pearly *Nautilus*. *J. Mar. Biol. Ass. U.K.*, **46**, pp. 723–759.
28. Denton, E.J., 1974, *Buoyancy in Marine Animals*. Oxford University Press, London.
29. Ward, P.D., 1982, Have shell, will float. *Nat. Hist.*, **91**(10), pp. 64–69.
30. Ward, P.D., 1986, Rates and processes of compensatory buoyancy change in *Nautilus macromphalus*. *Veliger*, 28(4), pp. 356–368.
31. Greenwald, L., Ward, P.D., and Greenwald, O., 1980, Cameral liquid transport and buoyancy control in chambered nautilus (*Nautilus macromphalus*). *Nature*, 286, pp. 55–56.

32. Ward, P.D., and Greenwald, L., 1982, Chamber refilling in *Nautilus*. *J. Mar. Biol. Ass. U.K.*, **62**, pp. 469–475.
33. Willey, A., 1902, Contributions to the natural history of the pearly nautilus. In *A. Willey's Zoological results*. Cambridge University Press, Part 6, pp. 691–830.
34. Heptonstall, W., 1970, Buoyancy control in ammonoids. *Lethaia*, **3**, pp. 317–328.
35. Birchall, J.D., and Thomas, W.L., 1983, On the architecture and function of cuttlefish bone. *J. Mater. Sci.*, **18**, pp. 2081–2086.
36. Denton, E.J., Gilpin-Brown, J.B., and Howarth, J.V., 1961, The osmotic mechanism of the cuttlebone. *J. Mar. Biol. Ass. U.K.*, **41**, pp. 351–364.
37. McNeill, A.R., 1982, In: *Locomotion of Animals*, Blackie, Glasgow, Chap. 3.
38. Clarke, M.R., 1966, A review of the systematics and ecology of oceanic squids. *Adv. Mar. Biol.*, **4**, pp. 91–300.
39. Steen, J.B., 1970, The swimbladder as a hydrostatic organ. In W.S. Hoar and D.J. Randall (Eds.). *Fish Physiology*, Vol. IV. Academic Press, New York and London.
40. Bone, Q., and Marshall, N.B., 1982, *Biology of Fishes*. Blackie, Glasgow.
41. Malins, D.C., and Barone, A., 1970, Glycerol ether metabolism: regulation of buoyancy in dogfish *Squalus acanthias*. *Science*, **167**, pp. 79–80.
42. Clarke, M.R., 1970, The function of the spermaceti organ of the sperm whale. *Nature*, **228**, pp. 873–874.
43. Ridgeway, S.H., 1970, Buoyancy regulation in deep diving whales. *Nature*, **232**, pp. 133–134.
44. Norris, K.S., and Harvey, G.W., 1972, A theory for the function of the spermaceti organ of the sperm whale. In S.R. Galler, K. Schmidt-Koenig, G.J. Jacobs and R.E. Belleville (Eds.). *Animal Orientation and Navigation*, NASA Special Publication.
45. Schenkkan, E.J., and Purves, P.E., 1973, The comparative anatomy of the nasal tract and the function of the spermaceti organ in the Physeteridae (Mammalia, Odontoceti). *Bijdragen tot de Dierkunde*, **43**, pp. 92–112.
46. Clarke, M.R., 1978, Structure and properties of the spermaceti organ in the sperm whale. *J. Mar. Biol. Ass. U.K.*, **58**, pp. 1–71.
47. Bonner, N., 1989, In *Whales of the World*, Blandford Press, Poole, pp. 89–93.
48. Davenport, J., 1994. Observations on the locomotion and buoyancy of *Phronima sedentariea* (Forskal 1775) (Crustacea, Amphipoda, Hyperiidea). *J. Nat. Hist.*, **28**(4), pp. 787–793.
49. Todd, C.D., Laverack, M.S., and Boxshall, G.A., 1996, *Coastal Marine Zooplankton*, 2nd Edition. Cambridge University Press, Cambridge.
50. Childress, J.J., and Nygaard, M.H., 1974, The chemical composition of midwater crustaceans as a function of depth of occurrence off Southern California. *Mar. Biol.*, **27**, pp. 225–238.
51. Allmendinger, E.E. (Ed.), 1990, *Submersible Vehicle Systems Design*. Society of Naval Architects and Marine Engineers.
52. MacDonald, A.G., 1975, *Physiological Aspects of Deep Sea Biology*. Cambridge University Press, Cambridge.
53. Kunzig, R., 1996, A thousand diving robots. *Discover*, April, pp. 60–71.
54. Webb, D.C., and Simonetti, P.J., 1999, The SLOCUM AUV: an environmentally propelled underwater glider. *11th International Symposium on Unmanned Untethered Submersible Technology*, pp. 75–85.
55. Gabler, U., 1986, *Submarine Design*. Bernard & Graefe Verlag, Koblenz.
56. Balmoral Hitec Buoyancy, 1989, *Buoyancy—In Depth*. Balmoral Group Ltd.
57. MIT Department of Ocean Engineering, http://web.mit.edu/towtank/www/pike.
58. Jalbert, J.C., Kasin, S., and Ayers, J., 1995, Design considerations and experiments of a biologically based undulatory lamprey AUV. *9th International Symposium on Unmanned Untethered Submersible Technology*, pp. 124–138.
59. Rose, C.J., and Myler, H.R., 1996, A design for a microelectronic fish robot. *1996 Florida Conference on Recent Advances in Robotics*. IEEE.
60. McCanna, J., and Rae, G.J., 1997, Shape memory alloy buoyancy regulator for subsea robots. *10th International Symposium on Unmanned Untethered Submersible Technology*, pp. 206–216.
61. Mide Technology Corporation, Cambridge, MA 02141. Proposal of Research to the Office of Naval Research Phase I Awards N96–161.
62. Molloy, P.J., Smith, M.J., and Cowling, M.J., 1999, The effects of salinity and temperature on the behaviour of polyacrylamide gels. *Materials and Design* (in press).

Volume and density changes in polymer gels in seawater environments

P J Molloy and **M J Cowling** *

Glasgow Marine Technology Centre, University of Glasgow, Scotland, UK.

Abstract: Some polymer gels are capable of undergoing large volume changes and significant density changes under the influence of solvent composition and temperature. Such characteristics are of interest in the design of small underwater devices. Studies have been conducted on the effects of temperature on the density and volume of poly(*N*-isopropylacrylamide), NIPA, gels. The gels were investigated in solutions of distilled water and solutions of natural seawater, which has an approximate salinity of 35 parts per thousand (ppt). For each solution, the effect of temperature from 5°C to 50°C was investigated. Such gels contract significantly when heated above their phase transition temperatures. The transition temperature for gels in seawater, 26-28°C, was found to be lower than for gels in distilled water, 33-34°C. Gels in seawater become more dense at higher temperatures, whereas gels in distilled water decrease in density. Short-term tests reveal that such NIPA gels realise full contraction after 4-6 hours, but re-swelling takes longer. Density values fluctuate greatly in the first few hours due to phase co-existence. Mechanical tests on the NIPA gels showed a marked increase in mechanical strength and elastic modulus as temperature was increased above the phase transition temperature.

Keywords: polymer gels; seawater, temperature, density

*Corresponding author: Glasgow Marine Technology Centre, University of Glasgow, Glasgow G12 8QQ, UK. Tel: +44 141 3304361; fax: +44 141 3304015; e-mail: mikejc@eng.gla.ac.uk

1. INTRODUCTION

There is a need for small autonomous marine devices that are able to traverse throughout the water column of the oceans and coastal seas, usually with limited power sources. Buoyancy control is important in these small underwater vehicles, which usually carry sensor packages, to enable greater flexibility in measurements in the ocean [**1**]. This paper has concentrated on the behaviour of polymer gel systems that exhibit large volume changes when subjected to certain stimuli, such as temperature. Such gel systems might be used as the basis for actuators to control buoyancy in underwater applications [**2**], particularly if the density of the gel also varies in a reproducible manner.

Some polymer gels respond to changes in their environment, such as pH [**3**], temperature [**4**], solvent composition [**5**], or applied voltage [**6**]. One response can be a change in size and shape [**7**], which offers the prospect of a conversion of chemical energy directly to mechanical work. The benefits of this conversion could be used wherever power for more conventional devices is limited or difficult to obtain, such as in an underwater environment.

The effects of salinity and temperature on the behaviour of polyacrylamide gels has been reported previously [**5**]. It was found that the salinity of seawater played a significant factor in gel volume, but that the temperature sensitivity was minimal. This paper represents an extension of the former study, but concentrates on thermo-sensitive poly(*N*-isopropylacrylamide), NIPA, gels and examines the correlation between changes in volume and density changes. A temperature-sensitive gel has advantages over the solvent-sensitive gel system examined previously [**5**], in terms of, potentially, easier control by onboard vehicle systems.

The volume phase transition of NIPA gels in distilled water has been extensively reported [**8-10**]. The transition occurs at a temperature of approximately 34°C in distilled water and the mechanism has been attributed to the change in the balance of hydrophilic and hydrophobic interactions [**9**]. The concentrations of monomer (*N*-isopropylacrylamide) and comonomer (*N,N'*-methylenebis(acrylamide)) also affect

the temperature of transition. The effect of seawater solutions has not previously been studied. The aim of the current study was to investigate the suitability of NIPA gels as possible elements in underwater vehicles, especially in the area of buoyancy control.

2. EXPERIMENTAL

2.1 Gel preparation

NIPA gels were prepared using an *N*-isopropylacrylamide monomer (Sigma) and the crosslinking comonomer, N'N-methylene-bis-acrylamide (Fluka). All chemicals were of reagent-grade quality and were used without further purification. The distilled water was produced by a Millipore-U10 system. Transparent rods of gel were prepared based on a method described by Tanaka [**11**]. The mass of crosslinking agent was doubled and the amount of water was halved, in order to produce a more mechanically robust gel. The gels were produced in polypropylene cylinders of various diameters and cured at ambient temperatures for one day. The gel rods so produced were 100mm long and had diameters of 4.8mm, 12.8mm, 15.4mm or 20.4mm. These were washed in distilled water to remove any residue monomers and the rods were allowed to equalise in distilled water at ambient temperatures for one week.

2.2 Optimum diameter study

After equalising, the rods were cut to roughly equal lengths of approximately 30mm. The gel rods were then immersed in distilled water for one day at 34°C, which is 0.5°C above the known phase transition temperature for NIPA gels [**4,9**]. All gel samples remained cylindrical after the transition period, therefore, the degree of swelling, or contraction in this case, was calculated as a ratio, V_{GEL}/V_0,

$$V_{GEL}/V_0 = (D/D_0)^2 \cdot (L/L_0) \qquad (1)$$

where V_0, D_0 and L_0 are the volume, diameter and length of the gel rod at preparation and V_{GEL}, D and L the subsequent respective dimensions after each temperature

change. The gels were then transferred to distilled water at 30°C for one day to allow them to swell again. After this the above test was repeated, but this time the period of time at each temperature was longer, at 6 days. All tests were carried out in triplicate. Gel dimensions were recorded using a Mitutoyo Profile Projector Type PJ-300, accurate to ±0.001mm.

2.3 Long-term density study

The gels used in this study had a diameter of 4.8mm and were roughly equal in length at 15mm. The density studies were carried out using distilled water or seawater collected from the Largs Channel in the Firth of Clyde, Scotland. The seawater had a salinity of 35ppt when collected and was filtered through Whatman glass microfibre filters (GF/C) to remove any bacterial cultures.

The density and volume of each NIPA gel was found using a density bottle. This consists of a pear-shaped flask and a ground glass stopper, which has a capillary hole through its centre, allowing liquid to escape. The volume contained in the density bottle can be determined to 0.001ml, which allows density measurements to be made with an accuracy of 0.01%. The empty density bottle is weighed, M_{DB}, and then re-weighed when filled with a liquid of known density and temperature, M_{DB+L}. The densities of distilled water and seawater are known at all temperatures [**12,13**]. Care was taken to ensure the exterior of the density bottle was dried of overflowed liquid before re-weighing. The internal volume of the density bottle, V_{DB}, was found from the equation,

$$V_{DB} = (M_{DB+L} - M_{DB}) / \rho_L \qquad (2)$$

where ρ_L = density of liquid at known temperature. For a gel sample, the empty density bottle was weighed with the gel inside, M_{DB+GEL}, and re-weighed with the bottle filled with liquid, $M_{DB+GEL+L}$. The volume of liquid entrained, V_L, was

calculated as $(M_{DB+GEL+L} - M_{DB+GEL}) / \rho_L$. The volume of the gel was then $V_{GEL} = V_{DB} - V_L$ and the density of the gel, ρ_{GEL}, was found from the equation

$$\rho_{GEL} = M_{GEL} / V_{GEL} = (M_{DB+GEL} - M_{DB}) / V_{GEL} \quad (3)$$

All experiments were carried out in triplicate. Tests began at 5°C and were taken through a temperature range up to 50°C. The temperature increments were 5°C, but were reduced to 2°C increments between the temperature range 28°C to 40°C. The solutions were kept at constant temperature using a Techne Flow Cooler FC-500 in conjunction with a Techne Circulator C-85D in a 10-litre polymethyl methacrylate (PMMA) tank of water. After each temperature increase the gels were left to adjust for one day in the respective solution (distilled water or seawater). The solutions were changed daily during the experiments to simulate the effects of a larger body of water. The volume and density of each gel was found as outlined above and these were used to determine the volume ratio at each temperature, V_{GEL} / V_0.

2.4 Short-term Density Study

NIPA gels in distilled water and seawater solutions were allowed to equalise at 25°C before being transferred to solutions at 50°C for a 12-hour period. As the gels shrank in size, the volumes and densities were recorded using a density bottle, with measurements taken every 2 hours. In a similar study, contracted gels, that had been equalised at 50°C, were transferred to distilled water and seawater solutions at 25°C for 12 hours and allowed to swell.

2.5 Mechanical Tests

Compression tests were performed on cylindrical samples (15.4mm diameter) of NIPA, contained in a volume of temperature controlled distilled water, using a Lloyd L10000 materials testing machine. The distilled water was circulated and kept at a constant temperature using a Techne Circulator C-85D. To determine the modulus of elasticity of the NIPA gels, they were subjected to a maximum strain of 10%, at the recommended rate of 50% strain per minute [14]. Tests were carried out in triplicate

at temperatures of 30°C to 46°C. Gel samples were also loaded to failure at temperatures of 30°C, 35°C, 40°C and 45°C.

3. RESULTS AND DISCUSSION

3.1 Optimum Diameter Study

The results of this study can be seen in Figure 1. At 34°C for one day, the volume change (contraction) increases as the gel diameter decreases. This is also true when the gel swells in solutions at 30°C for one day. Only the gels with the smallest diameter, 4.8mm, actually achieved a fully reversible volume change. Even after longer periods at respective temperatures, the larger diameter gels did not realise a volume transition comparable to smaller diameter samples. This is because the time needed for water diffusion into or out of the gel, to effect swelling and shrinking, is proportional to the square of the gel diameter [**15**]. In fact, most researchers now use gels of sub-millimetre size to speed up experiments [**8**]. If NIPA gels are to be used in applications involving buoyancy control, these response characteristics need to be taken into account.

3.2 Long-term Density Study

The volume ratios of NIPA gels, in both distilled water and seawater, as the temperature is increased slowly from 5°C to 50°C is shown in Figure 2a. The volume phase transition temperature for NIPA gels in distilled water is known to be about 34°C [**4**] and the gels in this study do achieve full contraction at, or just above, this temperature. A surprising outcome for NIPA gels in seawater is that the transition temperature is significantly lower at around 26 to 28°C. This is encouraging, as the power needed to heat the gels to this temperature would be less than if they were immersed in distilled water solutions. Saltwater effects on gel volume include polymer-polymer interactions and the combination of the three competitive interactions of polymer-water, polymer-ion and water-ion [**8**]. The polymer-water interaction is most important with respect to the shrinking force, as this depends on the association and release of structured water from the hydrophobic groups. The

addition of salt affects the structures of the bound water, causing a shift in transition temperature to the lower temperature side.

The corresponding densities of the gels as they shrink and undergo the phase transition are shown in Figure 2b. There is little change in density for gels in seawater or distilled water, below their respective transition temperatures. This, however, changes once the transition temperature is exceeded. For gels in distilled water, the density decreases by 15-25%. Gels in seawater exhibit the opposite effect after they exceed their transition point, in that they become denser (by as much 30-40%), before returning to their original densities at higher temperatures. The standard deviations tend to increase soon after the transition is reached. This may be due to the fact that the gels become a two-phase system during transition [**9**], with both shrunken and swollen phases in coexistence. As temperature increases, the shrunken phase becomes dominant due to the hydrophobic effect, but small pockets of swollen material may still exist which could affect the density of the gel. The large change in density seen at approximately 5°C above the transition temperature, coupled with the corresponding reduction in volume, could pave the way towards a variable volume/density device suitable for controlling the buoyancy of small underwater vehicles and sensor packages.

3.3 Short-term Density Study

Having a gel system with a fast response time is of great interest in the field of buoyancy control. Figure 3a shows the reduction in volume of NIPA gels when immersed in distilled water and seawater at 50°C for a period of 12 hours. Figure 3b shows the corresponding density changes. After 6 hours the gels have shrunk to a volume ratio comparable to the long-term study. There is much fluctuation in density for both distilled water and seawater gels during this period, including a brief drop in density at the 4-hour mark. The phase coexistence is most pronounced at this point, as can be seen in Figure 4, and this presence of collapsed sections and hydrated swollen sections has possibly caused the gels to become less dense. After 6 hours, however, the gels are predominantly collapsed and increase in density again.

Collapsed gels that are allowed to reswell at 25°C change volume at a slower rate than when they were shrinking, as can be seen in Figure 5a. After 12 hours they still have not returned to their original volume and need a full 24 hours to do so. The corresponding densities, in Figure 5b, fluctuate in the first 4 to 6 hours, where the coexistent phases are most prevalent, but seem to settle into a smaller range at longer times.

3.4 Mechanical Tests

Compression tests performed on NIPA gels in distilled water reveal that the mechanical properties also depend on the temperature of the gel and its volume phase transition temperature. These gel materials are very soft and mechanically quite weak. The elastic Young's modulus of NIPA gel at 30°C is 0.0152 N/mm^2, which is approximately 5% that of low modulus, acetoxy type silicone rubber sealant. The yield stress at 30°C is also very low (0.0395 N/mm^2). Figure 6 shows how the elastic modulus of a NIPA gel almost doubles in magnitude as the temperature is raised above the transition temperature. A corresponding increase is noted for the yield stress.

4. DESIGN IMPLICATIONS

The results of this study illustrate the possible uses of NIPA gels in the control of buoyancy in small, underwater vehicles. The significant change in compliance of the material could be exploited to create a passive or very low power, variable stiffness element, which could be controlled through a change in temperature, to counteract the effects of seawater pressure. A change in compressibility could be enough to correct deviations from the neutral buoyancy position.

The differences in density of NIPA material in seawater, compared to its density in distilled water, could also be effectively used in buoyancy control. From Figure 2b, it can be seen that the density of the NIPA gel in seawater changes from a value very close to that of natural seawater (1.024 g/cm^3 at 20°C), to a maximum of 1.344 g/cm^3 at 34°C. A marine organism capable of changing its density by such a margin could

increase or decrease its rate of sinking by almost 67% [2]. A small underwater device incorporating an element of the NIPA material could, with a suitable seawater or distilled water exchange system, bring about a substantial change in its overall density to control the buoyancy of the vehicle.

5. CONCLUSIONS

The purpose of this study was to investigate NIPA gels for their usefulness as possible actuators in marine applications, such as in the buoyancy control of small vehicles and sensor packages. The work demonstrated that for such gels there is a significant contraction in both distilled water and seawater solutions and that the volume phase transition temperature is lower for gels in seawater. The majority of contraction can occur within a couple of hours. The density of NIPA gels also changes above the transition temperature, increasing in seawater and decreasing in distilled water. The significant differences in mechanical properties, density and volume of NIPA gels, as temperature and solvent medium is changed, demonstrate the possible use of NIPA materials as controllable elements in specific marine applications, such as the control of buoyancy of small, autonomous marine devices.

ACKNOWLEDGEMENTS

This research was supported by the Engineering and Physical Sciences Research Council (EPSRC), Grant No. GR/L 27022, administered through the Marine Technology Directorate (MTD) Ltd. Such support is gratefully acknowledged.

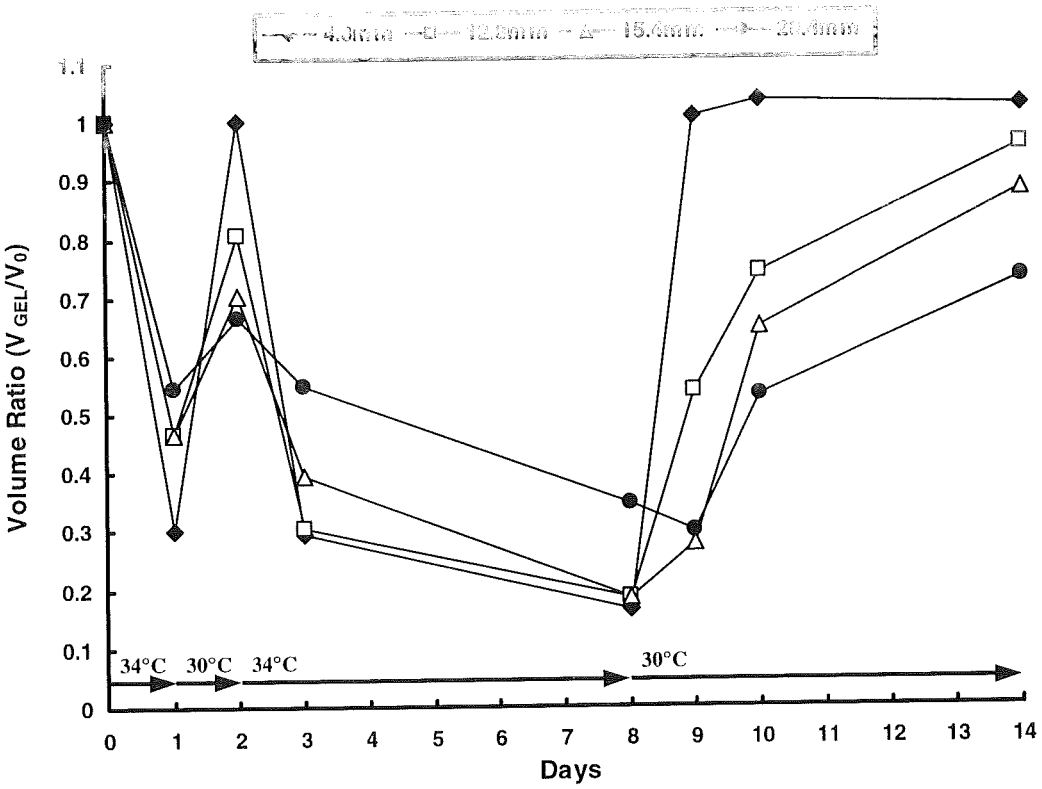
Volume Ratio (V_{GEL}/V_0)
Days
34°C
30°C
34°C
30°C

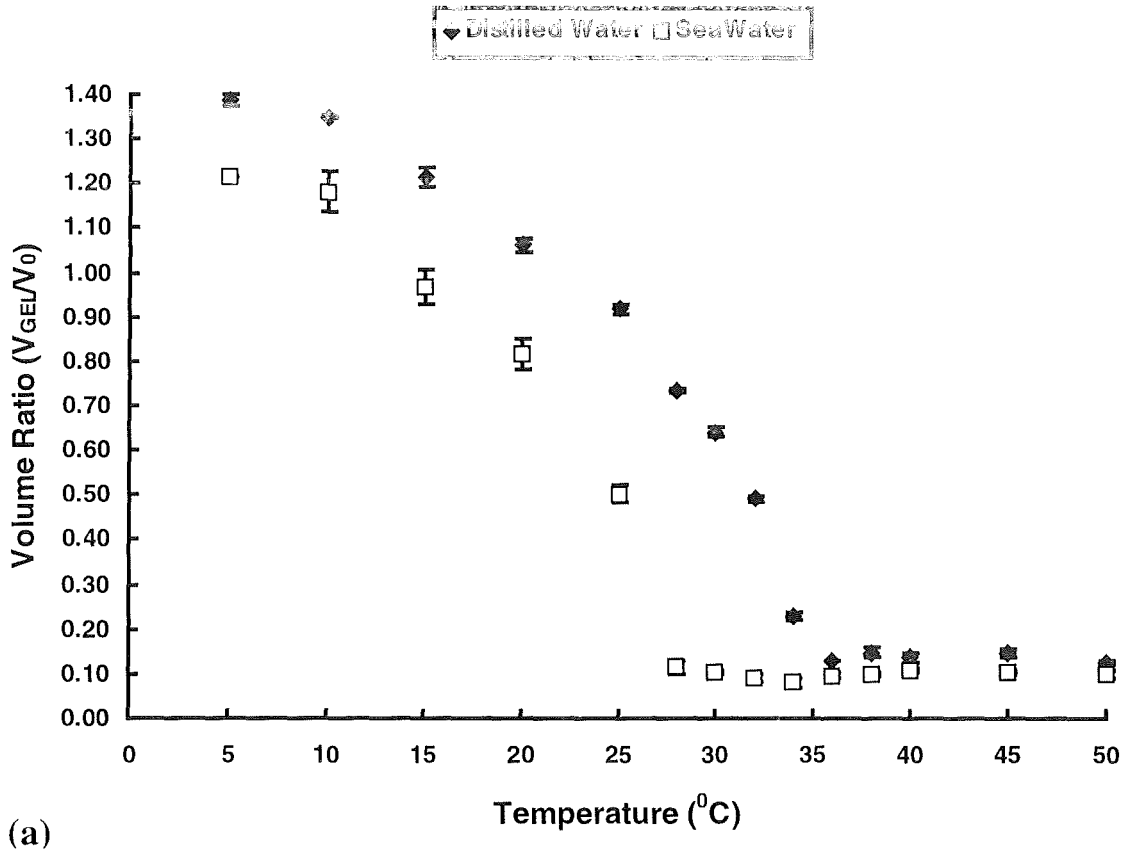
Distilled Water
SeaWater
Volume Ratio (V_{GEL}/V_0)
1.40
1.30
1.20
1.10
1.00
0.90
0.80
0.70
0.60
0.50
0.40
0.30
0.20
0.10
0.00
0
5
10
15
20
25
30
35
40
45
50
Temperature (^{0}C)

(a)

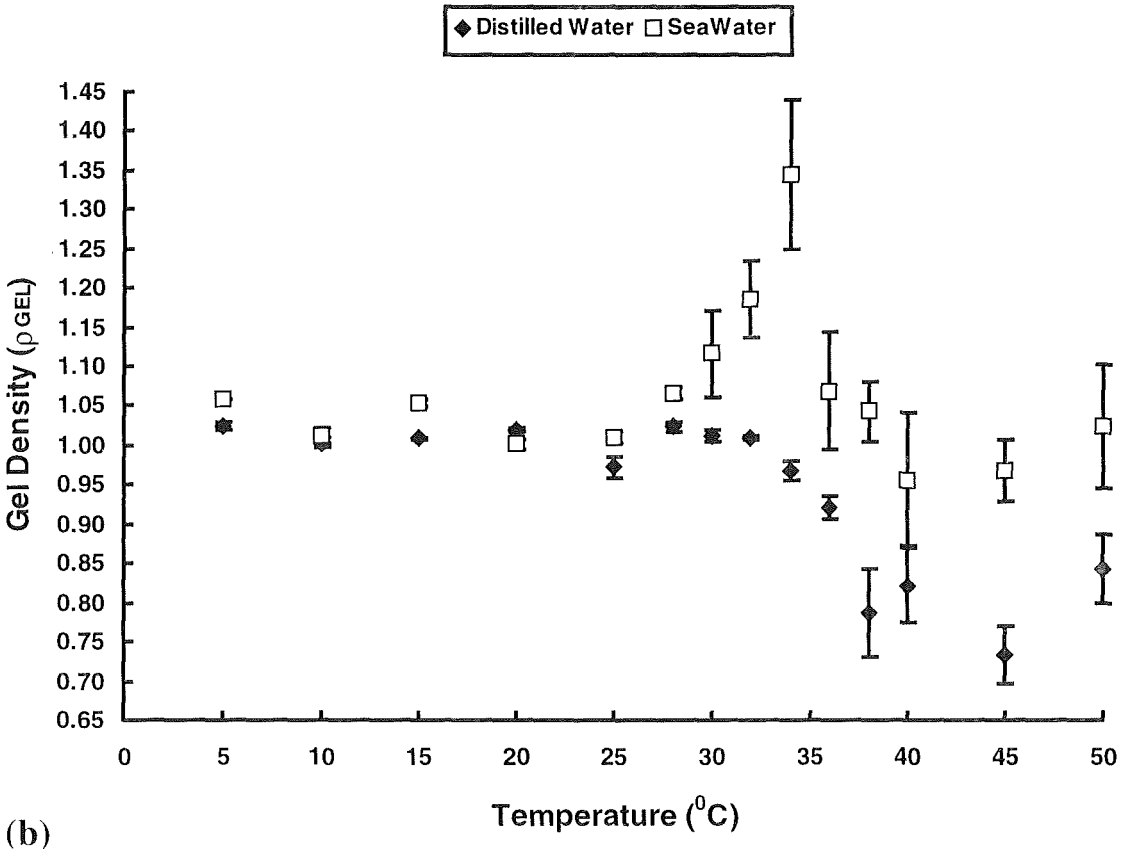
Distilled Water
SeaWater
Gel Density (ρ_{GEL})
1.45
1.40
1.35
1.30
1.25
1.20
1.15
1.10
1.05
1.00
0.95
0.90
0.85
0.80
0.75
0.70
0.65
0
5
10
15
20
25
30
35
40
45
50
Temperature (^{0}C)

(b)

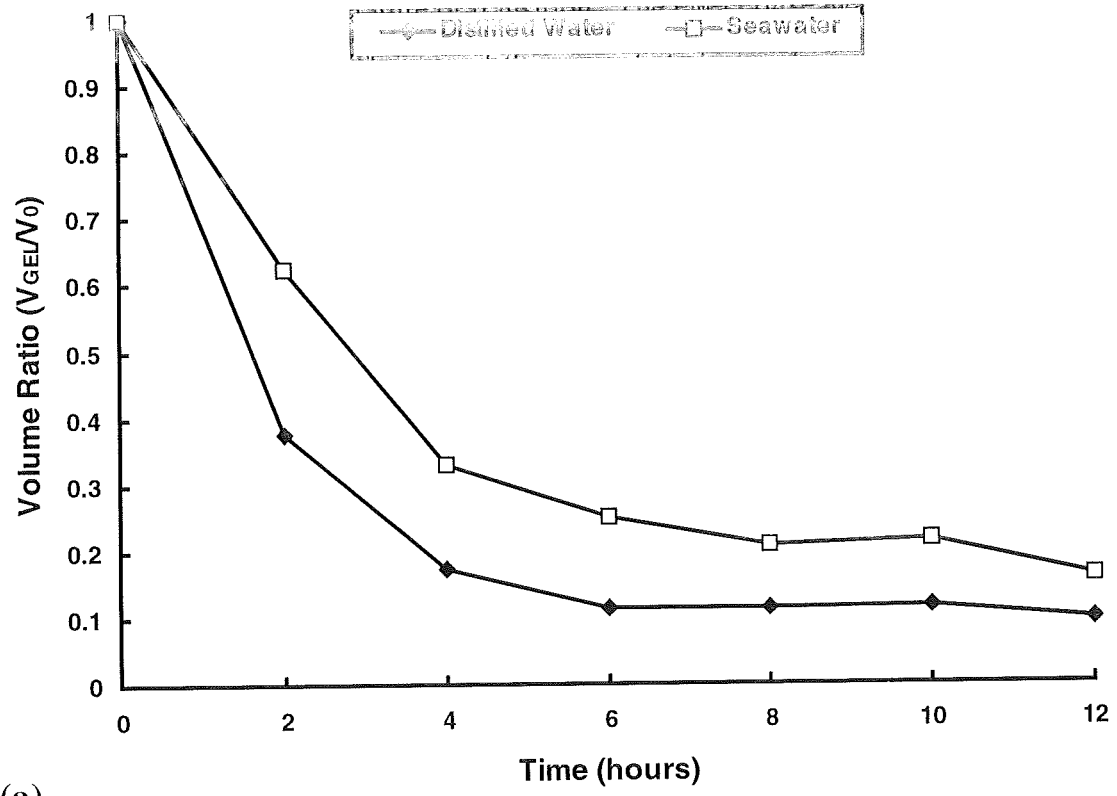
Distilled Water
Seawater
Volume Ratio (V_{GEL}/V_0)
1
0.9
0.8
0.7
0.6
0.5
0.4
0.3
0.2
0.1
0
0
2
4
6
8
10
12
Time (hours)

(a)

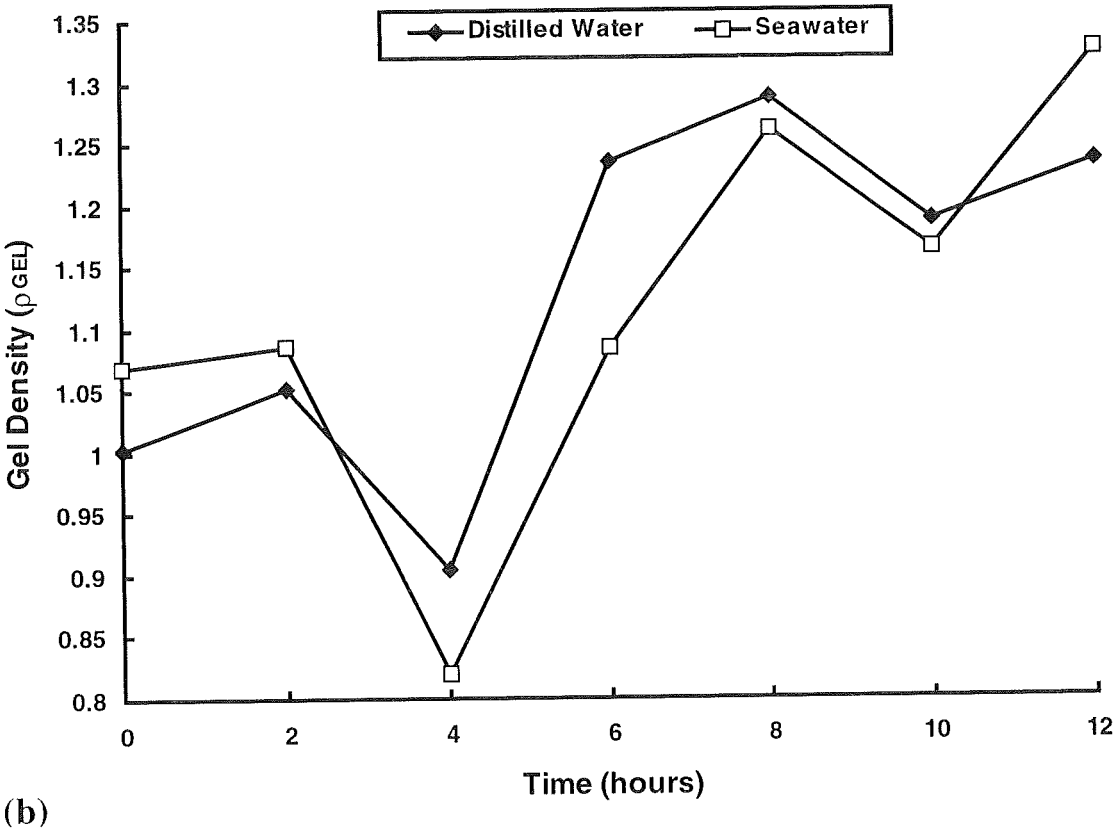
Distilled Water
Seawater
Gel Density (ρ_{GEL})
1.35
1.3
1.25
1.2
1.15
1.1
1.05
1
0.95
0.9
0.85
0.8
0
2
4
6
8
10
12
Time (hours)

(b)

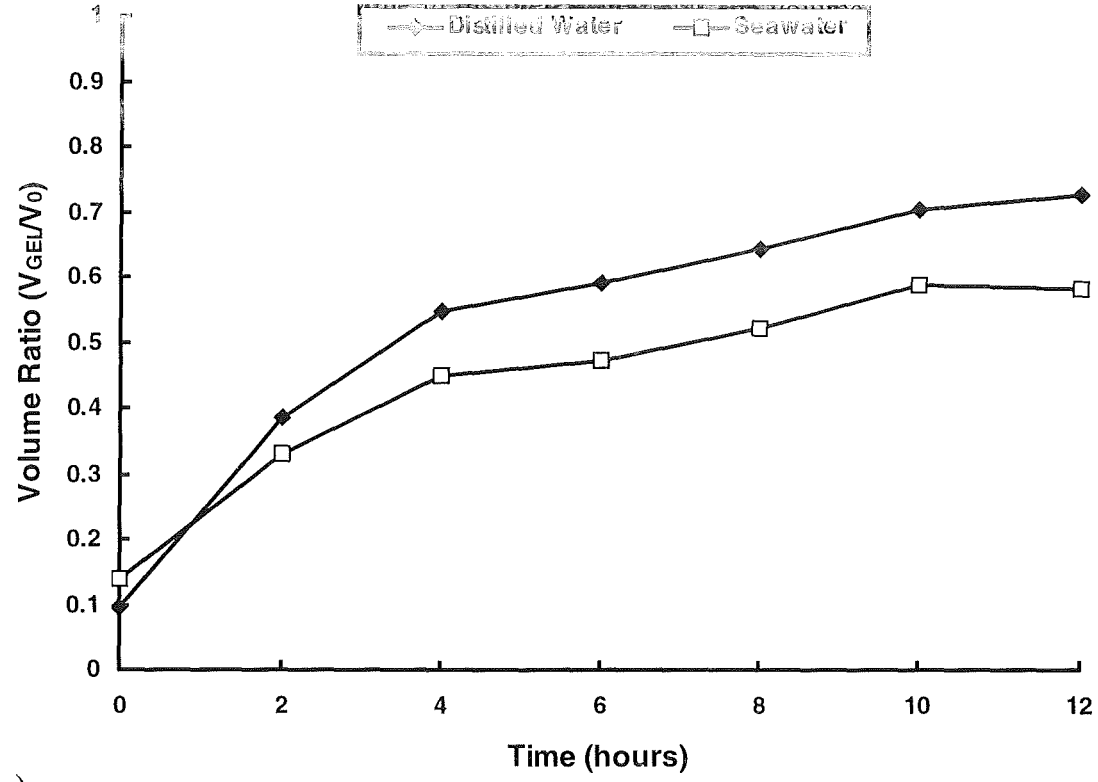

(a)

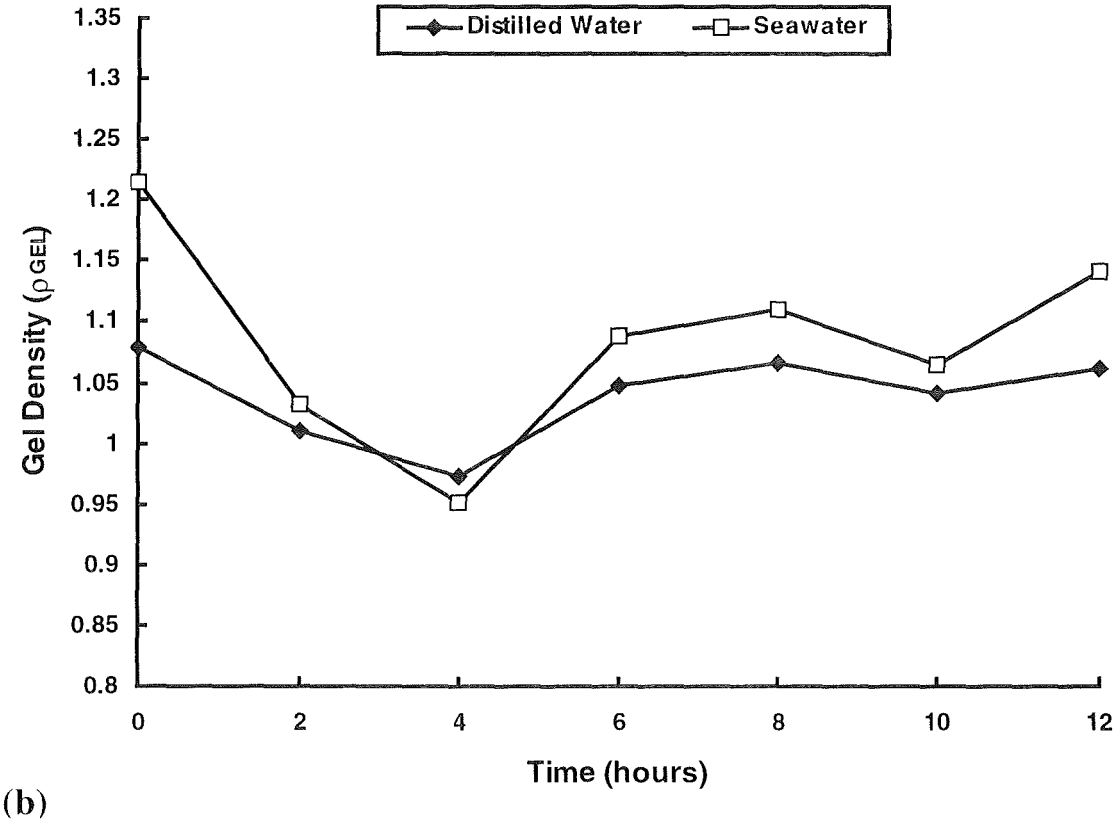

(b)

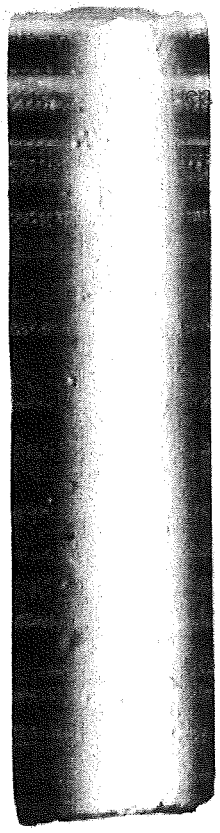

(a)

(b)

1 **Scrimshaw, K.H.** Aspects of buoyancy control and materials assessment applicable to deep submergence unmanned autonomous underwater vehicles (AUVs). *Oceanology International*, 1996, 245-262.

2 **Molloy, P.J.** and **Cowling, M.J.** Buoyancy mechanisms of marine organisms – learning from nature. *Journal of the Society for Underwater Technology*, 2000, **24** (2), 41-49.

3 **Katayama, S., Hirokawa, Y.** and **Tanaka, T.** Reentrant phase-transition in acrylamide-derivative copolymer gels. *Macromolecules*, 1984, **17**, 2641-2643.

4 **Hirokawa, Y.** and **Tanaka, T.** Volume phase transition in a nonionic gel. *J. Chem. Phys.*, 1984, **81** (12), 6379-6380.

5 **Molloy, P.J., Smith, M.J.** and **Cowling, M.J.** The effects of salinity and temperature on the behaviour of polyacrylamide gels. *Materials and Design*, 2000, **21**, 169-174.

6 **Tanaka, T., Nishio, I., Sun, S.T.** and **Ueno-Nishio, S.** Collapse of gels in an electric field. *Science*, 1982, **218**, 467-469.

7 **Tanaka, T.** Gels. *Scientific American*, 1981, **244** (Jan), 110-123.

8 **Suzuki, A.** Phase transition in gels of sub-millimeter size induced by interaction with stimuli. *Advances in Polymer Science*, 1993, **110**, 199-240.

9 **Hirotsu, S.** Static and time-dependent properties of polymer gels around the volume phase transition. *Phase Transitions*, 1994, **47**, 183-240.

10 **Suzuki, A., Yoshikawa, S.** and **Bai, G.** Shrinking pattern and phase transition velocity of poly(*N*-isopropylacrylamide) gel. *J. Chem. Phys.*, 1999, **111** (1), 360-367.

11 **Tanaka, T., Fillmore, D., Sun, S.-T., Nishio, I., Swislow, G.** and **Shah, A.** Phase transitions in ionic gels. *Phys. Rev. Lett.*, 1980, **45**, 1636-1639.

12 **Duxbury, A.B.** and **Duxbury, A.C.** In *Fundamentals of Oceanography*, 1993 (Wm. C. Brown, Boston, London, Sydney).

13 **Bretschneider, C.L., Corcoran, E.F., Jung, G.H., McAllister, R.F., Vine, A.C.** and **Zetler, B.D.** Basic Oceanography. In *Handbook of Ocean and Underwater Engineering* (Eds J.J. Myers, C.H. Holm and R.F. McAllister), 1969 (McGraw-Hill, London, San Francisco, Toronto, London, Sydney).

14 **Anseth, K.S., Bowman, C.N.** and **Brannon-Peppas, L.** Mechanical properties of hydrogels and their experimental determination. *Biomaterials*, 1996, **17**, 1647-1657.

15 **Tanaka, T.** and **Fillmore, D.J.** Kinetics of swelling of gels. *J. Chem. Phys.*, 1979, **70** (3), 1214-1218.

Fig. 1 Dependence of gel volume on gel sample diameter and time in distilled water during temperature cycles.

Fig. 2 (a) Gel volume as a function of temperature for gels in distilled water or seawater. (b) Corresponding dependence of gel density on temperature.

Fig. 3 Short term effects on gels in distilled water or seawater immersed at 50°C for a period of 12 hours. (a) Gel volume; (b) Gel density.

Fig. 4 (a) NIPA gel below the phase transition temperature. (b) Gel exhibiting phase co-existence as it contracts.

Fig. 5 Short term effects on gels in distilled water or seawater immersed at 25°C for a period of 12 hours. (a) Gel volume; (b) Gel density.

Fig. 6 Elastic modulus and yield stress as a function of temperature for NIPA gels tested in distilled water.